

OCS Study
BOEM 2021-055

Yakutat Wave Energy Converter Impact Assessment



US Department of the Interior
Bureau of Ocean Energy Management
Alaska Region

BOEM
Bureau of Ocean Energy
Management

Yakutat Wave Energy Converter Impact Assessment

August / 2021

Authors:

Jeremy Kasper
Manuel Castellote
Andrew Seitz
Kathleen Stafford
Michael Courtney
Eloise Brown

Prepared under Cooperative Agreement M17AC00021

By

University of Alaska Fairbanks
1764 Tanana Loop
Fairbanks AK 99775

University of Washington
1013 NE 40th St
Seattle WA 98105

US Department of the Interior
Bureau of Ocean Energy Management
Alaska Region



DISCLAIMER

Study collaboration and funding were provided by the US Department of the Interior, Bureau of Ocean Energy Management (BOEM), Environmental Studies Program, Washington, DC, under Agreement Number M17AC00021. This report has been technically reviewed by BOEM, and it has been approved for publication. The views and conclusions contained in this document are those of the authors and should not be interpreted as representing the opinions or policies of the US Government, nor does mention of trade names or commercial products constitute endorsement or recommendation for use.

REPORT AVAILABILITY

To download a PDF file of this report, go to the US Department of the Interior, Bureau of Ocean Energy Management [Data and Information Systems webpage \(http://www.boem.gov/Environmental-Studies-EnvData/\)](http://www.boem.gov/Environmental-Studies-EnvData/), click on the link for the Environmental Studies Program Information System (ESPIS), and search on 2021-055. The report is also available at the National Technical Reports Library at <https://ntrl.ntis.gov/NTRL/>.

CITATION

Kasper, J., Castellote, M., Seitz, A., Stafford, K., Courtney, M., Brown, E., 2021. Yakutat Wave Energy Converter Impact Assessment. Anchorage (AK): US Department of the Interior, Bureau of Ocean Energy Management. OCS Study BOEM 2021-055. 221 p.

ABOUT THE COVER

Photo by J. Kasper

Contents

1. List of Figures	3
2. List of Tables.....	5
3. List of Abbreviations and Acronyms	7
1.1 Summary	1
1.2 Marine Mammals and Acoustic Monitoring.....	1
1.2.1 Introduction	1
1.2.2 Methods	4
1.2.2.1 PAM Data Rescue	4
1.2.2.2 Collection of New PAM Data Through Mooring Deployments.....	5
1.2.2.2.1 2018 – 2019 PAM Equipment, Settings, and Deployments	4
1.2.2.2.2 2018 – 2019 Data Analysis	4
1.2.3 Results	7
1.2.3.1 2014 – 2015 PAM data	7
1.2.3.2 2018 – 2019 PAM Data.....	7
1.2.3.2.1 Cetacean Seasonal Occurrence	7
1.2.3.2.2 2018 – 2019 Study Area Soundscape	12
1.2.3.3 Sounds Produced by Wave Energy Converters	15
1.2.3.3.1 WEC Literature Reviewed.....	16
1.2.3.4 Entanglement rates of marine mammals in the general vicinity of Yakutat.....	18
1.2.4 Conclusions.....	19
1.3 Monitoring Fish and Information to Support an Essential Fish Habitat (EFH) Review.....	19
1.3.1 Introduction	19
1.3.2 Methods	21
1.3.2.1 Surface and bottom trawl sampling	21
1.1.1.1 Angling	28
1.3.2.2 Comprehensive species presence.....	24
1.3.3 Results	24
1.3.3.1 Surface and bottom trawl sampling	24
1.3.3.2 Angling	25
1.3.3.3 Species Presence	25
1.3.3.4 Archived Samples	26
1.3.4 Discussion.....	26
1.3.5 Conclusion	28

1.4	Information to Support an Archeological Review.....	38
1.4.1	Summary.....	38
1.4.2	Methods.....	38
1.4.3	Analysis.....	39
1.4.4	Results.....	39
1.4.5	Discussion and Conclusions.....	42
1.5	Evaluation of Oceanography and Sedimentation Effects of Wave Energy Converters.	42
1.5.1	Summary.....	42
1.5.2	Methods.....	43
1.5.2.1	Hydrography During the Trawl Survey.....	43
1.5.2.2	June 2018 Multibeam Bathymetry, Topographic Elevation and Hydrographic Surveys	47
1.5.2.3	Oceanographic Moorings.....	58
1.5.3	Results.....	59
1.5.3.1	Vessel-Based Hydrography.....	59
1.5.3.2	Topobathymetry.....	64
1.5.3.3	Moorings.....	66
1.5.4	Discussion.....	78
1.5.5	Summary and Conclusion.....	81
1.6	Evaluate Implications Findings from the Model Yakutat Wave Energy Project for Feasibility Studies in Other Coastal Regions of Alaska, Including Extensions onto the OCS.	81
1.7	References.....	86
•	Appendix B.....	198

1. List of Figures

1.	List of Figures	3
2.	List of Tables.....	5
3.	List of Abbreviations and Acronyms	7
1.1	Summary	1
1.2	Marine Mammals and Acoustic Monitoring.....	1
1.2.1	Introduction	1
1.2.2	Methods	4
1.2.2.1	PAM Data Rescue	4
1.2.2.2	Collection of New PAM Data Through Mooring Deployments.....	5
1.2.2.2.1	2018 – 2019 PAM Equipment, Settings, and Deployments	4
1.2.2.2.2	2018 – 2019 Data Analysis	4
1.2.3	Results	7
1.2.3.1	2014 – 2015 PAM data	7
1.2.3.2	2018 – 2019 PAM Data.....	7
1.2.3.2.1	Cetacean Seasonal Occurrence	7
1.2.3.2.2	2018 – 2019 Study Area Soundscape	12
1.2.3.3	Sounds Produced by Wave Energy Converters	15
1.2.3.3.1	WEC Literature Reviewed.....	16
1.2.3.4	Entanglement rates of marine mammals in the general vicinity of Yakutat.....	18
1.2.4	Conclusions.....	19
1.3	Monitoring Fish and Information to Support an Essential Fish Habitat (EFH) Review.....	19
1.3.1	Introduction	19
1.3.2	Methods	21
1.3.2.1	Surface and bottom trawl sampling	21
1.1.1.1	Angling	28
1.3.2.2	Comprehensive species presence.....	24
1.3.3	Results	24
1.3.3.1	Surface and bottom trawl sampling	24
1.3.3.2	Angling	25
1.3.3.3	Species Presence	25
1.3.3.4	Archived Samples	26
1.3.4	Discussion.....	26
1.3.5	Conclusion	28
1.4	Information to Support an Archeological Review.....	38

1.4.1	Summary	38
1.4.2	Methods	38
1.4.3	Analysis.....	39
1.4.4	Results	39
1.4.5	Discussion and Conclusions	42
1.5	Evaluation of Oceanography and Sedimentation Effects of Wave Energy Converters.	42
1.5.1	Summary	42
1.5.2	Methods	43
1.5.2.1	Hydrography During the Trawl Survey.....	43
1.5.2.2	June 2018 Multibeam Bathymetry, Topographic Elevation and Hydrographic Surveys	47
1.5.2.3	Oceanographic Moorings.....	58
1.5.3	Results	59
1.5.3.1	Vessel-Based Hydrography	59
1.5.3.2	Topobathymetry	64
1.5.3.3	Moorings	66
1.5.4	Discussion.....	78
1.5.5	Summary and Conclusion.....	81
1.6	Evaluate Implications Findings from the Model Yakutat Wave Energy Project for Feasibility Studies in Other Coastal Regions of Alaska, Including Extensions onto the OCS.	81
1.7	References.....	86
•	Appendix B.....	198

2. List of Tables

1.	List of Figures	3
2.	List of Tables.....	5
3.	List of Abbreviations and Acronyms	7
1.1	Summary	1
1.2	Marine Mammals and Acoustic Monitoring.....	1
1.2.1	Introduction	1
1.2.2	Methods	4
1.2.2.1	PAM Data Rescue	4
1.2.2.2	Collection of New PAM Data Through Mooring Deployments.....	5
1.2.2.2.1	2018 – 2019 PAM Equipment, Settings, and Deployments	4
1.2.2.2.2	2018 – 2019 Data Analysis	4
1.2.3	Results	7
1.2.3.1	2014 – 2015 PAM data	7
1.2.3.2	2018 – 2019 PAM Data.....	7
1.2.3.2.1	Cetacean Seasonal Occurrence	7
1.2.3.2.2	2018 – 2019 Study Area Soundscape	12
1.2.3.3	Sounds Produced by Wave Energy Converters	15
1.2.3.3.1	WEC Literature Reviewed.....	16
1.2.3.4	Entanglement rates of marine mammals in the general vicinity of Yakutat.....	18
1.2.4	Conclusions.....	19
1.3	Monitoring Fish and Information to Support an Essential Fish Habitat (EFH) Review.....	19
1.3.1	Introduction	19
1.3.2	Methods	21
1.3.2.1	Surface and bottom trawl sampling	21
1.1.1.1	Angling	28
1.3.2.2	Comprehensive species presence.....	24
1.3.3	Results	24
1.3.3.1	Surface and bottom trawl sampling	24
1.3.3.2	Angling	25
1.3.3.3	Species Presence	25
1.3.3.4	Archived Samples	26
1.3.4	Discussion.....	26
1.3.5	Conclusion	28
1.4	Information to Support an Archeological Review.....	38

1.4.1	Summary	38
1.4.2	Methods	38
1.4.3	Analysis.....	39
1.4.4	Results	39
1.4.5	Discussion and Conclusions	42
1.5	Evaluation of Oceanography and Sedimentation Effects of Wave Energy Converters.	42
1.5.1	Summary	42
1.5.2	Methods	43
1.5.2.1	Hydrography During the Trawl Survey.....	43
1.5.2.2	June 2018 Multibeam Bathymetry, Topographic Elevation and Hydrographic Surveys	47
1.5.2.3	Oceanographic Moorings.....	58
1.5.3	Results	59
1.5.3.1	Vessel-Based Hydrography	59
1.5.3.2	Topobathymetry	64
1.5.3.3	Moorings	66
1.5.4	Discussion.....	78
1.5.5	Summary and Conclusion.....	81
1.6	Evaluate Implications Findings from the Model Yakutat Wave Energy Project for Feasibility Studies in Other Coastal Regions of Alaska, Including Extensions onto the OCS.	81
1.7	References.....	86
•	Appendix B.....	198

3. List of Abbreviations and Acronyms

ADCP	Acoustic Doppler Current Profiler
BOEM	Bureau of Ocean Energy Management
AP&T	Alaska Power and Telephone
AVEC	Alaska Village Electric Cooperative
CPOD	Echolocation Logger
CPUE	Catch Per Unit Effort
CSE	Council of Science Editors
CTD	Conductivity/Temperature/Depth
dB	Decibel
DGGS	Alaska Division of Geological and Geophysical Survey
DEM	Digital Elevation Model
DSM	Digital Surface Model
DTM	Digital Terrain Model
DOI	Department of Interior
DPM	Detection Positive Minutes
EAR	Ecological Acoustic Recorder
EFH	Essential Fish Habitat
ESP	Environmental Studies Program
ESPIS	Environmental Studies Information Program
GNSS	Global Navigation Satellite System
GPS	Global Positioning System
LISST	Laser In Situ Sediment Size and Transmissivity
NMML	National Marine Mammal Laboratory
NMFS	National Marine Fisheries Service
OBS	Optical Backscatter Sensor
OCS	Outer Continental Shelf

OSU Oregon State University
OPUS Online Positioning User Service
PAM Passive Acoustic Monitoring
PPK Post Processed Kinematic
RME Resolute Marine Energy
RTK Real Time Kinematic
RMS Root Mean Squared
SPL Sound Pressure Level
TSS Total Suspended Solids
UA University of Alaska
UAF University of Alaska Fairbanks

1.1 Summary

Fisheries monitoring, hydrographic information, and passive acoustic monitoring (PAM) were undertaken in order to help assess the potential for environmental impacts resulting from any future deployments of wave energy converters offshore of the community of Yakutat, Alaska. Yakutat is a community along the northeast coast of the Gulf of Alaska that has been identified as a locale for the utilization of renewable, wave-based electricity generation in order to lessen their reliance on diesel fuel for electricity generation (Previsic and Bedard, 2009). Bottom-mount moorings instrumented with Acoustic Doppler Current Profilers, Conductivity/Temperature/Pressure loggers and turbidity sensors as well as hydrophone packages for ambient noise were deployed at three depths designated shallow (15 m), mid and deep (25 m and 40 m) over 15 months from late June 2018 to mid-September 2019. New topobathymetric, fisheries, hydrographic and PAM data sets were gathered from the region that can serve as a baseline upon which to assess impacts to protected species and/or essential fish habitat of any future marine energy projects in the region. One notable gap that remains is a lack of understanding of the connections between marine mammal, fish and water mass distributions at this site. Further study is required to develop a more comprehensive understanding of how these factors are interrelated. Current regulatory processes, timelines and lessons-learned from the permitting of other marine energy projects, including one in Alaska, are summarized as well. As noted elsewhere in the report, there is also a lack of studies on the potential for fish injuries by WECs. Overall, this and other related work (e.g. Tschetter et al., 2016; Chamberlain, 2021) provide a wealth of information for future wave and tidal energy projects in Yakutat or other Alaska coastal communities.

1.2 Marine Mammals and Acoustic Monitoring

1.2.1 Introduction

Yakutat, Alaska, is on the outer coast of the Northern Gulf of Alaska stretching from Cape Spencer to Cape Suckling. This region hosts numerous marine mammals, though there is relatively little quantitative information about their seasonal abundance and significance to the ecosystem. There are few baseline data on the occurrence of marine mammals that occur in the Yakutat region with the exception of information on pinnipeds, for which a robust research program led by the National Marine Fisheries Service's (NMFS) National Marine Mammal Laboratory (NMML) in Seattle, has been on-going (Jansen et al., 2018). This research includes aerial surveys for Steller sea lions (*Eumatopias jubatus*) and sea otters (*Enhydra lutra*) and aerial, shipboard and tagging studies of harbor seals (*Phoca vitulina*).

Only two broad-scale surveys focused on cetaceans (**Error! Reference source not found.**) have been carried out in this region, in 1993 and 1997 (NMML unpublished data), and only during June and July over the course of 1-3 days. These limited data show that multiple cetacean species occur offshore here: fin (*Balaenoptera physalus*), humpback (*Megaptera novaeangliae*), gray (*Eschrichtius robustus*), minke (*B. acutorostrata*), sperm (*Physeter macrocephalus*), killer whales (*Orcinus orca*), harbor (*Phocoena phocoena*) and Dall's (*Phocoenoides dalli*) porpoises in addition to a resident subpopulation of beluga whales (*Delphinapterus leucas*) that inhabits the northern area of Yakutat Bay (Laidre et al., 2000; O'Corry-Crowe, 2006; Lucey et al., 2015; Castellote et al., 2015). Additionally, opportunistic data include a sighting of four North Pacific right whales (*Eubalaena japonica*) in 1979, which is one of very few sightings of this endangered species outside of the Bering Sea (Shelden et al., 2005). A short-term project in Monti Bay in 2016 detected sea otters, harbor porpoise and a single sea lion (Bacon et al., 2016). In addition to these other studies, the City and Borough of Yakutat deployed several passive acoustic sensors including 2 echolocation loggers (C-PODs v0) and 2 EARs between 2014 and 2015 in

conjunction with the wave resource assessment work described by Tschetter et al., 2016. Rescue and analysis of these earlier data are described further in Section 1.2.2.1.

Though species occurrence has been measured only during a narrow window, these surveys suggest a high diversity of marine mammals near the proposed Wave Energy Converter (WEC) project site off the coast of Yakutat, Alaska. These surveys suggest that the proposed location of the WEC does not directly overlap harbor seal or sea lion haul outs, sea otter areas, or cetacean hot spots, though the general area is likely to be used as a transit corridor and could thus have seasonally high densities of some species. Some of the highest numbers of harbor seal in Alaska occur in the surrounding areas of Disenchantment Bay, the Alsek River mouth, and Icy Bay. Studies of harbor seal in Disenchantment Bay suggest that the population using floating ice is not static: large numbers of animals seemingly migrate in and out of the bay in response to environmental factors such as prey (Jansen et al. 2006; Jansen et al. 2010). It is likely that seals using Disenchantment Bay periodically respond to and capitalize on nearby prey resources, such as eulachon runs in the nearby Situk, Dangerous, Akwe, and Alsek Rivers (where feeding aggregations have been observed; Jansen et al., 2006). If this is the case, they would likely use the area along the coast and near the project site when embarking on foraging trips from their glacial haul outs to the river mouths. Seals would also be expected to transit near the project site when targeting offshore feeding areas.

Stellar sea lions occur in higher densities only at the mouth of the Alsek River. Sea lions are also known to travel long distances to target prey and so may also use the outer coast along the Yakutat Forelands and near the proposed WEC site for transiting. Sea otters, in contrast, are not expected to use the outer coastal areas in high numbers given their restricted range within the bay, their non-migratory nature, and their low abundance on the outer coast.

Cetacean species observed in the project area are migratory and cross the Gulf of Alaska twice annually on their migration to northern feeding grounds in spring and southern breeding grounds in fall (Perrin et al. 2008). Highly migratory, coastal species such as humpback and gray whales are the most likely to transit near or even within the project area. Other coastal species with high probability of being present in the WEC area are killer whales, harbor porpoises, and belugas. Killer whales have been tagged with satellite transmitters in 2010 and have been tracked passing by the WEC area and entering Yakutat Bay (Hanson et al., 2012). Harbor porpoises are commonly seen in shallow waters both inside and outside Yakutat Bay (Hobbs and Waite, 2010). Opportunistic beluga sightings have been reported around Khantaak Island, near Ocean Cape in Yakutat Bay, indicating that they could access the WEC site (Lucey et al., 2015).

The data available regarding the presence of marine mammals in the area of the proposed WEC suggests that there is a high potential for close-range interactions. Up to 12 different species of marine mammals have been observed in the area, including several with strong coastal habits (e.g. harbor seal, Stellar sea lion, humpback whale, gray whale, killer whale, beluga whale and harbor porpoise). The available data is limited to opportunistic sightings and summer aerial surveys, therefore there is no information regarding seasonal trends in abundance or distribution of these species. In order to properly document any potential displacement effect due to the presence of the WEC in the proposed site it is important to identify the natural variability in marine mammal presence for that particular area. The only way to characterize marine mammal seasonality and its variability is to continuously monitor their presence for multiple years, a condition that is hardly met anywhere for such a difficult animal group to study.

Passive acoustic methods are currently the most cost-effective way to monitor the occurrence of cetaceans over broad temporal scale (Mellinger and Barlow, 2003). The distribution and seasonal occurrence of most cetacean species are poorly understood. This deficit is due to several factors, including the difficulty of detecting them by sight, the high cost of operating survey ships or aerial surveys in remote habitats,

and, for most species, their far-ranging seasonal movements. Inferences drawn from these techniques are limited by weather, daylight, short sampling periods, and animal surfacing behavior. While passive acoustic techniques are also limited by behavior – in that they sample only calling or echolocating animals – they can be used 24 hours a day year-round and are generally independent of weather conditions. These methods have been very successfully applied in different regions of Alaska (e.g., Stafford, 2003, Moore et al., 2006, Stafford et al., 2010). Continuous, multi-year acoustic data can provide information on the presence over the year of cetacean species within several kilometers of the acoustic mooring (e.g., Stafford et al., 2007). The acoustic repertoires of most cetacean species known to occur near Yakutat are distinct enough from one another to be identified, therefore passive acoustics methods at the WEC site would provide cetacean seasonality as well as the species composition.

Passive acoustics data can also be used to isolate and analyze the sound of any WEC operating under different wave regimes. But it is expected that the background noise at the WEC site will mask any noise generated by the operating WEC devices, based on the high natural noise level from the nearby active wave beach front. However, onsite acoustic recordings before and after the installation of the WEC array are needed to confirm this hypothesis. By collecting and analyzing an acoustic dataset, the potential for noise impact on marine mammals and fish and the overall potential risk from the presence of the WEC in Yakutat can be estimated. Furthermore, this unique long time-series of acoustic data can better inform the limited worldwide set of noise-characterized wave devices. Because marine mammal seasonal presence is variable from year to year, monitoring the proposed WEC site requires identifying natural variations in seasonal presence.

Therefore, the primary objective of the marine mammal portion of this study was to provide a better understanding of the biotic and abiotic underwater acoustic environment near and adjacent to the area proposed for a wave energy converter. To accomplish this objective, we: 1) Rescued and evaluated rescued PAM data collected in the region between November 2014 to April 2015 ; 2) Instrumented bottom lander moorings with hydrophone packages to determine the seasonal presence of vocal marine mammals; 3) Described the abiotic seasonal soundscape of the study area; 4) Undertook a literature review of references that provide information on the sounds produce by WECs; 5) Evaluated information

on entanglement rates for marine mammals in the region to provide insight into the potential for interactions of marine mammals and WEC.

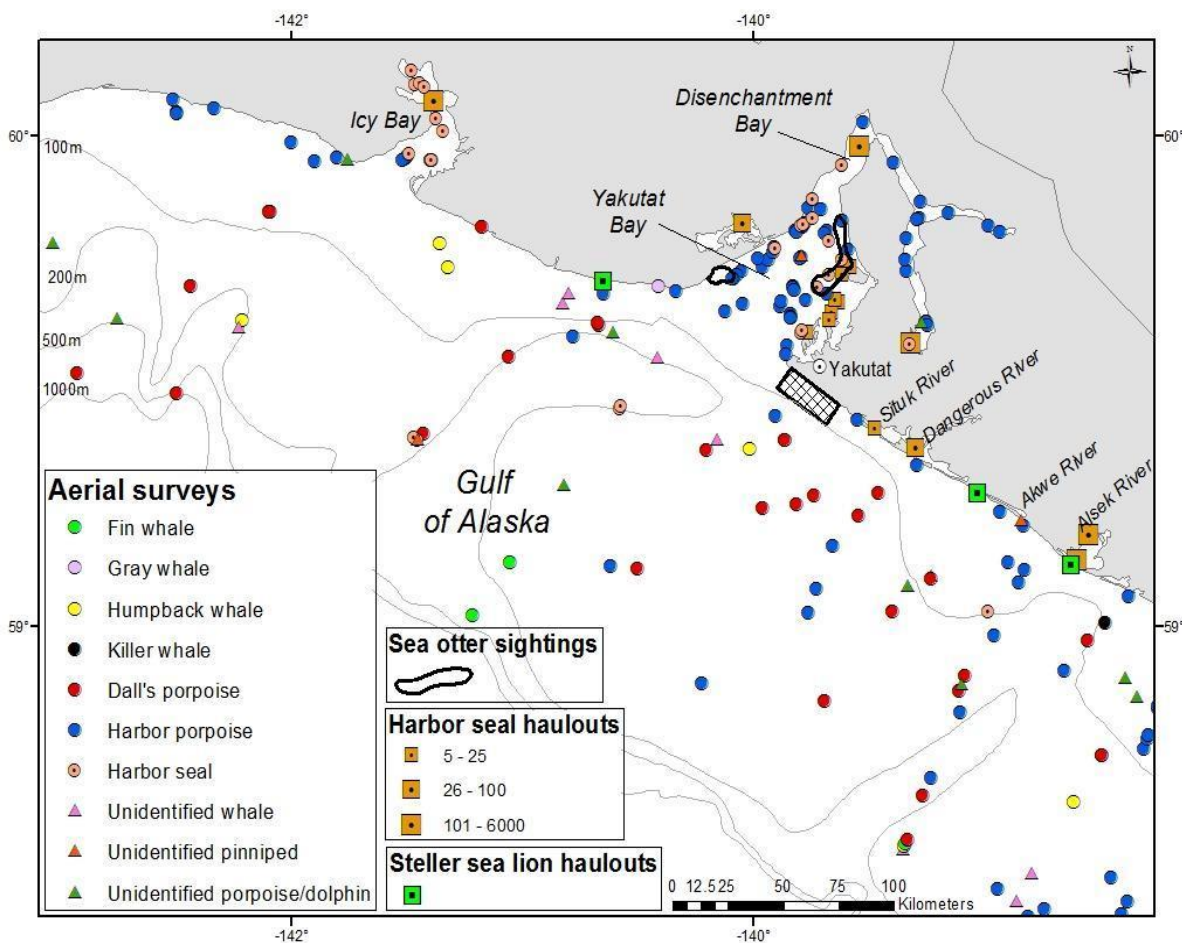


Figure 1. Map of marine mammal sightings from National Marine Mammal Laboratory surveys in the northern Gulf of Alaska showing species seen in the Yakutat area. The small gridded area indicates the study area for the current study.

1.2.2 Methods

1.2.2.1 PAM Data Rescue

In an attempt to retrieve acoustic data collected as part of a previous study, the City and Borough of Yakutat was contacted to find instruments that were deployed between November 2014 and April 2015. Two C-PODs v0 and 2 EARs were located by UAF in a City and Borough of Yakutat’s storage facility and were shipped to the NMML in Seattle in November of 2017. Both C-PODs had leaked in their last deployment destroying the internal electronics (Figure 2). There were no memory cards in either

instrument, nor was there any indication of where they might be stored, however seeing the conditions of the electronics it is likely that the C-POD data were lost.



Figure 2. Images of the two C-PODs.

Images show the housing rusty interior of the two C-PODs found in storage at the City and Borough of Yakutat building in November 2017. Rust was likely caused by a leak during deployment.

The two EARs were in good condition, and data from their hard drives were extracted and data downloaded. The data log indicated both EARs were programmed on a duty cycle of 45 seconds on every 5 minutes in stand-by. The instruments sampled at a rate of 25 kHz. One EAR started on 29 May 2014 and stopped recording on 2 November 2014. The second EAR contained only a few files corresponding to 29 and 30 May 2014 suggesting the instrument stopped recording before it was deployed. Inspection of the data from the EAR that recorded suggests this was deployed on 3 June and recovered on 23 October 2014. Based on emails and documentation found from the 2014-2015 effort, we think this EAR was deployed together with an acoustic Doppler current profiler (ADCP) and a Seabird SBE37 Conductivity/Temperature/Depth (CTD) sensor at the PAMN location (Tschetter et al., 2016), the same location as the DM site in this study (59.472°N, 139.732°W). There was also apparently a prior deployment of one mooring from December 2013 to May 2014. Data from that period were never found.

1.2.2.2 Collection of New PAM Data Through Mooring Deployments

Three oceanographic “bottom-lander” moorings were deployed between June 26-28, 2018. The three moorings, named shallow, mid, and deep based on their deployment depths of 15 meters, 25 meters, and 40 meters and designated SM, MM and DM, respectively. These moorings were deployed twice; the first deployment in June 2018 and the second in October 2018. All of the sensors were attached with brackets to a Teledyne Ocean Science “sea spider” fiberglass mooring frame; the frame consists of three legs mounted together with three stainless steel brackets and eyebolts attached to the center of the frame. 50-pound lead weights are attached to the bottom of each leg of the sea spider frames. The bottom landers at 25 m (MM) and 40 m depth (DM) were each instrumented with an echolocation logger (C-POD, Chelonia Ltd., UK) and a sound recorder (ST-500STD, Ocean Instruments, NZ). The echolocation logger covered the frequency range of 20 kHz to 160 kHz and recorded the presence of click trains in this frequency band and the recorder covered the range 10 Hz-24 kHz and collected data on a duty cycle of 10 minutes every 30 minutes (20 minutes total per hour). This approach allowed us to cover the full bandwidth of acoustic signals from all cetaceans (10 Hz to 160 kHz).



Figure 3. The shallow mooring, SM.

The shallow mooring was equipped with a Nortek Vector 300 meter ADV, a Teledyne RD Instruments Sentinel V20 acoustic Doppler current profiler (ADCP) with external battery case, two Sea-Bird Electronics (SBE) ECO-NTU SB Turbidity sensors, a SBE 37-SM MicroCAT CTD sensor, and a Teledyne Benthos R500 acoustic release (Figure 3, Table 1).

Table 1).



Figure 4. The mid mooring, MM.

The mid mooring was equipped with a Nortek Vector 300 meter ADV, two Sea-Bird Electronics ECO-NTU SB Turbidity sensors, a SBE 37-SM MicroCAT CTD, an echolocation logger (C-POD), a long-term acoustic recorder, the ST-500STD (Sound Trap, Ocean Instruments) and a Teledyne Benthos R500 acoustic release (Figure 4, Table 1).

Table 1).



Figure 5. The deep mooring, DM.

The deep mooring was equipped with a Nortek Vector 300 meter ADV with a Campbell Scientific OBS 3+ Turbidity sensor, a Teledyne RD Instruments Sentinel V50 ADCP with external battery case, an RBR concerto³ Tu CTD, a C-POD, a ST-500STD and a Teledyne Benthos R500 acoustic release (Figure 5, Table 1).

Table 1). The moorings were first deployed on June 28th and 29th of 2018 (Table 1).

Table 1. Instrument serial numbers and deployment and recovery times for each of the moorings.

Mooring	Latitude (°N)	Longitude (°E)	Deployment Time (UTC)	Recovery Time (UTC)	ADV SN	Turbidity SNs	CTD (Model and SN)	ADCP	Depth (m)
SM	59.472167	-139.729933	06/28/2018 21:47:19 UTC	10/07/2018 23:15:00 UTC	14520	SBE ECONTU 751 & 752	SBE 37- 16854	153	14.6
MM	59.474336	-139.746501	06/29/2018 20:13:51 UTC	10/07/2018 23:47:00 UTC	11074	SBE ECONTU 753 & 754	SBE 37- 16855	NA	22.3
DM	59.465667	-139.739383	06/28/2018 22:18:05 UTC	10/08/2018 02:15:00 UTC	14521	OBS 3+ T9381, Seapoint Tu 15984	RBR 66113	177	39.6

Table 2. October mooring deployment and final recovery times.

Mooring	Latitude (°N)	Longitude (°E)	Deployment Time (UTC)	Recovery Time (UTC)	ADV SN	Turbidity Make and SNs	CTD Make and SN	ADCP	Depth (m)
SM	59.475000	-139.726667	10/10/2018 20:15:00	Not recovered	14520	SBE ECONTU 751 & 752	SBE 37- 16854	153	NA
MM	59.476167	-139.755833	10/10/2018 19:58:00	Not recovered	11074	SBE ECONTU 753 & 754	SBE 37- 16855	NA	NA
DM	59.465200	-139.747133	10/10/2018 17:21:00	09/27/2019 21:50:00 UTC	14521	OBS 3+ T9381, Seapoint Tu 15984	RBR 66113	177	NA

Mooring recovery occurred on October 7th, 2018. The moorings were out of the water for three days to recover the data off the instruments, replace batteries, and remove biofouling (Figure 6).



Figure 6. Shallow and mid mooring on October 7, 2018 post-recovery.

The moorings were redeployed on October 10, 2018. Deployment and redeployment locations are shown in Figure 7.



Figure 7. Mooring deployment locations.

The Situk River estuary is clearly visible in the southeast corner of the image.

In November of 2018, the acoustic release for the shallow mooring was recovered by a fisherman in Yakutat after he snagged it ~7 miles from the deployment location. A recovery effort for the Yakutat moorings was made in June of 2019. Researchers went out on the F/V Quest and used the Teledyne deck

box and transducer to attempt to communicate with the acoustic releases on the mid and deep mooring. No communication was established with the mid mooring. The deep mooring's acoustic release communicated back but the buoy did not surface. Researchers spent the next two days towing an EdgeTech 4125 Series Dual-frequency Side Scan Sonar System over the three mooring deployment locations. A metal grappling hook was also used to drag the ocean floor where the deep mooring was deployed in an attempt to snag the mooring. In total, researchers spent three days attempting to recover the three moorings. None of the moorings were recovered in June of 2019.

Another recovery attempt was made on 27 and 28 September 2019. Alaska Marine Response (AMR) were contracted and two divers traveled to Yakutat to aid in locating and retrieving the moorings. The Yakutat resident who snagged the shallow moorings acoustic release talked to researchers at the Yakutat harbor and identified the area where the release was snagged. The side scan sonar system was used again in a second attempt to locate the moorings, including the last known area of the shallow mooring. After an unsuccessful attempt to locate the shallow mooring, the boat made its way to the deep mooring deployment location where the acoustic release and buoy were on the surface. The deep mooring was recovered on 27 September 2019. The AMR divers dove twice on potential mid mooring locations, but the mid mooring was not located.

In the next section we discuss the PAM sensors, the ST-500STDs and the C-PODs. The Ocean Instruments Sound Trap ST-500STD instruments are small, lightweight and capable of sampling at high frequencies on duty cycles exceeding 6 months (<https://www.oceaninstruments.co.nz/product/soundtrap-st500-std/>). Each instrument is individually calibrated allowing for absolute sound levels to be calculated over time. C-PODs are click-detectors which have been developed and extensively tested to detect odontocetes (Castellote et al., 2015). The physical oceanographic sensors on the moorings are discussed further in Section 1.5.2.

1.2.2.2.1 2018 – 2019 PAM Equipment, Settings, and Deployments

As described above, initial the mooring recovery occurred in October 2018, and all three moorings were recovered at this time. However, the ST-500STD from the MM mooring leaked and data were lost. Both C-PODs sampled the entire deployment period at both the DM and MM moorings. Instruments were serviced (the leaked ST-500STD was replaced) and redeployed in October 2018. The DM mooring was successfully recovered in October 2019, but the MM mooring was never found. The ST-500STD from the DM mooring recorded from October 2018 to August 2019. The C-POD from the DM mooring had data from October 2018 until 24 April 2019, when the batteries ran out.

The ST-500STD was programmed for the June-October 2018 deployment with a duty cycle of 10 minutes on every 30 minutes at a sampling rate of 48 kHz. These settings were optimized for maximum usage of memory and power. However, this duty cycle resulted in an overlap with the ADCP sampling period that was active for 17 minutes at the start of each hour. For the overwinter deployment (October 2018 to June 2019) the duty cycle was modified to 30 minutes starting at minute 25 of each hour to avoid any overlap with the ADCP sampling. Also, because the 2018 deployment showed less memory usage than anticipated (sound files are compressed, and compression rate depends on noise conditions of each site) the sampling rate was increased to 96 kHz to maximize memory and power usage for the overwinter deployment.

1.2.2.2.2 2018 – 2019 Data Analysis

C-POD data were analyzed using C-POD.exe version 2.043, using the default settings; that is, “Hi and Mod train quality,” “all cetacean species,” unmodified “train values,” and “click filters.” Default settings only exclude doubtful and low quality click trains, which could include false detections, particularly in noisy conditions. We manually validated all the “Hi” and “Mod” click train detections by plotting the

peak click frequency in the POD.exe analysis window with a time resolution of 100 ms (screen pixel width matching 100 ms in duration) which typically gives a screen window of 2 to 3 min in length (depending on the display size). Click train type classification (narrowband high frequency clicks, termed NBHF by CPOD.exe to refer to porpoise species, or other cetacean clicks) was also manually validated for each click train in the POD.exe analysis window based on considerable differences in peak frequency and click bandwidth among the echolocation clicks of killer whales, Pacific white-sided dolphins (*Lagenorhynchus obliquidens*), and harbor porpoises (Au et al., 2004; Simon et al., 2007). Our C-POD manual validation analysis permitted the exclusion of multiple false detections caused by noise, which were easily recognized by the broad frequency coverage and lack of coherence in temporal scale, peak frequency, and pulse bandwidth.

Table 3. PAMGuard whistle and moan detector parameter settings used to detect cetacean calls in the ST-500 STD data.

FFT parameters	FFT length = 4096 FFT hop = 2048 Window type = Hann Sample rate = 96 kHz Time resolution = 42.67 ms Frequency resolution = 23.44 Hz Time step size = 21.33 ms
Noise and thresholding	Median Filter length = 61 Average Subtraction = 0.02 Gaussian Kernel Smoothing = on Threshold = 7.0 dB
Detection connections	Minimum Hz = 50 Maximum Hz = 12000 Type = connect 8 (sides and diagonals) Minimum length = 5 time slices Minimum total size = 50 pixels Crossing and joining = Re-link across joins Max cross length = 5 time slices

ST-500STD data were analyzed using a semi-automated detector for social signals (i.e., moans, calls, and whistles), specifically the whistle and moan detector implemented in PAMGuard software version 2.00.14 beta ([https:// www.pamguard.org/](https://www.pamguard.org/)), following the configuration detailed in Table 3. Fin whale (*Balaneoptera physalus*) signals were detected using a spectrogram correlator in the program Ishmael (Mellinger, 2001).

The whistle and moan detector implemented in PAMGuard was set up with a relatively low classification threshold (whistle and moan detector v2.00.14 Beta, threshold = 8 dB, see Table 3) to reduce the risk of missing low amplitude cetacean signals at the expense of triggering false detections, due to wave action or anthropogenic noise. In order to detect fin whale signals, wave data were decimated to a sampling rate

of 2000 Hz, and analyzed using the spectrogram correlation detector in Ishmael (version 3.0.2) following the configuration detailed in Table 4. PAMGuard detection results were manually validated through visual and aural inspection of spectrograms in PAMGuard Viewer Mode, and Ishmael detections in Raven Pro (version 1.6) and labeled as either a true detection and species class, or false detection and its source when known (i.e., waves, seismic airguns).

Table 4. Ishmael spectrogram correlation detector parameter settings used to detect fin whale notes in the ST-500 STD data.

Spectrogram parameters	Frame size: 64 samples Zero padding: 1x Hop size: 1/8x Window type: Hamming Contour width: 1 Hz Start/End times: 0/1.8 s Start/end frequencies: 35/19 Hz
Detection options	Smoothing time constant: 0.6 s Detection threshold: 0.7 Min/Max duration: 0.1/3 s Detection neighborhood: 5 s

We estimated cetacean presence for each species on a minute-by-minute basis. Specifically, any minute in which moans, echolocation click trains, calls, or whistles were detected, by either data from the ST-500STD or C-POD, was categorized as a detection positive minute (DPM). As such, a DPM could include a single type of signal, or up to 3 types (echolocation, calls, and whistles in the case of killer whales), and could include signals at different rates (e.g., a single call or many calls). This DPM approach reduced behavioral effects when quantifying cetacean presence (e.g., avoided using number of signals as a metric of presence). Seasonal occurrence was described with daily DPM time series of each acoustically active species.

Noise analysis was computed using the Matlab tool “Acoustic Ecology Toolbox” developed by Cornell Lab's Center for Conservation Bioacoustics (Dugan et al., 2011). Data were processed to obtain fully calibrated spectral contents in 1-hour averages for the band 20 Hz to 24 kHz for the full deployment period. The hour before and after deployment/recovery of the moorings was excluded to avoid the contribution of the research vessel noise. Long-term spectrogram averages (LTSA) were computed to provide a visual representation of the full deployment period. Sound pressure level (SPL, dB rms re 1 μ Pa) for the band 20 Hz to 24 kHz, and spectral percentiles were calculated for the entire deployment period. Results were aggregated on a monthly basis to report monthly metrics.

In order to correlate broad-band noise levels (sound pressure level) with wave height and wind speed, a regression analysis was completed with wave height obtained from the ADCP data at the DM mooring, and wind speed. Wind data were downloaded from ECMWF ERA5 reanalysis dataset from the years 2009 - 2019. A subset of the data was used from 2018 - 2019 at the closest grid point to the study area at 59.5° N, 139.75° W.

1.2.3 Results

1.2.3.1 2014 – 2015 PAM data

These data were processed to obtain hourly sound pressure levels (SPL, dB_{rms} re 1 μ Pa) and to produce a long-term spectrogram average plot for an initial exploration of the data quality (Figure 8).

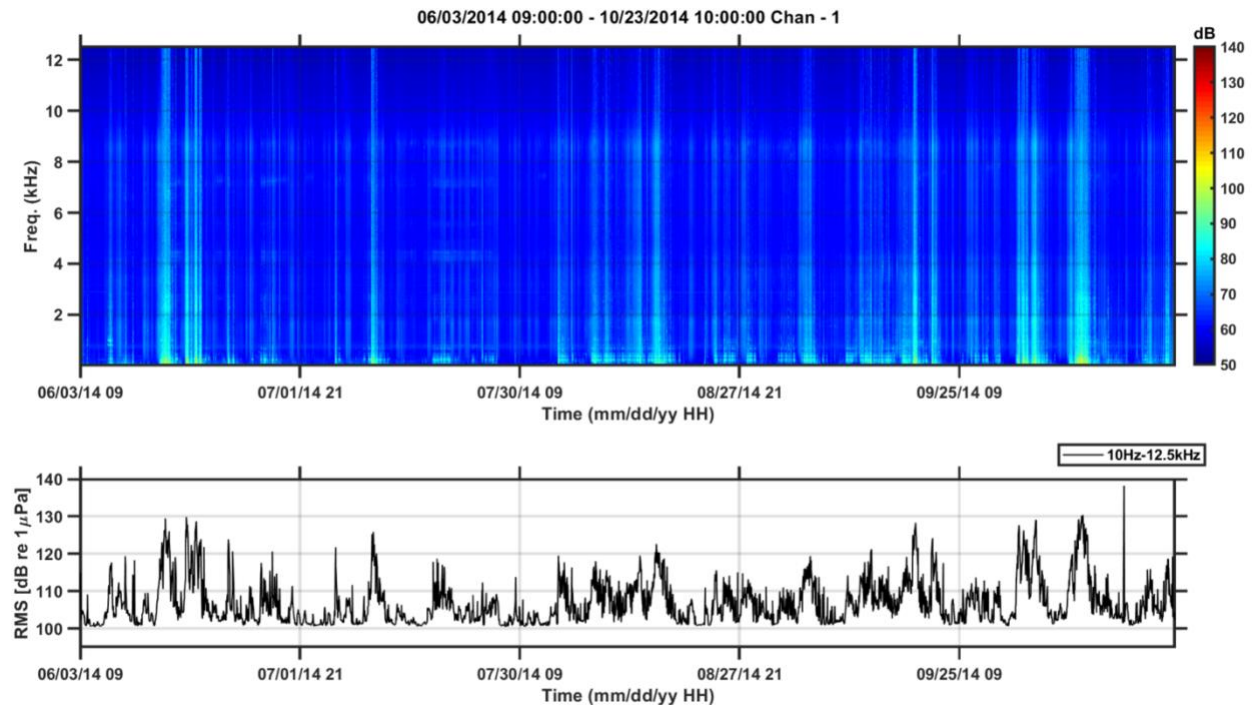


Figure 8. Data from the EAR.

Upper panel: Long-term spectrogram of EAR data from June 3rd to October 23rd 2014. Lower panel: SPL for the frequency range 10 Hz 12.5 kHz.

Data analysis showed no signs of obvious interference by other mooring instruments (i.e., ADCP) or self-noise caused by the mooring system. Closer inspection of periods of elevated noise levels confirm these are caused by breaking waves during stormy weather. The full band spectral content allowed an evaluation of the amount of flow noise generated by the cyclic wave movement in the deployment area, and it was concluded that a flow shield would be beneficial for the recorders in this project. SPL levels ranged from 100.5 dB to 138.2 dB re 1 μ Pa @ 1 m. In conclusion, only one usable dataset was obtained from the 2014 effort in Yakutat. The initial exploration of these data suggests there are periods of usable quality for noise description and marine mammal detection.

1.2.3.2 2018 – 2019 PAM Data

1.2.3.2.1 Cetacean Seasonal Occurrence

Five cetacean species were identified in the data. Humpback whales (Figure 9), fin whales (Figure 10), killer whales (Figure 11), Pacific white-sided dolphins (Figure 12), and harbor porpoises (Figure 13). Humpback whale detections included feeding calls, moans, and song notes. Fin whale detections including short sequences of 20 Hz notes, downsweeps and song sequences composed of both classic and backbeat note types. Killer whale detections included calls, buzzes and echolocation, Pacific white-sided

dolphin detections included whistles, and harbor porpoise detection were composed of 130-140 kHz clicks and buzzes.

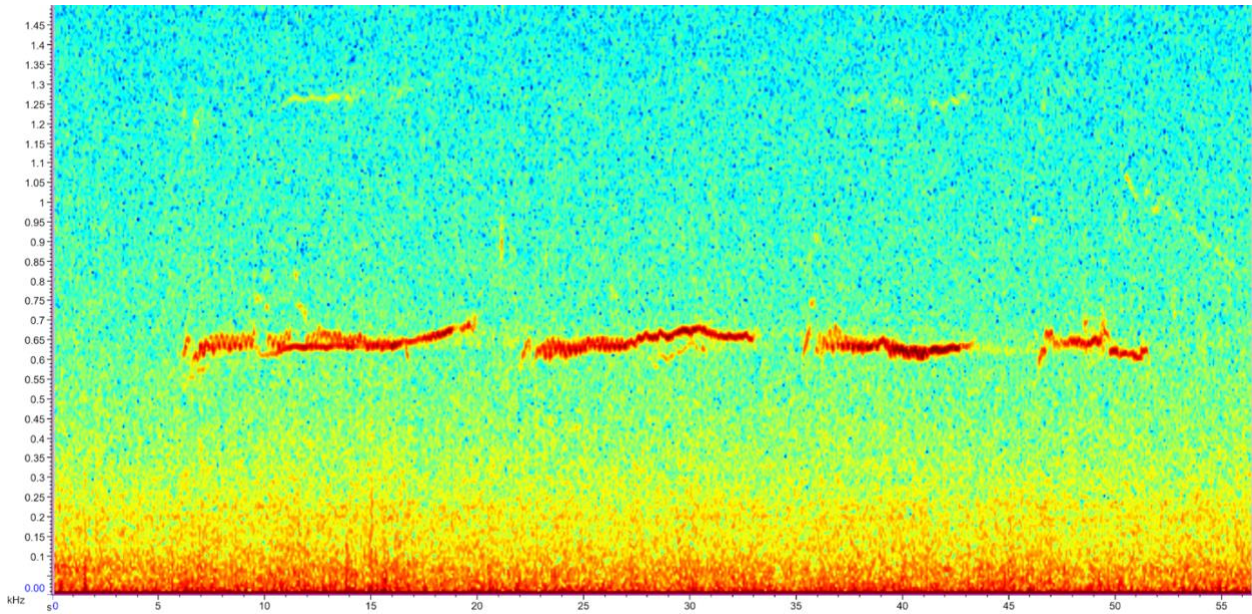


Figure 9. Spectrogram with humpback whale bubble net feeding calls recorded 19 June 2019. Frequency is shown on the y-axis from 0-1500 Hz and time on the x-axis from 0-55 s.

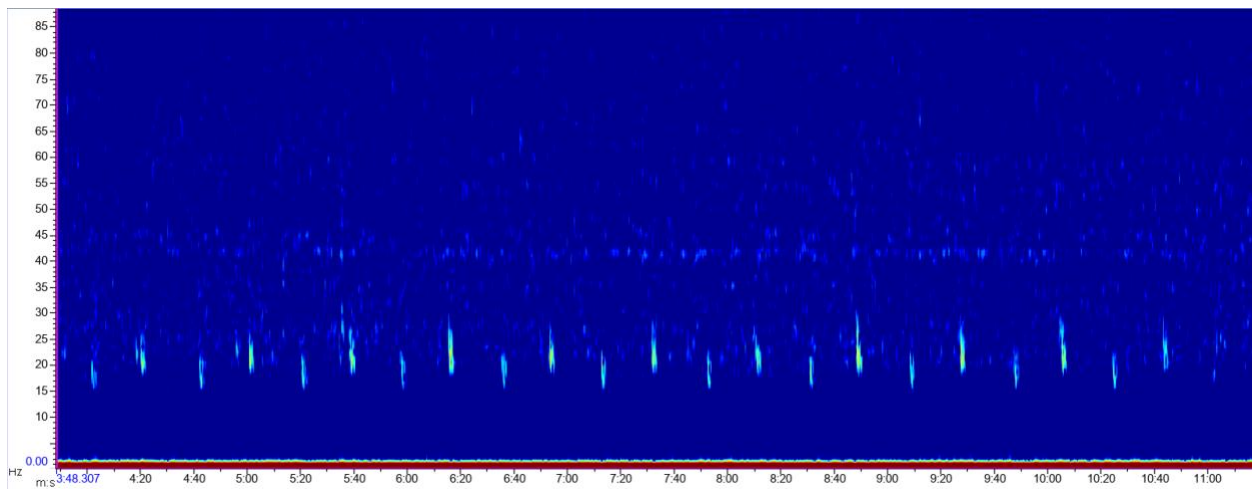


Figure 10. Spectrogram with fin whale song sequence composed of classic and backbeat notes recorded 24 December 2018. Frequency is shown on the y-axis from 0-90 Hz and time on the x-axis from 0:00-11:40 min.

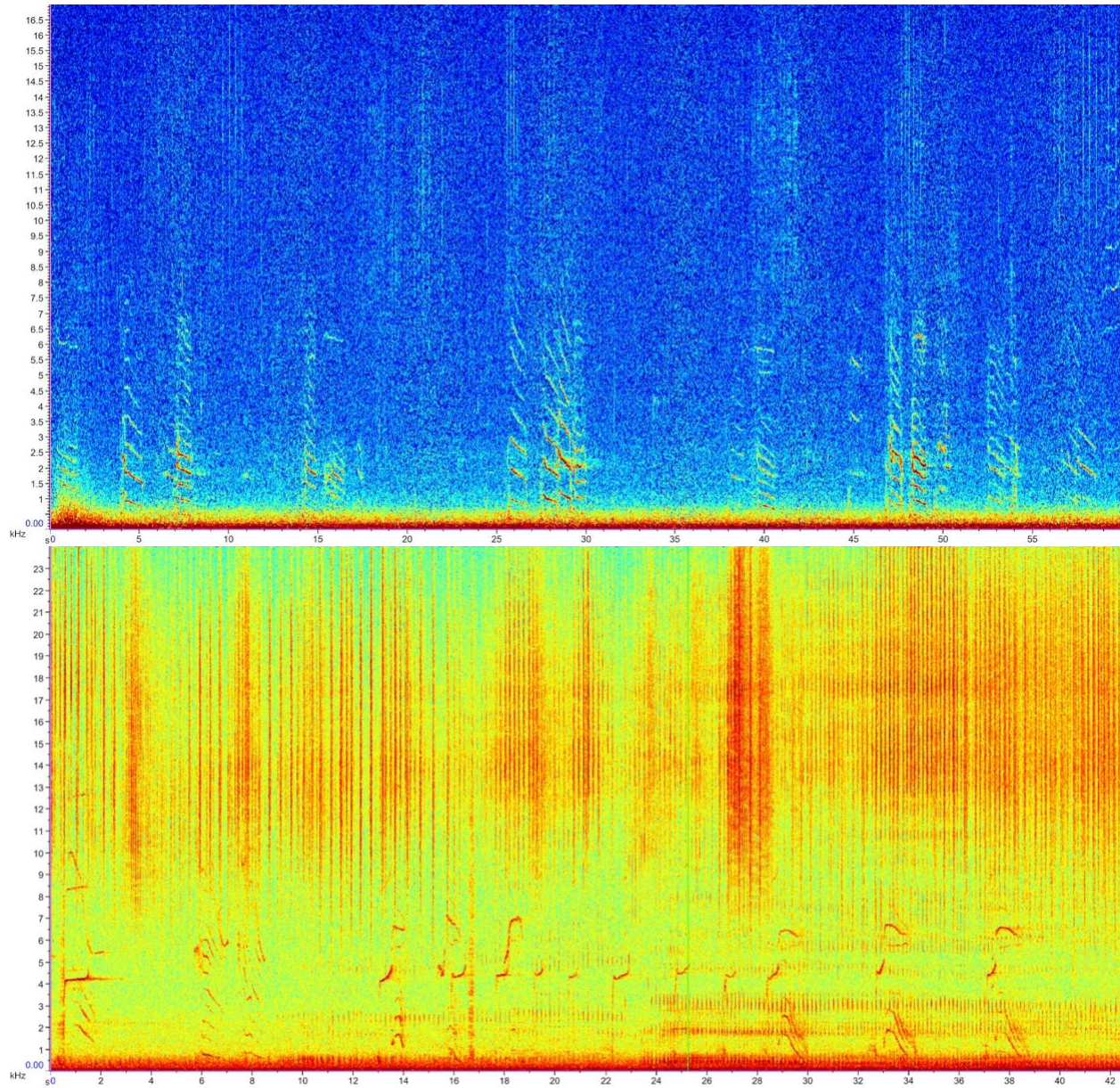


Figure 11. Spectrogram with killer whale detections. Upper panel shows a series of killer whale calls with no echolocation recorded on 9 August 2018. Frequency is shown on the y-axis from 0-24000 Hz and time on the x-axis from 0-60 s. Lower panel shows killer whale detections with calls and loud echolocation recorded on 6 July 2018. Frequency is shown on the y-axis from 0-24000 Hz and time on the x-axis from 0-42 s.

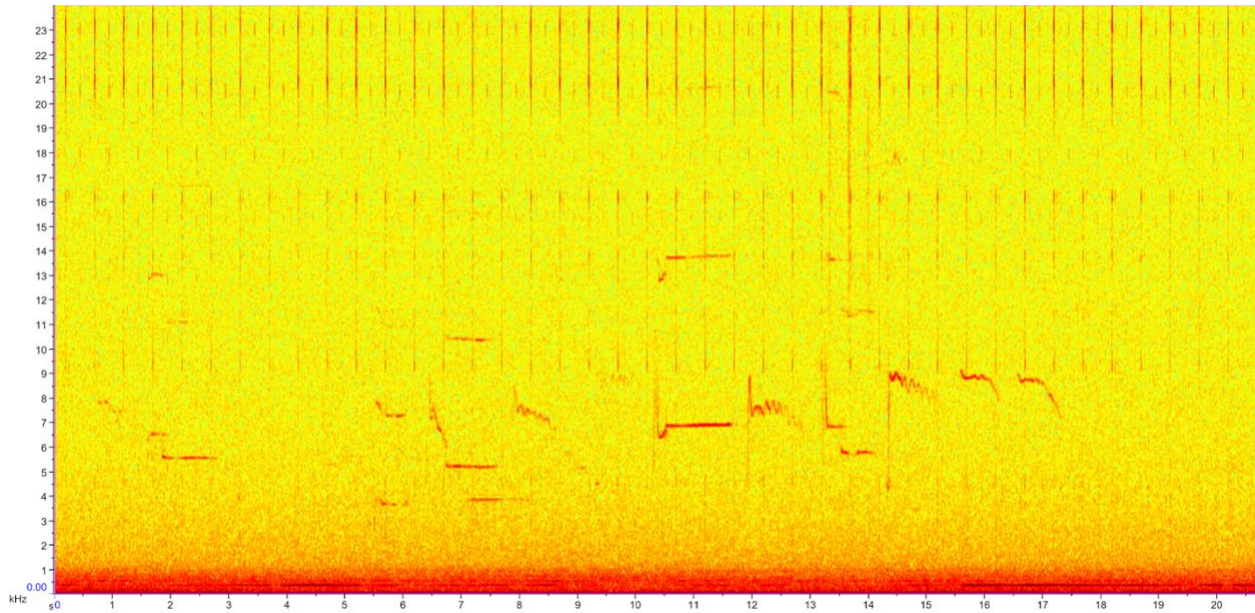


Figure 12. Spectrogram with Pacific white-sided dolphins on 13 June 2019. Note that the impulsive high frequency signals are the ADCP emission ticks, not marine mammals. Frequency is shown on the y-axis from 0-24000 Hz and time on the x-axis from 0-21 s.

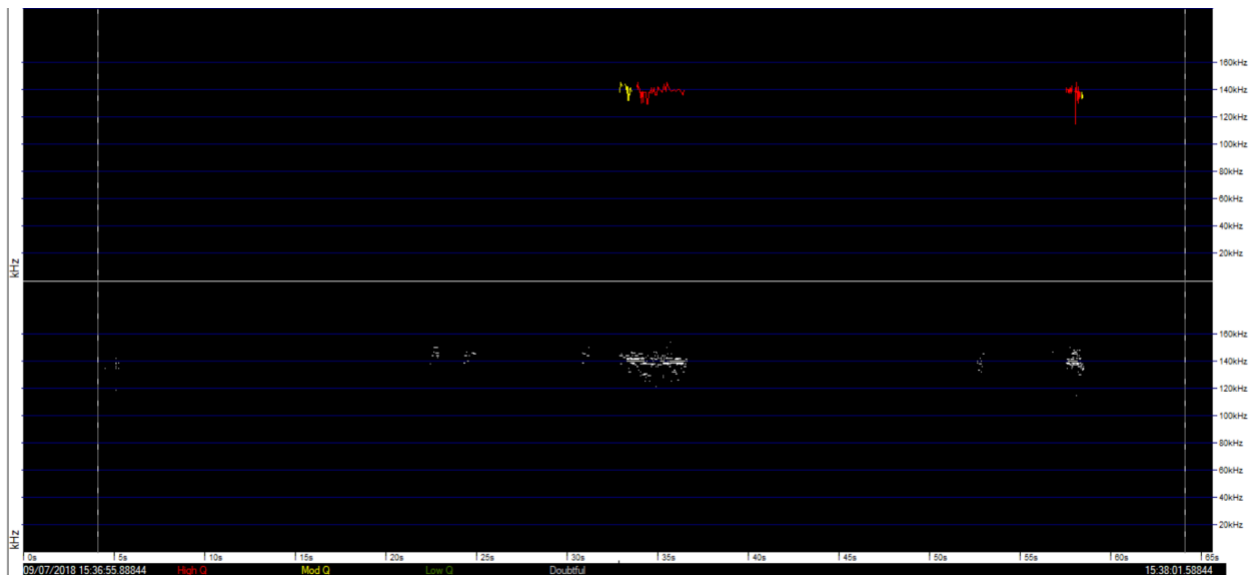


Figure 13. Clickogram (C-POD.exe screen) of harbor porpoise clicks (red lines) centered at 140 kHz detected on 9 July 2018.

Additionally, airgun pulses were detected for several days starting on 8 June 2019 (Figure 14). A geophysical experiment seismic survey was identified off Kodiak Island corresponding with the dates of the detected activity (8th to 23rd of June 2019), as well as the airgun interpulse interval of 155 s (atypical for commercial geophysical surveys). The source of these airgun signals was estimated to be ~1014 km away from the hydrophone location based on the location of the source vessel for the days and times detected, obtained in technical reports from this geophysical experiment (Barcheck et al., 2020; Moore et al., 2020).

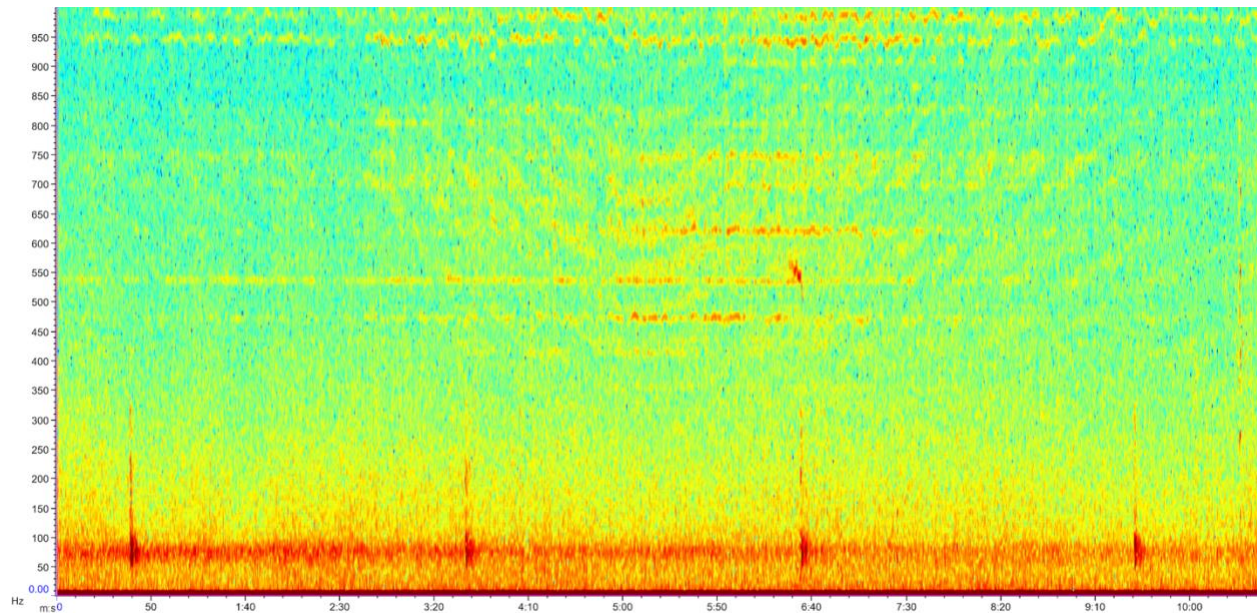


Figure 14. Spectrogram with four airgun pulses with an interval of 155 s.

Humpback whales were commonly heard throughout the year and the signals recorded included social calls, bubblenet feeding calls, and song (Figure 15A). We did not distinguish among the call types in Figure 15A as the purpose of this study is to determine when in the year these species occur. The presence of feeding calls suggests that schooling forage fish, such as herring, are common in the area. Fin whales were also surprisingly numerous with fin whale 20-Hz song detected primarily during winter and spring (Figure 15). Fin whales are a pelagic species, but we suspect the narrow shelf off Yakutat permits their signals to be detected on our mooring even if singing individuals might be off the shelf.

Killer whales were recorded surprisingly often (Figure 15C). We did not distinguish between the different ecotypes of killer whales but believe both fish-eating and mammal-eating killer whales were detected. Harbor porpoise were also detected year-round off Yakutat (Figure 15D). Interestingly, the occurrence of harbor porpoise and killer whales appear to have opposite patterns of occurrence. It is likely that mammal eating killer whales would target harbor porpoise. Finally, a very few detections of whistles of an unidentified odontocete, likely Pacific white-sided dolphins, were heard in the region but these were too few to plot. These signals were heard just a few times in July (4 DPM), August (10 DPM), November (1 DPM) and December (3 DPM) 2018 and January (6 DPM) and April (3 DPM) 2019.

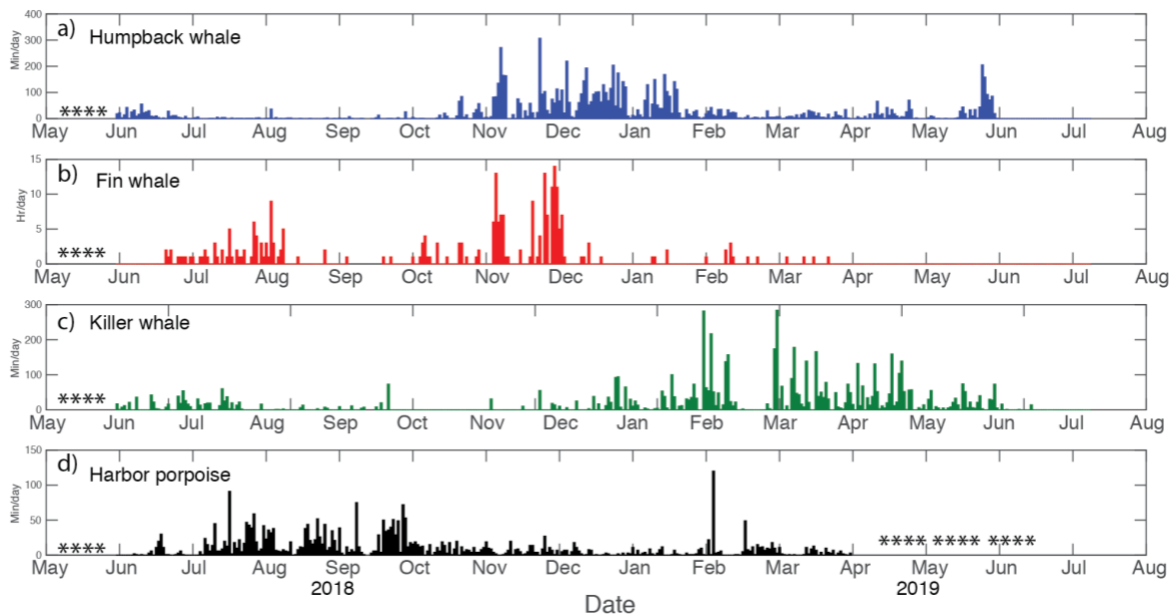


Figure 15. Detections of marine mammals from May 2018 to August 2019.

Panel A) Humpback whale detections in minutes per day from October 2018 to July 2019. These signals were automatically detected using a whistle and moan detector in Pamguard. B) Number of hours per day with fin whale detections from June 2018 - August 2018. These signals were detected with a spectrogram correlator in Ishmael. C) Killer whale detections in minutes per day from June 2018-August 2019. These signals were detected using a whistle and moan detector in Pamguard. D) Detections of harbor porpoise clicks in minutes per day. These data were collected with a CPOD and the detections derived from software provided by the manufacturer.

1.2.3.2.2 2018 – 2019 Study Area Soundscape

To establish the soundscape for the study area from June 2018 to March 2019, both sound pressure levels (SPL in dB re 1 μ Pa) and spectral content were computed. SPL averaged over 1-hour bins are presented in Figure 16, monthly average SPL and standard deviation is presented in Figure 17, the 50th percentile (median) monthly power spectral density (dB re 1 μ Pa²/Hz) is presented in Figure 18, and seasonal SPL results are presented in a box-whisker plot in Figure 19.

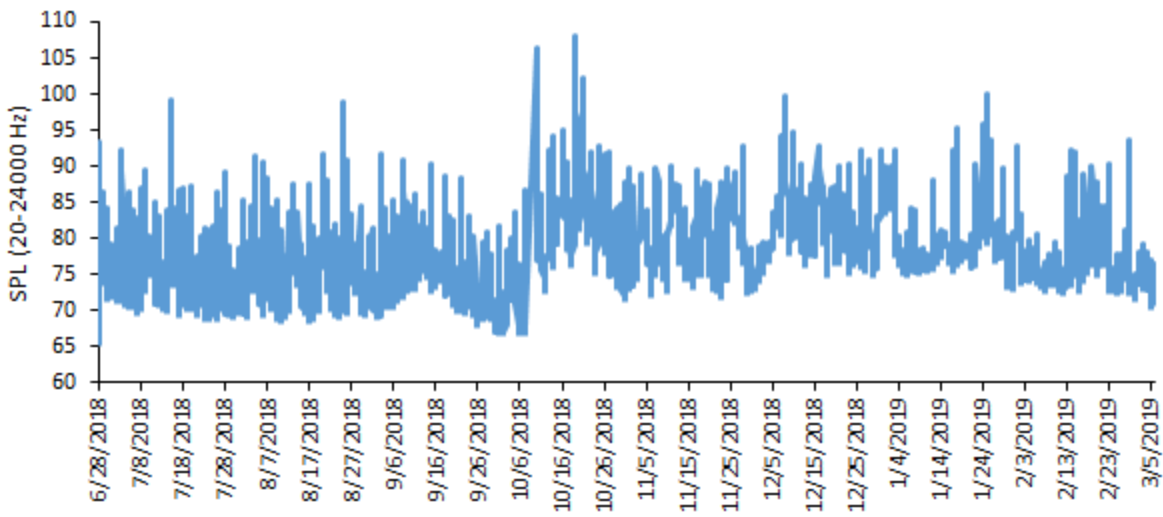


Figure 16. Sound pressure level (SPL) averaged over 1-hour bins for the frequency range 20 Hz to 24 kHz from 28 May 2018 to 5 March 2019.

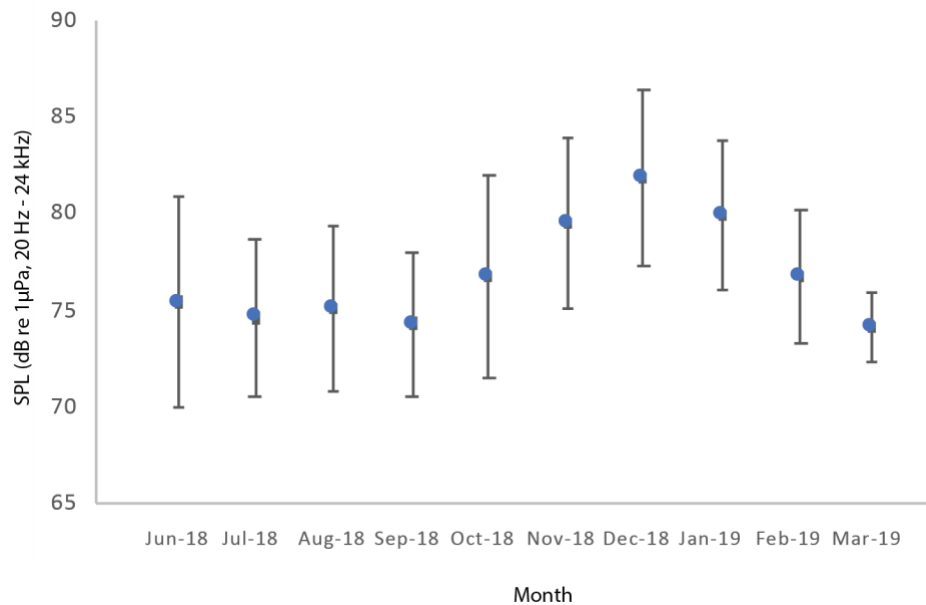


Figure 17. Sound pressure level (SPL dB re 1 μ Pa) and one standard deviation averaged over each full month for the frequency range 20 Hz to 24 kHz from 28 May 2018 to 5 March 2019 at the DM location.

The 50th percentile (median) monthly power spectral density (dB re 1 μ Pa²/Hz), presented in Figure 18, determines which frequency bands predominate by season. The period November to January shows higher SPL values, particularly below 100 Hz, likely due to an increase in wave activity.

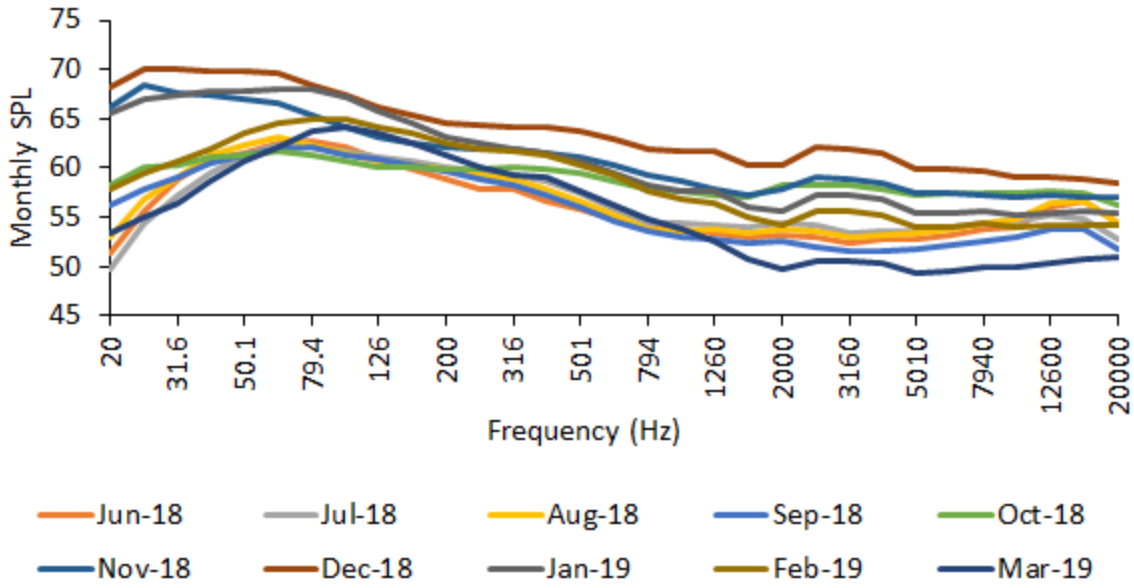


Figure 18. The 50th percentile (median) monthly power spectral density (dB re 1μPa²/Hz) for third-octave levels from June 2018 to March 2019.

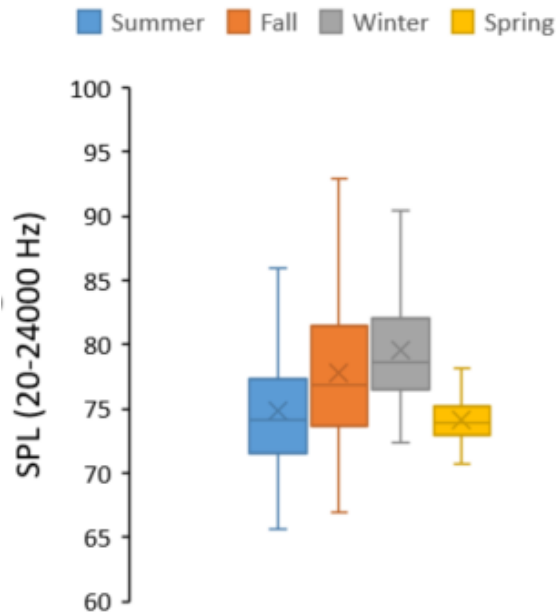


Figure 19. Seasonal SPL results in box-whiskers (whiskers = minimum/maximum, box = first/third quartile, line = median, cross = mean). Note Spring is truncated (ending on 6 March 2019) due to the instrument's clock drift and interference produced by the ADCP starting on 7 March 2019.

To determine the acoustic contribution of storms (wind and waves), we compared broadband acoustic SPL from the DM site with surface wave height and wind speed. Surface wave data were collected at the DM site with a Teledyne Sentinel V S50 ADCP. Time series of significant wave height (H_s), peak wave period (T_p) and water temperature were recorded in hourly bursts. The processing is described in detail in section 1.5.3.3. Wind data (m/s) were downloaded from ECMWF ERA5 reanalysis dataset from the years 2009 – 2019. Wind speed vectors were derived from the northing and easting vectors from the native data format. A subset of the data was used from 2018 – 2019 at the closest grid point to the study area 59.5°N

139.75 °W. Correlation analysis between the hourly SPL noise level and wave height and wind speed are presented in Figure 20.

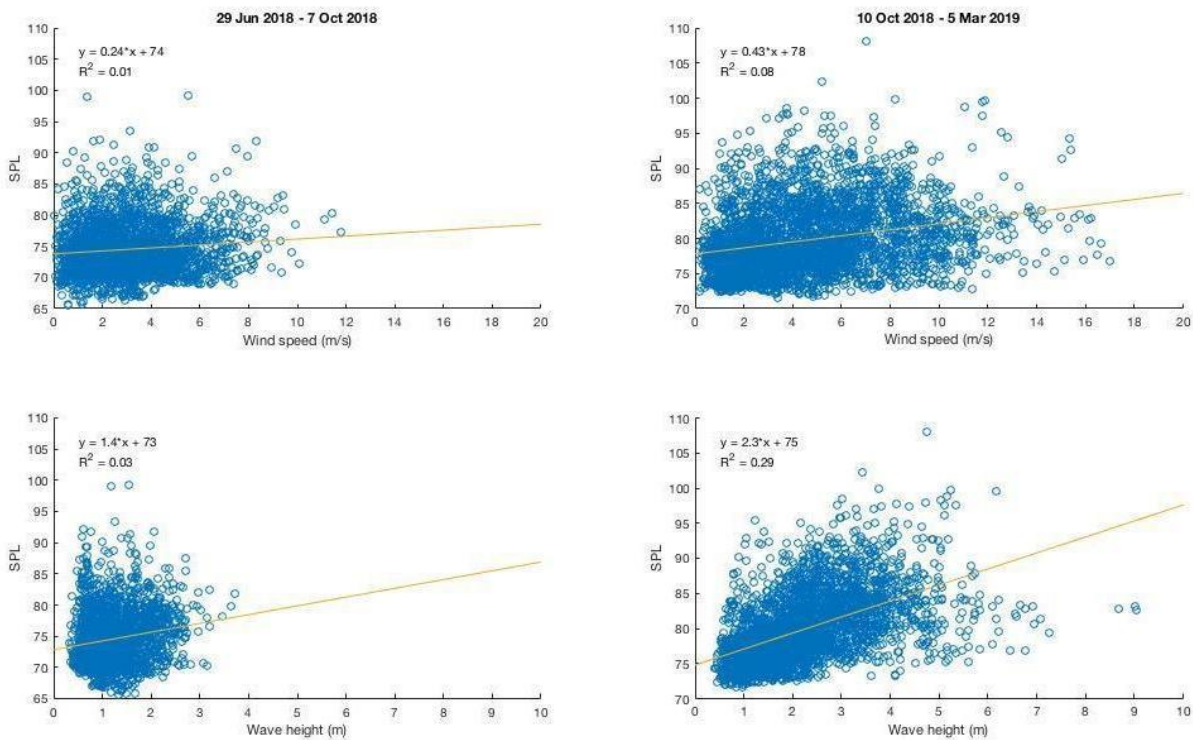


Figure 20. Correlation between wind speed and SPL (top panel) and wave height and SPL (bottom panel) for the first and second deployment periods.

Not surprisingly, there was a correlation between wind speed and SPL and wave height and SPL (wave height being highly related to wind speed) during the over-winter deployment. The first deployment, which went from the end of June until early October, was surprisingly calm for the Gulf of Alaska but surprisingly was louder on average than the overwinter period. The mean broadband SPL for the first deployment was 74.5 dB (std 4.2, range 65.6 - 99.2) and wind speeds ranged from 0.1 m/s to 11.8 m/s (mean 3.12 m/s std 1.83). During the second deployment, for 10 October 2018 - 5 March 2019 (the period for which we had reliable broadband noise levels) mean broadband SPL was 79.7 dB (std 4.9 dB, range 70.7 to 108.1) and wind speeds ranged from 0.1 m/s to 17 m/s (mean 4.6 m/s std 2.8).

1.2.3.3 Sounds Produced by Wave Energy Converters

Currently, our range of knowledge on WEC source levels and noise propagation is limited. This is partly due to the fact that noise measurements are challenging in wave environments, as well as the very diverse range of types of design of current WEC devices with different sources of noise emission. This makes extrapolation of noise production challenging and likely inaccurate. Multiple WEC devices per wave field are typical, thus noise needs to be measured from an ensemble of units to consider the additive effects. Most current knowledge is based on scaled-down and/or single units. In general, sound emission of WEC devices once operational, is expected to be low and comparable to that emitted by machinery on-board typical vessels (Tougaard, 2015). However, higher amplitude noise emissions would likely occur during the installation and decommission phases of a project due to an increase in machinery needed to complete the process, including in some cases pile driving operations. How the WEC converts waves to energy will

largely determine both the amplitude of the sound emissions, and the duration and frequency content. Potential noise emissions from WEC may include that produced by turbulence, self-noise from hydraulics, hinges, moorings, surface waves impacting the WEC, rotational machinery (turbine blades, gearboxes, shafts, etc.), etc. Whether these sources overlap in frequency and amplitude with the hearing or sound production of marine mammals is the overarching question with regards to permitting of WEC. However, based on numerous reviews, including the most recent by Polayge and Bassett (2020), it appears that in many cases, underwater noise emission by WEC is unlikely to affect marine mammal hearing (i.e., TTS or PTS), however for areas where background noise levels are not affected by anthropogenic activities, the average reported WEC noise emissions could easily exceed the background levels. For example, many of the WECs for which there are noise measurements produced source levels in the range of 126 to 129 dB re 1 μ Pa (Austin et al., 2009; Patricio and Soares, 2012; Garrett et al., 2013; Robinson et al., 2013; Polayge et al., 2014; Tougaard, 2015). In our study area, average monthly SPL ranged from 74 to 83 dB (Figure 17 **Figure** 16), a differential of 43 to 55 dB. Therefore, depending on the frequency spectrum distribution of the WEC emissions, these could have a significant masking effect to marine mammal communication.

In 2020, a fairly exhaustive report on known noise produced by wave energy devices was published as part of a broader “state of the science” of marine renewable energy devices (Polayge and Bassett, 2020). The Polayge and Bassett (2020) report should be considered the authoritative state of the science at the present time and we therefore did not ‘reinvent the wheel’ in our review. That document was a follow-on to Robinson et al. (2013). Below, we provide a list of extant WEC and a literature review of publications and reports from 2013-onward to avoid duplication from Robinson et al. (2013) review on this subject. We also added reports prior to 2013 not included in Robinson et al (2013).

1.2.3.3.1 WEC Literature Reviewed

Austin M, Chorney N, Ferguson J, Leary D, O’Neill C, Sneddon H. 2009. Assessment of Underwater Noise Generated by Wave Energy Devices. Tech Report prepared for Oregon Wave Energy Trust. 58 pp.

Boehlert GW, Gill AB. 2010. Environmental and Ecological Effects of Ocean Renewable Energy Development: A Current Synthesis. *Oceanography*. Vol. 23, No.2.

Denes SL, Zeddies DG, Weirathmueller MM. 2018. Turbine Foundation and Cable Installation at South Fork Wind Farm: Underwater Acoustic Modeling of Construction Noise. Document 01584, Version 4.0. Technical report by JASCO Applied Sciences for Jacobs Engineering Group Inc.

Lepper PA, Robinson SP. 2015. Measurement of Underwater Operational Noise Emitted by Wave and Tidal Stream Energy Devices. *Advances in Experimental Medicine and Biology*

Lusseau D, Christiansen F, Harwood J, Mendes S, Thompson PM, Smith K, Hastie G. 2012. Assessing the risks to marine mammal populations from renewable energy devices: an interim approach. Peterborough: Joint Nature Conservation Committee.

Madsen PT, Wahlberg M, Tougaard J, Lucke K, Tyack PL. 2006. Wind turbine underwater noise and marine mammals: Implications of current knowledge and data needs. *Mar Ecol Prog Ser*. 2006; 309:279–95.

Martin B, Whitt C, Horwich L. 2018. Acoustic Data Analysis of the OpenHydro Open-Centre Turbine at FORCE: Final Report. Document 01588, Version 3.0b. Technical report by JASCO Applied Sciences for Cape Sharp Tidal and FORCE.

Pine MK, Schmitt P, Culloch RM, Lieber L, Kregting LT. 2019. Providing ecological context to anthropogenic subsea noise: assessing listening space reductions of marine mammals from tidal energy devices. *Renew Sustain Energy Rev*. 103:49–57.

Polagye B, Copping A, Suryan R, Kramer S, Brown-Saracino J, Smith C. 2014. Instrumentation for Monitoring Around Marine Renewable Energy Converters: Workshop Final Report. PNNL-23110 Pacific Northwest National Laboratory, Seattle, Washington.

Polagye B, Bassett C. 2020. Risk to Marine Animals from Underwater Noise Generated by Marine Renewable Energy Devices. In A.E. Copping and L.G. Hemery (Eds.), OES-Environmental 2020 State of the Science Report: Environmental Effects of Marine Renewable Energy Development Around the World. Report for Ocean Energy Systems (OES). (pp. 67-85). DOI: 10.2172/1633082.

Pyć C, Zeddies D, Denes S, Weirathmueller M. 2018. Appendix III-M: REVISED DRAFT - Supplemental Information for the Assessment of Potential Acoustic and Non-acoustic Impact Producing Factors on Marine Fauna during Construction of the Vineyard Wind Project. Document 001639, Version 3.1. Technical report by JASCO Applied Sciences (USA) Inc. for Vineyard Wind.

Robinson SP, Lepper PA. 2013. Scoping Study: Review of Current Knowledge of Underwater Noise Emissions from Wave and Tidal Stream Energy Devices. Technical Report. The Crown Estate.

SeaGen environmental monitoring program, final report, 2011.

Sparling C, Smith K, Benjamins S, Wilson B, Gordon J, Stringell T, Morris C, Hastie G, Thompson D, Pomeroy P. 2015. Guidance to inform marine mammal site characterization requirements at wave and tidal stream energy sites in Wales. SMRUC-NRW-2015-012.

Tougaard J. 2015. Underwater Noise from a Wave Energy Converter is Unlikely to Affect Marine Mammals. PLoS ONE 10(7).

A literature review of extant WEC suggests that presently there are 10 different types of WEC:

1. **Attenuator**- Attenuators lie parallel to the predominant wave direction and move with the waves. An example of an attenuator is the Pelamis, developed by Ocean Power Delivery Ltd, now Pelamis Wave Power. <http://www.emec.org.uk/about-us/wave-clients/pelamis-wave-power/>
2. **Bulge Wave**- A bulge wave device is a large water filled distensible rubber tube floating just beneath the surface at right angles to the waves. As a wave passes, the bulge tube is lifted with the surrounding water and causes a bulge wave to be excited which passes down the tube's diameter, gathering energy from the wave as it moves. An example of this is the Anaconda by Checkmate Sea Energy UK Ltd. <https://www.checkmateukseaenergy.com/anaconda-technology/>
3. **Oscillating Water Column/Terminator**- Oscillating Water Column devices, sometimes called Terminators, have their principal axis parallel to the wave front and perpendicular to the wave motion and physically intercept waves. Usually, a subsurface opening feeds into a vertical compression chamber, in which the water surface oscillates with the wave action, forcing air out and across a turbine to create energy. Two examples are the Salter's Duck, developed at the University of Edinburgh and SPERBOY <http://www.paddocks1.co.uk/>
4. **Point Absorber**- Point absorbers utilize a mechanism consisting of two components: one immobile, either weighted or moored to the seafloor, and the other following the wave motion. The relative motion at a single point on the device is used for energy conversion. Two examples are the WaveStar and Ocean Power Technology's Powerbuoy. <http://wavestarenergy.com/>
5. **Oscillating Wave Surge Converter**- A sub-type of a point absorber device but where the floating component moves transversely as well as vertically. One example is the Oyster (Aquamarine Power Ltd.) and is a hinged device that moves under the action of passing waves. This movement drives two hydraulic pistons which push high pressure water onshore to drive a

conventional hydroelectric turbine to create electricity. <http://www.emec.org.uk/about-us/wave-clients/aquamarine-power/>

6. **Overtopping**- Overtopping devices consist of elevated reservoirs that are filled by waves spilling over a ramp and empty back into the ocean below through a drain. The potential difference creates a head pressure across the outlet that forces water through hydro turbines to create energy. An example of this is the Wave Dragon <http://www.wavedragon.co.uk/technology-2/>
7. **Rotating Mass**- A rotating mass, like the Subwave turbine, is a double-winged, counter-rotating water mill, hanging about 100 meters under a buoy floating on the surface. When the buoy is affected by ocean waves, the turbine will alternately be lifted up and sinking down, forcing the turbine blades to excerpt torque on the rotors and generate electricity. An example of this is the Subwave turbine by WaveCo <https://www.waveco.no/technology.html>
8. **Submerged Pressure Differential**- A sub-type of a point absorber where the floating component is submerged. An example of this is the mWave by Bombora Wave. This device has a series of air-inflated membranes on a structure on the sea floor arranged at an angle to the incoming waves. As waves pass over, the air is transferred into a duct via a turbine which causes the turbine to spin and generate electricity. <https://www.bomborawave.com/mwave/>
9. **WaveRoller**- WaveRoller devices consists of a large panel anchored to the sea floor in near shore areas (< 20 m deep) that moves back and forth along a hinge. This blade captures the energy from wave surge and converts it to electricity on site which is then transferred to shore via a cable. An example of this device is from Aw-Energy <https://aw-energy.com/waveroller/>
10. **Wave energy floaters**- Floaters use fixed arms attached to buoys that move up and down with wave motion. The resultant energy is used to rotate a generator and create electricity, which is transferred into the electricity grid. An example of this device is from Eco Wave Power. <https://www.ecowavepower.com>

1.2.3.4 Entanglement rates of marine mammals in the general vicinity of Yakutat

The only available data for marine mammal entanglements near Yakutat come from annual National Marine Fisheries Service Stock Assessment Reports (SARS) and associated Severe Injury and Mortality data. Unfortunately, there are very few recent assessments of marine mammal entanglements because most of the fisheries in the region are not currently monitored. Historically, harbor porpoise have been entangled in subsistence and commercial set nets for salmon, including in the waters surrounding Yakutat with an estimated 22 harbor porpoise per year entangled for the entire Southeast Alaska region (Muto et al., 2019; Delean et al., 2020). No other species have been reported to NMFS as entangled in the past decade near Yakutat however, in 2016 one killer whale was found dead entangled in unknown fishing gear in southeast Alaska and humpback whales have been observed entangled in various pot fishery and long line fishery gear which generally involve floating lines and surface buoys in which they are entangled (Muto et al., 2019; Delean et al., 2020). Overall, in the southeast Alaska region, there are relatively few observations annually of marine mammal entanglement in fishing gear, although many of the fisheries are not observed. There is no information on marine mammal entanglement in wave energy devices to date and a recent global assessment of the impact of wave energy devices on marine animals found no deleterious effects (Copping and Hemery, 2020). That report examined collision risk, impacts of noise, impacts of electromagnetic radiation and encounters with underwater cables and mooring structures and suggested that there was little chance for or evidence of impacts to marine mammals. Potential impacts of wave energy devices should be related to the design of such devices, including where they are

placed in the water column, whether they have moving parts or tethers, how they are moored and what their overall footprint is in the environment. Wave energy generators with underwater turbines have the potential to injure marine mammals should they collide with moving parts. Wave attenuators may present entanglement or entrapment hazards to marine mammals. Entanglement and injury impacts on marine mammals are separate questions from noise-related injury or impacts from installation and operation of wave energy devices.

1.2.4 Conclusions

In this study, we documented the seasonal acoustic occurrence of at least 5 species of marine mammals, including two endangered species, occurring in the survey area adjacent to Cannon Beach. We also determined seasonal ambient noise levels. Although we could only detect animals that were actively producing sound, the results of this study may be useful in determining interactions between marine mammals and future energy devices, as well as directions for marine mammal research. For example, based on the overall low densities and species diversity in the survey area, hydrokinetic devices deployed in this area are likely to have few negative interactions with marine mammals. Furthermore, a literature review of the noise levels of many WEC devices, when compared to ambient noise levels measured here, suggest that, post-deployment, there is unlikely to be masking of marine mammal signals. Likewise, entanglements of marine mammals in the current suite of wave energy conversion devices is unlikely. Future, multi-year research on the presence of vocal marine mammals in the area would be helpful to elucidate interannual variability. On-going passive acoustic monitoring concurrent with the installation and operation of future WEC devices will be needed to unequivocally determine if and what the impact of such devices will have on the overall soundscape of the nearshore region off Yakutat and the presence of marine mammals in the region.

1.3 Monitoring Fish and Information to Support an Essential Fish Habitat (EFH) Review

1.3.1 Introduction

Understanding the nearshore distribution and behavior of fishes can aid in evaluating their potential interactions with marine renewable energy activities (Shen et al., 2016; Viehman and Zydlewski, 2015; Viehman et al., 2015). One example of a nearshore marine renewable energy activity is the deployment of wave energy converters (Drew et al., 2009). Currently, to reduce expense incurred by diesel generators, wave-based electricity generation has been suggested for adoption by the community of Yakutat, located on the northeast coast of the Gulf of Alaska (Previsic and Bedard, 2009; Tschetter et al., 2016). Based on previous oceanographic research, the nearshore zone (< 1 km from shore; 0–20 m depth) of Cannon Beach, AK, (Figure 21) was identified as the most likely candidate location for wave energy converter deployment (Previsic and Bedard, 2009; Tschetter et al., 2016).

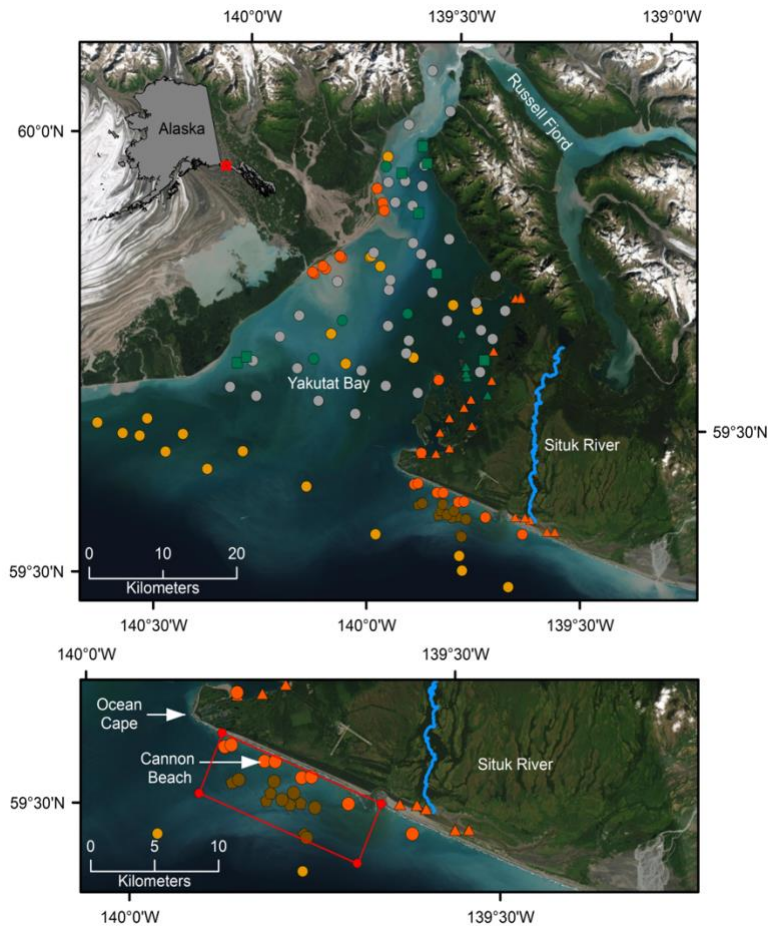


Figure 21. Mid-water trawl (squares), bottom trawl (circles), surface trawl (pentagons), and beach seining sites (triangles) from Arimitsu et al., 2002 (green symbols), Arimitsu et al., 2016 (gray symbols), Neff, 2016 (dark orange symbols), NOAA’s annual bottom trawl surveys (light orange symbols), and this study (brown symbols) in nearshore waters adjacent to Yakutat, AK. Bottom panels represent close up depiction of sampling sites that occurred near the proposed hydrokinetic wave energy site (red polygon = survey site), near Cannon Beach.

The Gulf of Alaska, near Yakutat supports lucrative sport (Marston and Power, 2016), commercial (Zeiser and Woods, 2016), personal use (Conrad and Gray, 2014), and culturally important subsistence fisheries (Naves et al., 2010). These fisheries target dozens of species, including pelagic fishes such as salmonids (family salmonidae), smelts (family osmeridae), and Pacific herring *Clupea pallasii*, as well as demersal fishes such as flatfishes (family pleuronectidae), rockfishes (*Sebastes* spp.), cods and pollock (family gadidae), and sablefish *Anoplopoma fimbria*, and Lingcod *Ophiodon elongatus* (Olson et al., 2017; Tingley and Davidson, 2011). In addition, dozens of other fish species occur in the central Gulf of Alaska that are not captured in fisheries, but are nonetheless important in pelagic and/or demersal food webs (Johnson et al. 2012).

In addition to supporting valuable fisheries, past fisheries research has suggested that nearshore waters of Yakutat are highly productive and may be important feeding areas of upper trophic level predators, such as marine mammals (Arimitsu et al., 2016; Castellote et al., 2015; Neff, 2016). Most research to understand the fish community in this area has primarily aimed to inventory marine and estuarine fishes throughout the region (Arimitsu et al., 2003; Neff, 2016), while other research has sought to understand influences of glacier runoff on the distribution and abundance of zooplankton, forage fishes, and seabirds (Arimitsu et al., 2016). While these research activities are informative, most of these efforts have

occurred in Yakutat Bay, and only one study has conducted limited sampling activities in the proposed wave energy device deployment location. Therefore, many questions remain concerning the species presence and distribution in this area, and past researchers have suggested that additional efforts with different gear types (e.g., mid-water, surface trawls) are needed to accurately portray species diversity and relative abundance in the area.

Many methodologies exist to study the spatial and temporal distribution of nearshore fish assemblages. For example, state and federal fisheries agencies commonly use a variety of fisheries survey styles including bottom trawl (von Szalay and Raring, 2018), mid-water trawl (Arimitsu et al., 2008), surface trawls (Orsi and Fergusson, 2016), acoustic technology (Honkalehto and McCarthy, 2015), longlines (Lunsford et al., 2017), gillnets (Sigler et al., 2001), beach seines (Johnson et al., 2012), and aerial imagery (Hebert, 2013) to characterize the relative abundance and distribution of fishes. When interpreting data from all of these sampling methods, it is important to recognize that they all have inherent species and size specific capture biases. Therefore, to comprehensively characterize fish assemblages, research needs to incorporate multiple sampling techniques.

To understand potential impacts of energy exploration and development on fishes, it is critical to determine the overlap in time and space between potential development activities and animals. Although the broad-scale distribution of fishes is well described in the central Gulf of Alaska near Yakutat, fish presence/absence near Cannon Beach at the proposed wave energy site has not been described in detail. Therefore, the primary objective of this study was to provide a better understanding of the demersal and pelagic fish communities near and adjacent to the area proposed for a wave energy converter. To accomplish this objective, we 1) conducted surface and bottom trawl sampling in 2018, 2) conducted hook and line sampling in 2019 and, 3) aggregated catch data from all known previous research campaigns (n = 4; Table 5) conducted in the vicinity of Cannon Beach and Yakutat Bay to better understand species presence near Cannon Beach.

1.3.2 Methods

1.3.2.1 Surface and bottom trawl sampling

From 19 to 25 May 2018, we conducted surface (n = 6 tows) and bottom trawls (n = 6 tows) in nearshore areas adjacent to Cannon Beach (hereafter referred to as the survey area), near Yakutat, AK (Figure 22a). To best characterize the fish community, a variety of bottom depths (18–86 m) were trawl sampled in the survey area. Trawling was conducted aboard the Alaska Department of Fish and Game’s Research Vessel Solstice (Figure 23). The surface trawl was a Nordic 264 rope trawl with 3-m doors and a 1.2-cm mesh liner cod end that fished approximately 11 m deep with a width of 14.3 m (Moss et al., 2005). The bottom trawl was a 400-mesh eastern trawl with 3.2 cm mesh in the cod end, 8.9 cm in the intermediate and 10.2 cm in the body and wings, and 364 kg Nor-Eastern Astoria V trawl doors (Bouwens et al., 1999). Duration of trawl tows was restricted to very short durations (~5 min), due to concerns expressed by the Alaska Department of Fish and Game Division of Commercial Fisheries Area Management Biologist about the possibility of catching Chinook Salmon *Oncorhynchus tshawytscha*.

After the trawl net was brought aboard the research vessel, fish were identified to species and fork length to the nearest mm was measured. Priority fish species, including Pacific Halibut, Lingcod, and Sablefish, were sorted in an expedited manner and released overboard as quickly as possible to increase survivorship. In addition to species identification and measuring captured fishes, a subsample of species of captured fish were frozen in Ziploc bags and shipped to the UAF Fisheries laboratory where scales, otoliths and tissue samples were collected and archived for potential later analyses. For data analyses of trawl catches, catch-per-unit-effort (CPUE; no. fish·min⁻¹) for each species was calculated and qualitative comparisons of CPUE and species captured were made between bottom and surface trawls.

1.3.2.2 Surface and bottom trawl sampling

During 7–10 May, 1–5 June, 29–31 August, 3–4 October, and 2–5 November 2019, we conducted 100.7 hours of hook and line sampling (hereafter referred to as angling) in the survey area, and in adjacent control areas (Figure 22b). Control areas were chosen by the boat captain, and are locations known to support productive recreational and commercial fisheries. Based on previous sampling programs (Neff 2016) and local fishing knowledge (M. Sappington), the survey area was often referred to as a “dead zone,” and catches were expected to be low through the sampling period. Therefore, to validate efficacy of the angling gear and tactics used and to provide a qualitative comparison to catches in the survey area, angling at nearby control areas was executed. During angling activities, we opportunistically used several techniques, including bottom jigging (bait, jigs, sabiki rigs), mooching (herring), and trolling with divers and lead weights (herring, artificial lures). Typically, 3–6 rods were concurrently used depending on environmental conditions (e.g., winds, currents) and angling technique. Upon capture, relatively small fishes were brought aboard, identified to species, and measured (mm). Additionally, the GPS location and time of catch was recorded. For relatively large fishes, such as Pacific Halibut *Hippoglossus stenolepis* and Big Skate *Beringraja binoculata*, lengths were estimated visually from the side of the vessel to avoid injury to captured specimens and research personnel. For qualitative analyses of angling catches, comparisons of number of fish and species captured were made between survey and control areas. No quantitative comparisons on angling catches were conducted due to the inconsistency of effort, angling techniques, and small durations of sampling events spread out over the spring, summer and fall seasons.

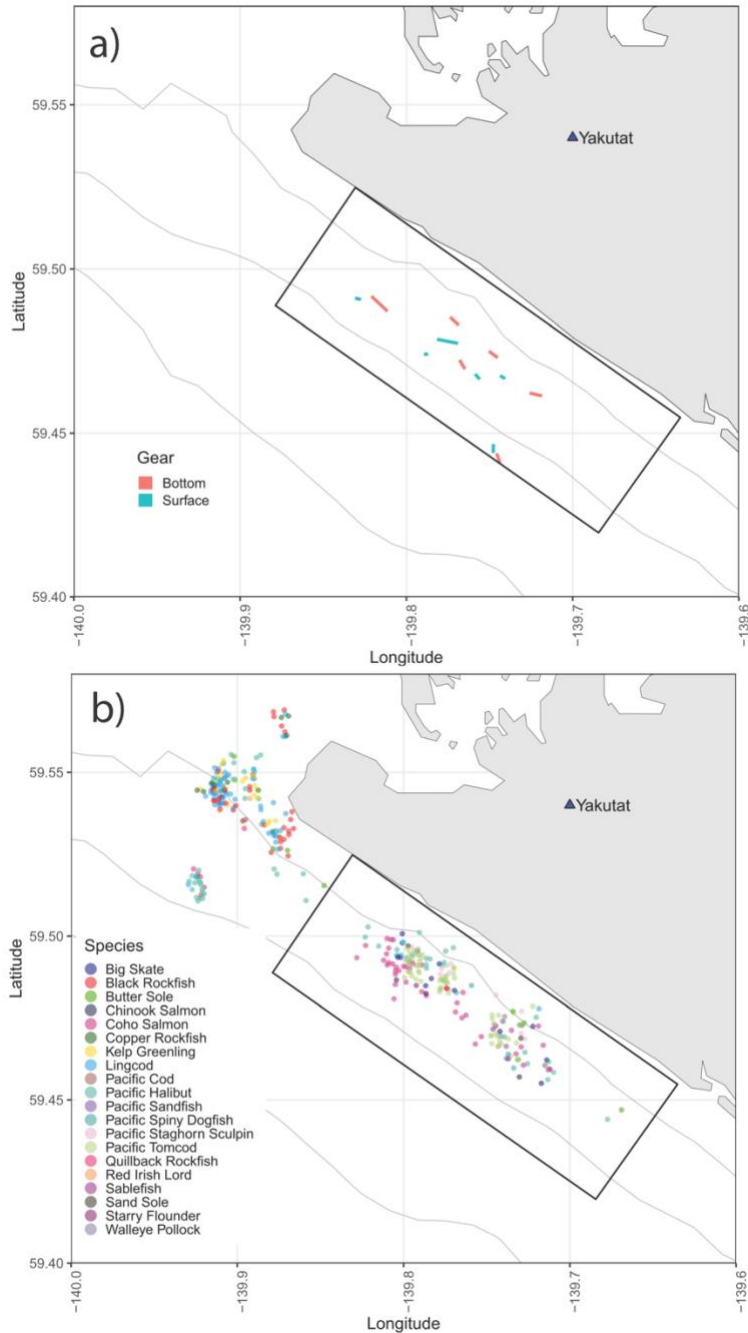


Figure 22. Trawl sampling transects (a), and angling capture locations for this study (b). Black polygon denotes the Cannon Beach survey area. The area where angling occurred northwest of the black polygon was considered the control area.

1.3.2.3 Comprehensive species presence

To comprehensively document species encountered in nearshore waters adjacent to Yakutat, AK, results from trawl and angling surveys in this study were combined with datasets from all known previous sampling activities (Table 5; Figure 21). After aggregating these data, a list of all fish species captured, by gear type (bottom trawl, mid-water trawl, surface trawl, beach seine, and angling) was tabulated. Additionally, the spatial distribution (presence/absence) of each species was mapped throughout the Yakutat region. Catch per unit effort from the other three studies were not aggregated nor compared with one another because sampling in these programs was sporadic, inconsistent, infrequent, and did not have standardized gear types, specimen sampling procedures, or data analyses.

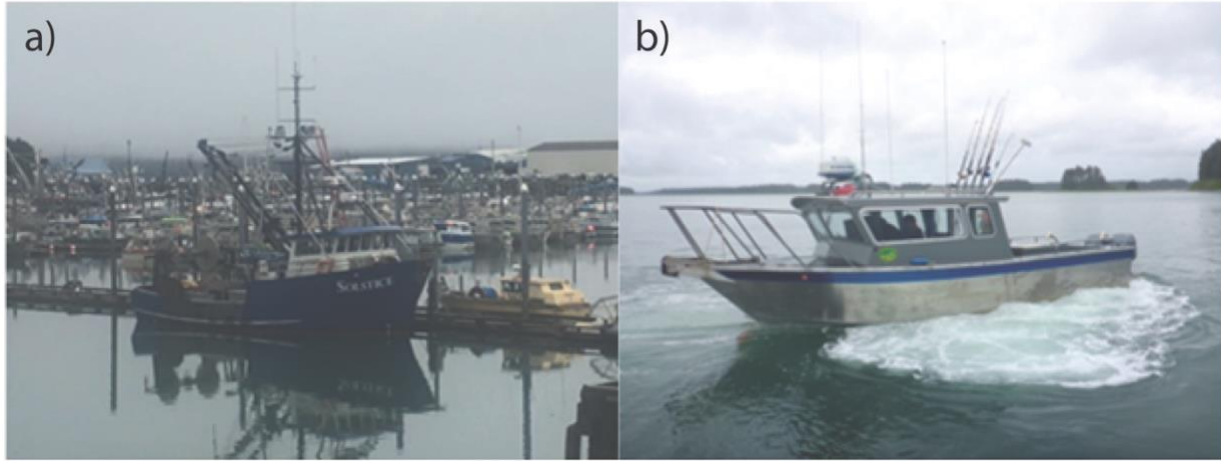


Figure 23. Alaska Department of Fish and Game's R/V Solstice used for the trawl surveys in 2018 (a). The F/V Quest used for angling surveys in 2019 (b).

1.3.3 Results

1.3.3.1 Surface and bottom trawl sampling

During surface and bottom trawl sampling, a total of 1190 fishes were captured representing 18 unique species (Table 6; Figure 24a). While 18 species were captured with trawl efforts, overall species diversity was relatively low, as over 80% of the total catch was comprised of only four species, including Butter Sole *Isopsetta isolepis* (49%), Pacific Tomcod *Microgadus proximus* (13%), Sand Sole *Psettichthys melanostictus* (10%), and Arrowtooth Flounder *Atheresthes stomias* (8%) (Table 7 Figure 24a). Besides Arrowtooth flounder ($n = 99$), commercially and recreationally important fishes including Pacific Halibut ($n = 30$), Sablefish ($n = 1$), and Lingcod ($n = 3$), were rare in catches (Table 7; Figure 24a).

The number of individual fishes, number of unique species, and catch per unit effort (CPUE) varied substantially between bottom and surface trawls (Table 6). Bottom trawling yielded 16 unique species with relatively high CPUEs ranging from 10.1 to 76.3 (36.4 ± 26.1 , mean \pm SD) fishes per minute (Table 6). The most commonly captured species were Butter Sole ($n = 581$), Pacific Tomcod ($n = 159$), Sand Sole ($n = 123$), and Arrowtooth flounder ($n = 99$). In contrast, surface trawling yielded only three unique species, low catches ($n = 9$ individuals), and relatively low CPUEs ranging from 0 to 0.3 (0.15 ± 0.12 , mean \pm SD) fishes per minute (Table 6). Catch composition of surface trawls consisted of Capelin ($n = 3$), Surf Smelt ($n = 1$), and Threespine Stickleback ($n = 5$).

1.3.3.2 Angling

During angling, a total of 381 fishes, representing 20 unique species was captured in 100.7 hours of sampling (Table 8; Figure 22b). Over 70% of the catch was comprised of just five species, including Pacific Tomcod (19.4%), Lingcod (17.6%), Pacific Halibut (16.8%), Coho Salmon *Oncorhynchus kisutch* (10.5%), and Black Rockfish *Sebastes melanops* (9.2%) (Figure 24b). Some catches varied seasonally, with Coho Salmon (n = 40) and Chinook Salmon *Oncorhynchus tshawytscha* (n = 4) only being captured during the month of August. In contrast, species such as Pacific Tomcod (n = 74), Pacific Halibut (n = 64) and Lingcod (n = 67) were caught during all sampling periods (Figure 25). While catches in different sampling areas (survey area vs. control area) are not directly comparable due to differences in effort (e.g., number of rods) and methods (e.g., bottom jigging, trolling, mooching, etc.) used, in general, daily catches were smaller and few commercially and recreationally important species were captured in the survey area, when qualitatively compared to the adjacent control areas (Table 8; Figure 24b). Specifically, in the survey area, a total of 195 fishes, mostly Pacific tomcod (n = 74), was captured in 78.1 hours of angling (Table 5; Figure 24). In contrast, 185 fishes including Pacific halibut (n = 35), Lingcod (n = 64), Black Rockfish (n = 34), Quillback Rockfish *Sebastes maliger* (n = 10), Copper Rockfish *Sebastes caurinus* (n = 10), of relatively large sizes were captured in only 13.1 hours of angling in the control areas (Table 8). An exception to these results is that adult Coho Salmon were frequently captured in the survey area during August sampling (Figure 25). Note angling methods successful for catching salmon and a variety of other species were used in all months of the study.

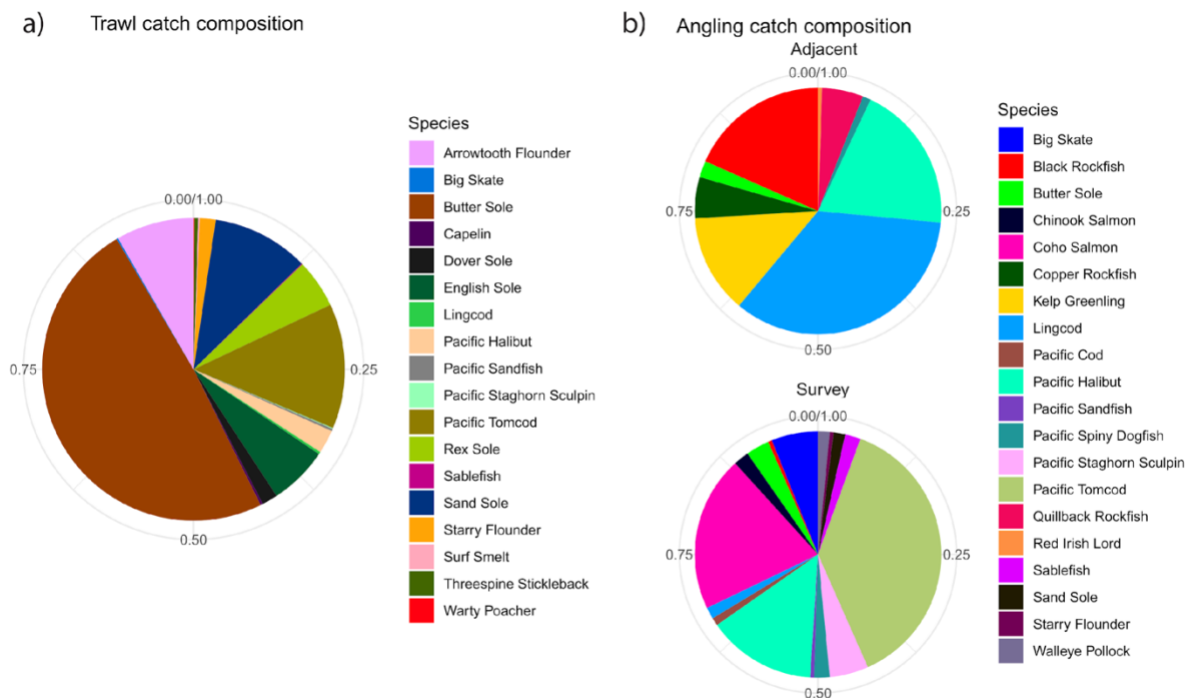


Figure 24. Species composition (%) of trawl (a) and angling catches (b) near Yakutat, Alaska.

1.3.3.3 Species Presence

After aggregating all catch data from relevant fisheries research efforts (Table 5), we identified 105 fish species present in nearshore waters adjacent to Yakutat, AK (Table 9). Of these species, 60 were captured with beach seines, 73 with bottom trawls, 10 with mid-water trawls, 3 with surface trawls, and 20 via angling (Table 8). In all, combining our research efforts with Neff (2016), 1,478 individual fishes were

captured in the survey area (i.e., Cannon Beach), representing 28 unique species. Similar to this study’s angling survey, past research has documented that catches were relatively low and less species diverse in the survey area, compared to other adjacent habitats. For example, Neff (2016) only captured 92 fishes (13 species) in 30 bottom trawl tows in the survey area, whereas she captured 1,186 fishes (23 species) in 48 trawl tows in west Yakutat Bay. Individual maps (n = 105) of species presence, by species and gear type, are included in Appendix A.

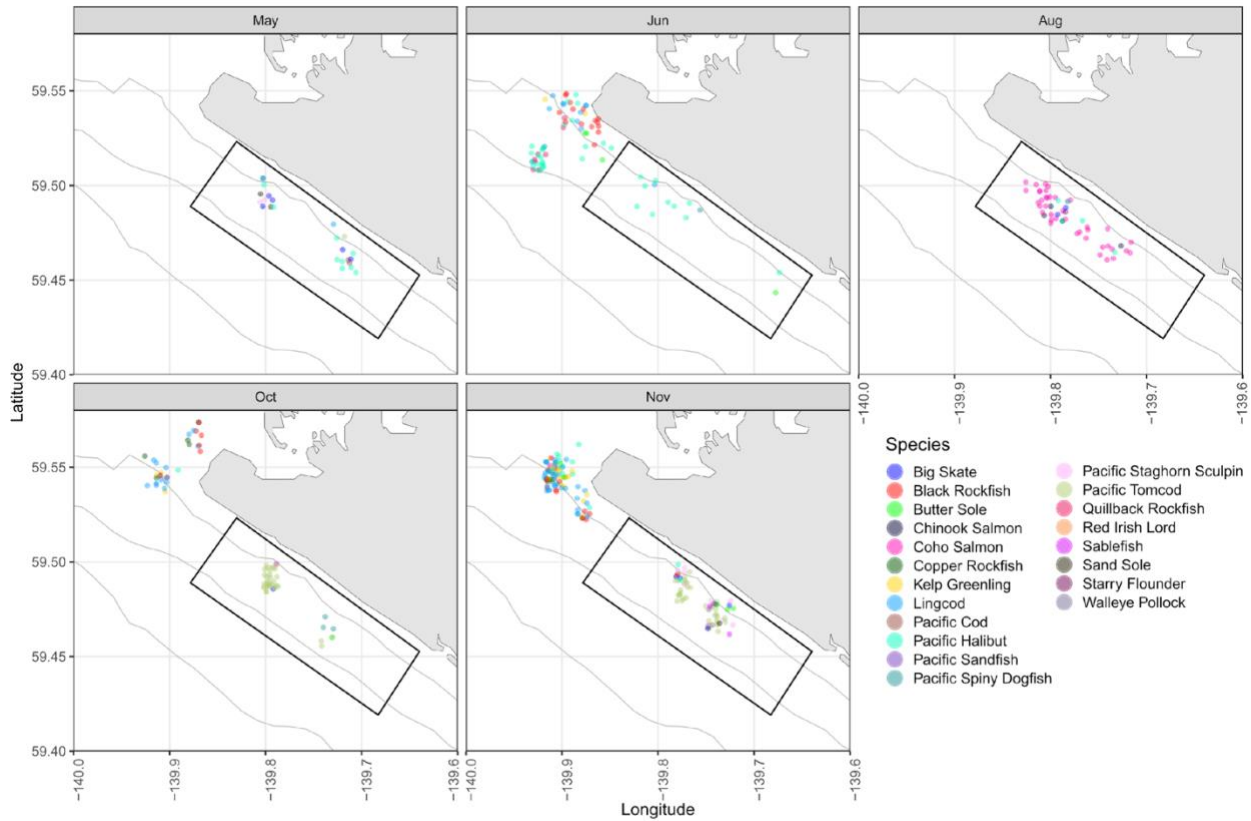


Figure 25. Monthly spatial distribution of angling catches, by species. Black polygon denotes Cannon Beach survey area. Points are jittered to separate overlapping locations.

1.3.3.4 Archived Samples

A total of 194 fishes, including Arrowtooth Flounder (n = 9), Butter Sole (n = 42), Dover Sole *Microstomus pacificus* (n = 24), English Sole *Parophrys vetulus* (n = 19), and Pacific Tomcod (n = 100) was sampled for weight (g), and otolith and tissue samples, all of which were frozen and archived at UAF. Additionally, several fish species including, Rex Sole (n = 3), Pacific Staghorn Sculpin (n = 1), Pacific Sandfish (n = 2), Threespine Stickleback *Gasterosteus aculeatus* (n = 4), Pricklebreast Poacher *Stellerina xyosterna* (n = 1), Surf Smelt *Hypomesus pretiosus* (n = 10), and Capelin *Mallotus villosus* (n = 5), were frozen and provided as voucher specimens to the University of Alaska Museum of the North.

1.3.4 Discussion

During this study we captured a total of 1,385 fishes representing 24 species, updating lacking information about species presence in the area adjacent to Cannon Beach that is proposed for a wave energy converter. Additionally, this study provides substantial information on recreationally important

fish species, captured via angling surveys, a methodology that had not previously been used in the survey area. The catches provide valuable baseline information about the fish species presence in the area that may be used for assessing potential impacts of a wave energy converter.

In all, while small in duration and geographic extent, our research suggests that benthic fishes (e.g., Butter Sole, Sand Sole, Pacific Tomcod) that are not targeted in fisheries are frequently encountered in survey area during the summer and fall months. The density of these benthic fishes as documented in this study differs from the perceived fish densities reported from past research (Neff 2016), and from local fishing knowledge (Captain M. Sappington, personal communication). The Cannon Beach area is often referred to as a “dead zone” by fishers in Yakutat as it is frequently compared to adjacent highly productive areas where commercial, recreational, and subsistence fishing efforts are focused. The perception of the Cannon Beach area being a dead zone is exacerbated as it appears that few recreationally and commercially important species occupy this area. Our research suggests that the survey area is not necessarily a “dead zone,” but rather it has comparably lower densities of fishes than that of some adjacent areas and it has fishes that are not readily captured with recreational and commercial fishing gear. This is likely why local fishers perceive the study area to be a “dead zone.”

The reasons for the apparent lack of fish species targeted in fisheries occurring in the survey area, except for ephemeral Coho Salmon migrating through the area in August, could be due to a variety of physical gradients (e.g., temperature, salinity, currents, or bottom structure), or biological (e.g. prey density, type, diversity) factors. Further exposition on this in a multidisciplinary context would be highly speculative thus we refrain from doing so in this report. For example, waters of the survey site are likely less productive compared to waters inside Yakutat Bay, which is heavily influenced by the fresh, cold, and nutrient-rich glacial runoff from Yakutat Bay (e.g., Arimitsu et al. 2016). Additionally, the seafloor of the survey area is characterized as a gentle slope composed of sand and silt. However, just to the north of the survey area (e.g., Ocean Cape), the seafloor becomes more heterogeneous, with rocky outcroppings (Author’s personal observations). The likely physical and biological differences between the control and survey areas likely explains the relative low catches in the survey area. While some Pacific Halibut and Lingcod were captured in the survey area, catches were sparse and no large individuals from these species were captured. Given this, this area may be used as a migratory corridor rather than foraging habitat for large individuals of these species.

We did not capture any juvenile (ocean age 0) Pacific salmon, and only four immature salmon (~ ocean age 1 Chinook salmon) were captured, via angling efforts. These results are similar to past bottom trawl research (Neff 2016) which captured only one juvenile Sockeye Salmon in 30 individual (5 min) trawl tows conducted in the survey area of the current study. Interestingly, the Situk River, along with several others (e.g., Dangerous, Italio, Lost, Alsek), are all large salmon producing watersheds that drain into the Gulf of Alaska near the survey area. Given this, at some time period, most likely spring to early summer, juvenile salmon likely occupy, or at a minimum, transit through the survey area as smolts. This migration is likely very short in duration, as some species of juvenile salmon may quickly emigrate from river mouths to coastal or offshore feeding areas (Moulton 1997; Trudel et al. 2009; Tucker et al. 2011). While many factors may be related to the absence of juvenile salmon in our catches (e.g., season of trawls, distance from shore), it is likely related to the limited number ($n = 6$) and short durations (5 min) of surface trawl efforts in this study. Surface trawling is the method most likely to capture surface oriented juvenile salmon, but due to permitting restrictions, our efforts, which were severely limited, likely were not sufficient to capture the salmon smolts during their very short residence time in the area. Future research with more intense surface trawl efforts, extending into the months of June and July would likely provide a better understanding of if and when juvenile salmon occupy the survey area.

In the survey area, adult Coho Salmon were relatively abundant in late August, during this species’ return spawning migration to rivers in the area. These results are corroborated by the distribution of the commercial troll fishery, which commonly fishes in the northern vicinity of the survey area during the fall months (M. Sappington, personal communication). However, we did not capture adults of other Pacific

Salmon species (Chum Salmon, Sockeye Salmon, Pink Salmon), even though the nearby Situk River is home to large populations of Sockeye Salmon, Coho Salmon, and Pink Salmon, which likely transit through the survey area during their return to freshwater spawning habitats. While many factors may be related to the lack of adult Pacific salmon captured in this study outside of Coho salmon in August, the short sampling efforts and months sampled are likely responsible. For example, local fisherman commonly observe salmon including Sockeye and Pink Salmon (M. Sappington, personal communication) during time periods we did not sample (mid-June to mid-August). Additionally, Sockeye Salmon are less readily captured via angling techniques compared to Coho Salmon. Future angling during the summer months using techniques refined for species other than Coho salmon would likely capture other salmon species in the survey area.

In this study, few forage fishes (e.g., Pacific Herring, Pacific Sand Lance, Capelin, Eulachon) were captured. While many factors may be related to the absence of these species in our catches (e.g., season), it is likely related to the very limited trawl efforts, in this study. In contrast, past research has documented relatively high abundance of important forage fishes in the Yakutat area (Arimitsu et al., 2016; Neff, 2016). For example, Neff (2016) reported that forage fish species including Pacific Herring, Pacific Sand Lance, Surf Smelt, Capelin, and Eulachon accounted for almost 70% of the entire catch during her nearshore fish project (over 29,000 fish captured) in the Yakutat region, although sampling efforts indicated lower densities of forage fish in the wave energy survey site compared other habitats (i.e., western and eastern Yakutat Bay). Additionally, past research has suggested that Capelin, an important forage fish, may use Cannon Beach as spawning habitat (Pahlke, 1985; Rogers et al., 1980). Although claims of Capelin spawning near Cannon Beach have not been verified recently (R. Hoffman, Alaska Department of Fish and Game), this species, including individuals of the larval life stage, have been commonly captured throughout the survey area and inside Yakutat Bay (Arimitsu et al., 2016; Neff, 2016). Finally, Pacific Herring, another important forage fish species, is known to spawn in nearby Yakutat Bay and Russel Fjord (R. Hoffman, Alaska Department of Fish and Game, Yakutat). Similar to Capelin, whether this species spawns adjacent to Cannon Beach is currently unknown. Given indications from past research about relatively high densities of important forage species, it is likely that these species ephemerally occupy the survey area near Cannon Beach and we did not document them because of limited sampling. Gathering more comprehensive distribution information about forage species, including the spawning distribution of Capelin and Pacific herring would be a valuable direction in future research.

1.3.5 Conclusion

In this study, we have updated and comprehensively documented over 28 species, occurring in the survey area adjacent to Cannon Beach. While we considered this research a “snap shot” of the true nearshore fish assemblage of the survey area, the results of this study may be useful in determining interactions between fishes and future energy devices, as well as directions for future fisheries research. For example, based on the overall low densities and species diversity in the survey area, hydrokinetic devices deployed in this area are likely to have fewer fish interactions, compared to those deployed in surrounding habitats with higher fish densities and diversity (i.e., Ocean Cape, Yakutat Bay). Furthermore, past research has highlighted the importance of the Yakutat region to forage fishes, the primary diet of many marine mammals, seabirds, and commercially and recreationally important fish species. Because of their swimming capabilities, forage fish and juvenile salmonids are much less likely to be able to actively avoid potential wave energy devices compared to their adult counterparts or larger fish species. Therefore, future research describing the distribution of juvenile salmon and forage fish would be valuable. Systematic and larger trawl efforts, including surface and mid-water trawls are likely needed to address these questions.

Table 5. Datasets aggregated to provide information on the species of nearshore fishes encountered near Yakutat, AK.

Study Name	Gear type	Year	Stations (n)	Unique species (n)	Catch (n)
Arimitsu et al. 2003	Bottom trawl, Mid-water trawl	2002	20	27	3520
Neff 2016	Bottom trawl, Beach seine	2013, 2014	36	73	29655
Arimitsu et al. 2016	Bottom trawl	2011	39	26	44403
NOAA Survey	Bottom trawl	*	24	50	439
This Study 2018	Bottom trawl, surface trawl	2018	12	18	1190
This Study 2019	Angling	2019	NA	20	381

*1984, 1990, 1996, 2003, 2005, 2009, 2011, 2015, 2017

Table 6. Summary of trawl catches in nearshore marine waters adjacent to Cannon Beach, Yakutat, AK in 2018.

Trawl #	Duration (min)	Catch (n)	Unique species (n)	Catch per unit effort (# fish/minute)
Bottom Trawl				
B1	10	101	8	10.1
B2	6	458	8	76.3
B3	4	245	8	61.3
B4	6	139	10	23.2
B5	5	107	5	21.4
B6	5	131	8	26.2
Total	36	1181		32.8
Surface trawl				
S1	10	3	2	0.3
S2	10	2	1	0.2
S3	10	2	2	0.2
S4	10	2	1	0.2
S5	10	0	0	0.0
S5	15	0	0	0.0
Total	65	9		0.1

Table 7. Fish species captured in bottom and surface trawling efforts in nearshore areas adjacent to Cannon Beach near Yakutat, AK 2018.

Species	n	Mean length (mm)	Length range (mm)	Catch per unit effort (# fish/min)
Bottom trawl				
Arrowtooth Flounder	99	271±152	100–560	2.8
Big Skate	2	620±56.6	580–660	0.1
Butter Sole	581	246±57.9	87–370	16.1
Dover Sole	20	246±58.9	150–340	0.6
English Sole	75	296±125	90–490	2.1
^c Lingcod	3	655±91.2	550–715	0.1
^c Pacific Halibut	30	608±90.7	460–810	0.8
Pacific Sandfish	3	150±10	140–160	0.1
Pacific Staghorn Sculpin	1		280	<0.0
Pacific Tomcod	159	162±26.1	110–250	4.4
Rex Sole	62	275±72.3	110–410	1.7
^c Sablefish	1		410	<0.0
Sand Sole	123	264±100.4	90–440	3.4
Starry Flounder	20	517±71.7	390–650	0.6
Surf Smelt	1		125	<0.0
Pricklebreast Poacher	1		80	<0.0
Surface trawl				
Capelin	3	95±10.1	84–104	0.05
Surf Smelt	1		144	0.02
Threespine Stickleback	5	76±7.1	64–81	0.08

^c Noteworthy commercially important species

^r Noteworthy recreationally important species

Table 8. Fish species captured by angling in the Survey and Control areas near Yakutat, AK in 2019.

Species	Sample size	Mean length (mm)	Length range (mm)
Survey area			
Big Skate	12	1123 ± 356	700–1750
^c Black Rockfish	1		510–510
Butter Sole	6	352 ± 23	320–390
^c Chinook Salmon	4	348 ± 33	310–380
^c Coho Salmon	40	701 ± 64	560–820
^c Lingcod	3	730 ± 142	620–890
^c Pacific Cod	2	870 ± 28	850–890
^c Pacific Halibut	28	657 ± 123	440–1060
Pacific Sandfish	1		160
Pacific Spiny Dogfish	4	980 ± 103	850–1100
Pacific Staghorn Sculpin	10		250–380
Pacific Tomcod	74	240 ± 16	180–280
^c Sablefish	4	255 ± 24	240–290
Sand Sole	3	447 ± 58	380–480
Starry Flounder	1		610
^c Walleye Pollock	3	533 ± 35	500–570
Control area			
^c Black Rockfish	34	436 ± 84	270–570
Butter Sole	4	305 ± 45	240–340
^r Copper Rockfish	10	436 ± 76	280–590
Kelp Greenling	24	352 ± 60	240–470
^c Lingcod	64	627 ± 121	340–1000
^c Pacific Halibut	36	978 ± 374	400–1730
Pacific Spiny Dogfish	2	935 ± 35	910–960
^r Quillback Rockfish	10	430 ± 79	250–530
Red Irish Lord	1		340

^c Noteworthy commercially important species

^r Noteworthy recreationally important species

Table 9. Updated list (by alphabetic order of common name) of marine nearshore, pelagic, and demersal fish species (n = 105) documented near Yakutat, AK in previous and current sampling efforts. Sampling methods and references are noted.

Common name	Scientific name	Beach Seine	Surface Trawl	Midwater Trawl	Bottom Trawl	Angling	Reference
Arctic Shanny	<i>Stichaeus punctatus</i>				x		c
Arrowtooth Flounder	<i>Atheresthes stomias</i>				x		ade
Bay Pipefish	<i>Syngnathus leptorhynchus</i>	x					c
Bering Skate	<i>Bathyraja interrupta</i>				x		d
Big Skate	<i>Beringraja binoculata</i>				x	x	bcde
Bigfin Eelpout	<i>Lycodes cortezianus</i>				x		d
Bigmouth Sculpin	<i>Hemitripterus bolini</i>				x		ab
Black Rockfish	<i>Sebastes melanops</i>	x			x	x	cde
Blackbelly Eelpout	<i>Lycodes pacificus</i>				x		d
Bluntnose Sixgill Shark	<i>Hexanchus griseus</i>				x		d
Buffalo Sculpin	<i>Enophrys bison</i>	x			x		ac
Butter Sole	<i>Isopsetta isolepis</i>	x			x	x	cde
Cabezón	<i>Scorpaenichthys marmoratus</i>	x					c
Capelin	<i>Mallotus villosus</i>	x	x	x	x		abcde
Chinook Salmon	<i>Oncorhynchus tshawytscha</i>	x			x	x	bcde
Chum Salmon	<i>Oncorhynchus keta</i>	x					c
Coho Salmon	<i>Oncorhynchus kisutch</i>	x			x	x	bce
Copper Rockfish	<i>Sebastes caurinus</i>	x				x	ce
Crescent Gunnel	<i>Pholis laeta</i>	x					c
Crested Sculpin	<i>Blepsias bilobus</i>				x		b
Dark Rockfish	<i>Sebastes ciliatus</i>	x					c

Darkblotched Rockfish	<i>Sebastes crameri</i>				x		d
Daubed Shanny	<i>Leptoclinus maculatus</i>			x	x		abc
Dolly Varden	<i>Salvelinus malma</i>	x					c
Dover Sole	<i>Microstomus pacificus</i>				x		ade
Dusky Rockfish	<i>Sebastes variabilis</i>				x		d
English Sole	<i>Parophrys vetulus</i>	x			x		cde
Eulachon	<i>Thaleichthys pacificus</i>			x	x		abcd
Flathead Sole	<i>Hippoglossoides elassodon</i>				x		abd
Great Sculpin	<i>Myoxocephalus polyacanthocephalus</i>	x					a
Kelp Greenling	<i>Hexagrammos decagrammus</i>	x			x	x	bcde
Leister Sculpin	<i>Enophrys lucasi</i>	x					c
Lingcod	<i>Ophiodon elongatus</i>	x			x	x	cde
Longfin Smelt	<i>Spirinchus thaleichthys</i>	x			x		bcd
Longnose Skate	<i>Raja rhina</i>				x		d
Longsnout Prickleback	<i>Lumpenella longirostris</i>				x		abd
Manacled Sculpin	<i>Synchirus gilli</i>	x					c
Masked Greenling	<i>Hexagrammos octogrammus</i>	x					c
Night Smelt	<i>Spirinchus starksi</i>				x		d
Northern Rock Sole	<i>Lepidopsetta polyxystra</i>	x			x		cd
Northern Ronquil	<i>Ronquilus jordani</i>				x		b
Northern Sculpin	<i>Icelinus borealis</i>	x					c
Pacific Cod	<i>Gadus macrocephalus</i>	x		x	x	x	acde
Pacific Halibut	<i>Hippoglossus stenolepis</i>	x			x	x	cde
Pacific Herring	<i>Clupea pallasii</i>	x			x		abcd

Pacific Ocean Perch	<i>Sebastes alutus</i>				x		d
Pacific Sand Lance	<i>Ammodytes personatus</i>	x			x		c
Pacific Sanddab	<i>Citharichthys sordidus</i>	x			x		cd
Pacific Sandfish	<i>Trichodon trichodon</i>	x	x		x	x	abcde
Pacific Spiny Dogfish	<i>Squalus suckleyi</i>				x	x	de
Pacific Spiny Lumpsucker	<i>Eumicrotremus orbis</i>		x		x		abcd
Pacific Staghorn Sculpin	<i>Leptocottus armatus</i>	x			x	x	ce
Pacific Tomcod	<i>Microgadus proximus</i>	x			x	x	cde
Padded Sculpin	<i>Artedius fenestralis</i>	x					c
Painted Greenling	<i>Oxylebius pictus</i>	x					c
Penpoint Gunnel	<i>Apodichthys flavidus</i>	x					c
Petrale Sole	<i>Eopsetta jordani</i>				x		d
Pink Salmon	<i>Oncorhynchus gorbuscha</i>	x	x				ac
Pricklebreast Poacher	<i>Stellerina xyosterna</i>				x		ce
Puget Sound Rockfish	<i>Sebastes emphaeus</i>	x					c
Quillback Rockfish	<i>Sebastes maliger</i>	x				x	ce
Rainbow Smelt	<i>Osmerus mordax</i>				x		d
Red Irish Lord	<i>Hemilepidotus hemilepidotus</i>	x				x	ce
Rex Sole	<i>Glyptocephalus zachirus</i>				x		bde
Ringtail Snailfish	<i>Liparis rutteri</i>				x		c
Rock Greenling	<i>Hexagrammos lagocephalus</i>	x					ac
Rougheye Rockfish	<i>Sebastes aleutianus</i>				x		d
Sablefish	<i>Anoplopoma fimbria</i>				x	x	de
Saffron Cod	<i>Eleginus gracilis</i>				x		c

Sand Sole	<i>Psettichthys melanostictus</i>	x			x	x	ce
Scalyhead Sculpin	<i>Artedius harringtoni</i>	x			x		c
Sharpnose Sculpin	<i>Clinocottus acuticeps</i>	x					c
Shiner Perch	<i>Cymatogaster aggregata</i>	x					c
Shortfin Eelpout	<i>Lycodes brevipes</i>				x		ad
Shorthorn Sculpin	<i>Myoxocephalus scorpius</i>	x					c
Shortspine Thornyhead	<i>Sebastolobus alascanus</i>				x		d
Showy Snailfish	<i>Liparis pulchellus</i>				x		c
Silverspotted Sculpin	<i>Blepsias cirrhosus</i>	x			x		c
Slender Sole	<i>Lyopsetta exilis</i>				x		cd
Smooth Lump sucker	<i>Aptocyclus ventricosus</i>				x		d
Smoothhead Sculpin	<i>Artedius lateralis</i>	x					c
Snake Prickleback	<i>Lumpenus sagitta</i>	x			x		abc
Sockeye Salmon	<i>Oncorhynchus nerka</i>	x			x		bc
Soft Sculpin	<i>Psychrolutes sigalutes</i>			x	x		ab
Southern Rock Sole	<i>Lepidopsetta bilineata</i>				x		d
Speckled Sanddab	<i>Citharichthys stigmaeus</i>	x					c
Spinyhead Sculpin	<i>Dasycottus setiger</i>				x		abcd
Spotted Ratfish	<i>Hydrolagus colliei</i>				x		d
Starry Flounder	<i>Platichthys stellatus</i>	x			x	x	acde
Steelhead Trout	<i>Oncorhynchus mykiss</i>	x					c
Stout Eelblenny	<i>Anisarchus medius</i>			x	x		ab
Sturgeon Poacher	<i>Podothecus accipenserinus</i>				x		cd
Surf Smelt	<i>Hypomesus pretiosus</i>	x	x		x		ce

Tadpole Sculpin	<i>Psychrolutes paradoxus</i>				x		d
Threespine Stickleback	<i>Gasterosteus aculeatus</i>	x	x				ce
Tidepool Sculpin	<i>Oligocottus maculosus</i>	x					a
Tidepool Snailfish	<i>Liparis flarae</i>	x					c
Tube-nose Poacher	<i>Pallasina barbata</i>	x					c
Tube-nout	<i>Aulorhynchus flavidus</i>	x					c
Walleye Pollock	<i>Gadus chalcogrammus</i>	x		x	x	x	abcde
Wattled Eelpout	<i>Lycodes palearis</i>				x		ad
Whitebarred Prickleback	<i>Poroclinus rothrocki</i>				x		d
Whitespotted Greenling	<i>Hexagrammos stelleri</i>	x			x		ac
Wolf-Eel	<i>Anarrhichthys ocellatus</i>				x		d
Yellowfin Sole	<i>Limanda aspera</i>	x					c

a) Arimitsu et al. 2013

b) Arimitsu et al. 2017

c) Neff 2016

d) NOAA GAP

e) This Study

1.4 Information to Support an Archeological Review

1.4.1 Summary

A side scan sonar survey of the seafloor was carried out May 25-26, 2018 to the Southwest of Icy Bay and centered on a pre identified site at 59.858114° N, 142.190939° W. This survey provided a field test of the side scan sonar during the transit to the primary study area. Consistent with the preliminary analysis of the real-time side scan data, post survey reevaluation of the data revealed no further evidence of any man-made structures, aside from multiple rectangular anomalies, likely shipping containers, on the seabed adjacent to the site (e.g. Figure 26). A second survey was planned as a follow-up, but no suitable vessel was ever available when ocean conditions were favorable. Finally, the COVID-19 pandemic eliminated any remaining chance to re-survey the region around the site.

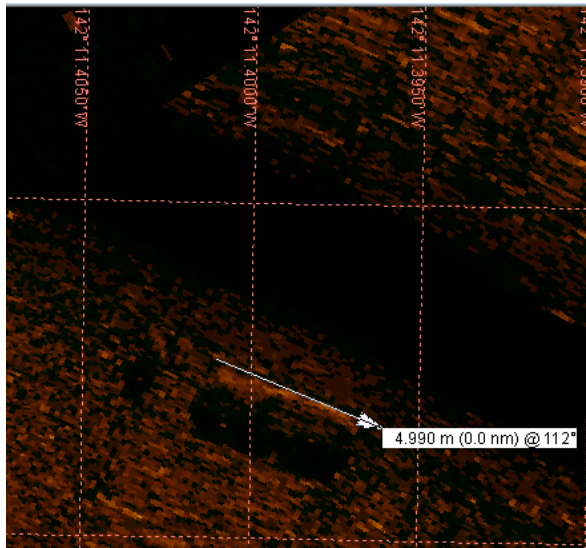


Figure 26. Side scan sonar image of a seafloor anomaly.

1.4.2 Methods

An Edgetech dual frequency 4125P dual frequency (1600 / 600 kHz) sidescan sonar tow fish package equipped with a depressor wing and weight (Figure 27) was deployed from the R/V Solstice the night of May 25- 26, 2018. The tow fish was deployed from a fixed davit off the starboard side of the vessel and cabled to the topside processor located in the wheelhouse. Water depths varied from 60-90 m in the survey area. A 150 m cable was employed along with speeds of 4-5 knots to maintain as deep a depth for the tow-fish as possible. Taking into consideration the 15 m length of the cable run from to davit to the wheelhouse, the tow-fish was expected to swim at approximately 45 m, the length of the cable scope between the davit and the towfish, divided by 3. A 64-bit Windows 10 Toughbook laptop computer located in the wheelhouse and equipped with Edgetech Discover Software (V. 37.0.1.108) and a USB GPS were used to log real time side scan data, vessel position, heading and speed. The vessel maintained a speed of 4-5 knots during the survey, less than the 6 knots maximum specified by the IHO to produce sufficient resolution to identify small targets (IHO, 2011). Weather during the survey deteriorated to the point where the side scan system was unable to continue to gather quality imagery despite being submerged to a depth of at least 20 m for the duration of the survey. The survey was concluded abruptly when the sonar stopped communicating with topside unit. It is likely the heaving vessel either accelerated the towfish into the bottom or allowed for enough slack in the cable for the towfish to sink and hit the

bottom, since upon retrieval, one of the stabilizing fins was found to be missing. Communication was reestablished the following day and the unit apparently suffered no permanent damage.



Figure 27. Edgetech 4125 side scan sonar equipped with depressor wing.

1.4.3 Analysis

The Edgetech Discover software package (V. 39.0.1.122), SonarWiz (V.5.03.0023) and Google Earth Pro (v. 7.3.3.7786) were used to review the data, identify and map and further investigate any seafloor anomalies identified during review of the data.

1.4.4 Results

Sixteen features of interest were identified during review of the sonar imagery. These sixteen anomalies were mapped (**Figure 28.**, Figure 28, Figure 29) and then individual sonar data frames were examined to extract details of the features such length, width and height (based on shadow length, when possible).



Figure 28. Wide area map of the location of the side scan seafloor survey.

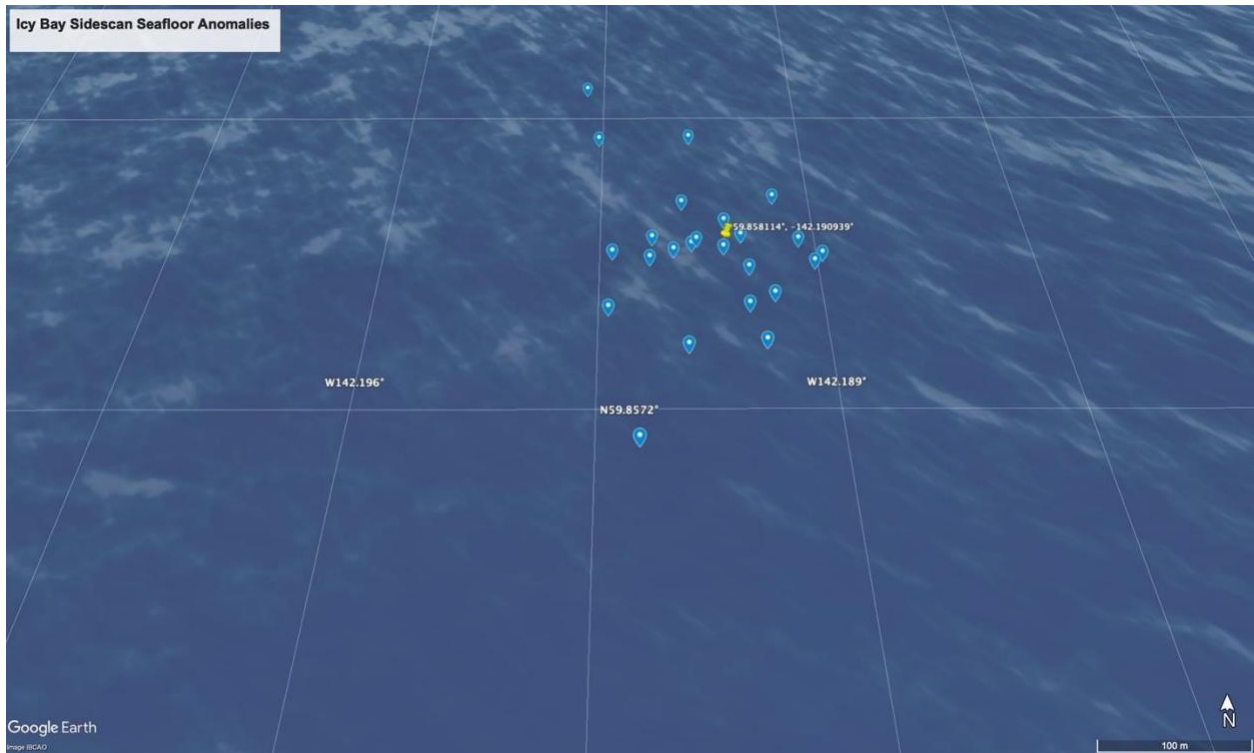


Figure 28. Detailed view of side scan sea floor anomalies.

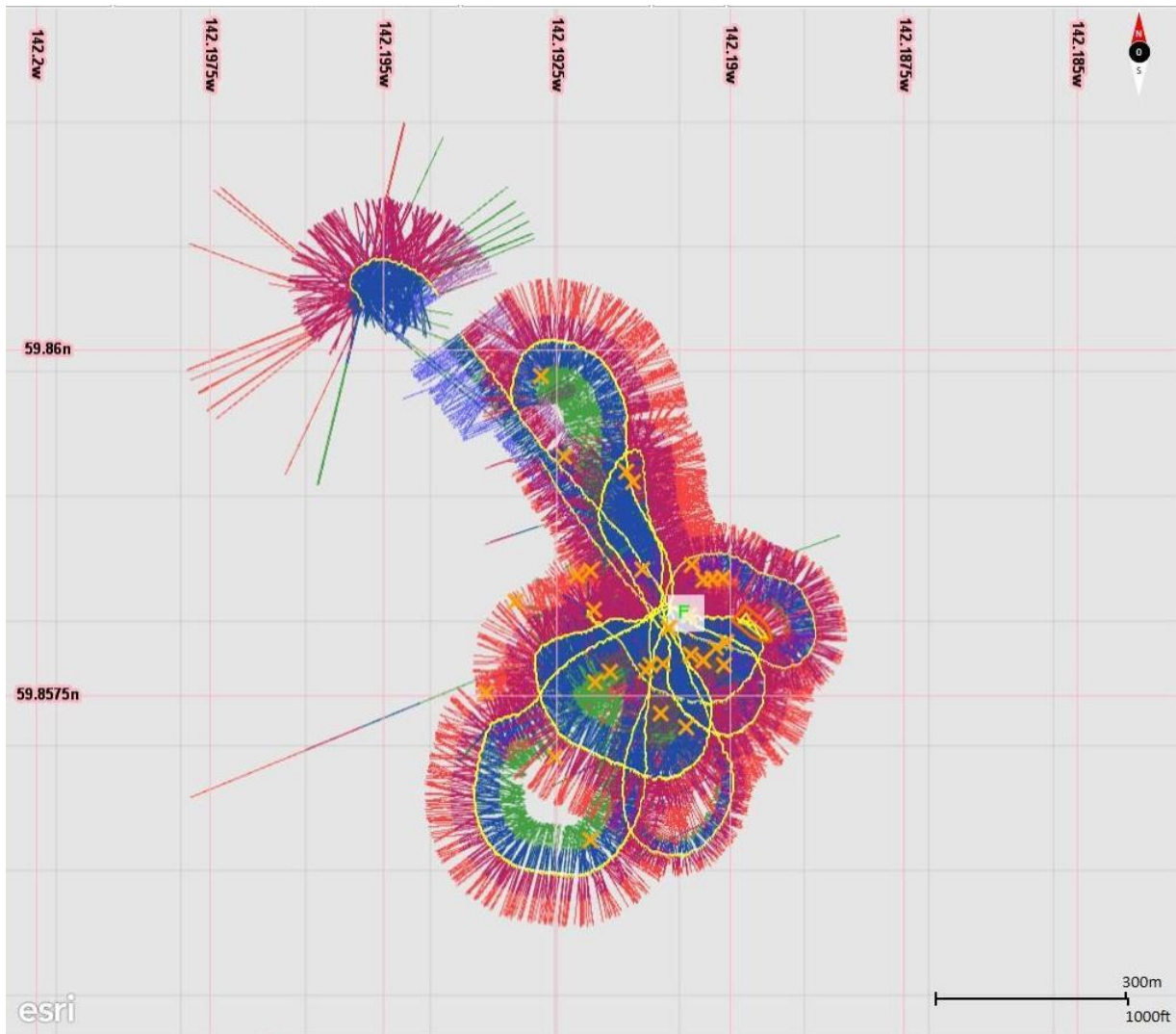


Figure 29. Side scan survey path. X's mark the location of the anomalies shown in previous figures.

Different color palettes and contrast values were used to enhance anomaly features during review of the data (e.g. Fish and Carr, 1990). Example images are shown above (Figure 26) and below (Figure 30, Figure 31). The images are illustrative of the multiple, rectangular seafloor targets, i.e., likely shipping containers, identified during the survey.

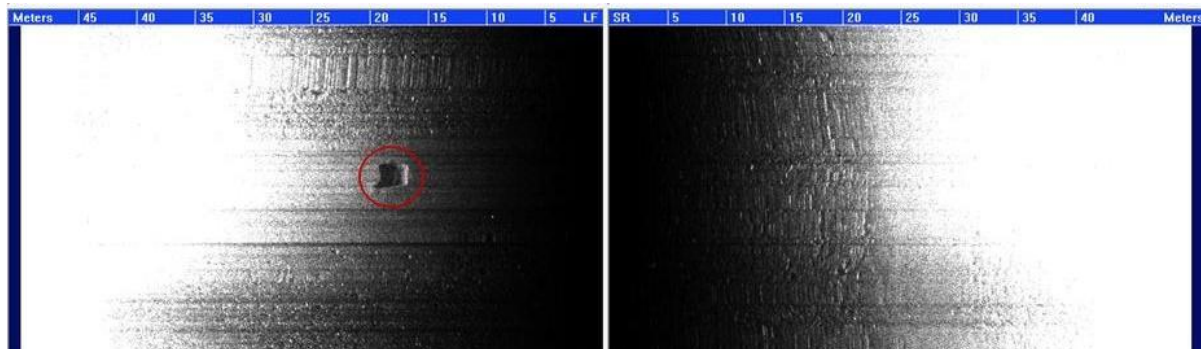


Figure 30. Example output from Edgetech Discover software.

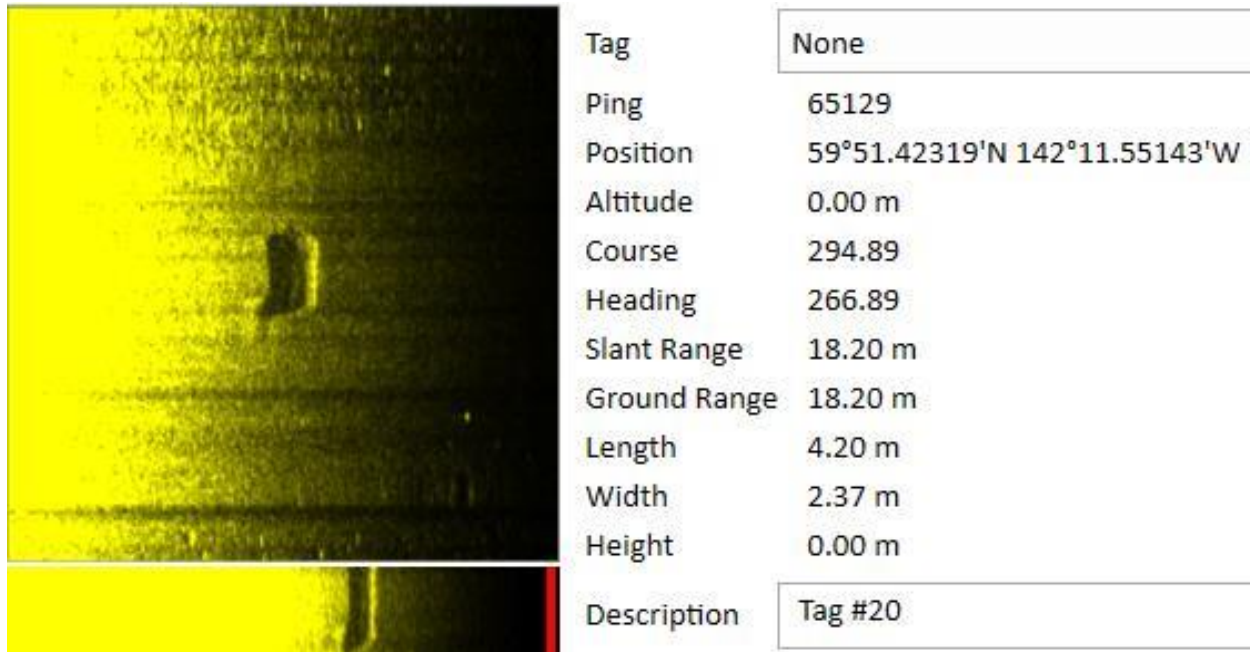


Figure 31. Close up view with a different color palette of the anomaly shown in Figure 30.

1.4.5 Discussion and Conclusions

While the side scan seafloor survey was abbreviated due to deteriorating weather and a subsequent equipment malfunction, no evidence was found of any man-made structures on the seafloor aside from numerous rectangular objects that appear to be shipping containers. Overall, no targets were identified during this work that would justify further fine scale surveys such as the one carried out as part of this work and described herein. If any further reconnaissance work is undertaken, a wide(r) area grid should first be surveyed using a lower frequency side scan sonar unit (e.g., an Edgetech 4125 400/900 kHz unit or similar) and/or a multibeam echo sounder capable of collecting backscatter and water column information in order to identify targets for follow-on surveying with a higher frequency side scan sonar system (IHO, 2011).

1.5 Evaluation of Oceanography and Sedimentation Effects of Wave Energy Converters.

1.5.1 Summary

Oceanographic sampling was carried out in conjunction with the other tasks outlined above. In particular, 24 CTD stations were occupied from the R/V Solstice between May 22-24, 2018, overlapping with the trawl survey work. A towed ADCP-sled system was deployed at this time as well, but due to rough sea conditions that induced significant motion in the sled, the data proved unusable. This data is not discussed further. Immediately following the trawl survey, a multibeam bathymetric survey including 110 CTD casts was carried out between May 30 and June 7, 2018 from the F/V Quest. Twenty topographic beach elevation transects were surveyed at the same time the multibeam survey was being carried out. A photogrammetric elevation survey was carried out at this time as well using an Unmanned Aerial Vehicle. Unfortunately, the UAV suffered from navigation issues during the survey including inconsistent flight altitudes and angled camera photo captures likely caused by strong winds. A lack of ground control points during the survey meant there was no way to correct for these issues in postprocessing. Comparisons

between the photogrammetrically derived elevations and the transect data showed large and inconsistent errors in the UAV measured elevations that were not able to be corrected. A subsequent survey in 2019 carried out with separate funding was used to generate a useful and accurate Digital Terrain Model (10 cm accuracy in the vertical and horizontal, Kasper, 2021). So the 2019 DTM is compared to the transect measurements.

As described in section 1.2.2.2, three oceanographic moorings equipped with ADVs, ADCPs, CTDs and turbidity sensors were deployed as part of this work. Overall, the deep mooring, DM, produced a 1+ year time series of waves, currents and hydrography at the deep site. Even though they were ultimately lost, the shallow (SM) and mid (MM) moorings produced 6 months of usable data.

1.5.2 Methods

1.5.2.1 Hydrography During the Trawl Survey

A total of 24 CTD casts were taken during the trawl survey from the F/V Solstice using a Seabird 25 CTD/SBE 55 water sampler and a Sequoia Laser In Situ Size and Transmissivity 100X sensor (Figure 33; Figure 34; Table 10). The SBE CTD package was equipped with external PAR (Biospherical Instruments QSP 2300), Transmissivity (WET Labs ECO FLNTURT), Fluorometry (WET Labs ECO FLNTURT) and altimetry sensors for making water column measurements of conductivity (Salinity), temperature, pressure as well as of photosynthetically available radiation (PAR), transmissivity and chlorophyll A (fluorometer) and elevation above the bottom (altimeter). The LISST measures scattering angles and transmissivity. The SBE-25 sampled at 16 Hz and was lowered through the water column at a rate of $\sim 3 \text{ m s}^{-1}$ so that 5 samples/ meter were collected. Measured variables include pressure, temperature, conductivity, beam transmission, fluorescence and PAR. Derived variables include depth (m), salinity, potential temperature ($^{\circ}\text{C}$), density (kg /m^3) and speed of sound (m/s). A particle size distribution is derived from the scattering measurements made by the LISST.

The SBE 55 water sampler includes a 6-bottle carousel equipped with 4-liter bottles as well as a deck unit (SBE 33) and an electronics control module to allow for real time read out of the measurements. Bottles were used for taking discrete water column samples for nutrients (ammonium, nitrite, nitrate, phosphate, silicate) and total suspended solids (TSS) (Table 10). Also, two bottom grab samples were collected with a Wildco “petite” Stainless steel ponar grab with 0.1 m^2 sample area with additional weight added to obtain better grabs in challenging bottom conditions. The grab samples were sent to the Central Analytical Laboratory at Oregon State University for analysis. The analysis procedure is described in Appendix II. More unsuccessful attempts were made to gather additional grab samples but the drifting vessel and challenging bottom conditions made sampling difficult.

To measure TSS, water samples were filtered through a $1.5 \mu\text{m}$ binder free, glass microfiber filter that was vacuum rinsed three times with 20mL aliquots of reagent free water and dried at 105°C for at least one hour. The samples were processed following ASTM standard methods 2005, 2540D and EPA (1983) Method 160.2 (Residue, non-filterable) in the UAF WERC lab.

Nutrient samples were analyzed by the UAF Nutrient Analytical Facility. Field samples were prepared following Mordy et al. (2005). Samples were syringe-filtered using $0.45\text{-}\mu\text{m}$ cellulose acetate membranes, and the filtrate was collected in 30-mL acid-washed high-density polyethylene bottles after three rinses. Samples were frozen at -20°C with care to leave appropriate head space and to freeze upright. Nutrient Analyses (nitrate plus nitrite, nitrite, phosphate, silicate, and ammonia) are performed on a Seal Analytical continuous-flow QuAAtro39 AutoAnalyzer. Frozen samples are thawed overnight at approximately 1.8°C and brought to room temperature prior to analysis. Following each run peaks are reviewed for any problems, any blank is subtracted and final concentrations (in micromoles per liter) are calculated based on a linear curve fit using Seal Analytical AACE 7.07 software.

For nitrate analysis a modification of the Armstrong et al. (1967) procedure is used where nitrate is reduced to nitrite at pH 8 in a copperized cadmium reduction coil. The nitrite reduced from nitrate plus any nitrite react with sulfanilamide to form a diazo compound that then couples with N-1-naphthylethylenediamine dihydrochloride (NEDD) to form a red dye that is measured at 550 nm. The procedure is the same for the nitrite analysis but without the cadmium column.

Phosphate is analyzed using a modification of Murphy and Riley (1962) where a blue color is formed when phosphate reacts with molybdate ion and antimony ion followed by reduction with ascorbic acid. The reduced blue phosphor-molybdenum complex is read at 880 nm.

The procedure for the determination of soluble silicates, using a modification of Armstrong (1967), is based on the reduction of silico molybdate in acid solution to molybdenum blue by ascorbic acid. Oxalic acid is added to inhibit phosphate color interference. Absorbance is measured at 820 nm. To avoid low silicate values caused by potential polymerization during frozen storage the samples are returned to the refrigerator for 24 hours and analyzed a second time for silicate the following day.

Ammonia is measured fluorometrically using a modification of Kerouel and Aminot (1997). The sample reacts with o-phthalaldehyde at 75°C in the presence of borate buffer and sodium sulfite to form a fluorescent compound proportional to the ammonia concentration. The fluorescence is measured at 460 nm following excitation at 370 nm.

Reagent solutions and primary and secondary standards are prepared with fresh Milli-Q water and working standards are prepared daily with low nutrient artificial seawater. Primary standards for nitrate (KNO_3), nitrite (NaNO_2), phosphate (KH_2PO_4), silicate (Na_2SiF_6), and ammonia ($(\text{NH}_4)_2\text{SO}_4$) with reported purities of 99.999%, 99.999%, 99+%, 99%, and 99+%, respectively, are sourced from Fisher Scientific and/or VWR. For each sample run, standardizations are performed at the beginning and Certified Reference Materials for Nutrients in Seawater (RMNS) obtained from KANSO CO., LTD. are measured throughout.

SEAL Analytical methods and laboratory detection limits (in $\mu\text{mol/L}$):

Nitrate: No. Q-119-11 Rev. 1, detection limit 0.05

Nitrite: No. Q-054-04 Rev. 2, detection limit 0.02

Phosphate: No. Q-048-04 Rev. 3, detection limit 0.02

Silicate: No. Q-050-04 Rev. 1, detection limit 0.06

Ammonia: No. Q-080-06 Rev. 5, detection limit 0.01 (published SEAL LoD)



Figure 32. The Seabird 25 CTD and SBE55 water sampler with the LISST100X attached to the frame.



Figure 33. Location SBE (green diamonds) and of AML (red circles) CTD casts taken between May and June 2018.

Table 10. Location of CTD stations+LISST100X carried out using the SBE25 CTD during the trawl survey.

Station Type	Station Name	Latitude (°N)	Longitude (°E)	UTC Date	UTC Time	# of Nutrient samples	# of Total Suspended Solids sampled
CTD+LI SST	YB1	59.615467	-139.84623	5/22/2018	17:46	0	0
CTD+LI SST	YB2	59.604283	-139.85578	5/22/2018	18:09	0	0
CTD+LI SST	CB1	59.484217	-139.82568	5/22/2018	21:28	0	0
CTD+LI SST	CB2	59.478167	-139.80608	5/22/2018	22:32	3	0
CTD+LI SST	CB3	59.467017	-139.74212	5/22/2018	23:42	0	0
CTD+LI SST	CB4	59.4736	-139.77272	5/23/2018	20:52	0	0
CTD+LI SST	CB7	59.440167	-139.75477	5/23/2018	23:12	2	2
CTD+LI SST	CB8	59.4749	-139.75223	5/24/2018	0:43	2	2
CTD+LI SST	CB9	59.484333	-139.84308	5/24/2018	17:50	1	1
CTD+LI SST	CB10	59.486817	-139.82787	5/24/2018	18:07	1	1
CTD+LI SST	CB12	59.495217	-139.803	5/24/2018	18:30	3	2
CTD+LI SST	CB13	59.487567	-139.7779	5/24/2018	18:49	3	3
CTD+LI SST	CB14	59.483383	-139.78927	5/24/2018	19:11	0	0

CTD+LI SST	CB15	59.476483	-139.79937	5/24/2018	19:21	3	3
CTD+LI SST	CB16	59.473267	-139.81368	5/24/2018	19:42	0	0
CTD+LI SST	CB17	59.397567	-139.61523	5/24/2018	20:45	3	3
CTD+LI SST	CB18	59.403	-139.60438	5/24/2018	21:06	0	0
CTD+LI SST	CB19	59.408683	-139.59188	5/24/2018	21:16	2	2
CTD+LI SST	CB20	59.415533	-139.58407	5/24/2018	21:29	3	3
CTD+LI SST	CB21	59.405633	-139.55885	5/24/2018	21:50	0	0
CTD+LI SST	CB22	59.399917	-139.55952	5/24/2018	21:58	3	3
CTD+LI SST	CB23	59.392967	-139.57762	5/24/2018	22:17	0	0
CTD+LI SST	CB24	59.387967	-139.58198	5/24/2018	22:25	3	3

1.5.2.2 June 2018 Multibeam Bathymetry, Topographic Elevation and Hydrographic Surveys

To carry out the multibeam survey, a Reson 7125 Seabat multibeam sonar was mounted to the gunwale of the F/V Quest using a pole mount. An Applanix POSMV GNSS + Inertial Measurement Unit was mounted on pole on the starboard gunwale (Figure 34- Figure 36). The sonar transducer and projector were mounted on the same pole, in the water. The pole is swung up to remove the transducers from the water during transit. The transducer is swung back into the water for survey operations. A GNSS base station was setup on the beach each day to provide real time kinematic (RTK) position corrections to the POSMV (Figure 37).

The multibeam sonar was installed on the F/V Quest and a calibration was conducted on 5/29 in Yakutat Bay. Survey operations off Cannon Beach were initiated on 5/30 and continued until 6/7/2018. At any one time, two staff members were conducting vessel-based survey work while two staff members were conducting shoreside elevation and UAV surveys. Staff rotated between vessel and shore-based surveying to reduce fatigue.

To determine whether post processed kinematic (PPK) corrections improved upon the RTK corrections, position data for the bathymetric survey were post-processed using the Applanix POSPAC software

package and compared to RTK positions. Overall, positional accuracies of ± 2 cm were achieved in both the vertical and horizontal using the RTK corrections. PPK corrections were accurate to ± 5 cm. Thus the RTK solution was used to produce the final product. Multibeam soundings were post processed with CARIS HIPS including correcting for sound speed variations derived from CTD measurements described below.

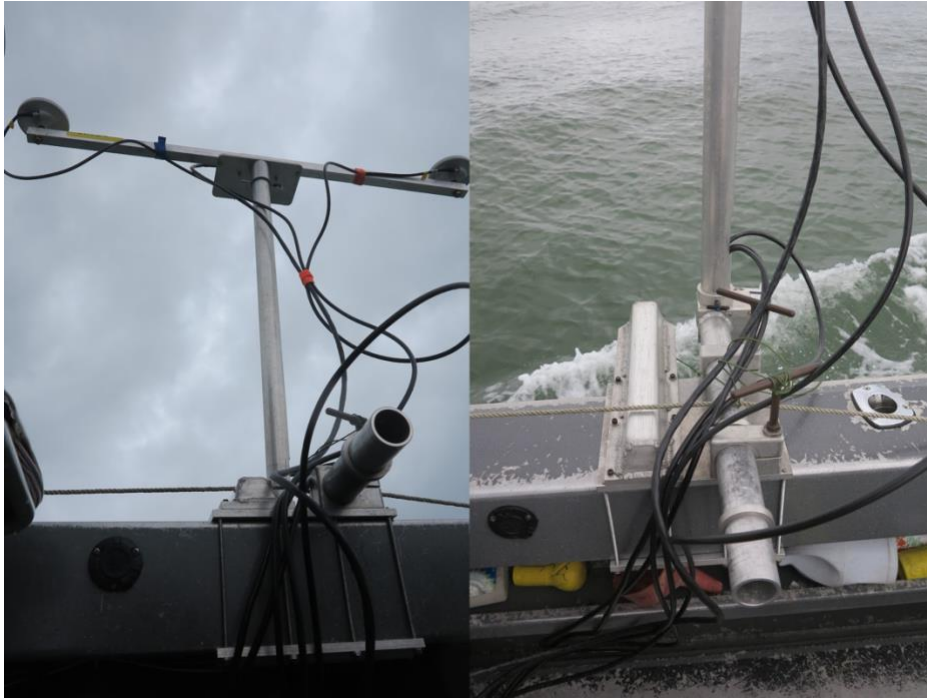


Figure 34 Left: GNSS antennae and IMU mounted on a pole on the starboard gunwale of the F/V Quest. Right.: gunwale adapter.



Figure 35. Vertical pole stabilizer for the multibeam pole mount on the starboard gunwale of the F/V Quest.



Figure 36. Setup of the Reson Seabat operating system in the cabin of the F/V Quest.



Figure 37. Setting up the Trimble R8 base station broadcasting real time kinematic corrections to the F/V Quest for the multibeam survey.

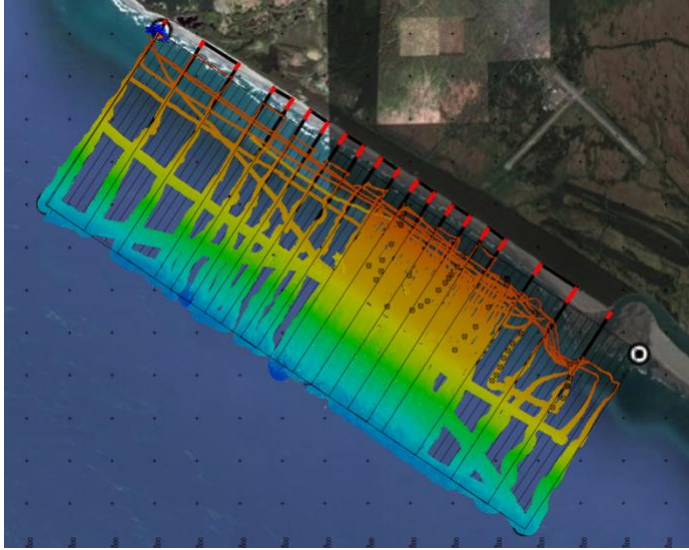


Figure 38. 2018 multibeam survey coverage. Historical penetrometer samples (circles with crosses) are shown as well. The Situk River estuary is in the SE corner of this image.

An AML Oceanographic MinosX CTD equipped with an nephelometric turbidity sensor (AML Turbidity Xchange autoranging, 0-3000 NTU nephelometric sensor, compliant with the ISO 7027 standard, and calibrated with AMCO Clear, an EPA-certified primary standard, designated CTD+Tu) was utilized during the multibeam survey (Figure 40); 110 sensor only CTD+Tu casts were taken during the multibeam survey (Table 11; Figure 34). CTD data was used for soundspeed correction of the multibeam sounding data. The AML CTD sampled at 25 Hz and was lowered at ~3 m/s so that 8 samples/ meter were collected. Measured variables include pressure, temperature, conductivity and optical backscatter. Derived variables include depth (m), salinity, potential temperature ($^{\circ}\text{C}$), density (kg/m^3), speed of sound (m/s) and turbidity (NTU).

CTD data were processed following Kelley (2018) and were screened for anomalous spikes, dropouts, and density inversions. Both the SBE and AML CTD data were separated into up- and down-cast data. Downcast data were then binned into 0.5 m bins.



Figure 39. The AML CTD+Tu being deployed from the F/V Quest.

Two halibut fishing rods were used to deploy the AML CTD+Tu.

Table 11. Location, date and time of the AML CTD (CTD+Tu) casts taken during the multibeam sonar survey.

Station Type	Station Name	Lat (°N)	Long (°E)	UTC Date	UTC Time
CTD+Tu	AML1	59.52323	-139.83027	5/30/18	13:54
CTD+Tu	AML2	59.50783	-139.85292	5/30/18	14:15
CTD+Tu	AML3	59.48898	-139.87835	5/30/18	14:41
CTD+Tu	AML4	59.48366	-139.86267	5/30/18	14:53
CTD+Tu	AML5	59.50345	-139.83645	5/30/18	15:12
CTD+Tu	AML6	59.51945	-139.81685	5/30/18	15:31
CTD+Tu	AML7	59.51438	-139.80159	5/30/18	15:38
CTD+Tu	AML8	59.49782	-139.82393	5/30/18	15:55

CTD+Tu	AML9	59.47779	-139.84885	5/30/18	16:19
CTD+Tu	AML10	59.47278	-139.83370	5/30/18	16:33
CTD+Tu	AML11	59.49345	-139.80802	5/30/18	16:52
CTD+Tu	AML12	59.50888	-139.78909	5/30/18	17:07
CTD+Tu	AML13	59.50609	-139.78049	5/30/18	17:12
CTD+Tu	AML14	59.48971	-139.80137	5/30/18	17:29
CTD+Tu	AML15	59.46999	-139.82764	5/30/18	17:53
CTD+Tu	AML16	59.46759	-139.81807	5/31/18	9:16
CTD+Tu	AML17	59.48786	-139.79419	5/31/18	9:35
CTD+Tu	AML18	59.50188	-139.77624	5/31/18	9:48
CTD+Tu	AML19	59.49888	-139.76818	5/31/18	9:52
CTD+Tu	AML20	59.48373	-139.78908	5/31/18	10:09
CTD+Tu	AML21	59.46492	-139.81527	5/31/18	10:33
CTD+Tu	AML22	59.46294	-139.80611	5/31/18	10:42
CTD+Tu	AML23	59.48263	-139.78165	5/31/18	10:59
CTD+Tu	AML24	59.49664	-139.76300	5/31/18	11:14
CTD+Tu	AML25	59.49395	-139.75468	5/31/18	11:18
CTD+Tu	AML26	59.47895	-139.77396	5/31/18	11:34
CTD+Tu	AML27	59.45983	-139.79739	5/31/18	12:00
CTD+Tu	AML28	59.45784	-139.79040	5/31/18	12:08
CTD+Tu	AML29	59.47760	-139.76564	5/31/18	12:26
CTD+Tu	AML30	59.49158	-139.74591	5/31/18	12:40

CTD+Tu	AML31	59.49029	-139.73849	5/31/18	12:45
CTD+Tu	AML32	59.47360	-139.75928	5/31/18	13:02
CTD+Tu	AML33	59.45454	-139.78310	5/31/18	13:23
CTD+Tu	AML34	59.48719	-139.87835	6/3/18	9:03
CTD+Tu	AML35	59.48719	-139.87835	6/3/18	9:03
CTD+Tu	AML36	59.47283	-139.76188	6/3/18	9:52
CTD+Tu	AML37	59.46266	-139.67451	6/3/18	10:26
CTD+Tu	AML38	59.48646	-139.74019	6/3/18	11:03
CTD+Tu	AML39	59.52148	-139.83691	6/3/18	11:43
CTD+Tu	AML40	59.43747	-139.66971	6/3/18	13:15
CTD+Tu	AML41	59.50478	-139.85450	6/3/18	14:46
CTD+Tu	AML42	59.46834	-139.72764	6/4/18	9:29
CTD+Tu	AML43	59.48728	-139.73186	6/4/18	9:50
CTD+Tu	AML44	59.47423	-139.70865	6/4/18	10:05
CTD+Tu	AML45	59.46429	-139.72877	6/4/18	10:19
CTD+Tu	AML46	59.45548	-139.71043	6/4/18	10:29
CTD+Tu	AML47	59.46990	-139.68896	6/4/18	10:45
CTD+Tu	AML48	59.46332	-139.67847	6/4/18	10:52
CTD+Tu	AML49	59.44841	-139.69684	6/4/18	11:06
CTD+Tu	AML50	59.44351	-139.67127	6/4/18	11:18
CTD+Tu	AML51	59.45313	-139.66015	6/4/18	11:30
CTD+Tu	AML52	59.43069	-139.71876	6/4/18	12:03

CTD+Tu	AML53	59.44529	-139.75869	6/4/18	12:27
CTD+Tu	AML54	59.47421	-139.72242	6/4/18	12:55
CTD+Tu	AML55	59.49379	-139.78224	6/4/18	13:25
CTD+Tu	AML56	59.51459	-139.84399	6/4/18	13:55
CTD+Tu	AML57	59.51444	-139.84360	6/4/18	13:56
CTD+Tu	AML58	59.47645	-139.75973	6/7/18	8:52
CTD+Tu	AML59	59.48587	-139.74134	6/7/18	9:07
CTD+Tu	AML60	59.48723	-139.74192	6/7/18	11:49
CTD+Tu	AML61	59.46749	-139.68774	6/7/18	12:19
CTD+Tu	AML62	59.51921	-139.83337	6/7/18	13:16
CTD+Tu	AML63	59.45295	-139.78368	6/1/18	9:08
CTD+Tu	AML64	59.45224	-139.77705	6/1/18	9:16
CTD+Tu	AML65	59.47171	-139.75273	6/1/18	9:35
CTD+Tu	AML66	59.48615	-139.73195	6/1/18	9:50
CTD+Tu	AML67	59.48435	-139.72497	6/1/18	9:55
CTD+Tu	AML68	59.46966	-139.73476	6/1/18	10:09
CTD+Tu	AML69	59.44946	-139.76917	6/1/18	10:30
CTD+Tu	AML70	59.44842	-139.76128	6/1/18	10:37
CTD+Tu	AML71	59.46704	-139.73978	6/1/18	10:53
CTD+Tu	AML72	59.48196	-139.71725	6/1/18	11:06
CTD+Tu	AML73	59.47956	-139.70959	6/1/18	11:10
CTD+Tu	AML74	59.46470	-139.72895	6/1/18	11:24

CTD+Tu	AML75	59.44430	-139.75431	6/1/18	11:46
CTD+Tu	AML76	59.44235	-139.74612	6/1/18	11:55
CTD+Tu	AML77	59.46119	-139.72295	6/1/18	12:11
CTD+Tu	AML78	59.47835	-139.70073	6/1/18	12:26
CTD+Tu	AML79	59.47561	-139.69403	6/1/18	12:31
CTD+Tu	AML80	59.45885	-139.71424	6/1/18	12:46
CTD+Tu	AML81	59.44039	-139.74405	6/2/18	10:08
CTD+Tu	AML82	59.43512	-139.72812	6/2/18	10:16
CTD+Tu	AML83	59.45616	-139.70368	6/2/18	10:42
CTD+Tu	AML84	59.46825	-139.68377	6/2/18	11:00
CTD+Tu	AML85	59.46160	-139.67121	6/2/18	11:09
CTD+Tu	AML86	59.44993	-139.68777	6/2/18	11:21
CTD+Tu	AML87	59.42980	-139.71295	6/2/18	11:40
CTD+Tu	AML88	59.42465	-139.69866	6/2/18	11:52
CTD+Tu	AML89	59.44600	-139.67047	6/2/18	12:18
CTD+Tu	AML90	59.45432	-139.65905	6/2/18	12:28
CTD+Tu	AML91	59.44861	-139.64411	6/2/18	12:37
CTD+Tu	AML92	59.43652	-139.66062	6/2/18	12:47
CTD+Tu	AML93	59.41908	-139.68270	6/2/18	13:24
CTD+Tu	AML94	59.48411	-139.73743	6/5/18	9:26
CTD+Tu	AML95	59.47255	-139.75615	6/5/18	9:39
CTD+Tu	AML96	59.45278	-139.77146	6/5/18	10:01

CTD+Tu	AML97	59.46016	-139.72990	6/5/18	11:20
CTD+Tu	AML98	59.46179	-139.73683	6/5/18	11:57
CTD+Tu	AML99	59.48253	-139.72117	6/5/18	12:23
CTD+Tu	AML100	59.47985	-139.71572	6/5/18	12:27
CTD+Tu	AML101	59.46885	-139.68825	6/6/18	9:45
CTD+Tu	AML102	59.43838	-139.73288	6/6/18	10:10
CTD+Tu	AML103	59.47132	-139.69298	6/6/18	10:44
CTD+Tu	AML104	59.47124	-139.69685	6/6/18	10:48
CTD+Tu	AML105	59.47414	-139.74642	6/6/18	11:28
CTD+Tu	AML106	59.46564	-139.73943	6/6/18	12:09
CTD+Tu	AML107	59.47211	-139.72994	6/6/18	12:54
CTD+Tu	AML108	59.46267	-139.72358	6/6/18	13:20
CTD+Tu	AML109	59.47207	-139.70696	6/6/18	13:46
CTD+Tu	AML110	59.44226	-139.74203	6/6/18	14:11

A Trimble GNSS base station (Figure 40) and rover (Figure 41) were used to re-survey elevations of 20 transects along Cannon Beach. Transect survey data were post-processed using OPUS corrections to obtain positional accuracy of +/- 3 cm in both the vertical and horizontal. These same transects were previously occupied the Alaska Division of Geological and Geophysical Surveys in 2014. The original 2014 transect data can be accessed through the DGGs Coastal Hazards Alaska Coastal Profile Tool (<https://maps.dggs.alaska.gov/acpt/>). Transect locations (red) are shown in relation to multibeam transects (black) in Figure 42.



Figure 40. The Trimble GNSS base station set up to broadcast real time kinematic position corrections to the GNSS rover used to survey beach elevations.



Figure 41. UAF staff preparing to survey Cannon Beach using a GNSS rover.

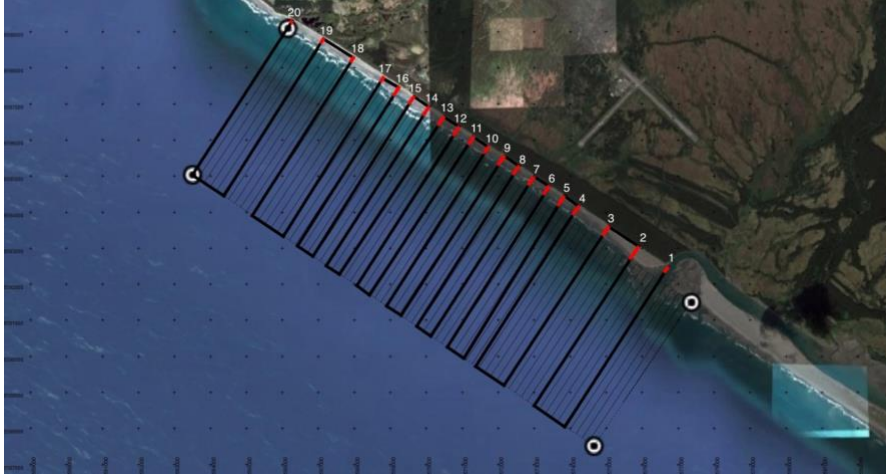


Figure 42. Beach elevation transects occupied in 2018 and 2014 in red using GNSS surveying techniques.

Black transects offshore are the multibeam transects occupied in 2018. Beach elevation transect 1 marks the edge of the Situk River estuary.

1.5.2.3 Oceanographic Moorings

Spectral analyses of velocity and pressure data recorded by the ADCPs with RDI Velocity software (Teledyne 2017a and 2017b) provided estimates of surface wave parameters, including significant wave height (H_s), peak wave period (T_p), peak (D_p) and mean (D_m) wave direction and directional spreading (S_0), where

$$S_0 = \sum_{i=loFreq}^{hiFreq} \left(\sqrt{2.0 \times \left(1 - \sqrt{A1_i^2 + B1_i^2} \right)} \right) \Delta f \quad (1)$$

the high and low frequency thresholds were 0.5 and 0.05 seconds, respectively, $A1$ and $B1$ represent the Fourier coefficients from the Fast Fourier Transform, and Δf is the step in frequency (Teledyne 2017a). Time series of surface wave parameters and water temperature ($^{\circ}\text{C}$) were compiled from burst data in MATLAB following Sullivan et al. (2006) and shown here as timeseries figures and a wave rose for each mooring over the duration of the deployments. Annual and monthly statistics of wave data were calculated in MATLAB (MathWorks 2019) for both moorings, including the mean (μ), median, maximum, minimum, 10th and 90th percentiles, and the standard deviation (σ), defined as the square root of the variance with Eq. 2,

$$\sigma = \sqrt{\frac{1}{N-1} \sum_{i=1}^N |X_i - \mu|^2} \quad (2)$$

where N represents the number of observations, and X is the variable of interest (e.g., H_s , T_p , D_p).

Overall, ~6 months of sensor data is available from the shallow and mid moorings while ~1 year of data is available from the deep mooring with the following exceptions: it was apparent when examining the CTD

and turbidity records from the deep mooring that the mooring was buried early in second half of the deployment at which point the OBS sensors and CTD no longer provided accurate measurements. Similarly, the OBS sensors at the shallow mooring only provided ~3 months of valid measurements. Thus there is an incomplete record of turbidity and hydrography for the deep mooring and an incomplete record of turbidity from the shallow mooring.

1.5.3 Results

1.5.3.1 Vessel-Based Hydrography

Selected results from the water samples are shown in Figure 43 through Figure 45.

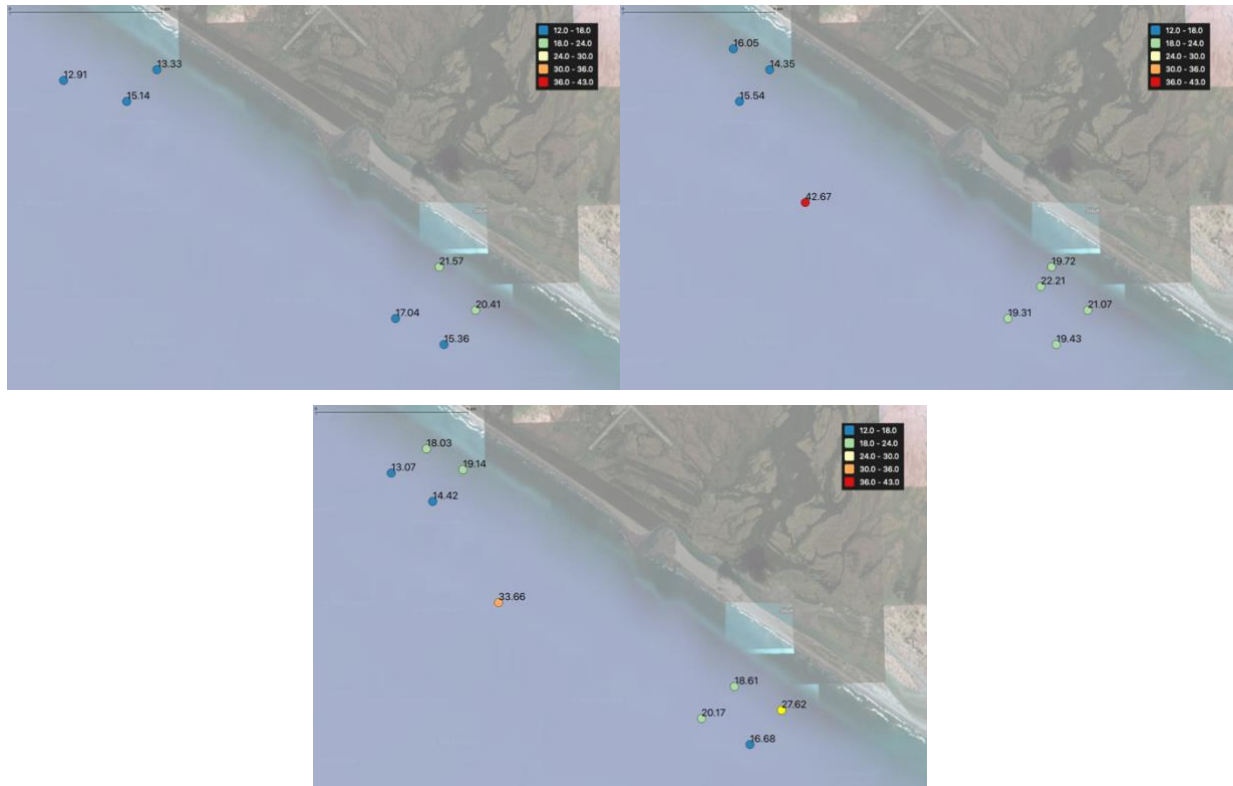


Figure 43. Total Suspended Solids (mg/L) from May 2018. Top left: TSS at the surface (water depths < 2 m). Top right: TSS in the middle of the water column (water depths between 2 and 20 m). Bottom: TSS at the bottom (water depth > 20 m).

There are no clear trends in TSS though there are only a limited number of samples.



Figure 44 Nitrate (µM) from May 2018. Top left: Nitrate at the surface (water depths < 2 m). Top right: Nitrate in the middle of the water column (water depths between 2 and 20 m). Bottom: Nitrate at the bottom (water depth > 20 m).

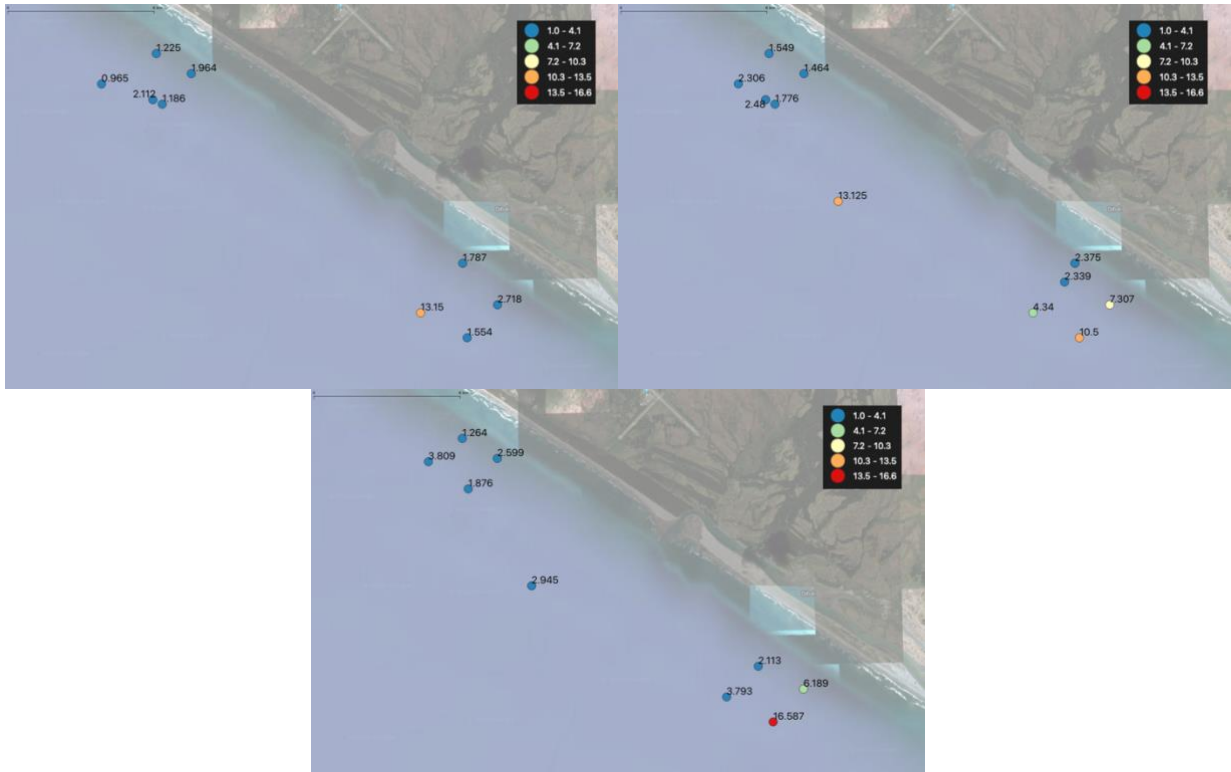


Figure 45. Ammonium (μM) from May 2018. Top left: Ammonium at the surface (water depths $< 2\text{ m}$). Top right: Ammonium in the middle of the water column (water depths between 2 and 20 m). Bottom: Ammonium at the bottom (water depth $> 20\text{ m}$).

In general, the water offshore Cannon Beach during May and June 2018 was warm and salty (temperatures of $\sim 8\text{ }^{\circ}\text{C}$ and bottom temperatures $\sim 7\text{ }^{\circ}\text{C}$) and low in nutrients (Figure 43 through Figure 45). At depths $> 10\text{ m}$, salinities ranged from 31.7 to 28.5 (Figure 46 and Figure 47). Data from two representative casts, one SE of the Situk River and one to the NW of the Situk are shown below. Only at depths shallower than 10m, is there strong evidence of very fresh riverine water (salinities of 5) along the coast in this region during the May and June sampling.

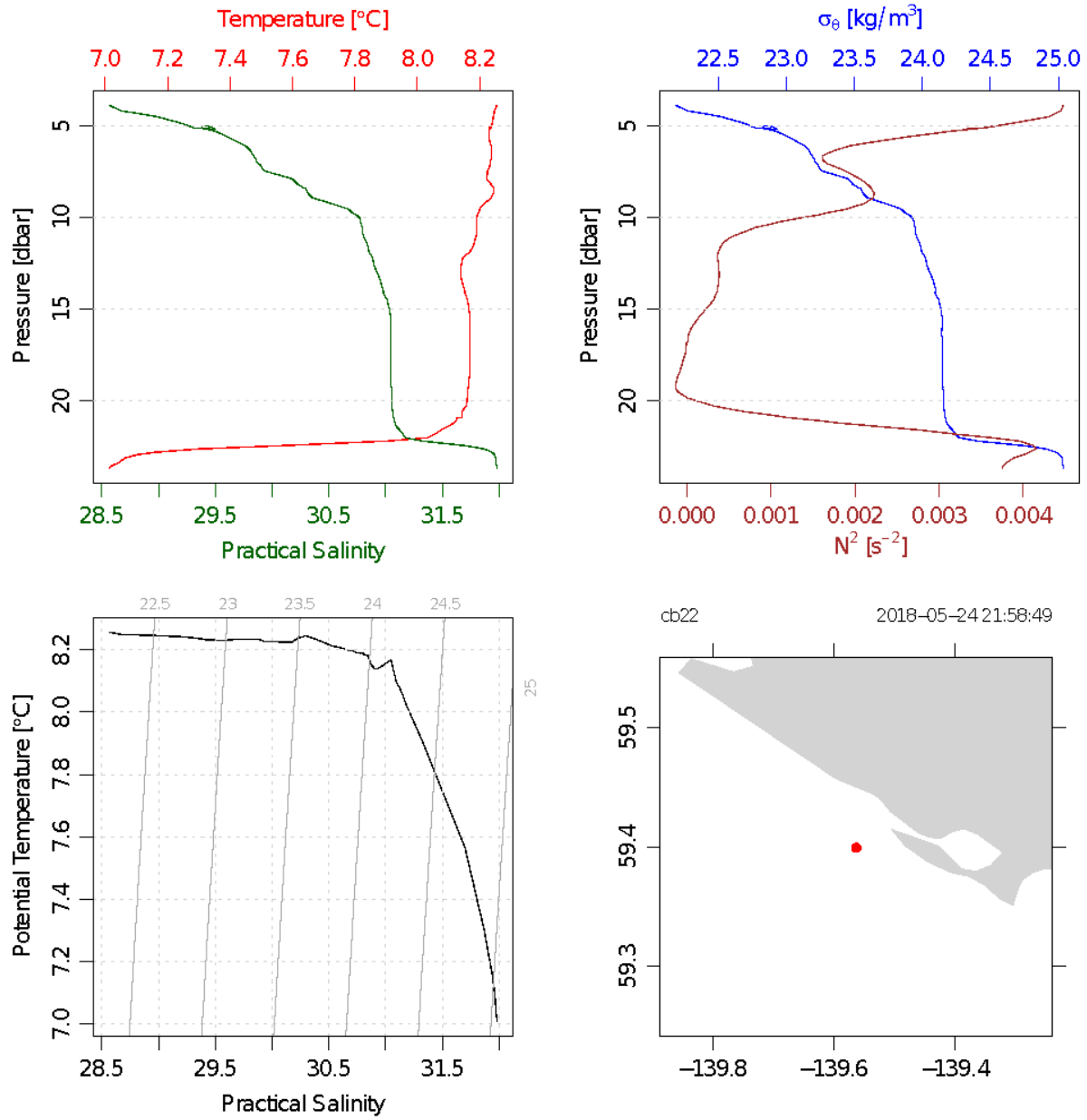


Figure 46. CTD cast from station CB22 to the SW of the Situk River.

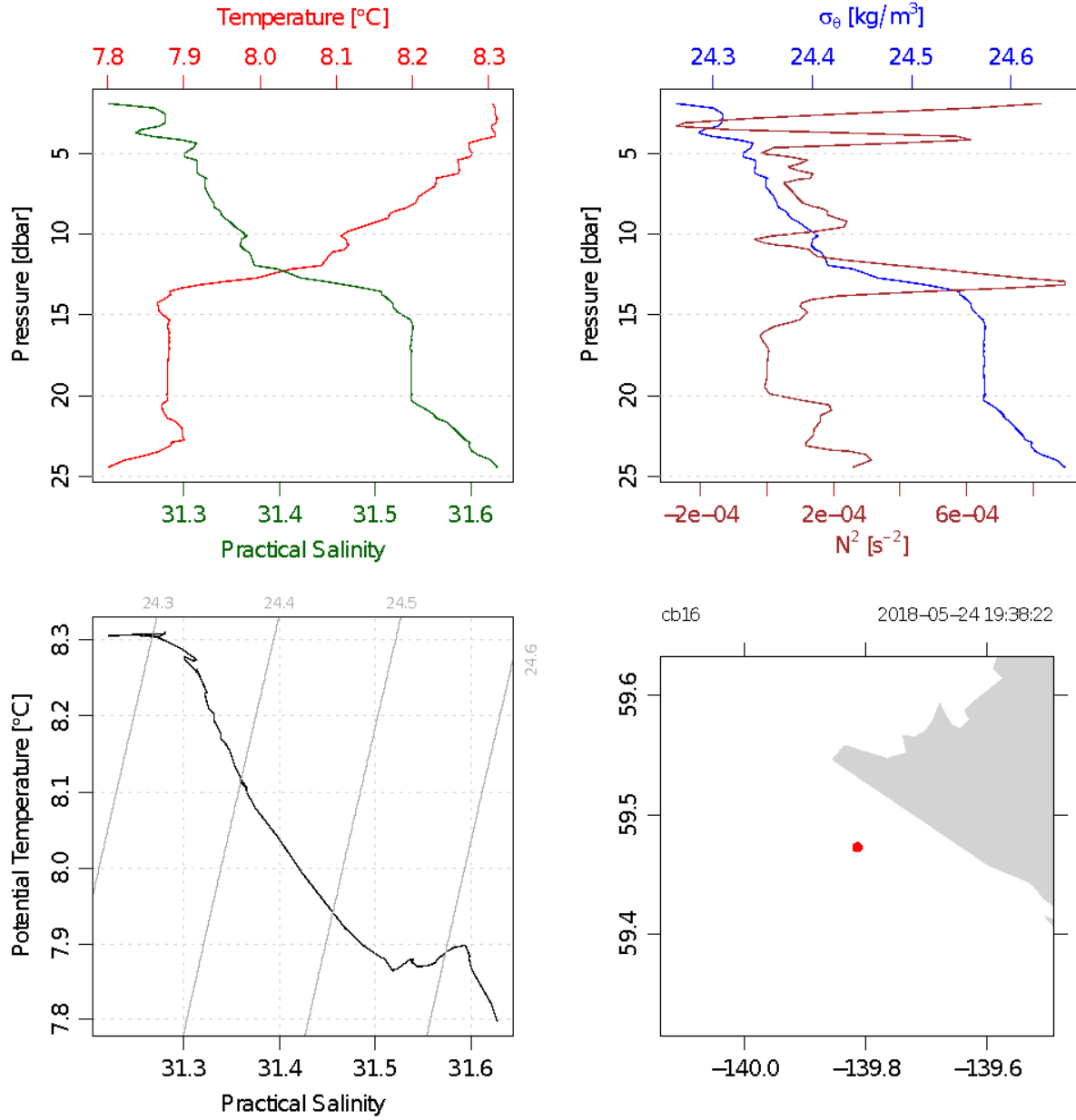


Figure 47. CTD cast from station CB16 to the NW of the Situk River.

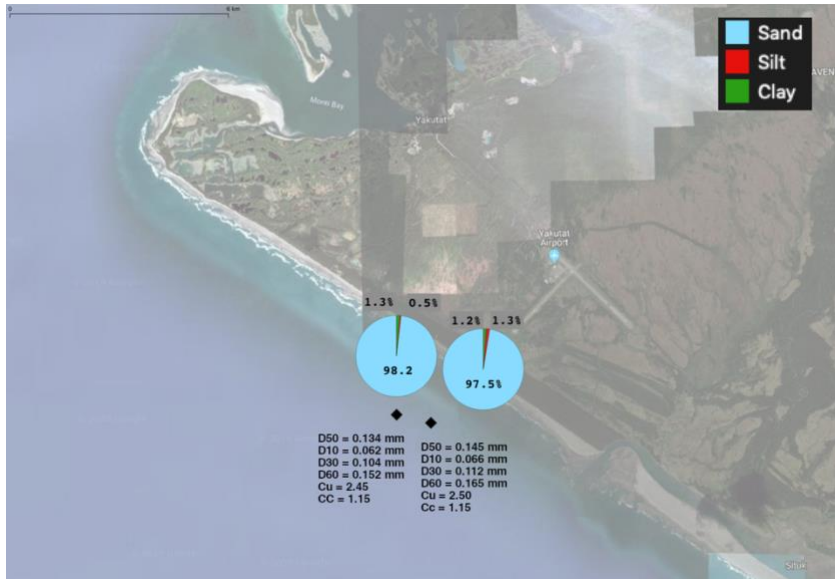


Figure 48. Analysis of grain size from two bottom grabs collected in May 2018.

Sediment samples from the bottom are consistent with sediments from Cannon Beach (DGGs, pers. comm. 2014) and consist primarily of sand. The median particle diameter, expressed as D50, varied between samples from 0.134m and 0.145 mm (Figure 48).

1.5.3.2 Topobathymetry

Elevations derived from a 2019 UAV survey of the Cannon Beach in the form of Digital Terrain Model (DTM) are shown in Figure 49. Elevations from this DTM are compared to the 2014 and 2018 GNSS-measured elevation transects in **Figure 51**.

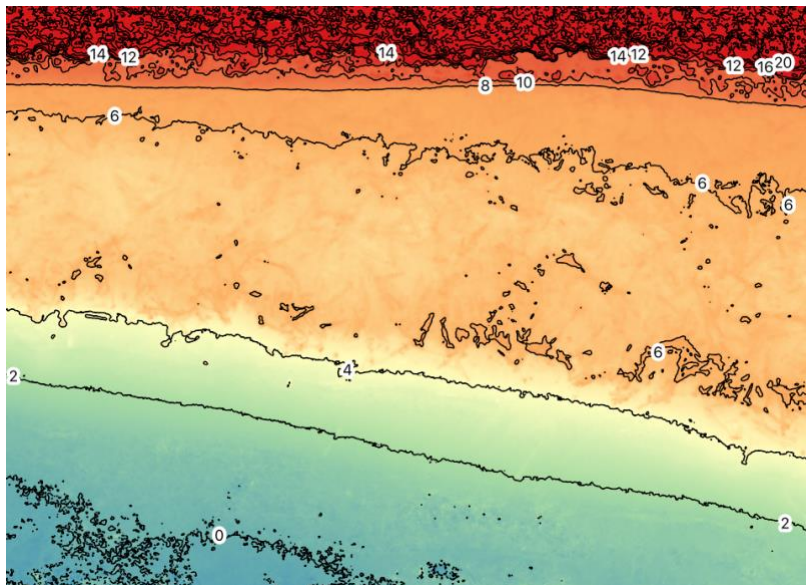


Figure 49. Digital Terrain Model of Cannon Beach (NAVD88 vertical datum).

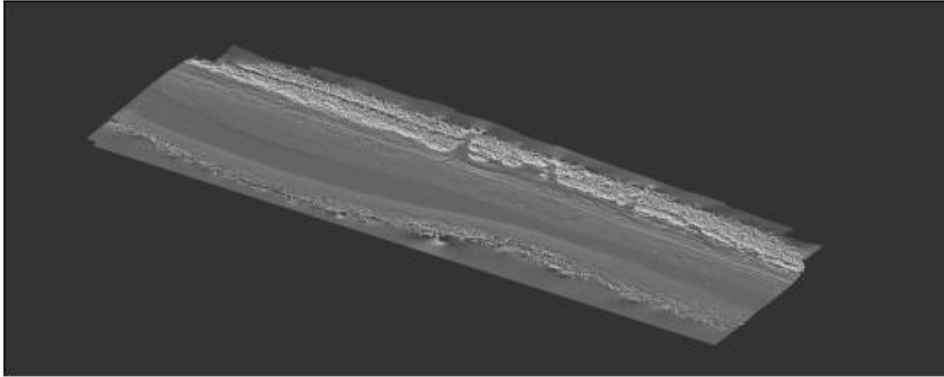


Figure 50. DTM draped over a hillshade to aid in visualization of the elevation change from the water to the beach scarp.

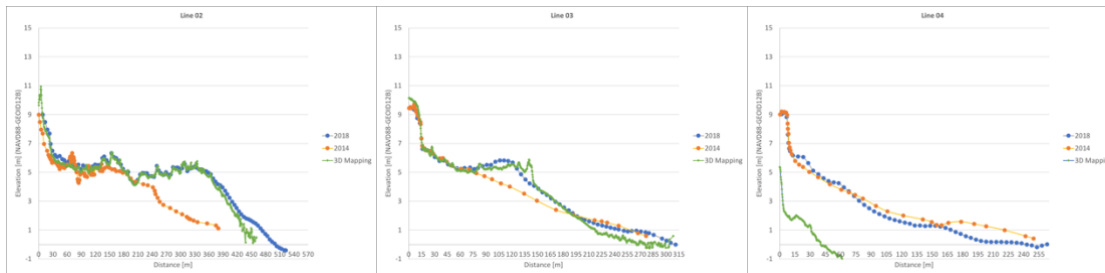


Figure 51. Comparison between 2014, 2018 and 2019 measurements of beach elevation from three transects on Cannon Beach.

The location of lines 2, 3 and 4 are shown in Figure 42.

Between 2014 and 2018 changes in the beach elevations were minimal whereas there were significant changes in elevations between 2018 and 2019, especially for Line 4. Note transect 1 which was first occupied in 2014 was not able to be re-occupied because the Situk River estuary had cut into the bank at this location and eroded it away entirely including the trees that were presumably helping to anchor the bank in place. As an aside, river bank erosion is a likely source of the numerous trees that blanket Cannon Beach.

The final bathymetric surface is shown in Figure 52. Nearly 100% coverage was obtained for the region just offshore of the airport, a promising spot for any future wave energy installations because of land ownership and proximity to electrical distribution lines.

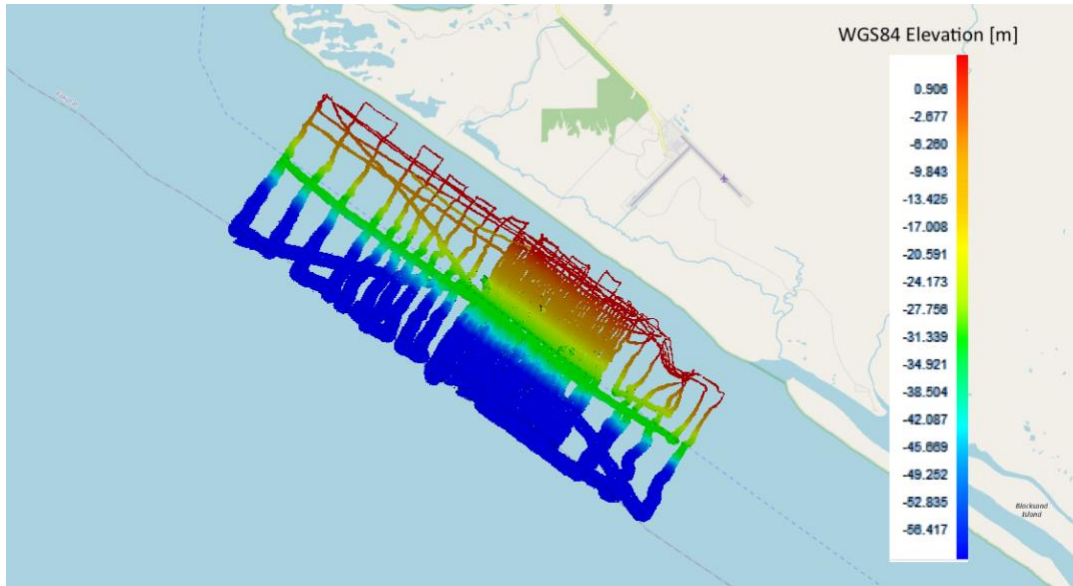


Figure 52. Final 2018 bathymetry.

1.5.3.3 Moorings

The ADCP on mooring DM recorded data from July 2018-July 2019 at ~40m water depth. Following Tschetter et al. (2016) time series of wave parameters are shown in Figure 53 while the wave rose is shown in Figure 54. Monthly and annual statistics for this mooring are shown in Figure 55 and tabulated in Table 12.

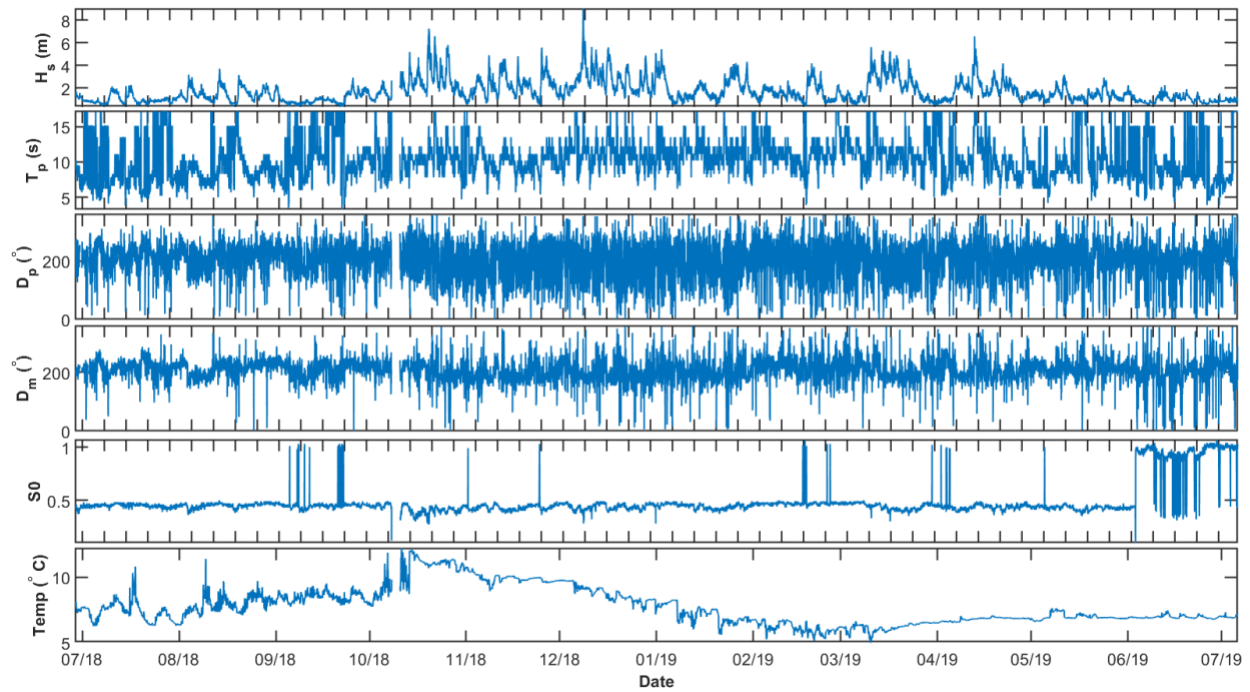


Figure 53. Time series of significant wave height (H_s), peak period (T_p), peak direction (D_p), mean direction (D_m), directional spreading (S_0), and water temperature ($^{\circ}$ C) from the Yakutat deep mooring located at 40 m water depth over the period July 2018-July 2019.

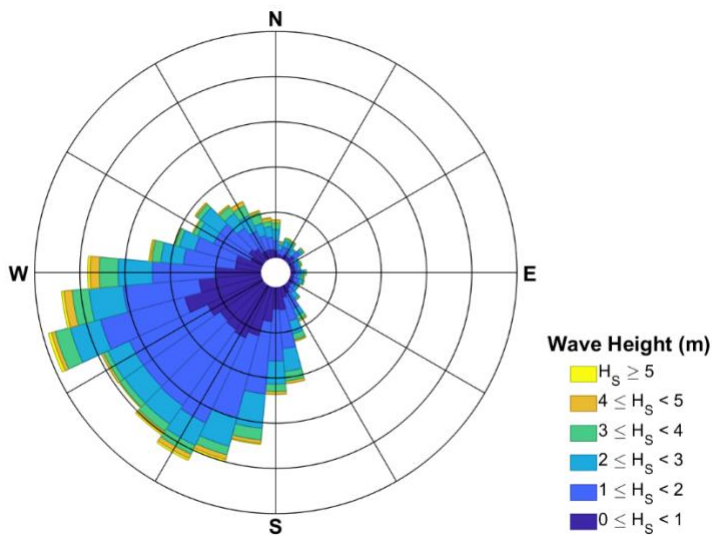


Figure 54. Wave rose showing histogram of dominant wave direction (D_p) and frequency of significant wave height (H_s) at each D_p from the Yakutat deep mooring located at 40 m water depth over the period July 2018-July 2019.

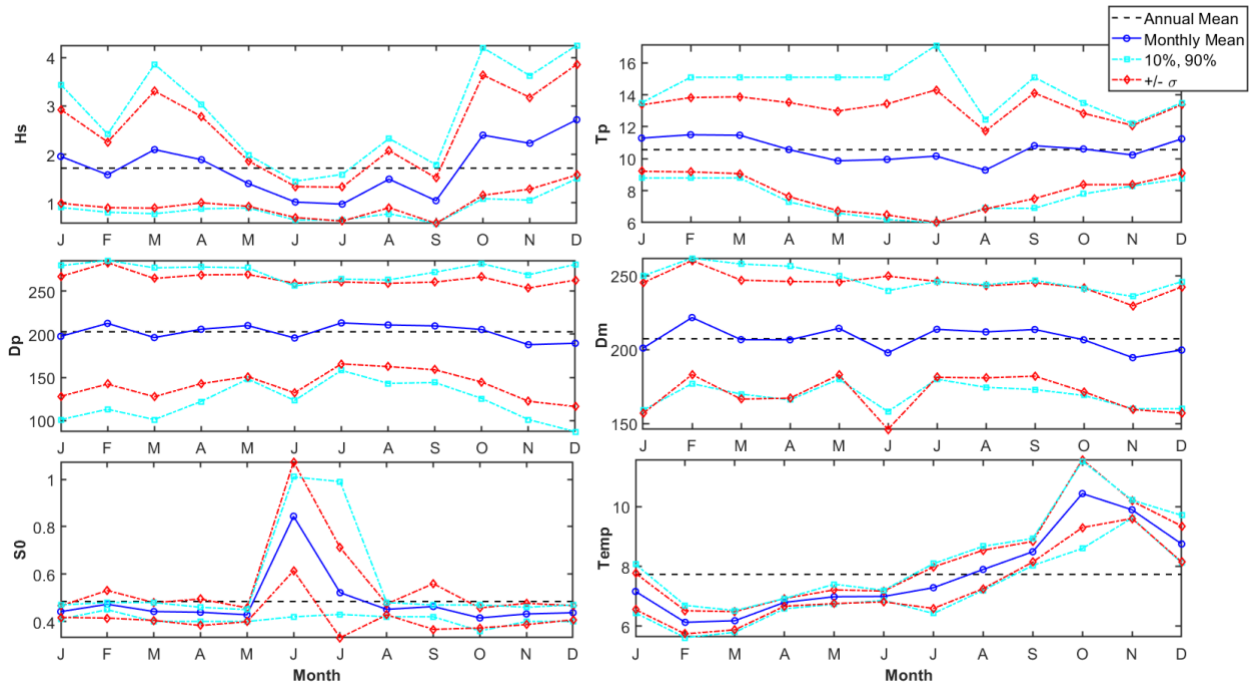


Figure 55. Monthly and annual statistics of wave data from the deep mooring over a one year deployment from July 2018 – July 2019.

Table 12. Monthly and annual statistics of wave data for the deep mooring over a one-year deployment from June 28, 2018 at 23:00 – July 6, 2019 at 02:00 UTC. Note that the total represents the annual mean over that period.

		Jan	Feb	Mar	Apr	May	June	July	Aug	Sept	Oct	Nov	Dec	Total
Hs	Mean	2.0	1.6	2.1	1.9	1.4	1.0	1.0	1.5	1.0	2.4	2.2	2.7	1.7
	Standard Deviation	1.0	0.7	1.2	0.9	0.5	0.3	0.3	0.6	0.5	1.2	0.9	1.1	1.0
	Median	1.7	1.5	1.8	1.8	1.3	1.0	0.9	1.4	0.9	2.1	2.1	2.5	1.5
	10th Percentile	0.9	0.8	0.8	0.9	0.9	0.7	0.7	0.8	0.6	1.1	1.1	1.5	0.8
	90th Percentile	3.4	2.4	3.9	3.0	2.0	1.5	1.6	2.3	1.8	4.2	3.6	4.3	3.1
	Maximum	5.4	4.2	5.6	6.6	3.2	2.3	2.3	3.7	2.9	7.3	5.6	9.0	9.0
	Minimum	0.5	0.4	0.4	0.6	0.6	0.5	0.4	0.4	0.3	0.6	0.5	0.9	0.3
Tp	Mean	11.3	11.5	11.5	10.6	9.9	10.0	10.2	9.3	10.8	10.6	10.2	11.2	10.6
	Standard Deviation	2.1	2.3	2.4	2.9	3.1	3.5	4.1	2.4	3.3	2.2	1.8	2.1	2.9
	Median	11.1	11.1	11.1	10.2	8.8	8.8	8.3	8.8	10.2	10.2	10.2	11.1	10.2
	10th Percentile	8.8	8.8	8.8	7.3	6.6	6.2	6.0	6.9	6.9	7.8	8.3	8.8	6.9
	90th Percentile	13.5	15.1	15.1	15.1	15.1	15.1	17.1	12.5	15.1	13.5	12.2	13.5	15.1
	Maximum	17.1	17.1	17.1	17.1	17.1	17.1	17.1	17.1	17.1	17.1	17.1	17.1	17.1
	Minimum	6.2	3.9	5.0	5.2	4.2	3.9	3.8	4.7	3.3	4.7	5.4	6.0	3.3
Dp	Mean	198	213	196	206	210	196	213	211	210	205	188	190	203
	Standard Deviation	70	70	69	63	59	64	48	48	51	61	66	73	63

	Median	197	222	198	206	213	208	216	220	212	212	189	193	208
	10th Percentile	101	113	101	122	148	123	158	143	144	126	101	87	118
	90th Percentile	280	286	277	278	277	256	264	263	272	282	269	281	274
	Maximum	357	357	358	358	354	356	357	355	356	358	353	357	358
	Minimum	1	1	1	6	2	0	13	10	8	2	1	1	0
Dm	Mean	201	222	207	207	214	198	214	212	214	207	195	200	207
	Standard Deviation	44	39	40	40	31	52	33	31	32	35	35	43	39
	Median	199	224	201	200	214	203	217	218	216	209	191	196	208
	10th Percentile	159	177	170	166	180	158	180	175	173	169	160	160	168
	90th Percentile	250	262	258	257	250	240	246	244	247	242	236	246	248
	Maximum	358	351	359	347	342	359	355	334	326	356	349	357	359
	Minimum	6	35	9	17	4	3	7	1	0	5	30	6	0

(Table 1. cont'd on next page)

(Table 1. cont'd)

		Jan	Feb	Mar	Apr	May	June	July	Aug	Sept	Oct	Nov	Dec	Total
SO	Mean	0.4	0.5	0.4	0.4	0.4	0.8	0.5	0.5	0.5	0.4	0.4	0.4	0.5
	Standard Deviation	0.0	0.1	0.0	0.1	0.0	0.2	0.2	0.0	0.1	0.0	0.0	0.0	0.2
	Median	0.4	0.5	0.5	0.4	0.4	0.9	0.5	0.5	0.5	0.4	0.4	0.4	0.5
	10th Percentile	0.4	0.5	0.4	0.4	0.4	0.4	0.4	0.4	0.4	0.4	0.4	0.4	0.4
	90th Percentile	0.5	0.5	0.5	0.5	0.5	1.0	1.0	0.5	0.5	0.5	0.5	0.5	0.5
	Maximum	0.5	1.1	1.0	1.0	1.0	1.1	1.0	0.5	1.0	0.5	1.0	0.5	1.1
	Minimum	0.4	0.4	0.3	0.4	0.4	0.1	0.4	0.4	0.4	0.1	0.4	0.3	0.1
Temp eratu re	Mean	7.2	6.1	6.2	6.8	7.0	7.0	7.3	7.9	8.5	10.4	9.9	8.8	7.7
	Standard Deviation	0.6	0.4	0.3	0.1	0.2	0.2	0.7	0.6	0.3	1.1	0.3	0.6	1.4
	Median	7.1	6.1	6.2	6.8	6.9	6.9	7.2	7.9	8.5	11.0	9.9	8.7	7.2
	10th Percentile	6.4	5.6	5.8	6.6	6.7	6.9	6.4	7.2	8.0	8.6	9.6	8.1	6.3
	90th Percentile	8.1	6.7	6.5	6.9	7.4	7.2	8.1	8.7	8.9	11.5	10.2	9.7	9.9
	Maximum	8.3	6.8	6.6	7.1	7.6	8.1	10.8	11.4	9.5	12.2	10.8	9.8	12.2
	Minimum	5.6	5.1	5.0	6.5	6.6	6.8	6.3	6.3	7.8	7.8	8.9	7.2	5.0

Despite the eventual loss of the shallow and mid-moorings, they did provide ~6 months of data. Time series of wave statistics derived from the ADCP on the shallow mooring are shown in Figure 56. The wave rose for this mooring is shown in Figure 57. Monthly and annual wave statistics for this mooring are shown in Figure 58 and tabulated in Table 13. Note that the annual mean represents the mean of the deployment period during the summer months, from June 28, 2018 at 22:00 - Oct 4, 2018 at 18:00 UTC. Also note that 1) monthly means for June and October represent only 2.08 and 3.75 days of data for those two months, respectively, and 2) the total represents the summer mean over that period.

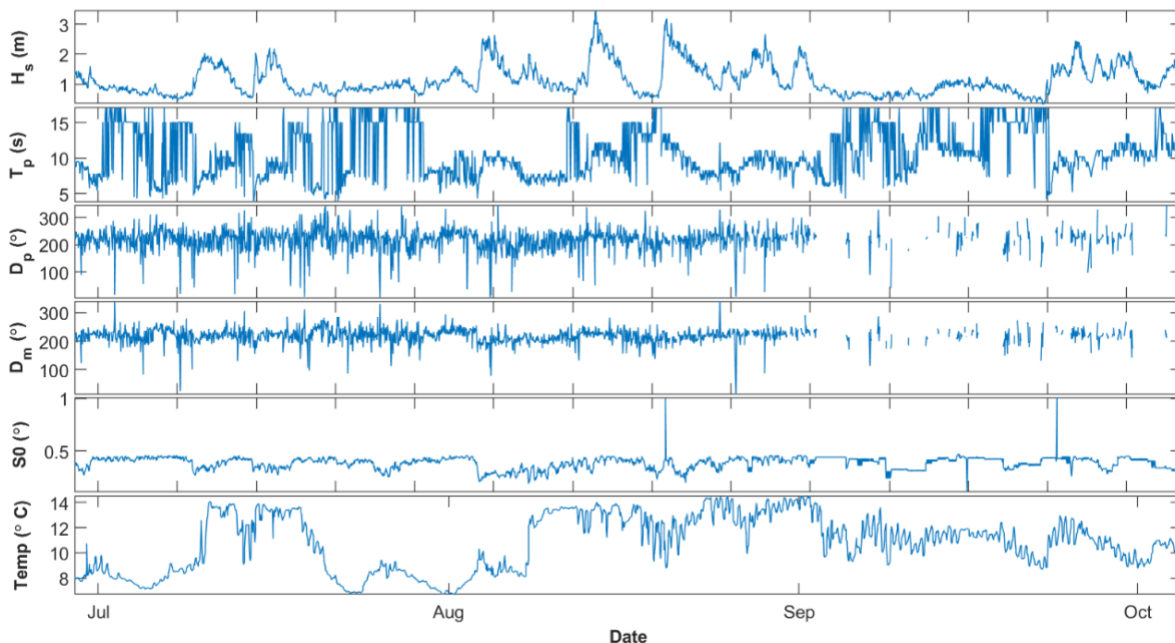


Figure 56. Time series of significant wave height (H_s), peak period (T_p), peak direction (D_p), mean direction (D_m), directional spreading (S_0) and water temperature ($^\circ$ C) from the Yakutat shallow mooring located at 14.7 m water depth over the period July-October 2018.

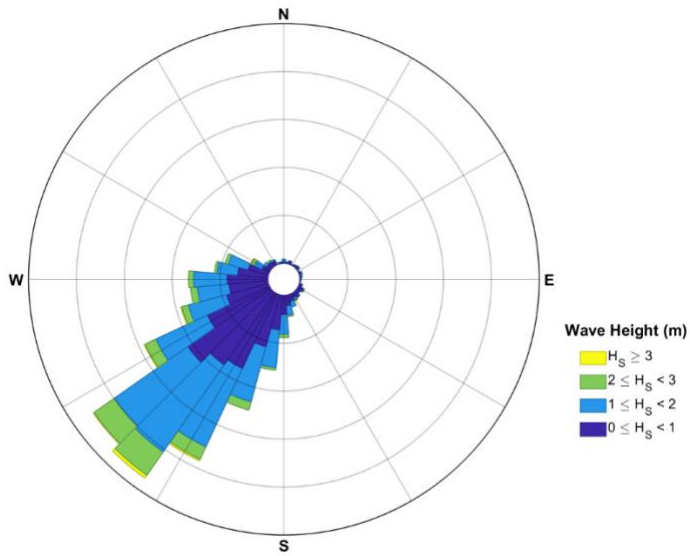


Figure 57. Wave rose showing histogram of dominant wave direction (D_p) and frequency of significant wave height (H_s) at each D_p from the Yakutat shallow mooring located at 14.7 m water depth over the period July-October 2018.

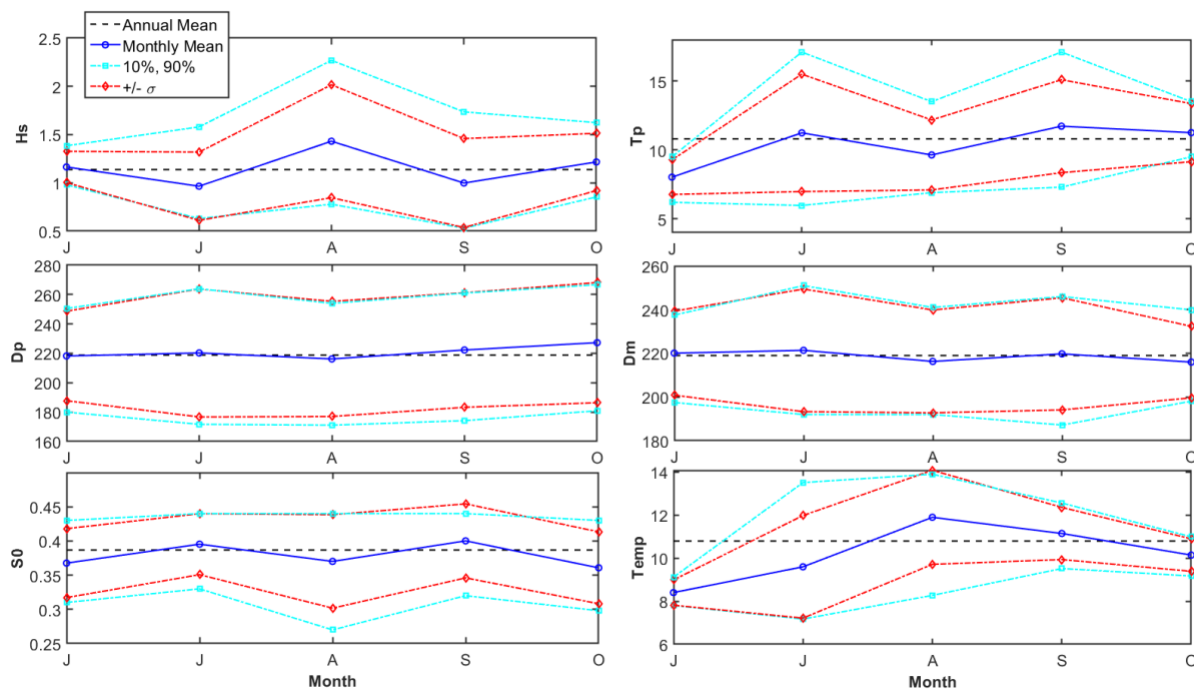


Figure 58. Monthly statistics of wave data for the shallow mooring from 2018.

Table 13. Monthly statistics of wave data for the shallow mooring from 2018.

		June	July	Aug	Sept	Oct	Total
H_s	Mean	1.2	1.0	1.4	1.0	1.2	1.1
	Standard Deviation	0.2	0.4	0.6	0.5	0.3	0.5
	Median	1.2	0.9	1.3	0.9	1.1	1.0
	10th Percentile	1.0	0.6	0.8	0.5	0.9	0.6
	90th Percentile	1.4	1.6	2.3	1.7	1.6	1.9
	Maximum	1.6	2.2	3.4	2.5	1.8	3.4
	Minimum	0.9	0.4	0.5	0.3	0.7	0.3
T_p	Mean	8.0	11.2	9.6	11.7	11.3	10.8
	Standard Deviation	1.3	4.3	2.5	3.4	2.1	3.5
	Median	8.3	10.2	9.5	11.1	11.1	10.2
	10th Percentile	6.2	6.0	6.9	7.3	9.5	6.6
	90th Percentile	9.5	17.1	13.5	17.1	13.5	17.1
	Maximum	10.2	17.1	17.1	17.1	17.1	17.1
	Minimum	5.4	3.8	4.3	4.2	5.2	3.8
D_p	Mean	218	220	216	222	227	219
	Standard Deviation	30	44	39	39	41	41
	Median	225	225	222	229	225	225
	10th Percentile	180	172	171	174	181	172
	90th Percentile	251	264	254	261	267	258
	Maximum	259	342	346	329	345	346
	Minimum	88	4	3	41	180	3
D_m	Mean	220	221	216	220	216	219

	Standard Deviation	19	28	24	26	16	26
	Median	224	224	218	223	213	221
	10th Percentile	198	192	192	187	198	192
	90th Percentile	238	251	241	246	240	246
	Maximum	248	336	340	291	248	340
	Minimum	123	25	13	113	190	13
S₀	Mean	0.4	0.4	0.4	0.4	0.4	0.4
	Standard Deviation	0.1	0.0	0.1	0.1	0.1	0.1
	Median	0.4	0.4	0.4	0.4	0.3	0.4
	10th Percentile	0.3	0.3	0.3	0.3	0.3	0.3
	90th Percentile	0.4	0.4	0.4	0.4	0.4	0.4
	Maximum	0.5	0.5	1.0	1.0	0.4	1.0
	Minimum	0.3	0.3	0.2	0.1	0.2	0.1
Temp eratu re	Mean	8.4	9.6	11.9	11.1	10.1	10.8

A TS diagram for the mid mooring is shown in Figure 59. In general, the water at the mid mooring is slightly saltier and cooler than the shallower mooring. Both moorings clearly show the persistent presence of Alaska Coastal Current water with the maximum salinities at the shallow (mid) mooring are ~32 (32.5) (e.g. Weingartner, 2005). Temperatures at the deep mooring during this same time are considerably cooler (Figure 60) though salinities are similar to the shallower sites.

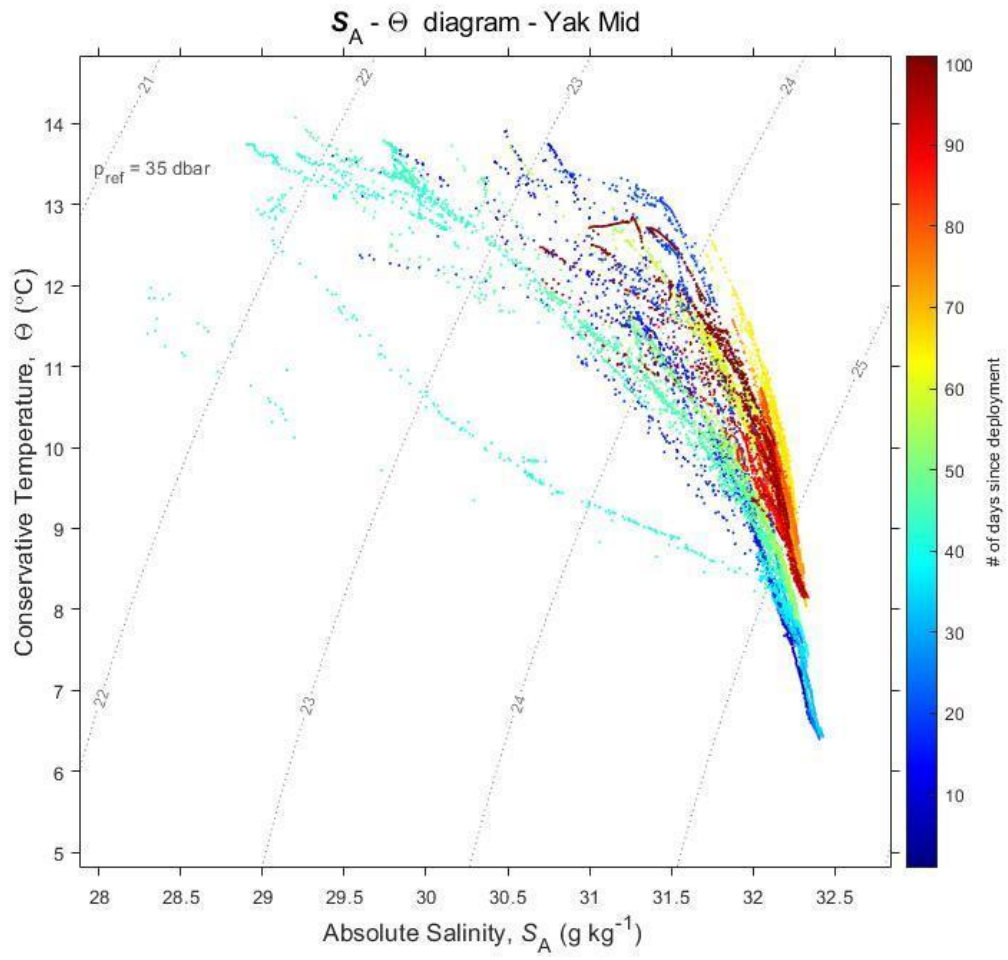


Figure 59. Conservative Temperature vs. Absolute Salinity from the mid mooring.

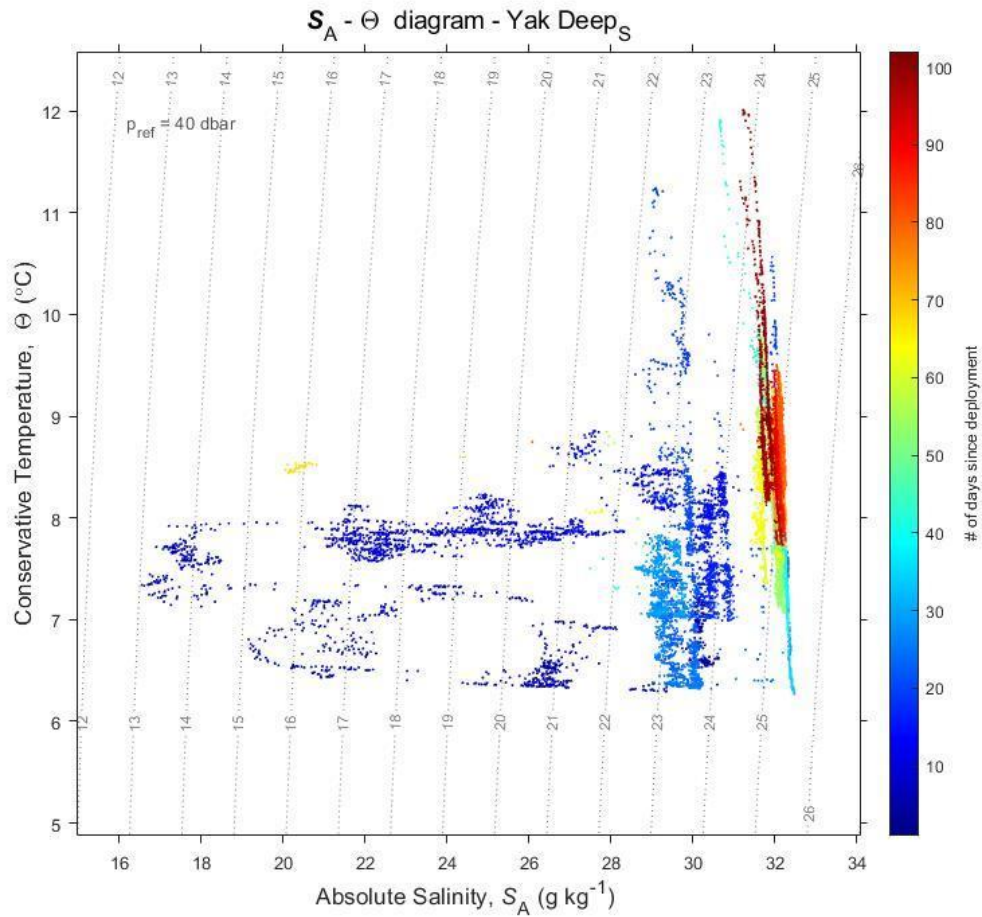


Figure 60. Conservative Temperature vs. Absolute Salinity from the deep mooring.

The turbidity time series from the mid mooring are shown in Figure 61. With the exception of one event in October, the turbidity values are clearly correlated through time and turbidity levels are generally lower at the downward facing OBS.

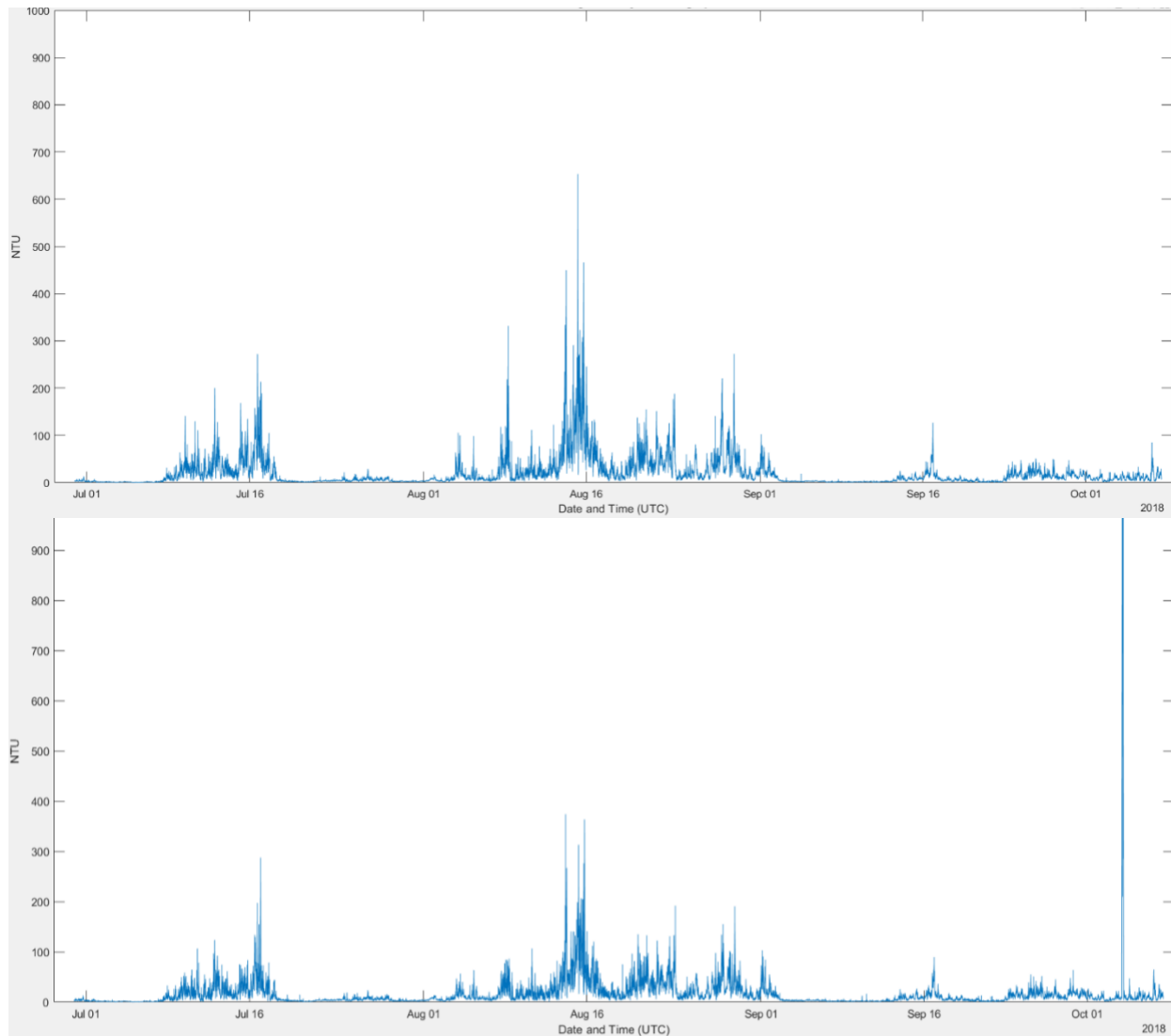


Figure 61. Top: turbidity from the upward facing OBS sensor. Bottom: turbidity from the downward facing OBS sensor.

1.5.4 Discussion

Surprisingly, despite proximity to both the shore and to the mouth of the Situk, there was no indication of riverine water signal in the CTD data except at depths of 10 m or less and immediately adjacent to the coast. This is relevant to this discussion because if freshwater dependent species are present, they will follow this freshwater and the location of this freshwater likely varies with winds and tides (e.g., Rijnsburger et al. 2018). This introduces the possibility that any species that follow the freshwater may interact with wave energy converters installed in the region. Deeper than 10m, the overall low nutrient concentrations compared to typical Gulf of Alaska values and the salinity and temperature are indicative that Alaska Coastal Current water is dominant at the time of sampling (e.g., Weingartner, 2005). A more comprehensive effort to map the presence of fish and/or marine mammals in relation to the hydrography would be beneficial to help understand the potential for impacts of wave energy converters on the region.

TSS values measured near the coast are significantly higher than those suggested by Hampton et al. (1986) but are consistent with the high energy wave environment and proximity to the multiple, glacial-fed rivers in the region as well as the apparent loss of beach material noted previously. Note the two closest rivers, the Alsek and the Situk are clearwater streams, but the Dangerous River further to the SE is glacial as are other rivers up and down the coast.

Elevation changes near the Situk River estuary and those further removed from the dynamic estuary (Transect Lines 3 and 4; **Figure 51**) indicate that at least two processes are driving the morphological change and supplying sediment to the offshore along this stretch of coast: erosion driven by the migrating estuary and wave driven erosion of the Gulf-facing Cannon Beach. The erosion along the Situk River estuary is consistent with past work in the region. Shepherd (1995) describes the tendency of the Situk River estuary to elongate in the NW direction through erosion and then eventually reset itself via the action of waves breaking through the spit directly in front of where the Situk enters the estuary (e.g. **Figure 7**). In contrast for sections of the Yakutat forelands removed from such dynamic estuaries, Boothroyd et al. (1976) characterize this coastal region as “neutral” meaning that sediment is moved offshore seasonally and then replenished. The changes between years for Lines 3 and 4 contradict this characterization. Longer term observations or other means of estimating change are required to determine whether this has changed or if our observations of large losses between years are anomalous.

In **Figure 62** the UAV derived Digital Terrain Model is compared to the ArcticDEM (Porter et al., 2018). In the region of interest, between the water line and the forest, the differences between the two products are smallest though still large (between 1.5 and 3 m difference) suggesting that the ArcticDEM is not accurate enough to make these types of comparisons in this region. Rather, repeat UAV surveys or GNSS-based transects are likely better tools for assessing elevation changes at this site.

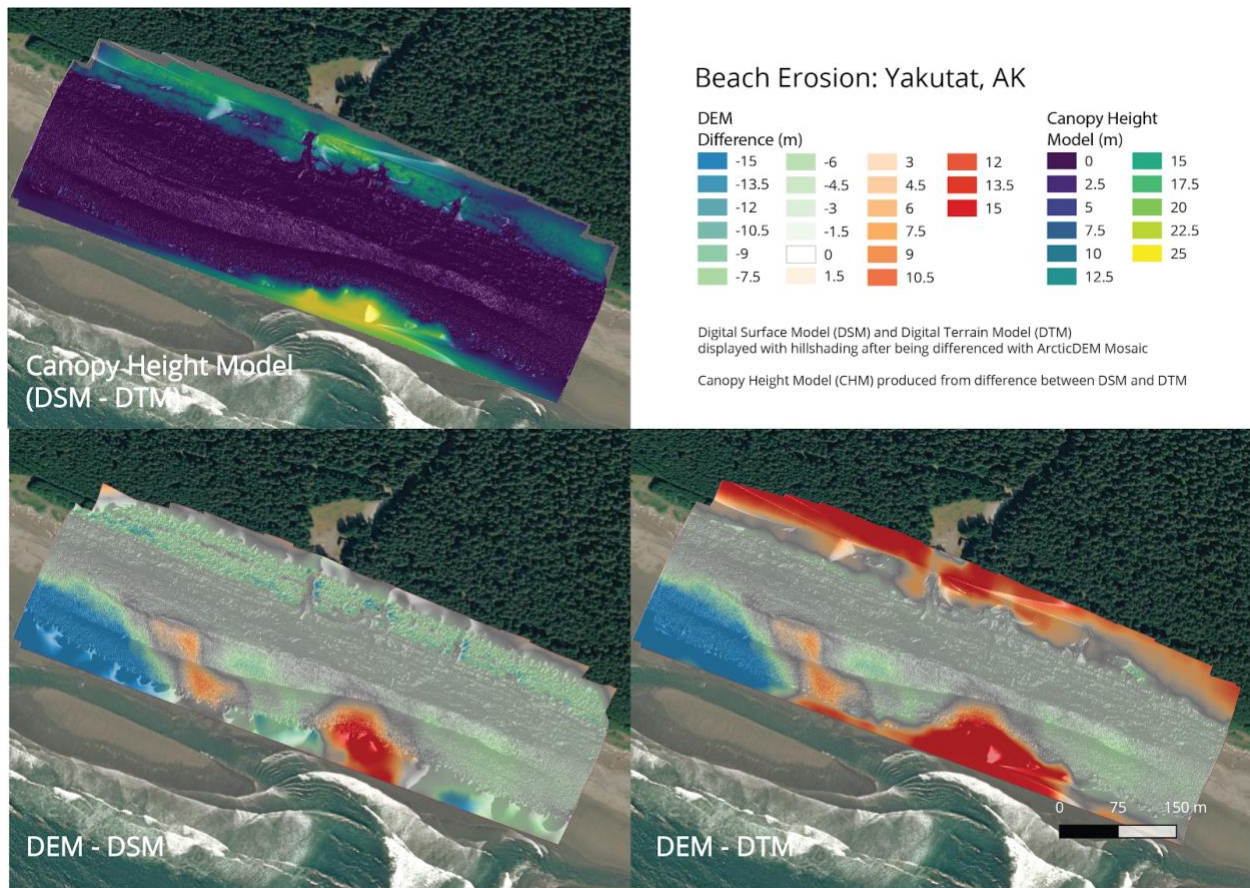


Figure 62. UAV derived elevations compared to the ArcticDEM.

The bathymetry described herein are sufficiently accurate to serve as an excellent base line from which to estimate change if a developer were to pursue a wave energy project in the region. Furthermore, the IEC Standards dictate a high-quality bathymetry and hazard survey (IEC, 2015) as part of a wave energy resource assessment. Unfortunately, because bathymetric surveys in this region are so sparse, it is not meaningful to make comparisons between this bathymetry and other regional bathymetric DEMs which are based on a limited number of survey datasets and sparse soundings (e.g., NOAA, 2009). However, since this elevation surface is now available for Yakutat it would be a simple matter to estimate change at the site, as needed, using repeat single beam surveys which are much less intensive to carry out and process than multibeam bathymetry surveys.

The wave statistics from the deep mooring are remarkably similar those from 2014-2015 (Tschetter et al., 2016) both in terms of magnitude but also in terms of direction and peak period. At the shallower mooring, the peak direction is more strongly from the southwest than further offshore, consistent with the shoaling depths that tend to align the incoming waves with the orientation of the coast (e.g., Holthuijsen, 2007).

Hydrography from the moorings shows that the sites are strongly influenced by Alaska Coastal Current water. Though it should be noted that all three CTD sensors were located on the bottom and not near the surface where we would expect the freshest water to be observed.

While incomplete, the turbidity records are quite interesting. The increase in turbidity with distance from the seafloor at the mid mooring suggests that the primary driver of turbidity at this site is suspended

matter. Although not shown, this contrasts with the shortened record from the shallow site where turbidity levels are higher for the downward facing OBS suggesting that wave resuspension is the dominant driver of elevated turbidity at the shallow site. This is consistent with wave forcing leading to more sediment resuspension at shallower depths (Holthuijsen, 2007).

1.5.5 Summary and Conclusion

The comparisons between past measurements of elevation and areal DEMs are illustrative of some of the challenges developers will likely encounter when undertaking projects in the Alaska region. In general, topobathymetric elevations are undersampled in Alaska (Overbeck, 2018) which could add considerable cost to any planned project. This is especially true for bathymetry since currently, remote sensing of bathymetry is still a time consuming and sometimes unreliable research endeavor (Pe'eri, pers. comm, 2020). NOAA is currently working on methods for predicting water clarity in an effort to automate analysis of satellite imagery for use in mapping bathymetry. In situ, sonar-based bathymetric surveys are both time consuming and challenging and thus expensive to carry out in the state's remote regions. Similarly, LIDAR-based bathymetry is expensive and in Alaska's turbid waters, often requires follow-up with sonar in order to generate continuous surfaces (J. Wozencraft, National Coastal Mapping Program, pers. comm, 2021). It should be noted that Yakutat is comparatively accessible since it has twice daily Alaska Airlines service as well as regular barge and ferry service. Many other sites will be considerably more difficult to access.

Overall, the oceanographic and topobathymetric measurements combine to produce a picture of a site with a dynamic seafloor driven by high energy wave events throughout the year. The loss of the two shallower moorings and the burial of the deep mooring in ~40m of water are anecdotal but illustrative that wave driven sediment transport at the site is significant, noisy and likely makes for challenging conditions for any life that would seek to make its home on the seafloor in this region. Because of this, any wave energy project developers will have to carefully consider their project design so that sediment transport does not negatively impact the installation of the converter, its cabling or other project infrastructure.

1.6 Implications for Feasibility Studies in Other Coastal Regions of Alaska

Before beginning this discussion, it should be noted that the Federal Energy Regulatory Commission (FERC) licensing process that governs all grid-connected marine energy projects is very dynamic at this time (<https://www.ferc.gov/licensing/hydrokinetic-projects>). Moreover, during the course of this project the Department of Interior updated their guidance on marine energy projects (BOEM, 2020). BOEM also produced guidelines for Renewable Energy Site Assessment Plans (BOEM, 2019). There are also numerous efforts underway to educate regulators on marine energy technology most notably efforts by researchers at the Pacific Northwest National Laboratory including Dr. Andrea Copping and colleagues (e.g. Copping and Hemery, 2020). The overall result of these research and education efforts and a dynamic legislative environment is that the regulatory process for marine energy is best described as fluid. The most up to date summary of the marine energy regulatory process is O'Neill et al. (2019).

When a project is connected to the electrical grid, it must go through the FERC process. It is also important to note that in contrast to the rest of the U.S., there are no grid interconnection standards in most of rural Alaska. Rather, the interconnection requirements for new generation devices on isolated microgrids are not bound by regulatory requirements and are specific to an individual microgrid. Practically this means that independent power producers or other project developers must engage early with the local utility. In Alaska, utilities range from individual, village-owned utilities such as the Village of Igiugig to electric cooperatives such as Alaska Village Electric Cooperative (AVEC) and Alaska Power and Telephone (AP&T). AVEC currently owns the Yakutat utility.

A growing number of entities have successfully navigated FERC’s marine energy process. Oregon State University (D. Hellin, Oregon State University, pers. comm., 2021), Ocean Renewable Power Company (ORPC, M. Jackinsky, pers. comm., 2021) and Verdant Power are several examples of entities that navigated, or in some cases, pioneered the process of filing preliminary FERC permits through to full FERC licenses.

ORPC recently obtained a full-FERC license for their Kvichak River project in Alaska (FERC Project No. 13511-003) so their example is particularly relevant to this discussion. There are important nuances to note that vary between the FERC processes noted above. For their Kvichak River project, ORPC maintains the following State permits: Alaska Department of Fish and Game Title 16 Fish Habitat Permit; Alaska Department of Natural Resources Water Use Permit and Alaska Department of Natural Resources Land Use Permit. In contrast the OSU project is in Federal Water on the Outer Continental Shelf (OCS), thus of the three, OSU is the only project that currently holds a BOEM Lease. Projects in state waters are not required to obtain an OCS lease. Though they are still required to follow the FERC process.

Several examples are given below to provide perspective on the range of permitting variations and timelines. Table 14 summarize the permits Oregon State University currently maintains for their grid-connected PacWave “South Energy Test Site” off the Oregon Coast.

Table 14. Oregon State University Permit Summary.

Federal Permits	
Agency	Permit
US Army Corps	Nationwide Permit #12
BOEM	OCS Lease
FERC	License
State of Oregon Permits	
Dept of Environmental Quality	401 Water Quality Certificate
Dept of State Lands	Easement, and Removal Fill Permit
Coastal Management Program	Federal Consistency Determination
Dept of Transportation	various

Parks & Recreation Dept	Easement, Intergovernmental Agreement, and Ocean Shore Permit
State Historic Preservation Office	Concurrence

The permits for UAF’s non-grid connected test site on the Tanana River in Nenana are summarized in Table 15.

Table 15. University of Alaska Fairbanks permit summary.

Federal	
Agency	Permit
US Army Corps	Nationwide Permit #12
State of Alaska	
Dept of Natural Resources	Land use permit
Dept of Fish and Game	Habitat permit
Local	
Nenana Village Tribal Council	Land use agreement

A summary of the permitting process for the Kvichak River project in State of Alaska waters is included in O’Neil et al., 2019 and reproduced below (Figure 63).

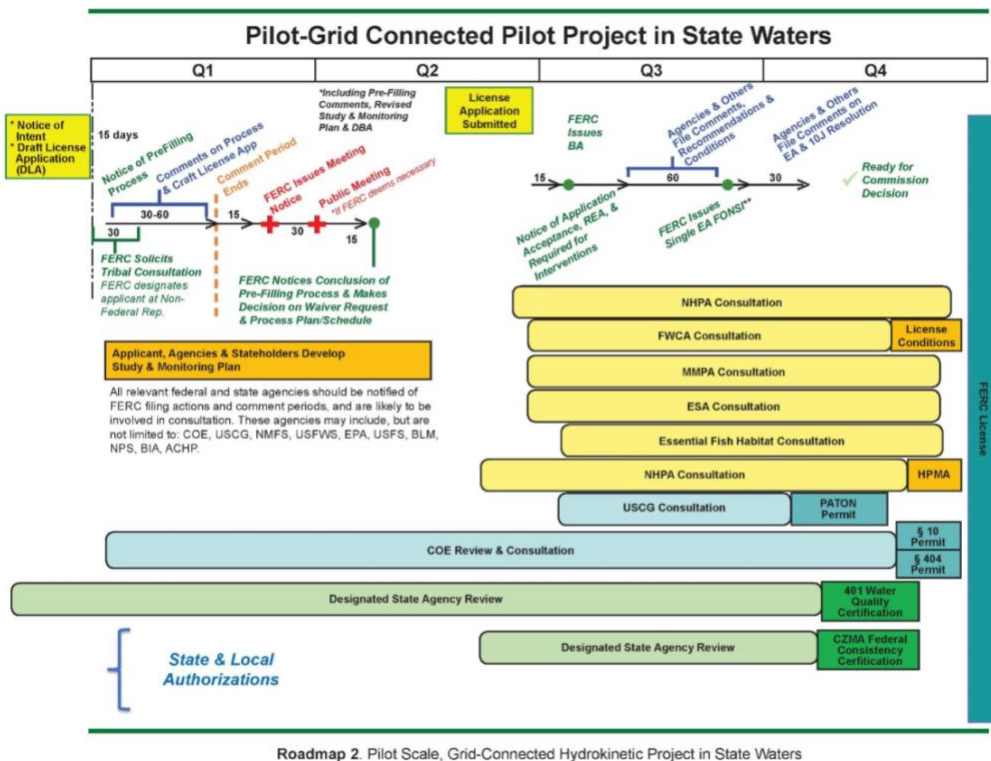


Figure 63. Timeline for permitting a pilot marine energy project in State waters from O’Neil et al., 2019.

In general, it is likely that state regulatory requirements in Alaska will be less onerous than in other states. OSU required 8 years to navigate the FERC process while ORPC only required approximately 3 years to obtain a full FERC License for their Igiugig project on the Kvichak River and they had a river turbine installed and connected to Igiugig’s electrical grid during most of that timeframe. Note that ORPC engaged with Igiugig at least 8 years prior to the finalization of the FERC Licensing process and the Igiugig Village Council, rather than ORPC, led many of DOE-funded efforts to install ORPC’s technology in the Kvichak River. UAF’s non-grid connected site took less than a year to permit and is illustrative of the shortest timeline companies can expect before installing their technology in Alaska.

The permitting of future projects in Alaska at locations such as Cook Inlet (tidal) or Yakutat (wave) will vary depending on several factors, the most fundamental of which is whether the deployment location is within the OCS or state waters. If the project is in OCS waters, a BOEM lease will be required. Regardless, the process begins with a preliminary FERC permit. There are currently at least three preliminary FERC permits pending for Alaska locations: one for Lower Cook Inlet (ORPC, tidal), one for Upper Cook Inlet (Turnagain Arm Tidal Energy Corp., tidal) and one for Angoon (Littoral Power, tidal). Resolute Marine Energy (RME) used to hold a preliminary FERC permit for the Cannon Beach area of Yakutat for a wave energy project but their permit lapsed some years ago (FERC Project No. 14438-000). The work described in Tschetter et al. (2016) was undertaken while RME held their preliminary FERC permit and RME used information from these and the earlier PAM studies described herein to demonstrate activity to FERC in order to maintain their permit.

In all of the Alaska-based scenarios, FERC requested that the permittee engage with the local utility. This engagement should be considered one of the most basic steps in beginning a project in Alaska. ORPC’s Kvichak River project and RME’s Yakutat engagement offer further guidance. In both cases, project

developers engaged extensively with the local tribal representatives, tribal and/or village corporations, Local, State and/or Federal Government representatives and/or regulators (e.g. Alaska Department of Fish and Game), utility owner/operators and landowners (Federal, State or Local). In Alaska, all of these entities may have a say in the processes either through land ownership, control of the local electrical grid or through other means. Thus, it cannot be emphasized enough that it is critical to understand and engage these entities at the very start of the process and this takes time. One other important constituent important to mention are fisheries: OSU spent considerable time (years) engaging with local and regional fisheries in order to identify suitable locations for their test site. In Alaska there are subsistence, sport and commercial fisheries, all of which must be engaged early in the process. Overall, while stakeholder engagement is a required part of the FERC process, it is important to begin this process as early as possible. If feasible, this should be started before the FERC process. Again, ORPC's experience in Igiugig can provide guidance: ORPC let IVC lead on many of these issues and successfully navigated the process.

Other unanticipated constraints commonly encountered in Alaska include but are not limited to a) the presence of critical habitat for endangered species within a region of interest/activity (either in the marine environment or on-shore); b) special land use areas such as national and state parks, monument, refuges, borough and municipal boundaries and shipping that may require additional coordination; c) the range of associated activity in addition to device operation itself that may involve impacts and permitting requirements above and beyond the operation of the device itself, such as collecting environmental field data, installation, and maintenance activities; d) turnover of local government and agency personnel. While this is daunting list of challenges, ORPC's success illustrates that it is possible to navigate this process successfully. The key to doing so is local engagement early and often.

In summary, while it is possible to quickly navigate from a preliminary FERC permit process (months) to the full FERC License (3+ years), doing so requires considerable effort before the FERC process even begins. Thus, timelines for project development need to take into account not just the basic IEC-specified resource assessments and National Environmental Permitting Act processes, they also require significant local engagement to help mitigate any unanticipated challenges. It should also be noted that ORPC's success in Igiugig also depended on an Alaska Energy Authority funded resource assessment and bathymetric survey work completed some years prior to the subsequent turbine deployment in Igiugig. Similar to Igiugig, this BOEM funded Yakutat work and future work at other high-potential marine energy sites such as Cook Inlet, Angoon and Gustavus could serve as a similarly important springboard for projects in other promising Alaska-locales.

1.7 References

- Arimitsu ML, Litzow MA, Piatt JF, Robards MD, Abookire AA, Drew GS. 2003. Inventory of marine and estuarine fish in southeast and central Alaska National Parks. Anchorage, Alaska: Alaska Science Center, Biological Resources Division, United States Geological Survey. Inventory and Monitoring Program Final Report.
- Arimitsu ML, Piatt JF, Litzow MA, Abookire AA, Romano MD, Robards MD. 2008. Distribution and spawning dynamics of capelin (*Mallotus villosus*) in Glacier Bay, Alaska: a cold water refugium. *Fish Oceanogr.* 17:137-146.
- Arimitsu ML, Piatt JF, Mueter F. 2016. Influence of glacier runoff on ecosystem structure in Gulf of Alaska fjords. *Mar Ecol Prog Ser.* 560:19-40.
- Armstrong FAJ, Stearns CR, Strickland JDH. 1967. "The measurement of upwelling and subsequent biological processes by means of the Technicon Autoanalyzer and associated equipment," *Deep-Sea Research*, 14, pp.381-389.
- Austin M, Chorney N, Ferguson J, Leary D, O'Neill C, Sneddon H. 2009. Assessment of Underwater Noise Generated by Wave Energy Devices. Tech Report prepared for Oregon Wave Energy Trust. 58 pp.
- Moore G, Onyango E, et al. 2020. The Alaska Amphibious Community Seismic Experiment, *Seismol. Res. Lett.* 91, 3054–3063, doi: 10.1785/0220200189.
- Barcheck, G., G. A. Abers, A. N. Adams, A. Bécel, J. Collins, J. B. Gaherty, P. J. Haeussler, Z. Li, G. Moore, E. Onyango, et al. (2020). The Alaska Amphibious Community Seismic Experiment, *Seismol. Res. Lett.* 91, 3054–3063, doi: 10.1785/0220200189.
- Boehlert GW, Gill AB. 2010. Environmental and Ecological Effects of Ocean Renewable Energy Development: A Current Synthesis. *Oceanography*. Vol. 23, No.2.
- Bureau of Ocean Energy Management (BOEM), US Department of Interior. 2019. Guidelines for Information Requirements for a Renewable Energy Site Assessment Plan (SAP). <https://www.boem.gov/sites/default/files/renewable-energy-program/BOEM-Renewable-SAP-Guidelines.pdf>
- Bureau of Ocean Energy Management (BOEM), US Department of Interior. 2020. BOEM / FERC Guidelines on Regulation of Marine Hydrokinetic Energy Projects on the OCS, Version 3 <https://www.ferc.gov/sites/default/files/2020-06/Guidance-document-on-Outer-Continental-Shelf-development-with-DOI.pdf>
- Boothroyd JC, Cable MS, Levey RA. 1976. *Coastal morphology and sedimentation, Gulf Coast of Alaska (glacial sedimentation)*. United States: N. p., 1976. Web.
- Bouwens KA, Paul AJ, Smith RL. 1999. Growth of juvenile Arrowtooth Flounders from Kachemak Bay, Alaska. *Alaska Fishery Research Bulletin.* 6:30-40.
- Castellote M, Stafford KM, Neff AD, Lucey W. 2015. Acoustic monitoring and prey association for Beluga Whale, *Delphinapterus leucas*, and Harbor Porpoise, *Phocoena phocoena*, off two river mouths in Yakutat Bay, Alaska. *Marine Fisheries Review.* 77:1-10.

- Chamberlain M. 2021. Techno-economic Investigation and Policy Implications of Renewable Energy Integration into an Islanded Diesel-based Microgrid in Rural Alaska, Master's Thesis, Swiss Federal Institute of Technology Zurich.
- Conrad S, Gray D. 2014. Overview of the 2013 Southeast Alaska and Yakutat commercial, personal use, and subsistence salmon fisheries Anchorage, Alaska: Alaska Department of Fish and Game. Fishery Management Report No. 14-28.
- Copping A, Battey H, Brown-Saracino J, Massaua M, Smith C. 2014. Ocean & Coastal Management. *Ocean and Coastal Management* 99:3–13
- Copping AE, Hemery LG., editors. 2020. OES-Environmental 2020 State of the Science Report: Environmental Effects of Marine Renewable Energy Development Around the World. Report for Ocean Energy Systems (OES). doi:10.2172/1632878
- Delean BJ, Helker V Muto M, Savage K, Teerlink S, Jemison LA, Wilkinson K, Jannot J, Young NC. 2020. Human-caused mortality and injury of NMFS-managed Alaska marine mammal stocks 2013-2017 U.S. Dep. Commer., NOAA Tech. Memo. NMFS-AFSC-401 86 pp.
- Denes SL, Zeddies DG, Weirathmueller MM. 2018. Turbine Foundation and Cable Installation at South Fork Wind Farm: Underwater Acoustic Modeling of Construction Noise. Document 01584, Version 4.0. Technical report by JASCO Applied Sciences for Jacobs Engineering Group Inc.
- Drew B, Plummer AR, Sahinkaya MN. 2009. A review of wave energy converter technology. *Proceeding of the Institution of Mechanical Engineers, Part A: Journal for Power and Energy*. 223:887-902.
- Dubuque A, Rios K, Salomon A, Balderas Y, Zavala A, Mares B. 2019. Protected Species Mitigation and Monitoring Report. Marine Geophysical (Seismic) Survey, North Pacific Ocean, Gulf of Alaska 08 June 2019 – 24 June 2019 R/V Marcus G. Langseth. Prepared for: Lamont-Doherty Earth Observatory of Columbia University for submission to: National Marine Fisheries Service, Office of Protected Resources. 94 p. Downloaded from: https://media.fisheries.noaa.gov/dam-migration/ldeo_goa_2019iha_monrep_opr1.pdf
- Dugan, PJ, Ponirakis DW, Zollweg JA, Pitzrick MS, Morano JL, Warde AM, Rice AN, Clark CW. 2011. SEDNA - Bioacoustic Analysis Toolbox Matlab Platform to Support High Performance Computing, Noise Analysis, Event Detection and Event Modeling. *IEEE Xplore*, vol. OCEANS-11, Kona, Hawaii.
- Fish JP, Carr HA. 1990. *Sound Underwater Images: A guide to the generation and interpretation of side scan sonar data*, Lower Cape Publishing, Orleans, MA., 189 pp.
- Hampton MA, Carlson PR, Lee HJ, Fealey RA. 1986. Geomorphology, sediment and sedimentary processes. In: *The Gulf of Alaska, Physical Environment and Biological Resources*, U.S. Dept. of Commerce, OCS Study, MMS 86-0095, 93-144.
- Hanson, M. B., M. E. Dalheim, D. L. Webster, C. K. Emmons, G. S. Shchorr, R. W. Baird, and R. D. Andrews. 2012. How "resident" are resident-type killer whales in Alaska? New data show similar widespread movement patterns in the fall (Poster Presentation). Alaska Marine Science Symposium, Anchorage, AK. Accessed at ftp://ftp.afsc.noaa.gov/posters/pMBHanson01_how-resident-killer-whales.pdf.
- Hebert K. 2013. Southeast Alaska 2012 herring stock assessment surveys. Anchorage, Alaska: Alaska Department of Fish and Game. Fishery Data Series No. 13-08.

- Hobbs RC, Waite JM. Abundance of harbor porpoise (*Phocoena phocoena*) in three Alaskan regions, corrected for observer errors due to perception bias and species misidentification, and corrected for animals submerged from view. *Fishery Bulletin*. 2010 Jul;108(3):251–67.
- Holthuijsen LH. 2007. *Waves in Oceanic and Coastal Waters*. Delft University of Technology and UNESCO-IHE. Cambridge University Press. New York. 387 pp.
- Honkalehto T, McCarthy A. 2015. Results of the acoustic-trawl survey of walleye pollock (*Gadus chalcogrammus*) on the U.S. and Russian Bering Sea Shelf in June - August 2014 (DY1407). Seattle, Washington: Alaska Fisheries Science Center, National Marine Fisheries Service, National Oceanic and Atmospheric Administration. AFSC Processed Report 2015-07.
- International Electrotechnical Commission (IEC). 2015. IEC TS 62600-101, Marine energy – Wave, tidal and other water current converters – Part 101: Wave energy resource assessment and characterization. International Electrotechnical Commission 62600-101: 2015(E). 53 pp.
- International Hydrographic Organization (IHO). 2011. *Manual on Hydrography*, 1st Edition, Monaco.
- Jansen J, Boveng P, Ver Hoef J, Dahle S, Bengtson J. 2014. Natural and human effects on harbor seal abundance and spatial distribution in an Alaskan glacial fjord. *Marine Mammal Science*. 31. 10.1111/mms.12140.
- Jansen J, Womble J, Gende S. 2018. *Studies of Harbor Seals Using Glacial Ice in Disenchantment Bay, Alaska, 2016-2017*.
- Jansen JK, Bengtson JL, Dahle SP, Ver Hoef JM. 2006. Disturbance of harbor seals by cruise ships in Disenchantment Bay, Alaska: an investigation at three spatial and temporal scales. AFSC Processed Report 2006-02, 75 p. National Marine Mammal Laboratory, Alaska Fisheries Science Center, National Marine Fisheries Service, 7600 Sand Point Way NE, Seattle, WA 98115.
- Jansen JK, Boveng PL, Dahle SP, Bengtson JL. 2010. Reaction of harbor seals to cruise ships. *Journal of Wildlife Management* 74:1186-1194.
- Johnson SW, Neff AD, Thedinga JF, Lindeberg MR, Maselko JM. 2012. *Atlas of nearshore fishes of Alaska: A synthesis of marine surveys from 1998 to 2011*. Juneau, Alaska: Alaska Fisheries Science Center, National Marine Fisheries Service, National Oceanic and Atmospheric Administration. NOAA Technical Memorandum NMFS-AFSC-239.
- Kasper JK. 2021. *Secure and Resilient Power Generation in Cold Region Environments Phase 0, Final Project Report to the US Army Corps of Engineers Engineering Research and Development Center, Cooperative Agreement W913E52020001*.
- Kelley DE. 2018. *Oceanographic Analysis with R*. New York. Springer-Verlag ISBN 978-1-4939-8844-0.
- Kerouel R, Aminot A. 1997. "Fluorometric determination of ammonia in sea and estuarine waters by direct segmented flow analysis," *Marine Chemistry* Vol. 57, no. 3-4, pp.265-275.
- Laidre KL, Sheldon KE, Rugh DJ, Mahoney BA. 2000. Beluga, *Delphinapterus leucas*, distribution and survey effort in the Gulf of Alaska. *Marine Fisheries Review*. 62(3):27–36.
- Lepper PA, Robinson SP, 2015. Measurement of Underwater Operational Noise Emitted by Wave and Tidal Stream Energy Devices. *Advances in Experimental Medicine and Biology*.
- Lucey, W G, E Henniger, E Abraham, G O’Corry-Crowe, K M Stafford, and M Castellote. 2015. “Traditional Knowledge and Historical and Opportunistic Sightings of Beluga Whales,

- Delphinapterus Leucas*, In Yakutat Bay, Alaska, 1938–2013.” Marine Fisheries Review 77 (1): 41–46. doi:10.7755/MFR.77.1.4.
- Lunsford C, Rodgveller C, Malecha P. 2017. The 2017 longline survey of the Gulf of Alaska and eastern Bering Sea on the FV Ocean Prowler: Cruise Report OP-17-01. Juneau, Alaska: Alaska Fisheries Science Center, National Marine Fisheries Service, National Oceanic and Atmospheric Administration. AFSC Processed Rep. 2018-01.
- Lusseau D, Christiansen F, Harwood J, Mendes S, Thompson PM, Smith K, Hastie G. 2012. Assessing the risks to marine mammal populations from renewable energy devices: an interim approach. Peterborough: Joint Nature Conservation Committee.
- Madsen PT, Wahlberg M, Tougaard J, Lucke K, Tyack PL. 2006. Wind turbine underwater noise and marine mammals: Implications of current knowledge and data needs. Mar Ecol Prog Ser. 2006; 309:279–95.
- Martin B, Whitt C, Horwich L. 2018. Acoustic Data Analysis of the OpenHydro Open-Centre Turbine at FORCE: Final Report. Document 01588, Version 3.0b. Technical report by JASCO Applied Sciences for Cape Sharp Tidal and FORCE.
- MathWorks. 2019. Statistics and Machine Learning Toolbox User’s Guide, MATLAB R2019b. 10,370 pp. https://www.mathworks.com/help/releases/R2019b/pdf_doc/stats/stats.pdf date accessed 7/6/2021.
- Moore G, Onyango E, et al. 2020. The Alaska Amphibious Community Seismic Experiment, Seismol. Res. Lett. 91, 3054–3063, doi: 10.1785/0220200189.
- Moss JH, Beauchamp DA, Cross AD, Myers KW, Farley Jr. EV, Murphy JM, Helle JH. 2005. Evidence for size-selective mortality after the first summer of ocean growth by Pink Salmon. Transactions of the American Fisheries Society. 134:1313-1322.
- Mordy CW, Stabeno PJ, Ladd C, Zeeman S, Wisegarver DP, Salo SA, Hunt GL. 2005. Nutrients and primary production along the eastern Aleutian Island Archipelago. Fisheries Oceanography, 14: 55-76. <https://doi.org/10.1111/j.1365-2419.2005.00364.x>
- Moulton LL. 1997. Early marine residence, growth, and feeding by juvenile salmon in northern Cook Inlet, Alaska. Alaska Fishery Research Bulletin. 4(2):154-177.
- Murphy J, Riley JP. 1962. A modified single solution method for the determination of phosphate in natural waters. Analytica Chimia Acta, Vol. 27 pp.31-36.
- Muto MM, Helker VT, Delean BJ, Angliss RP, Boveng PL, Breiwick JM, Brost BM, Cameron MF, Clapham PJ, Dahle SP, Dahlheim ME, Fadely BS, Ferguson MC, Fritz PLW, Hobbs RC, Ivashchenko YV, Kennedy AS, London JM, Mizroch SA, Ream RR, Richmond EL, Shelden KEW, Sweeney KL, Towell RG, Wade PR, Waite JM, Zerbini A. 2020. Alaska marine mammal stock assessments, 2019. U.S. Dep. Commer., NOAA Tech. Memo. NMFS-AFSC-404, 395 p.
- Naves LC, Turek MF, Simeone WE. 2010. Subsistence–personal use salmon harvest, Southeast–Yakutat Management Region, 1996–2006. Anchorage, Alaska: Alaska Department of Fish and Game. Technical Paper No. 350.
- Neff D. 2016. Nearshore faunal assemblages in the vicinity of Yakutat, Alaska. Anchorage, Alaska: Alaska BioMap, prepared for the U.S Army Corps of Engineers. Project Report 2012–2013.

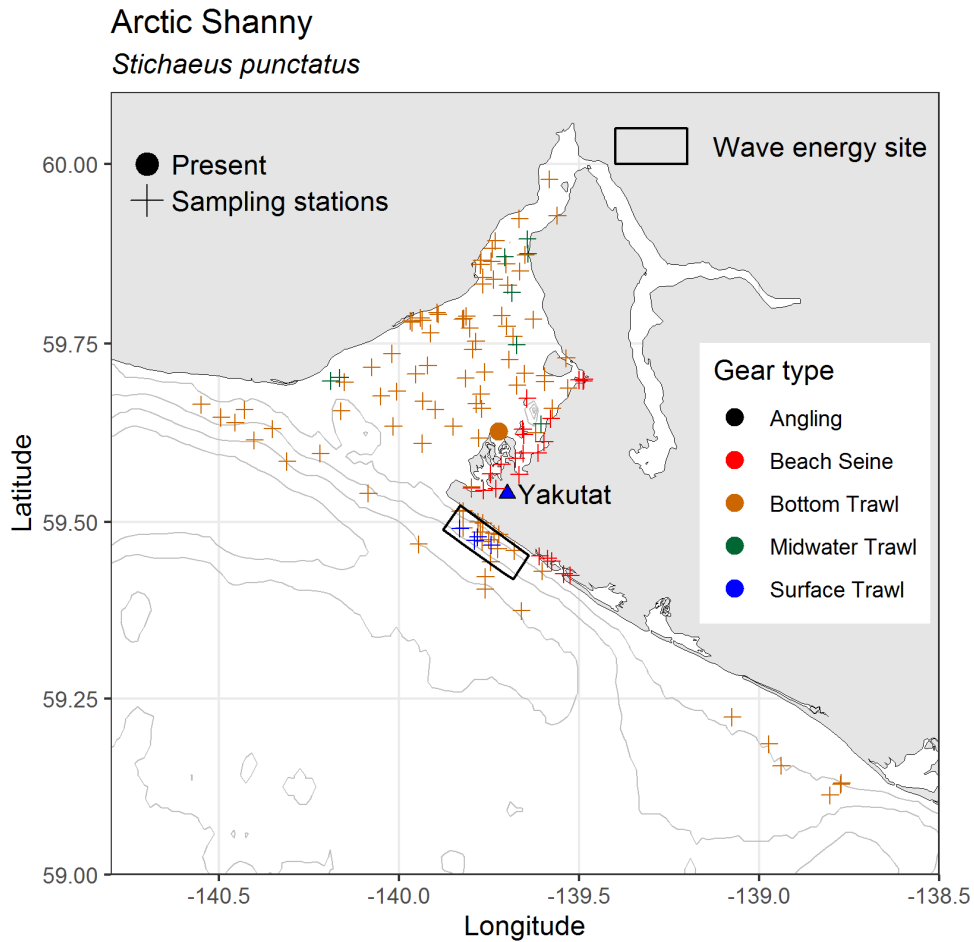
- NOAA National Geophysical Data Center. 2009: Yakutat, Alaska 8/15 Arc-second MHHW Coastal Digital Elevation Model. NOAA National Centers for Environmental Information. Accessed 07/01/2021.
- O’Corry-Crowe et al. 2006. The ecology, status and stock identity of beluga whales, *Delphinapterus leucas*, in Yakutat Bay, Alaska. Report to the U.S. Marine Mammal Commission. 22 pp.
- Olson A, Stahl J, Vaughn M, Carroll K, Baldwin A. 2017. Annual management report for the Southeast Alaska and Yakutat groundfish fisheries. Anchorage, Alaska: Alaska Department of Fish and Game. Fishery Management Report No. 17-54.
- Orsi JA, Fergusson EA. 2016. Annual survey of juvenile salmon, ecologically related species, and biophysical factors in the marine water of southeastern Alaska, May–August 2015. Juneau, Alaska: Alaska Fisheries Science Center, National Marine Fisheries Service, National Oceanic and Atmospheric Administration. NPAFC Document 1617.
- O’Neil R, Staines G, Freeman M. 2019. Marine Hydrokinetics Regulatory Processes Literature Review (Report No. PNNL-28608). Report by Pacific Northwest National Laboratory (PNNL). Report for US Department of Energy.
- Overbeck JR, ed. 2018, Alaska coastal mapping gaps & priorities, Alaska Division of Geological & Geophysical Surveys Information Circular 72. <http://doi.org/10.14509/30096>
- Pahlke KA. 1985. Preliminary studies of Capelin (*Mallotus villosus*) in Alaskan waters. Juneau, Alaska: Alaska Department of Fish and Game. Informational Leaflet 250.
- Perrin WF, Wursig B, Thewissen JGM. 2008. Encyclopedia of Marine Mammals. Academic Press. 1414 p.
- Pine MK, Schmitt P, Culloch RM, Lieber L, Kregting LT. 2019. Providing ecological context to anthropogenic subsea noise: assessing listening space reductions of marine mammals from tidal energy devices. *Renew Sustain Energy Rev.* 103:49–57.
- Polagye, B. and C. Bassett. 2020. Risk to Marine Animals from Underwater Noise Generated by Marine Renewable Energy Devices. In A.E. Copping and L.G. Hemery (Eds.), OES-Environmental 2020 State of the Science Report: Environmental Effects of Marine Renewable Energy Development Around the World. Report for Ocean Energy Systems (OES). (pp. 67-85). DOI: 10.2172/1633082.
- Polagye B, Copping A, Suryan R, Kramer S, Brown-Saracino J, Smith C. 2014. Instrumentation for Monitoring Around Marine Renewable Energy Converters: Workshop Final Report. PNNL-23110 Pacific Northwest National Laboratory, Seattle, Washington.
- Porter C, Morin P, Howat I, Noh M-J, Bates B, Peterman K, Keesey S, Schlenk M, Gardiner J, Tomko K, Willis M, Kelleher C, Cloutier M, Husby E, Foga S, Nakamura H, Platson M, Wethington Jr. M, Williamson C, Bauer G, Enos J, Arnold G, Kramer W, Becker P, Doshi A, Abhijit A, D’Souza C, Cummens P, Laurier F, Bojesen M. 2018. "ArcticDEM", <https://doi.org/10.7910/DVN/OHHUKH>, Harvard Dataverse, V1
- Previsic M, Bedard R. 2009. Yakutat conceptual design, performance, cost and economic wave power feasibility study. Electric Power Research Institute. Report ID: EPRI-WP-006-Alaska.
- Pyc C., Zeddies D, Denes S, Weirathmueller M. 2018. Appendix III-M: REVISED DRAFT - Supplemental Information for the Assessment of Potential Acoustic and Non-acoustic Impact Producing Factors on Marine Fauna during Construction of the Vineyard Wind Project.

- Document 001639, Version 3.1. Technical report by JASCO Applied Sciences (USA) Inc. for Vineyard Wind.
- Rijnsburger S, Flores RP, Pietrzak JD, Horner-Devine AR, Souza AJ. 2018. The influence of tide and wind on the propagation of fronts in a shallow river plume. *Journal of Geophysical Research: Oceans*, 123, 5426– 5442. <https://doi.org/10.1029/2017JC013422>
- Robinson SP, Lepper PA. 2013. Scoping Study: Review of Current Knowledge of Underwater Noise Emissions from Wave and Tidal Stream Energy Devices. Technical Report. The Crown Estate.
- Rogers BJ, Wangerin ME, Garrison KJ, Rogers DE. 1980. Epipelagic meroplankton, juvenile fish, and forage fish: distribution and relative abundance in coastal waters near Yakutat. Boulder, Colorado: National Oceanic and Atmospheric Administration, Outer Continental Shelf Environmental Assessment Program. Interim Report RU No. 603.
- SeaGen environmental monitoring program, final report, 2011.
- Shelden K, Moore SE, Waite J, Wade P, Rugh D. 2005. Historic and current habitat use by North Pacific right whales *Eubalaena japonica* in the Bering Sea and Gulf of Alaska. *Mammal Review*. 2005;35(2):129–55.
- Shen H, Zydlewski GB, Viehman HA, Staines G. 2016. Estimating the probability of fish encountering a marine hydrokinetic device. *Renewable Energy*. 97:746-756.
- Shephard ME. 1995. Plant community ecology and classification of the Yakutat Foreland, Alaska. Region 10, USDA Forest Service, Alaska Publication R10-TP-56. Juneau, AK. 214p.
- Sigler MF, Rutecki TL, Courtney DL, Karinen JF, Yang M-S. 2001. Young of the year Sablefish abundance, growth, and diet in the Gulf of Alaska. *Alaska Fishery Research Bulletin*. 8:57-70.
- Sparling C, Smith K, Benjamins S, Wilson B, Gordon J, Stringell T, Morris C, Hastie G, Thompson D, Pomeroy P. 2015. Guidance to inform marine mammal site characterization requirements at wave and tidal stream energy sites in Wales. SMRUC-NRW-2015-012.
- Stafford KM, Mellinger DK, Moore SE, Fox CG. 2007. Seasonal variability and detection range modeling of baleen whale calls in the Gulf of Alaska, 1999–2002. *Journal of the Acoustical Society of America* 122(6): 3378-3390.
- Stafford KM, Moore SE, Stabeno PJ, Holliday DV, Napp JM, Mellinger DK. 2010. Biophysical ocean observation in the southeastern Bering Sea. *Geophysical Research Letters* 37:L02606.
- Stafford KM. 2003. Two types of blue whale calls Recorded in the Gulf of Alaska. *Marine Mammal Science* 19(4):682-693.
- Sullivan C, Warner J, Martin M, Lightsom F, Voulgaris G, Work P. 2006. Waves Processing Toolbox Manual. Open-File Report 2005-1211. U.S. Department of the Interior. U.S. Geological Survey. 86 pp. <https://pubs.usgs.gov/of/2005/1211/> date accessed 1/1/2020.
- Teledyne RD Instruments. 2017a. Velocity Software User’s Guide. P/N 95D-6000-00 (January 2017) 116 pp. <http://www.teledynemarine.com/rdi/support#> date accessed 4/23/2020.
- Teledyne RD Instruments. 2017b. Waves Primer Wave Measurements and the TRDI ADCP Waves Array Technique. P/N 957-6279-00 (July 2017) 28 pp. <http://www.teledynemarine.com/rdi/support#> date accessed 5/11/2020.

- Tingley A, Davidson W. 2011. Overview of the 2010 Southeast Alaska and Yakutat commercial, personal use, and subsistence salmon fisheries. Anchorage, Alaska: Alaska Department of Fish and Game. Fishery Management Report No.11-39.
- Tougaard J. 2015. Underwater Noise from a Wave Energy Converter Is Unlikely to Affect Marine Mammals. Pavan G, editor. PLoS ONE. 2015 Jul 6;10(7):e0132391.
- Trudel M, Fisher J, Orsi JA, Morris JFT, Thiess ME, Sweeting RM, Hinton S, Fergusson EA, Welch DW. 2009. Distribution and migration of juvenile Chinook salmon derived from coded wire tag recoveries along the continental shelf of western North America. *Transactions of the American Fisheries Society*. 138(6):1369-1391.
- Tschetter T, Kasper JL, Duvoy PX. 2016. Yakutat area wave resource assessment. Fairbanks, Alaska: Alaska Center for Energy and Power. Final Report prepared for the Alaska Energy Authority and the City and Borough of Yakutat.
- Tucker S, Trudel M, Welch DW, Candy JR, Morris JFT, Thiess ME, Wallace C, Beacham TD. 2011. Life history and seasonal stock-specific ocean migration of juvenile Chinook Salmon. *Transactions of the American Fisheries Society*. 140:1101-1119.
- Viehman HA, Zydlewski GB. 2015. Fish interactions with a commercial-scale tidal energy device in the natural environment. *Estuaries and Coasts*. 38:241-252.
- Viehman HA, Zydlewski GB, McCleave JD, Staines GJ. 2015. Using hydroacoustics to understand fish presence and vertical distribution in a tidally dynamic region targeted for energy extraction. *Estuaries and Coasts*. 38:215-226.
- Viehman HA, Zydlewski GB. 2015. Fish interactions with a commercial-scale tidal energy device in the natural environment. *Estuaries and Coasts*. 38:241-252.
- von Szalay PG, Raring NW. 2018. Data report: 2017 Gulf of Alaska bottom trawl survey. Seattle, Washington: Alaska Fisheries Science Center, National Marine Fisheries Service, National Oceanic and Atmospheric Administration. NOAA Technical Memorandum NMFS-AFSC-374.
- Weingartner T. 2005. Physical and Geological Oceanography: Coastal Boundaries and Coastal and Ocean Circulation in Mundy, Phillip R. (ed.). *The Gulf of Alaska: Biology and Oceanography*. Alaska Sea Grant College Program, University of Alaska Fairbanks.
- Zeiser NL, Woods GF. 2016. Annual management report of the 2015 Yakutat area commercial salmon fisheries. Anchorage, Alaska: Alaska Department of Fish and Game. Fishery Management Report No.16-22.

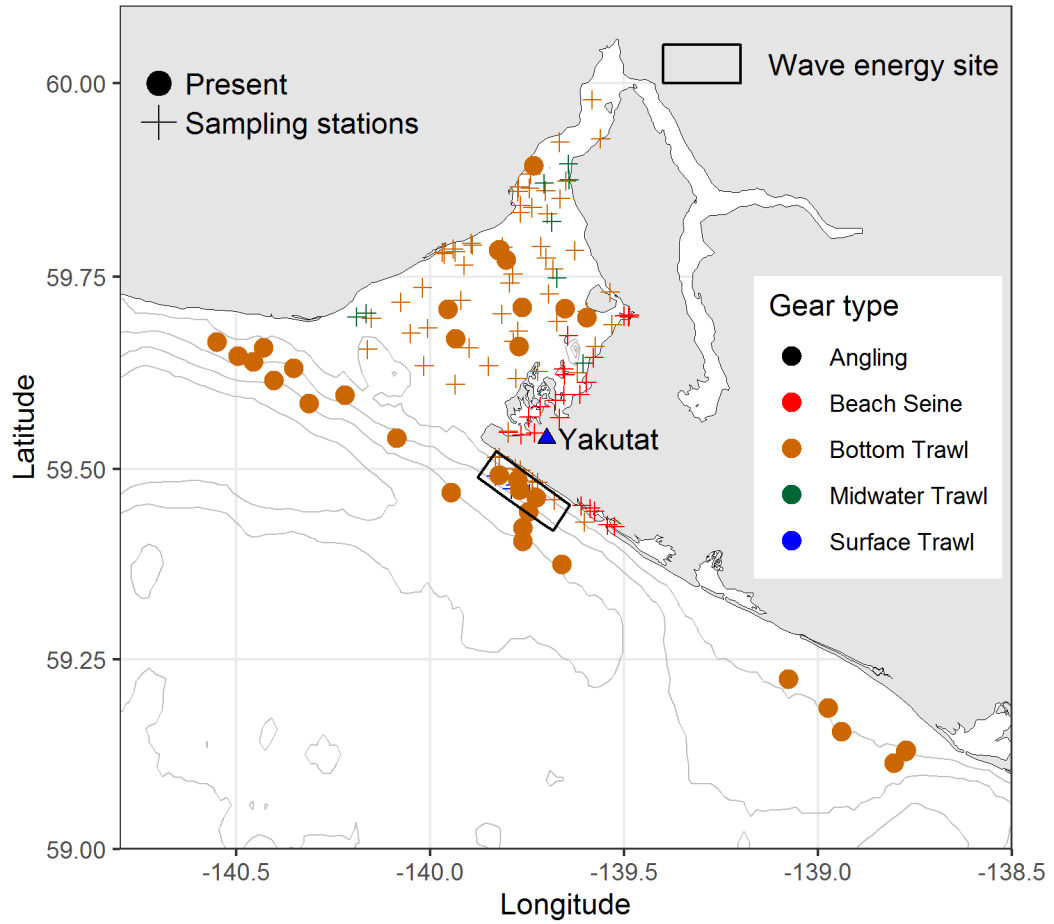
Appendix A

Figure captions: Fish species presence (solid circles) by gear type (beach seine = red, bottom trawl = orange, midwater trawl = green, surface trawl = blue) in nearshore regions adjacent to Cannon Beach, Yakutat, AK. + represents additional sampling sites where the species depicted in each figure was not captured. Small black dots denote fish captured by angling methods (note not all angling locations are depicted in figures). Black polygon denotes the wave-energy study site, near Cannon Beach. Gray lines denote 50, 100, 150, and 200 m isobaths.

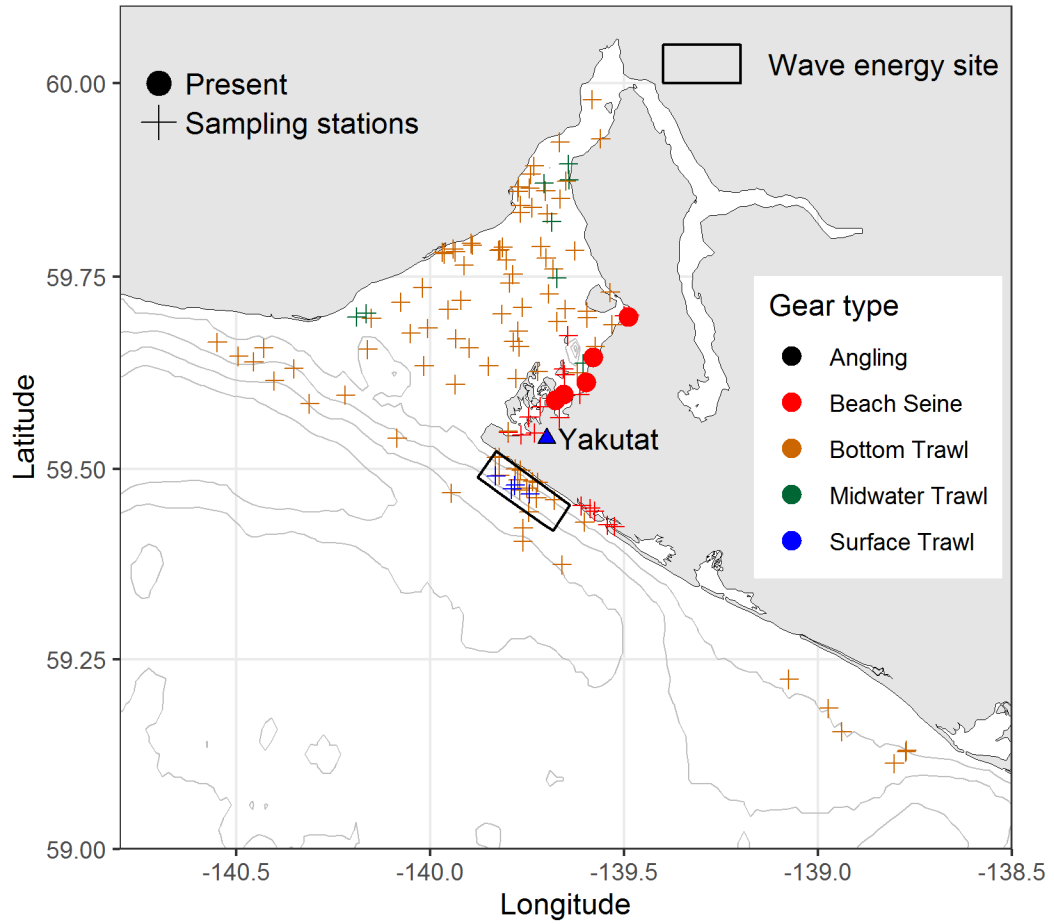


Arrowtooth Flounder

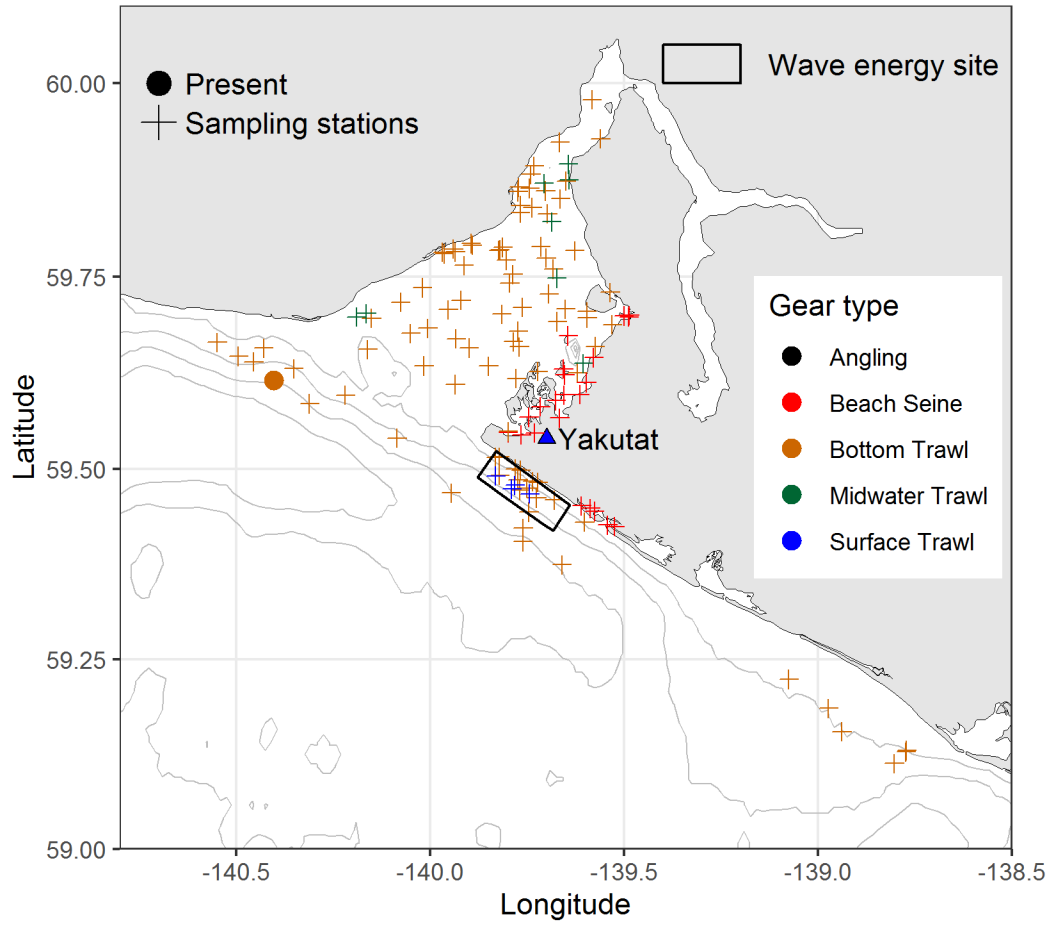
Atheresthes stomias



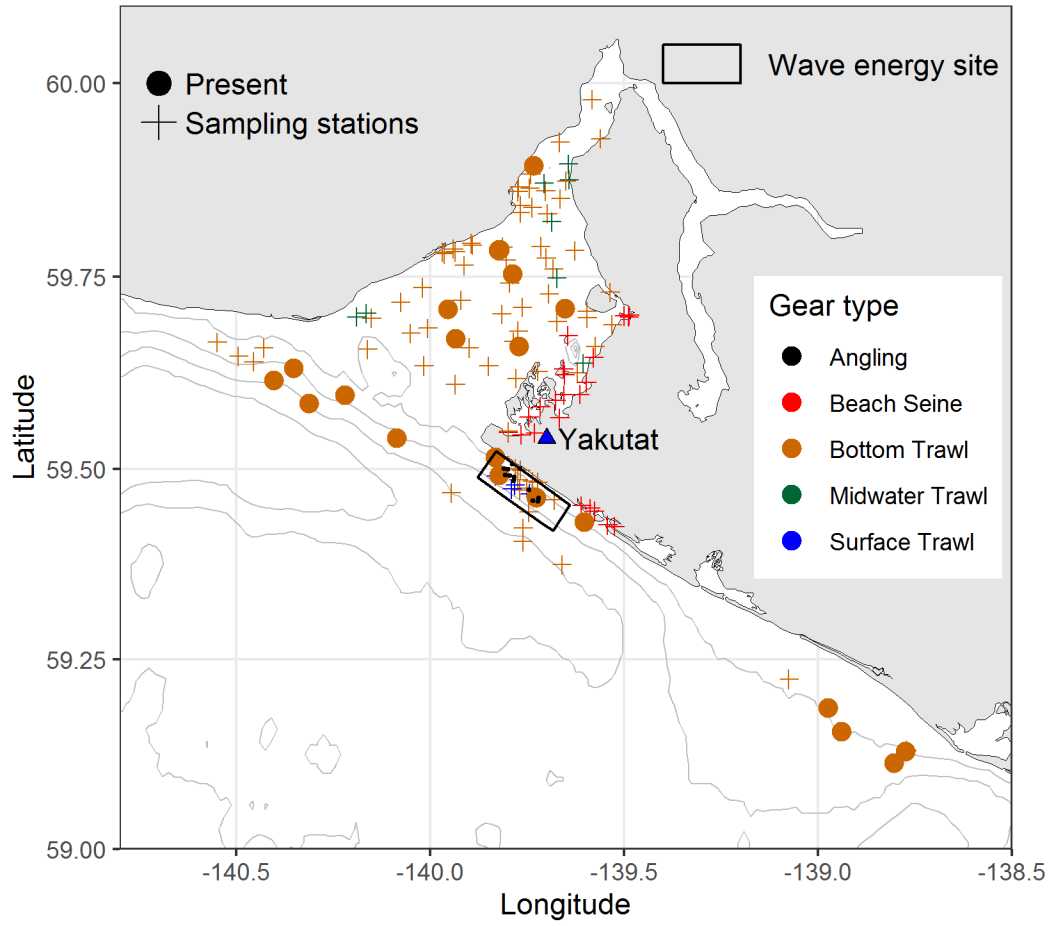
Bay Pipefish
Syngnathus leptorhynchus



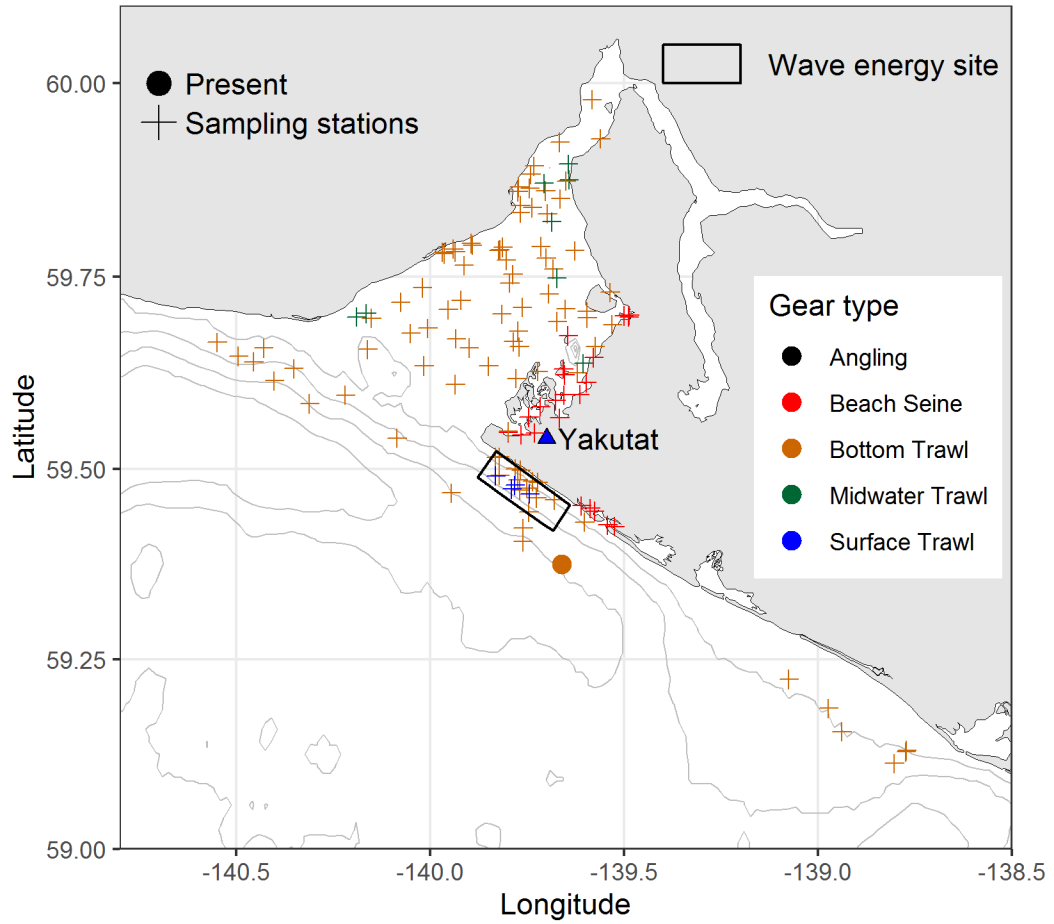
Bering Skate
Bathyraja interrupta



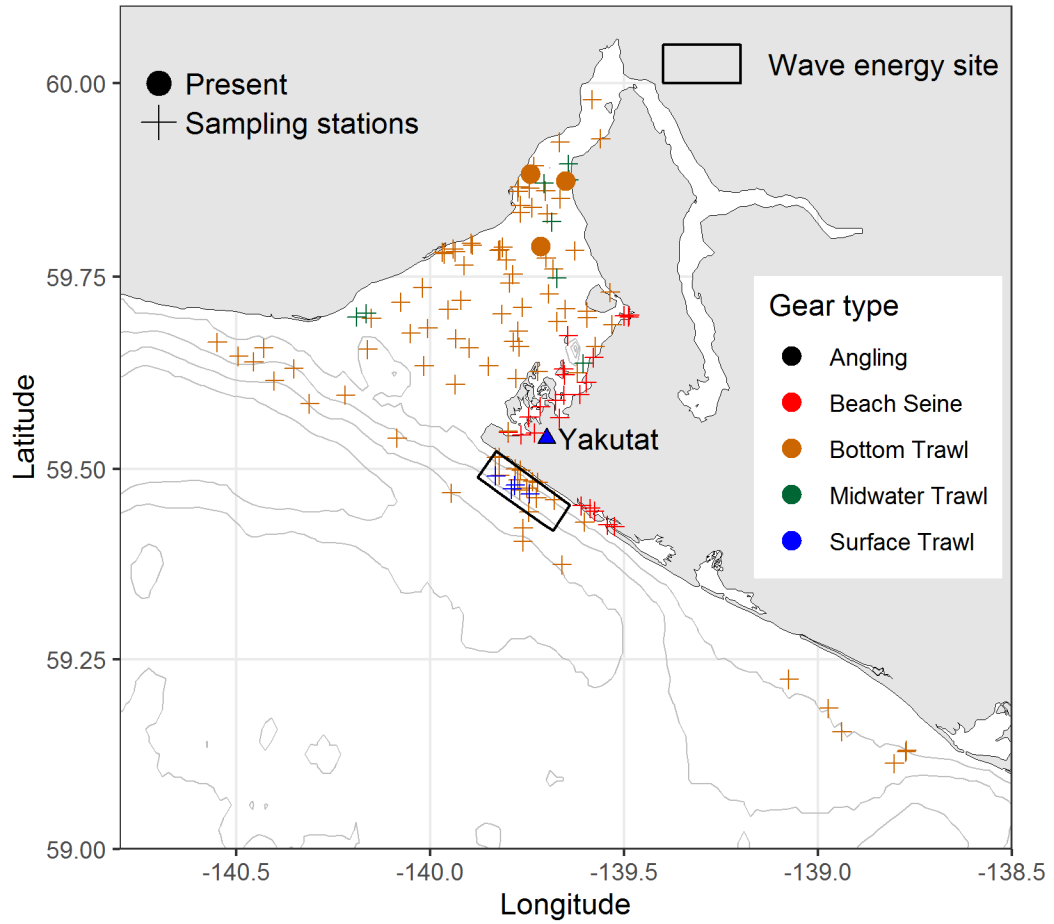
Big Skate
Beringraja binoculata



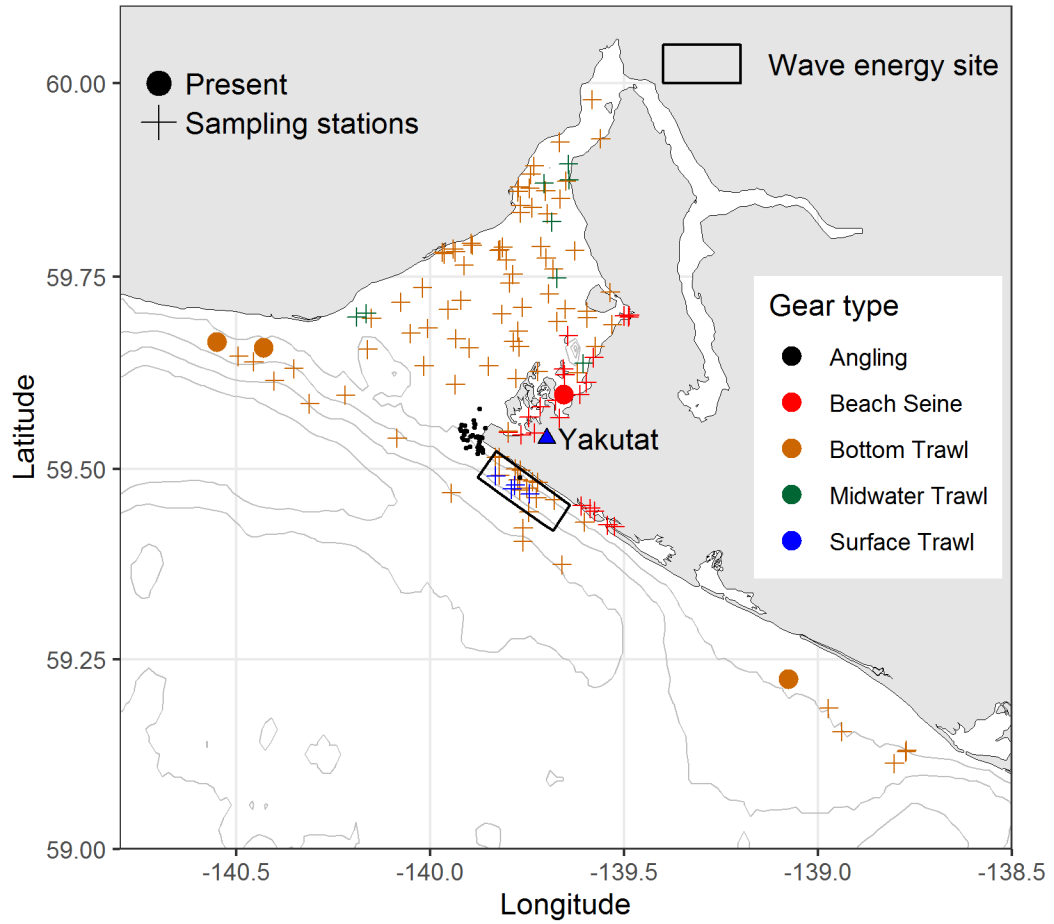
Bigfin Eelpout
Lycodes cortezius



Bigmouth Sculpin
Hemitripterus bolini

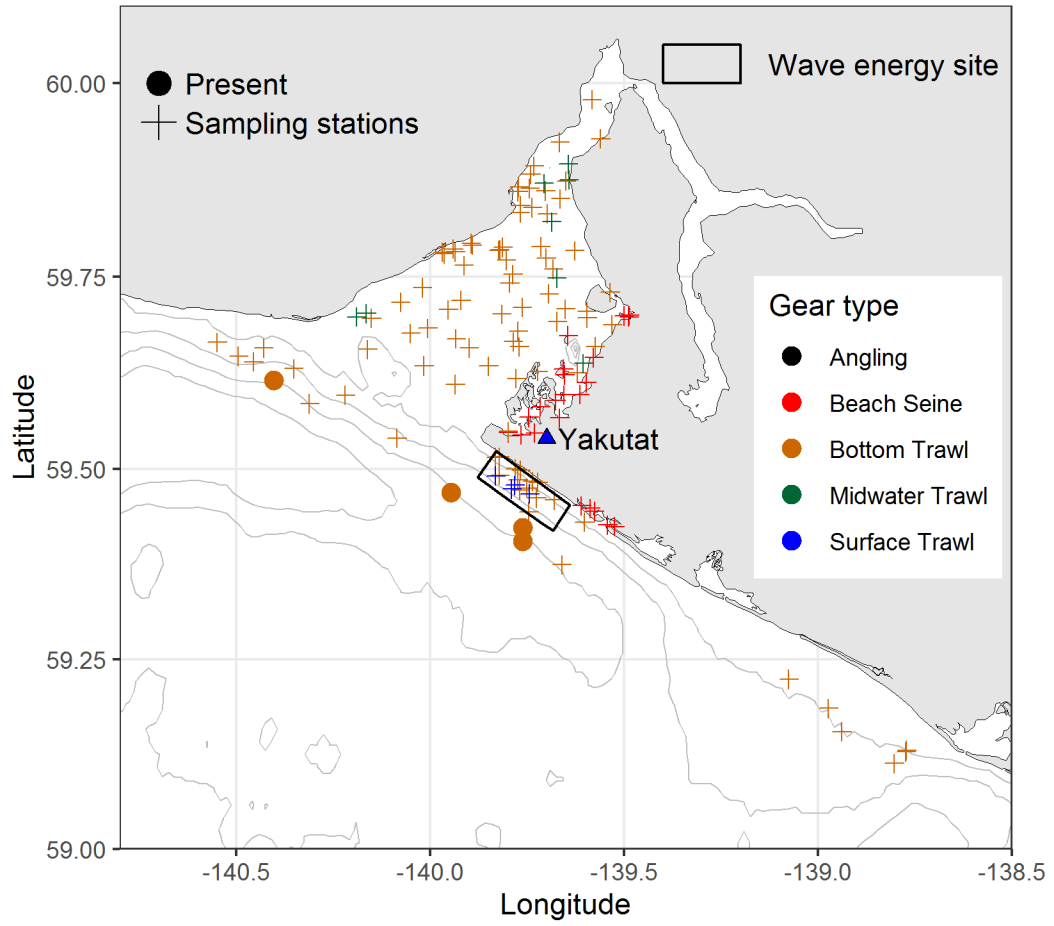


Black Rockfish
Sebastes melanops



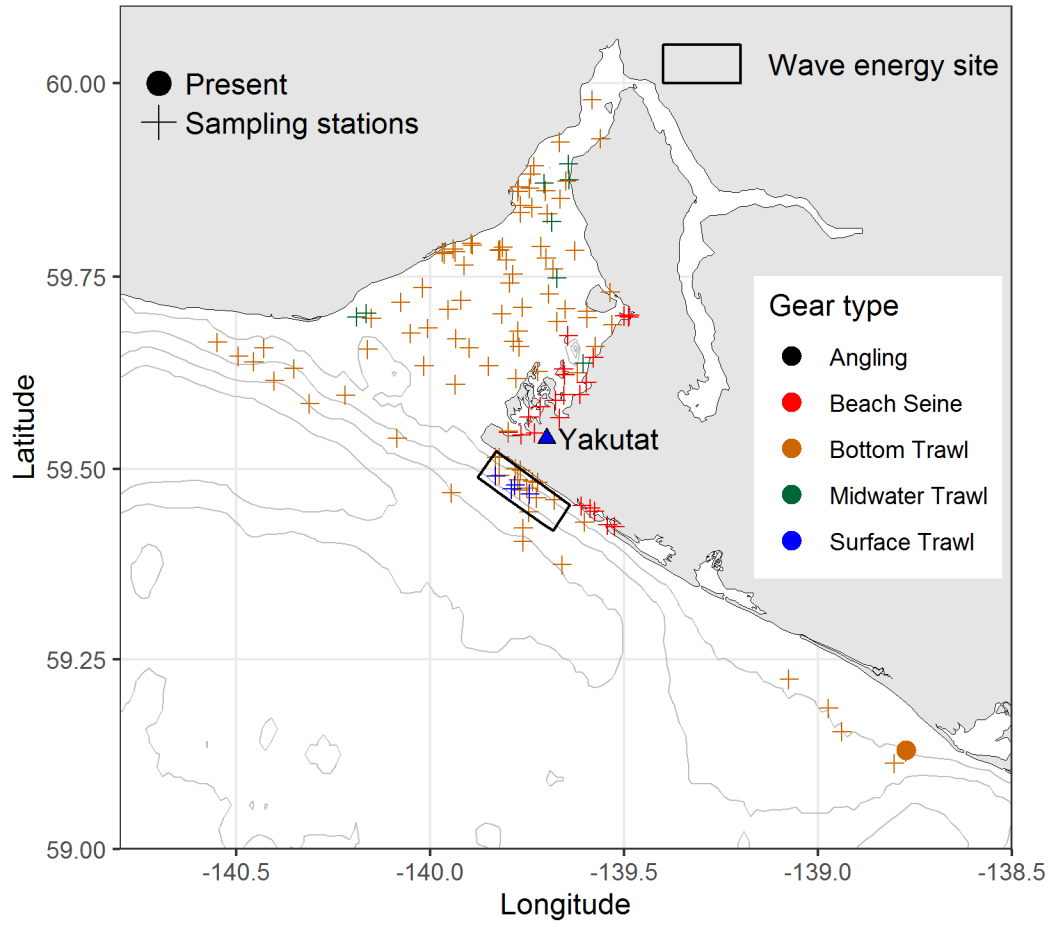
Blackbelly Eelpout

Lycodes pacificus



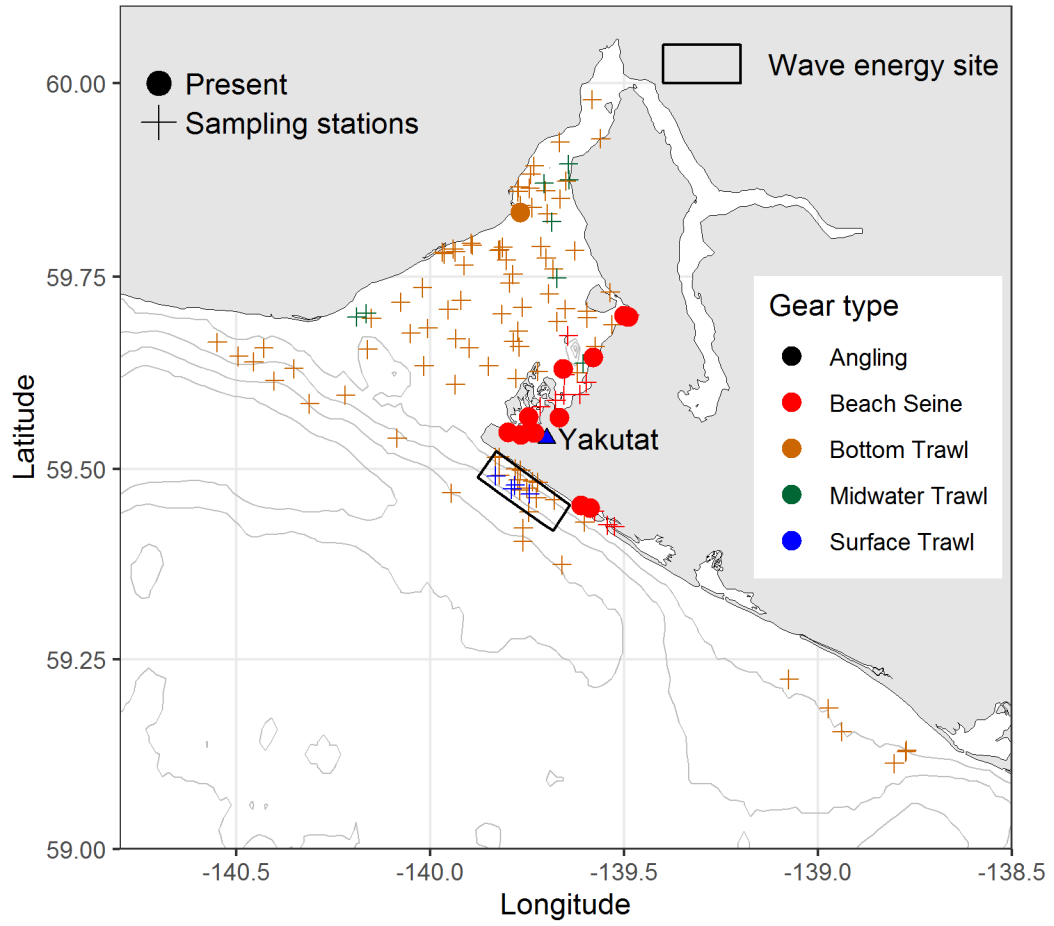
Bluntnose Sixgill Shark

Hexanchus griseus

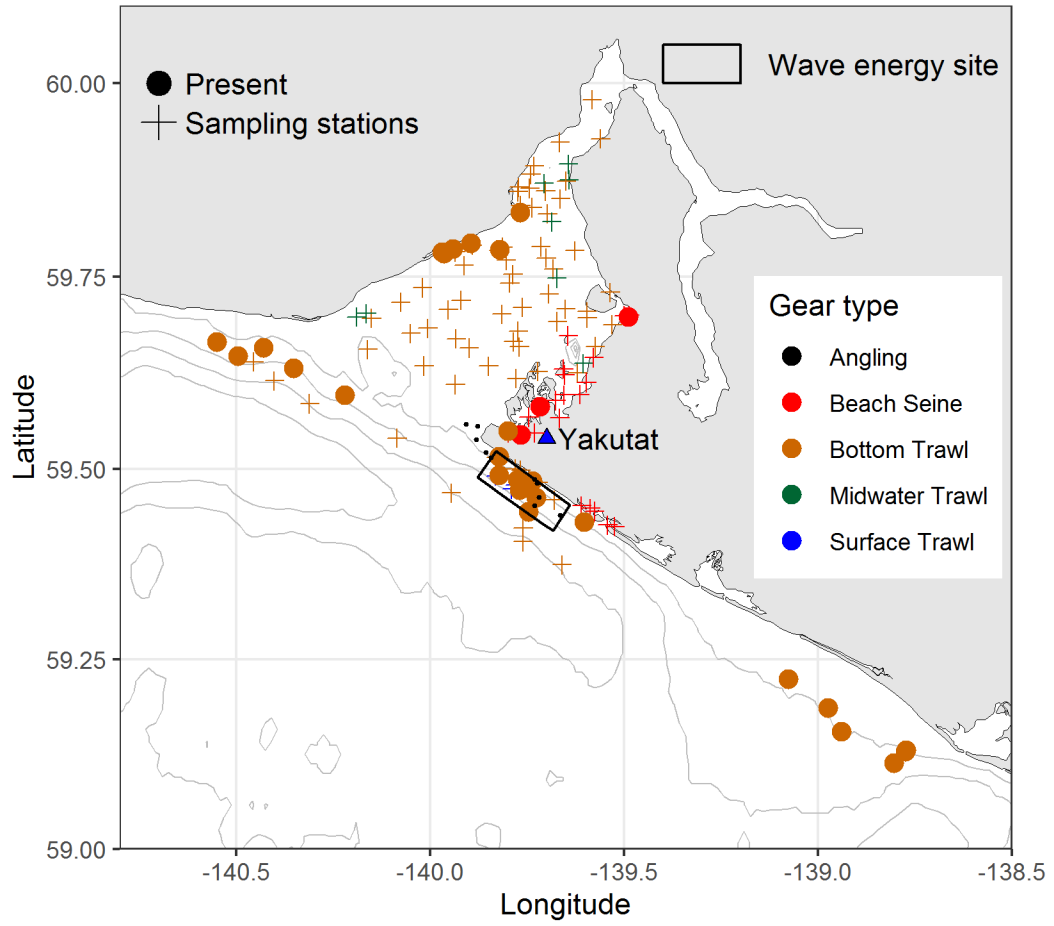


Buffalo Sculpin

Enophrys bison

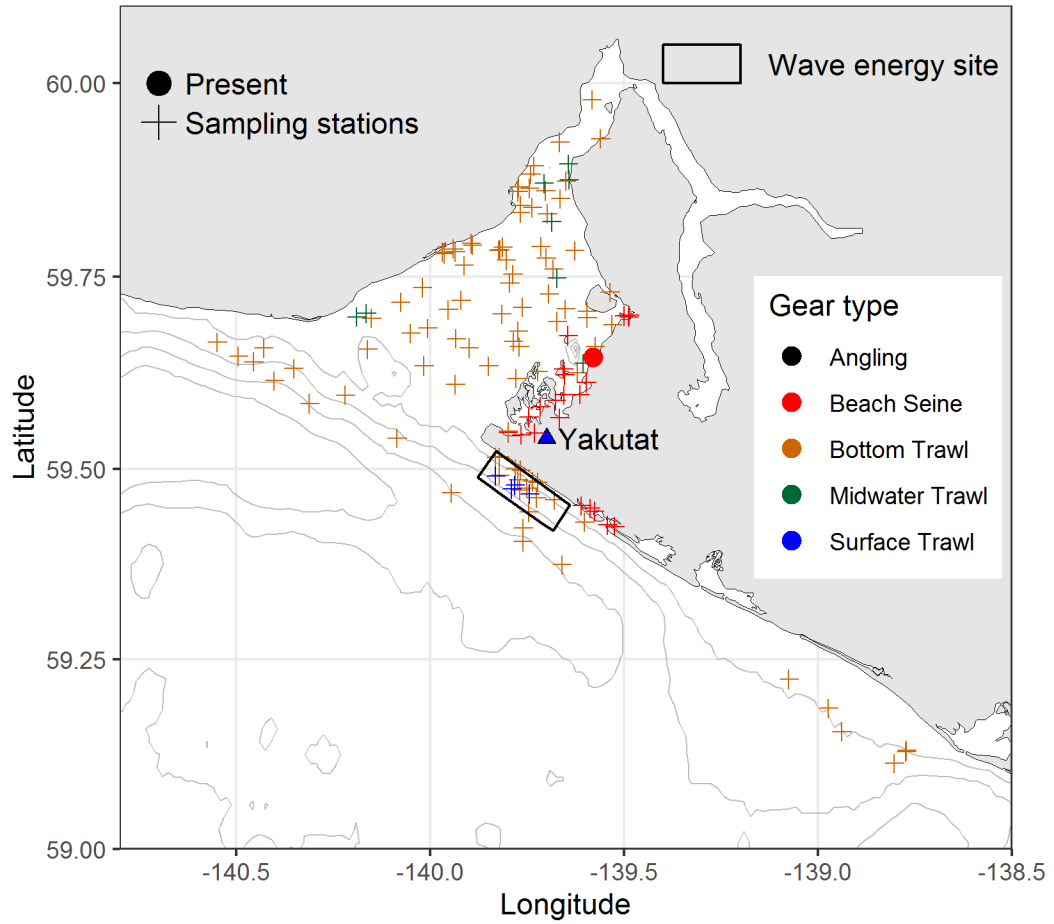


Butter Sole
Isopsetta isolepis

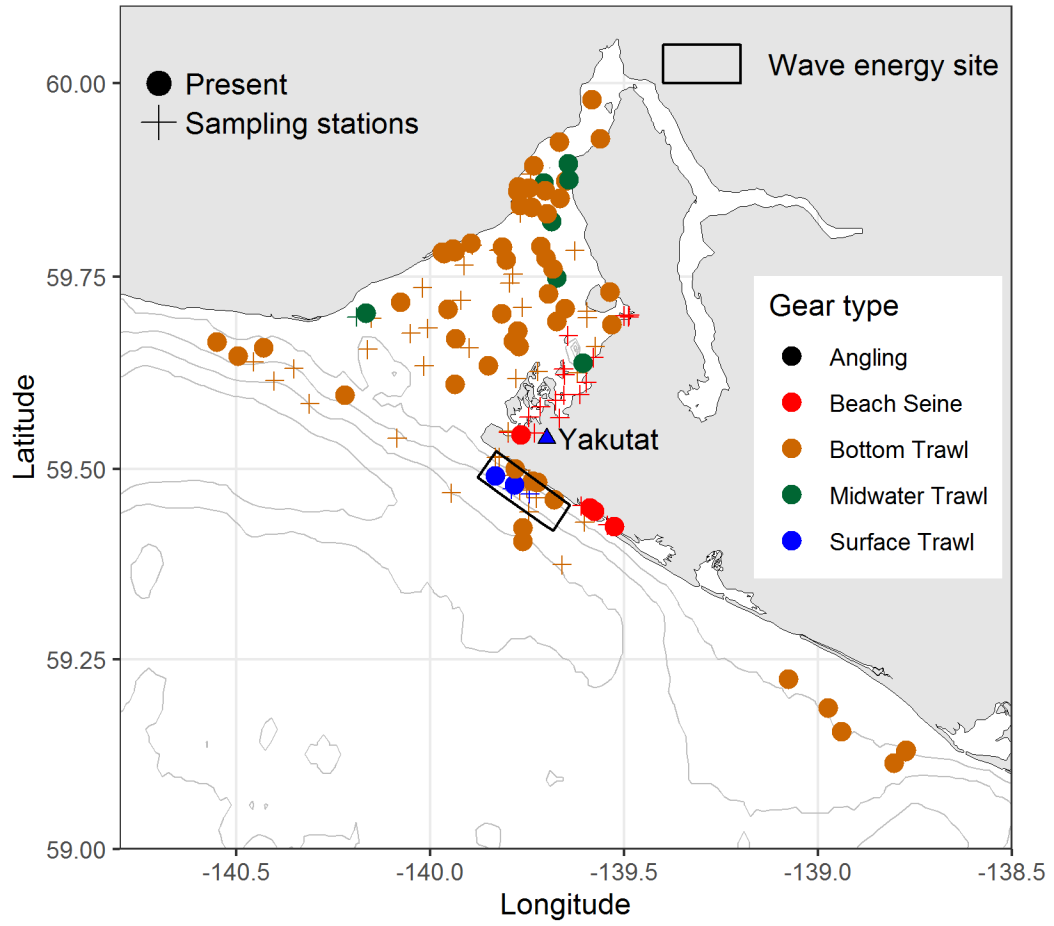


Cabezon

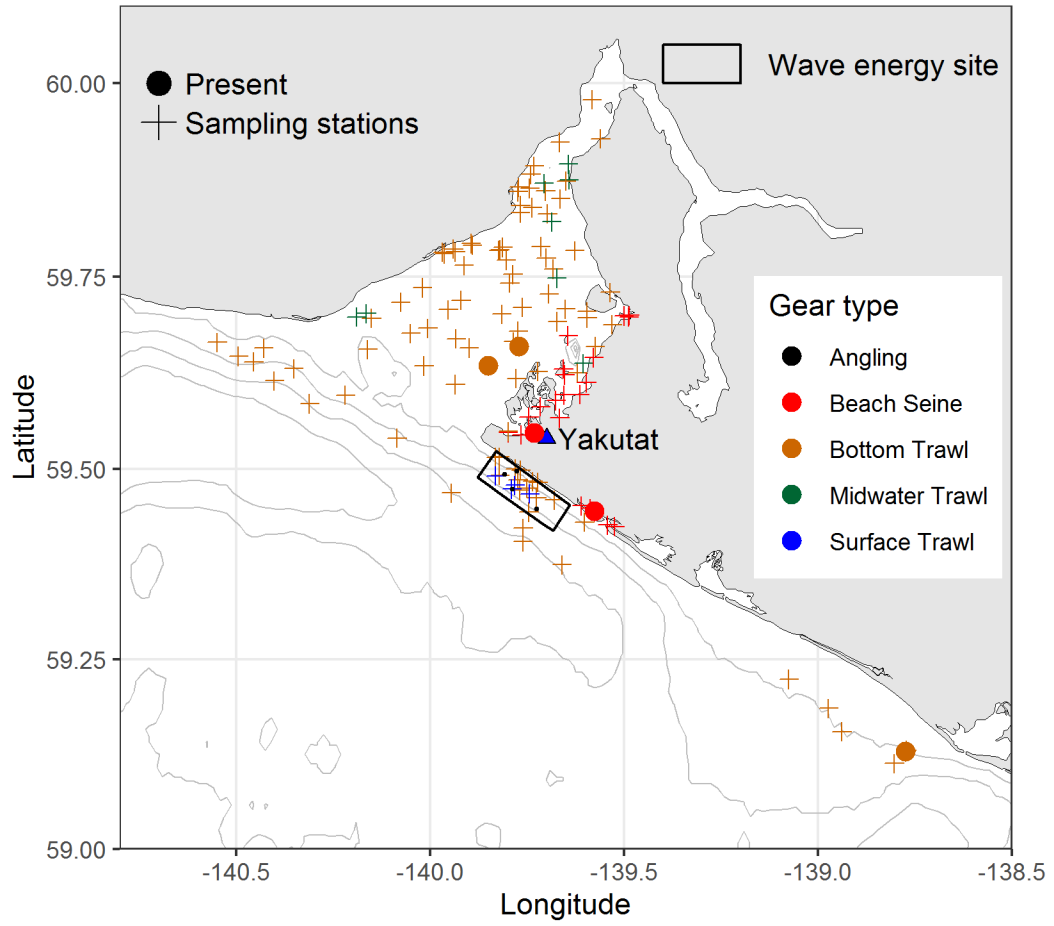
Scorpaenichthys marmoratus



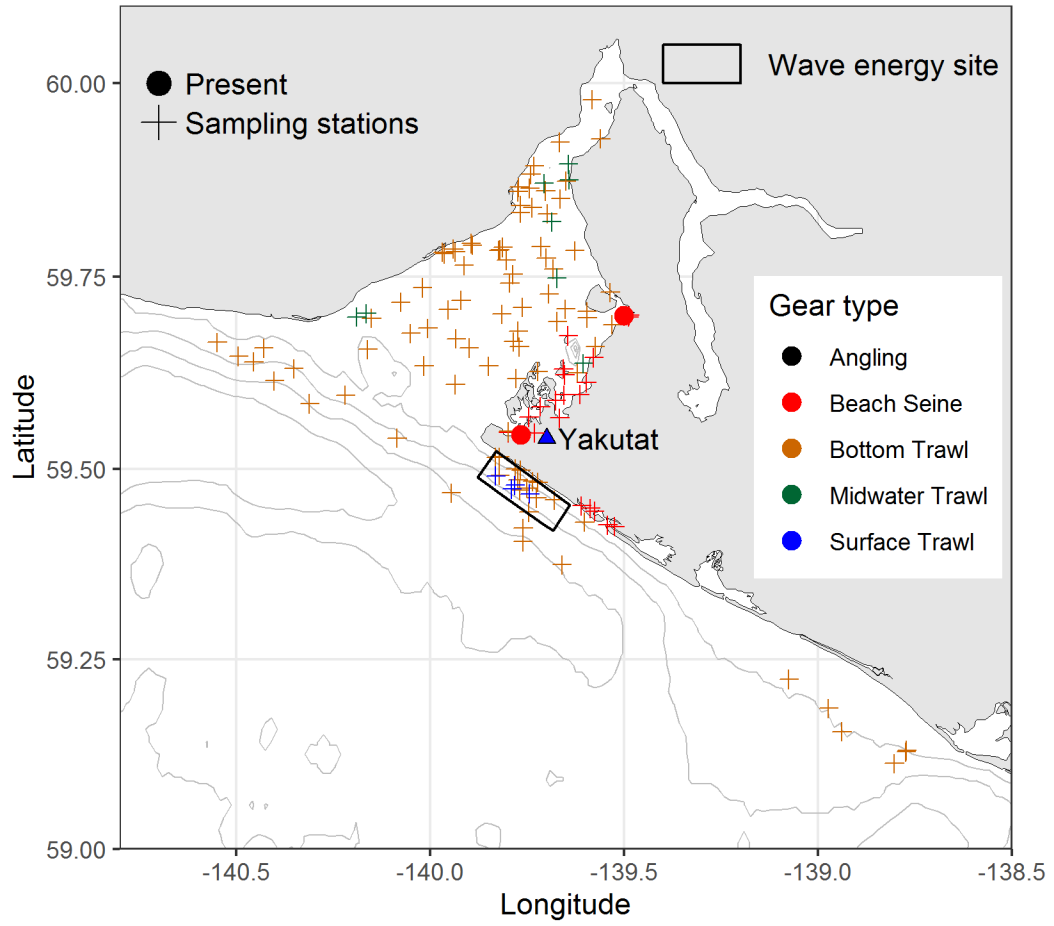
Capelin
Mallotus villosus



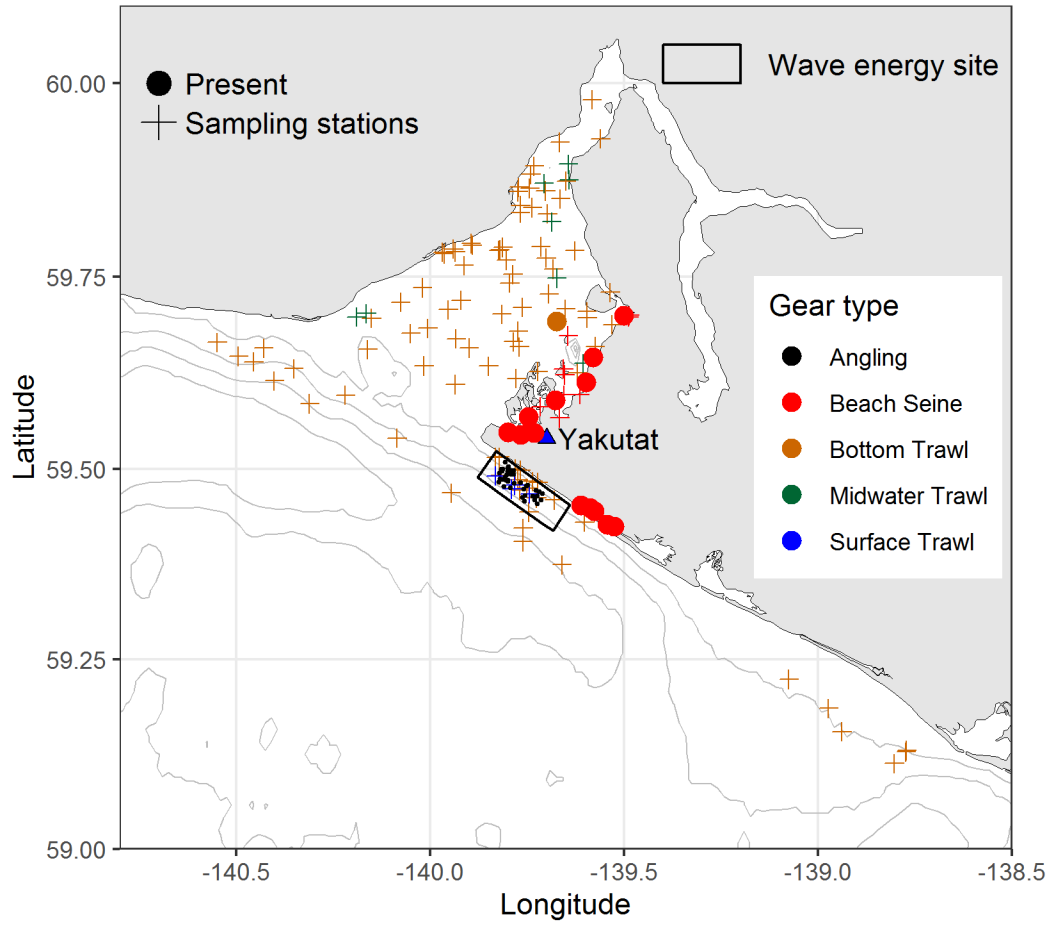
Chinook Salmon
Oncorhynchus tshawytscha



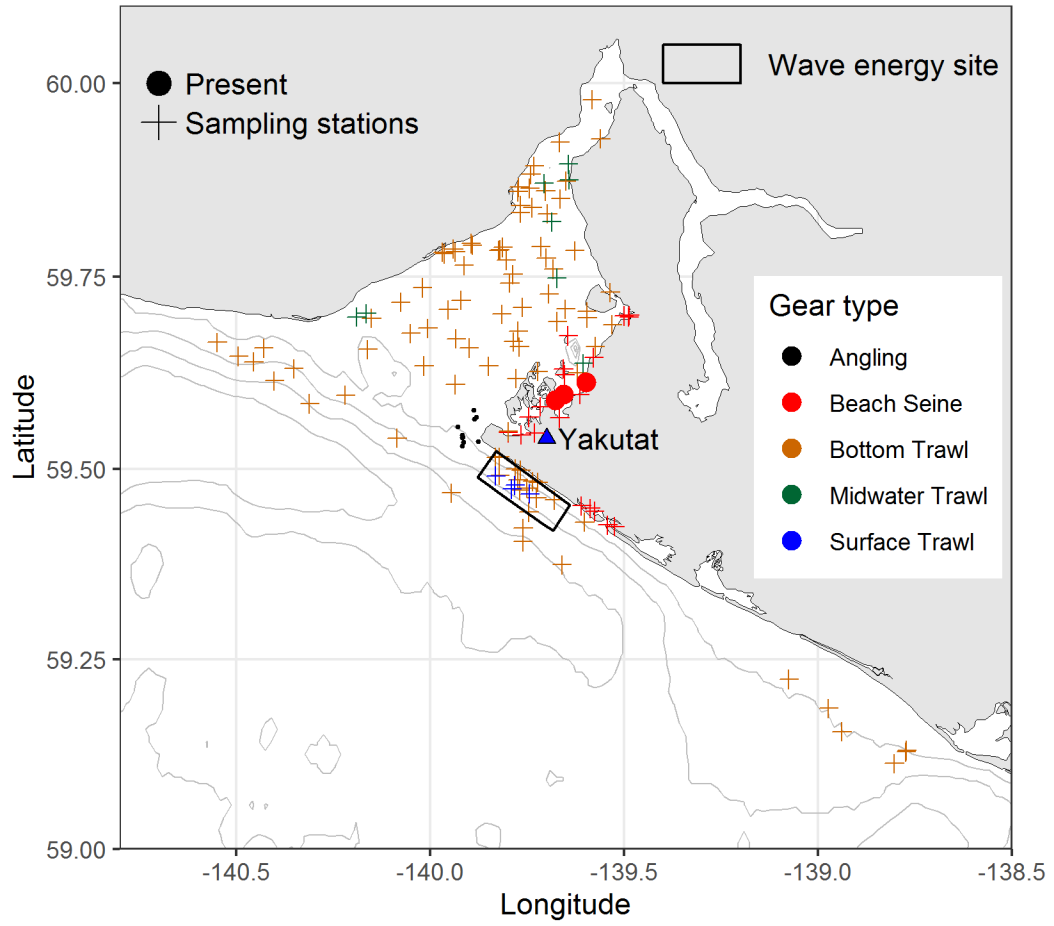
Chum Salmon
Oncorhynchus keta



Coho Salmon
Oncorhynchus kisutch

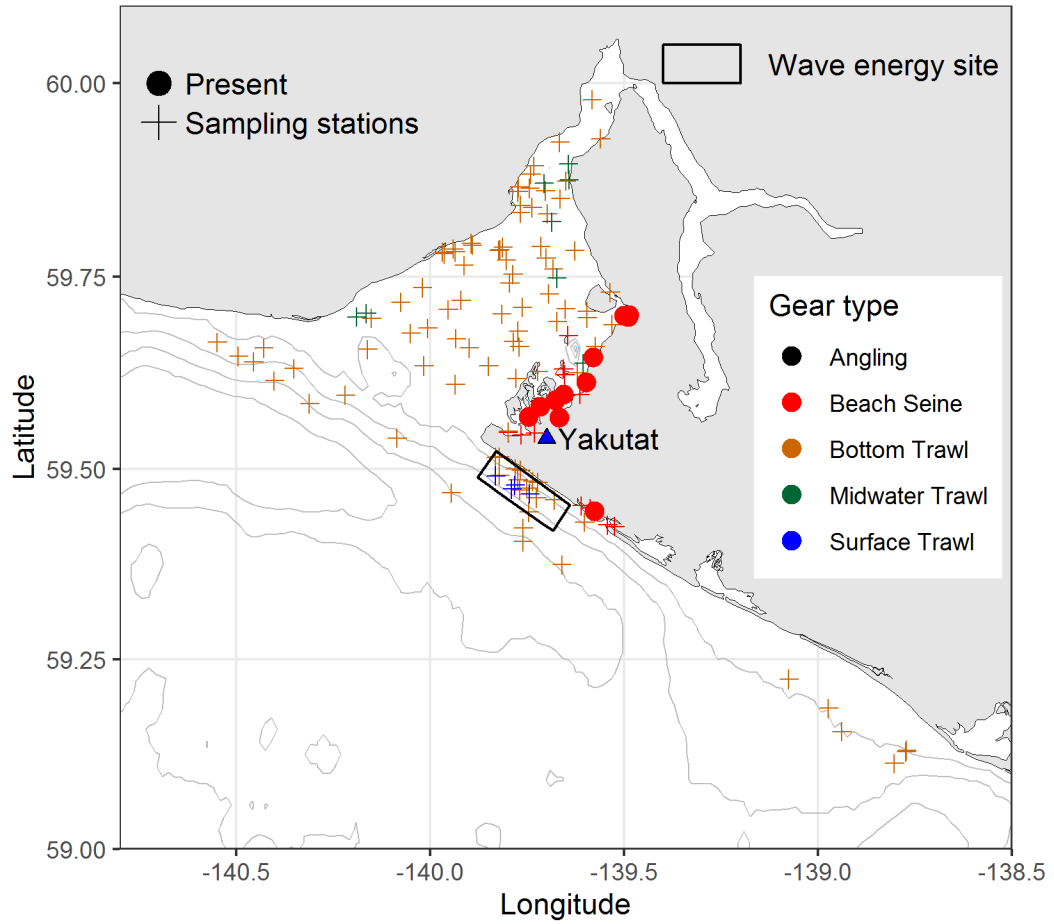


Copper Rockfish
Sebastes caurinus



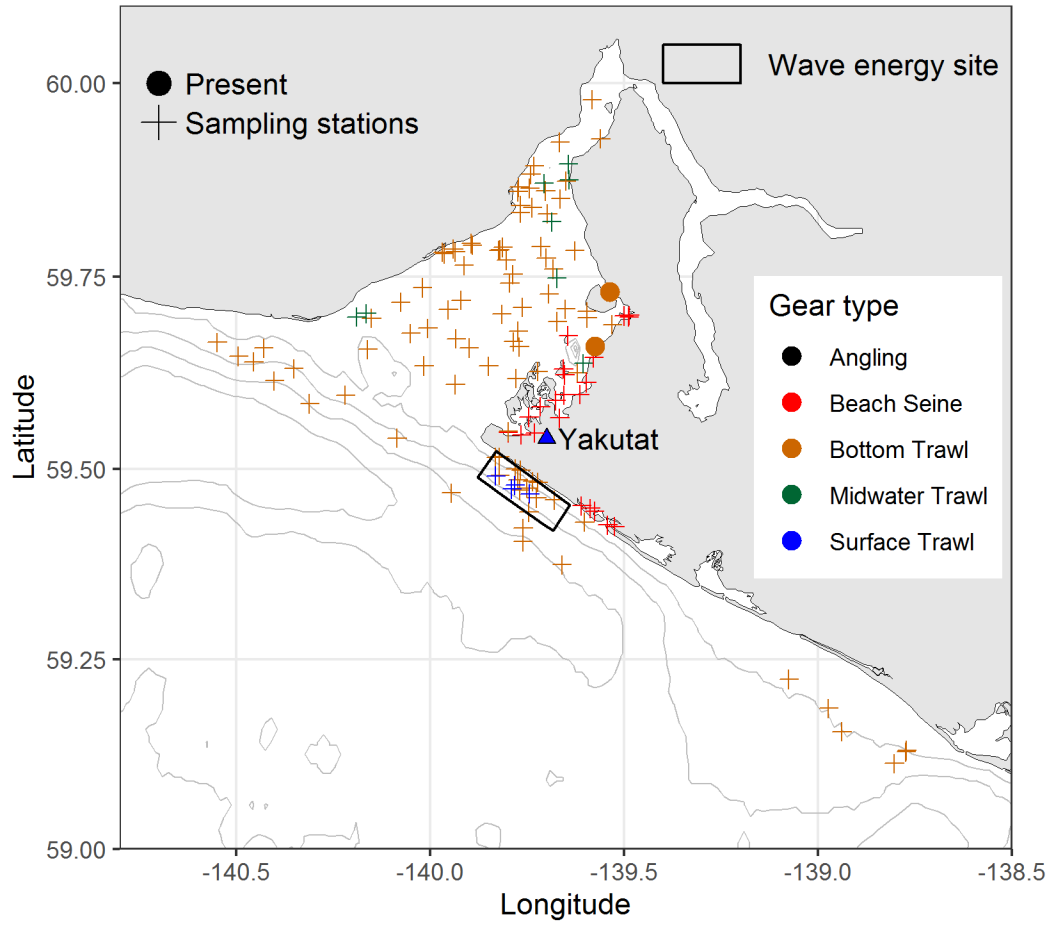
Crescent Gunnel

Pholis laeta



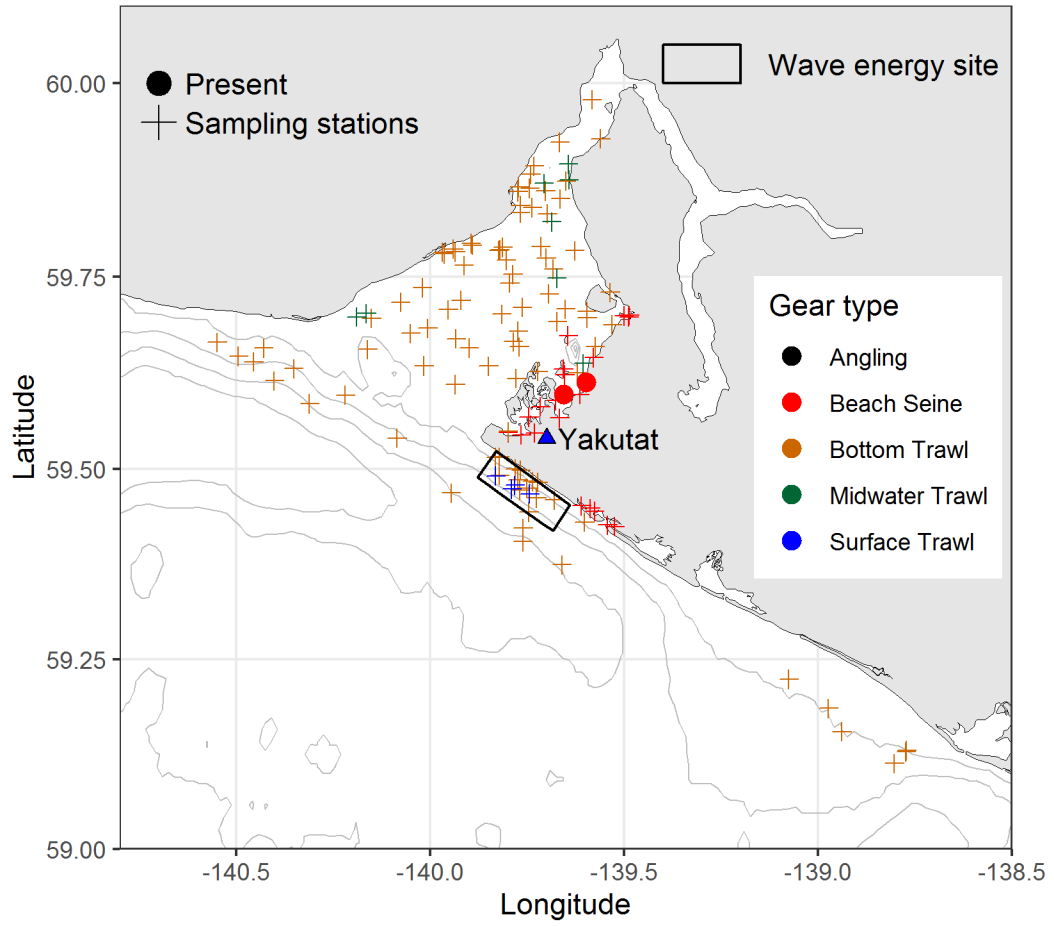
Crested Sculpin

Blepsias bilobus



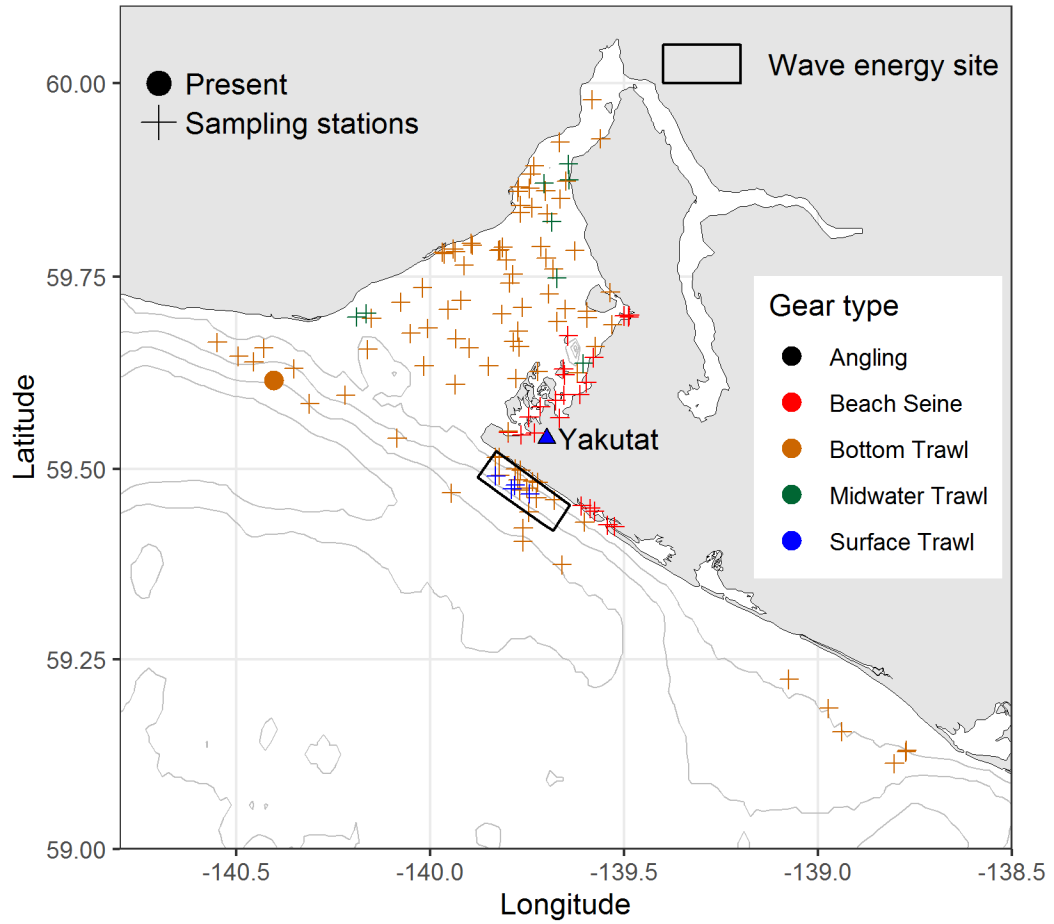
Dark Rockfish

Sebastes ciliatus

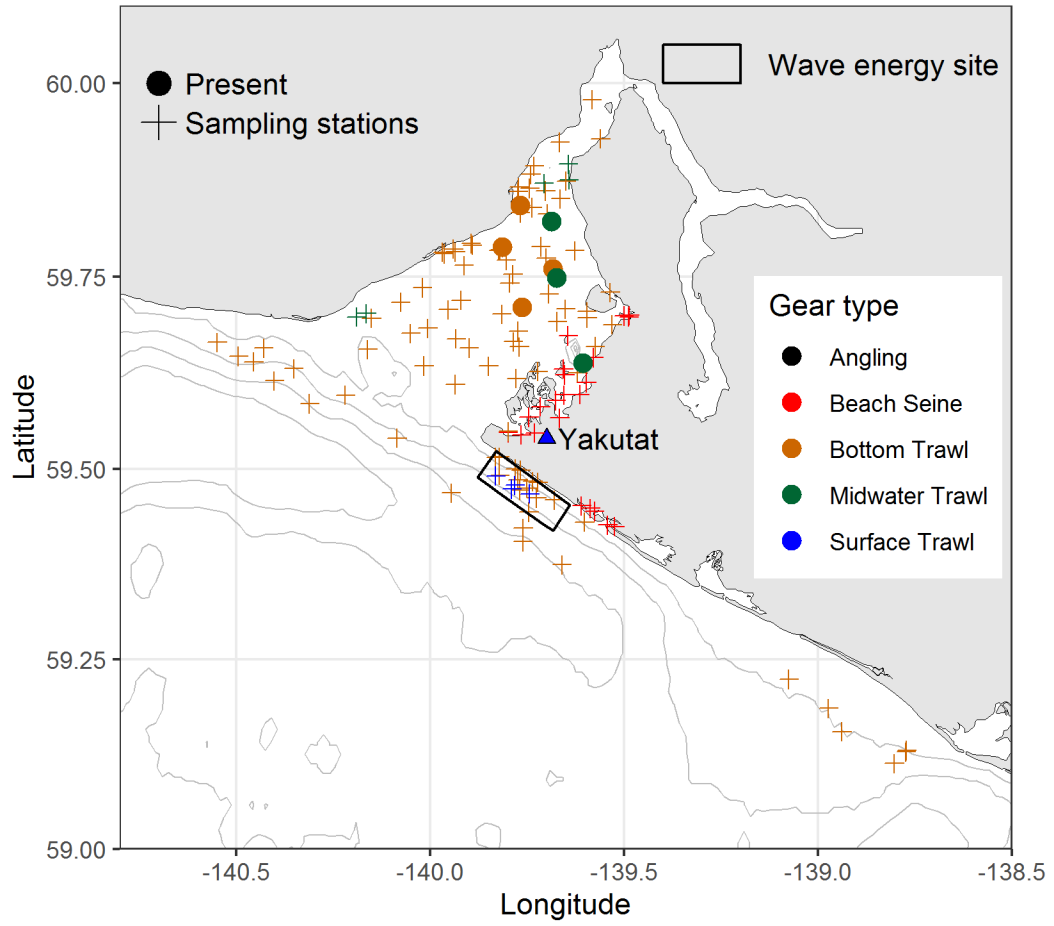


Darkblotched Rockfish

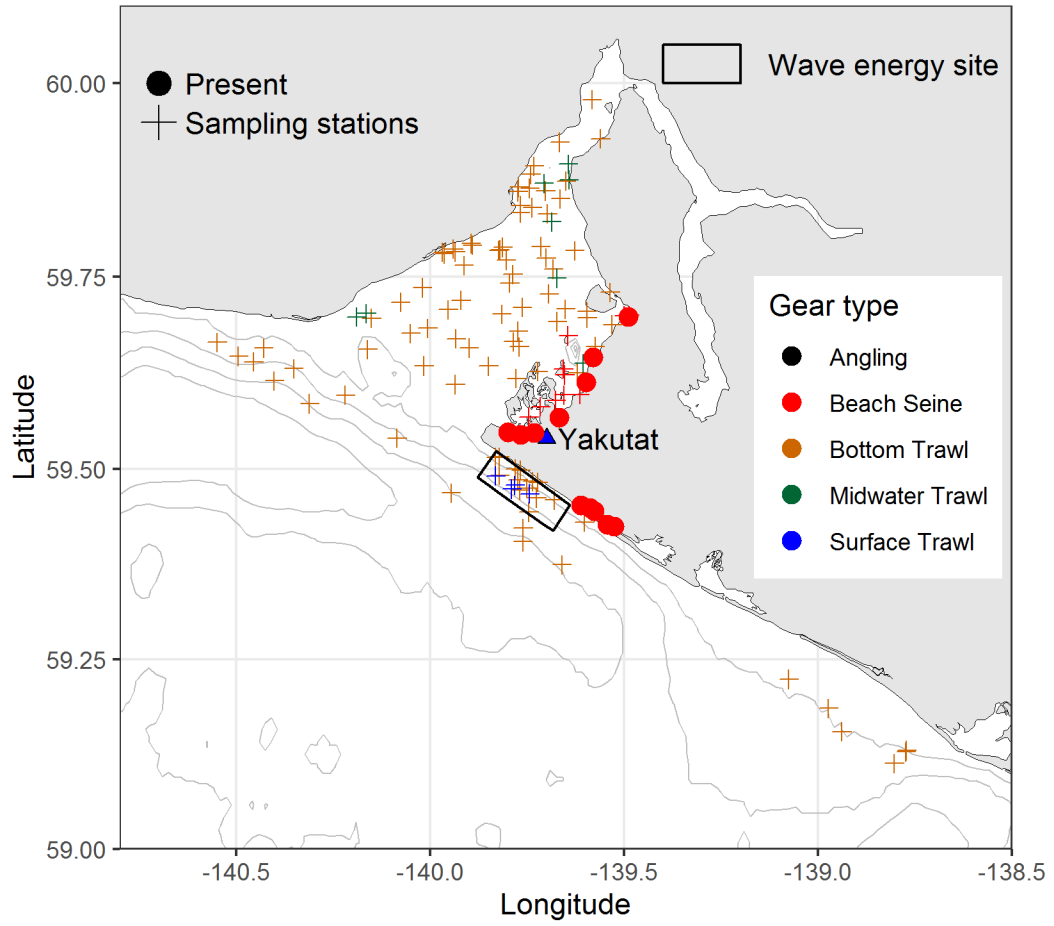
Sebastes crameri



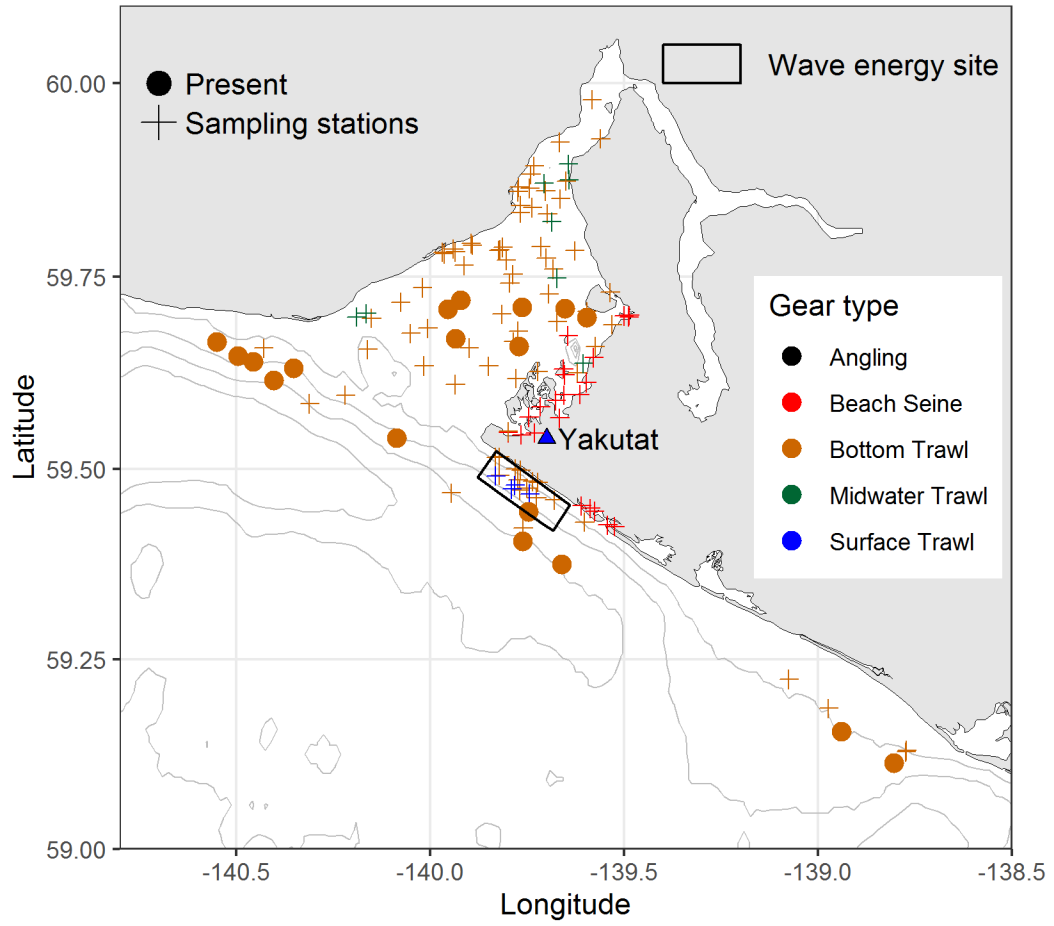
Daubed Shanny
Leptoclinus maculatus



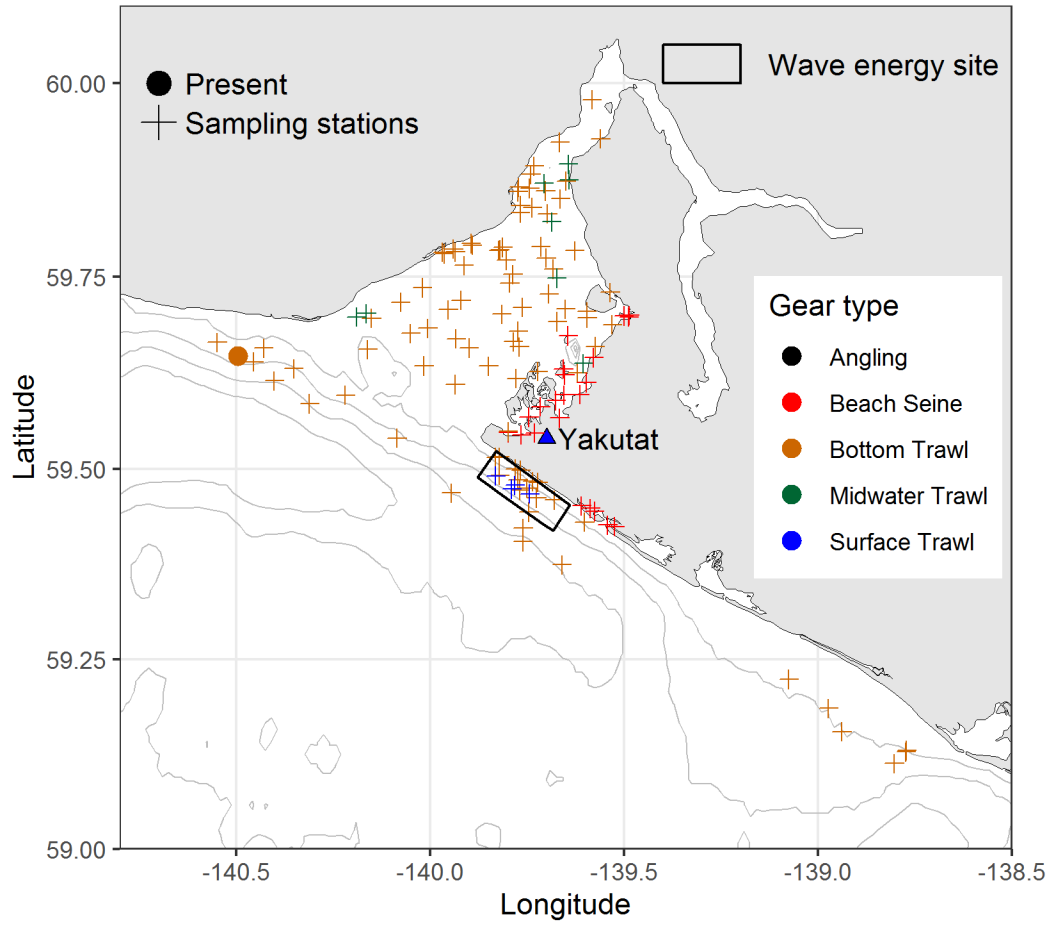
Dolly Varden
Salvelinus malma



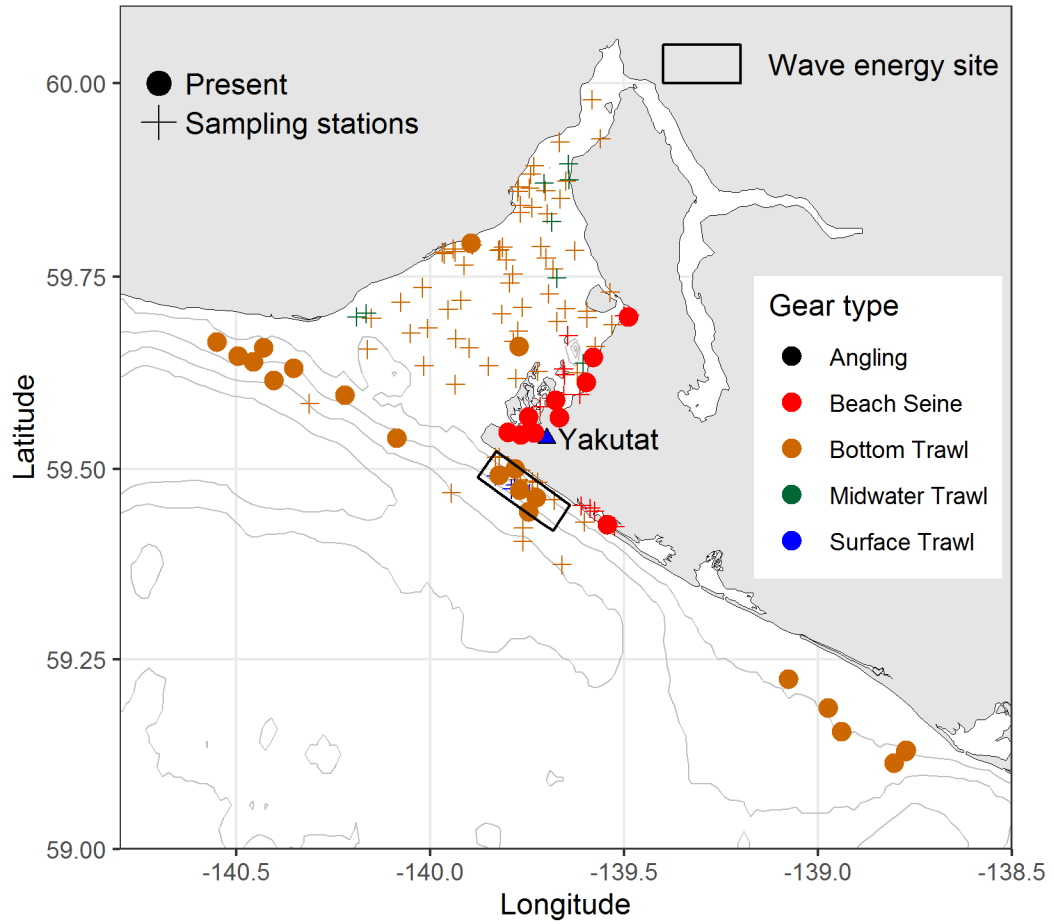
Dover Sole
Microstomus pacificus



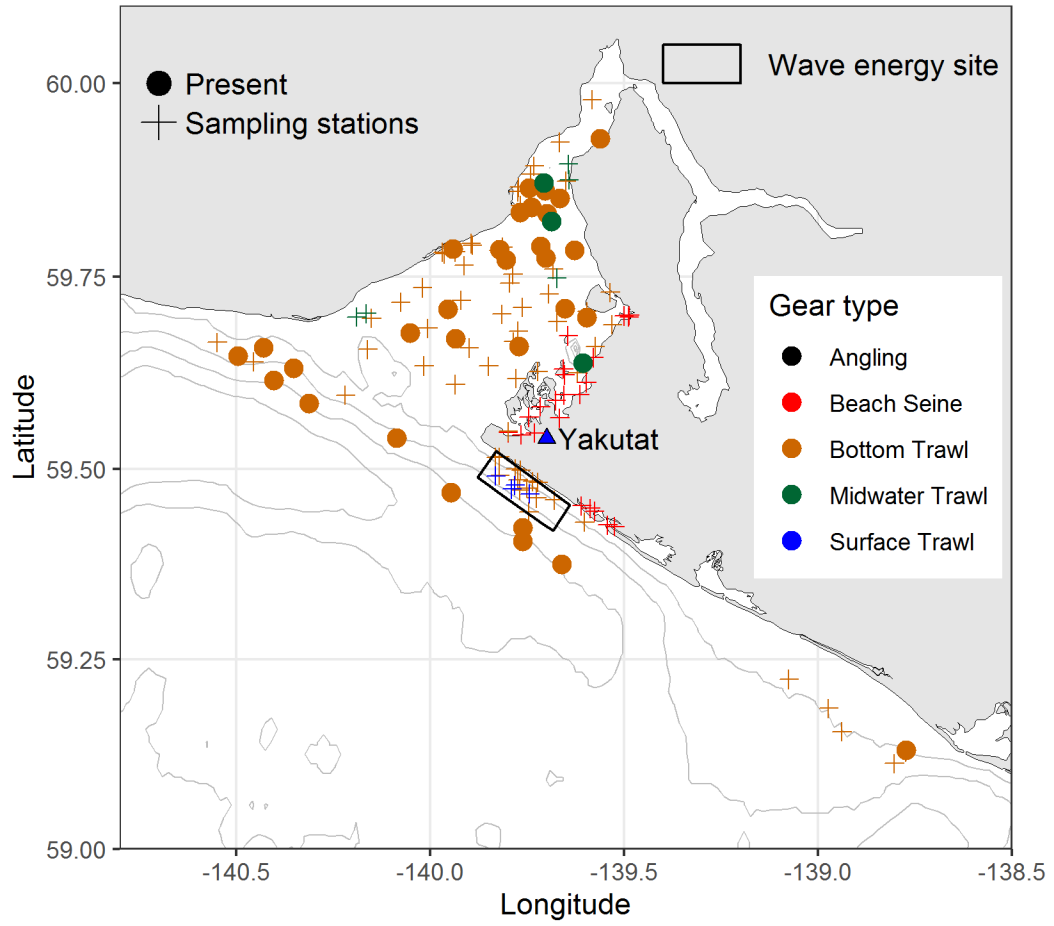
Dusky Rockfish
Sebastes variabilis



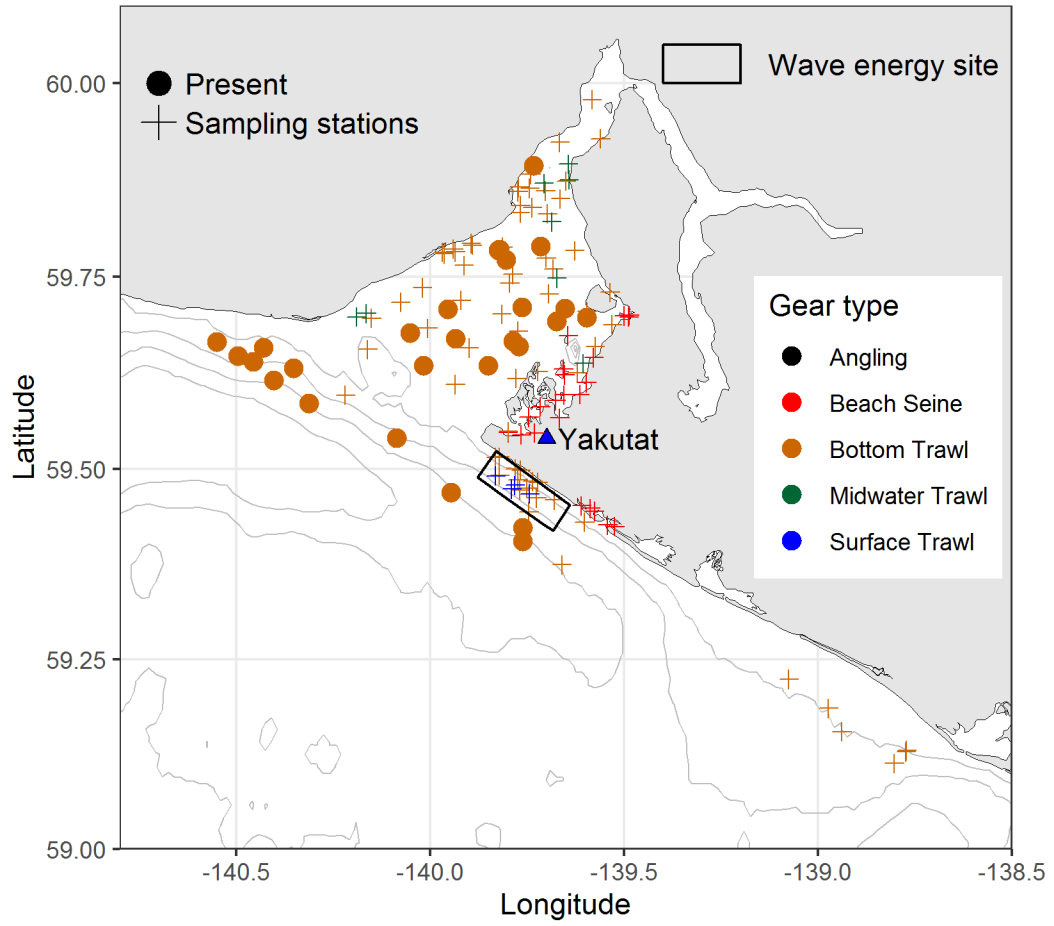
English Sole
Parophrys vetulus



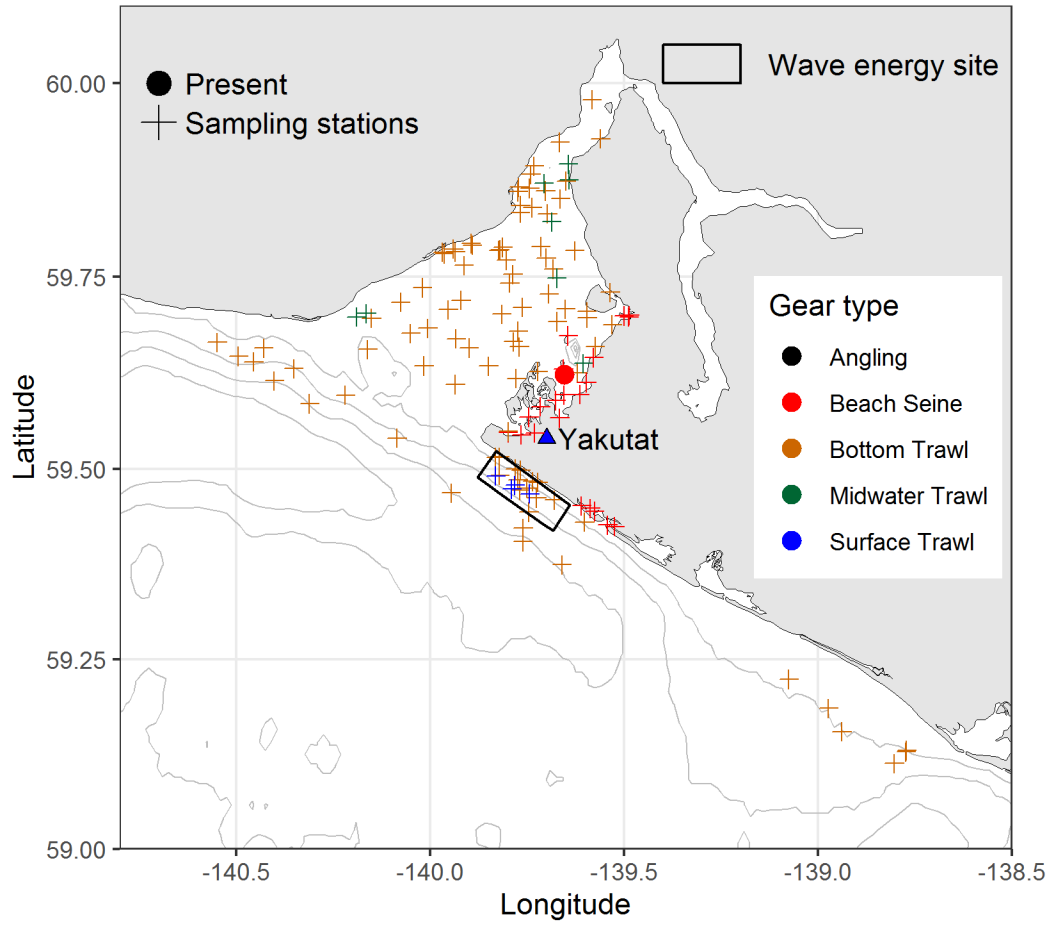
Eulachon
Thaleichthys pacificus



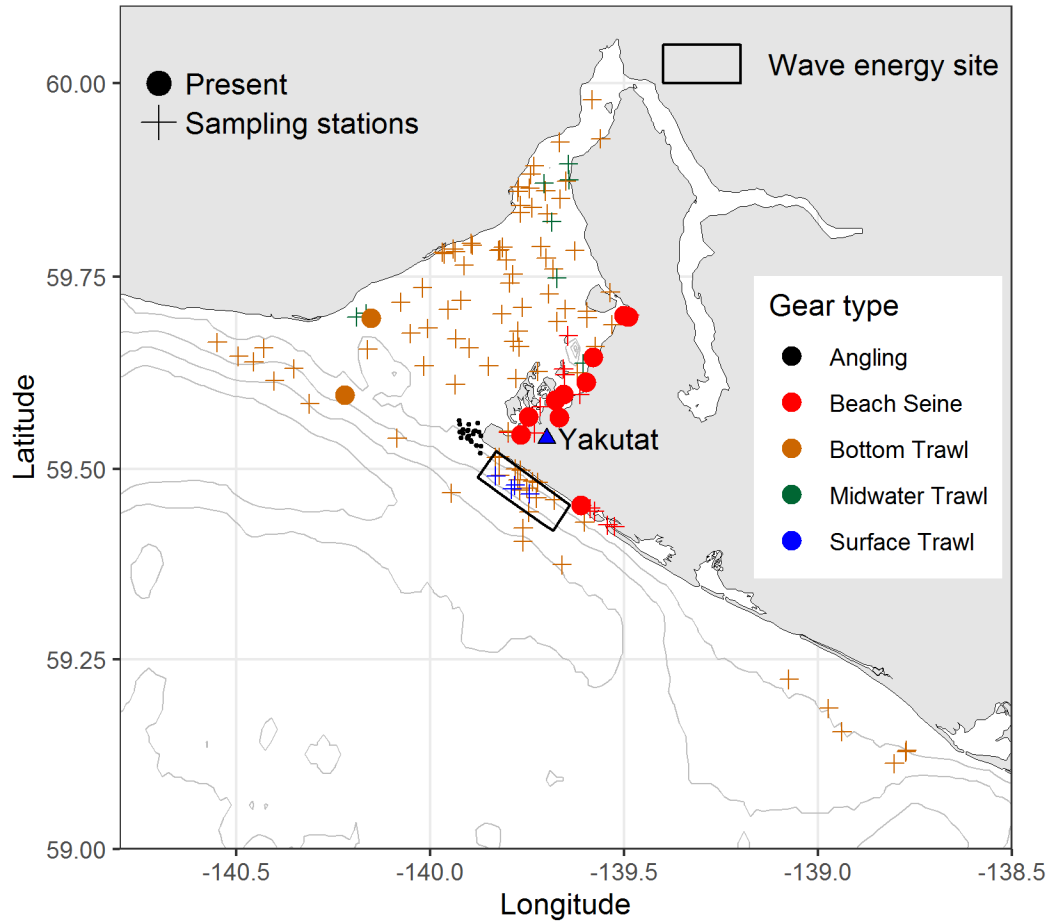
Flathead Sole
Hippoglossoides elassodon



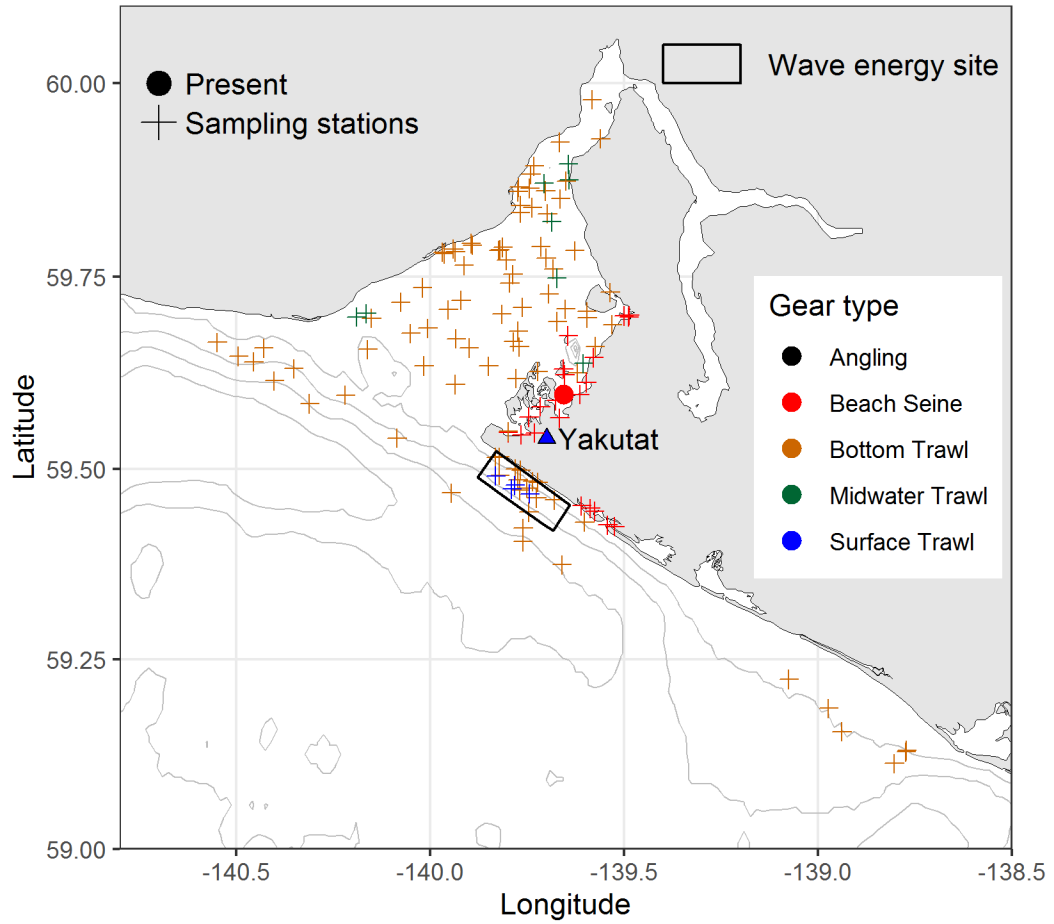
Great Sculpin
Myoxocephalus polyacanthocephalus



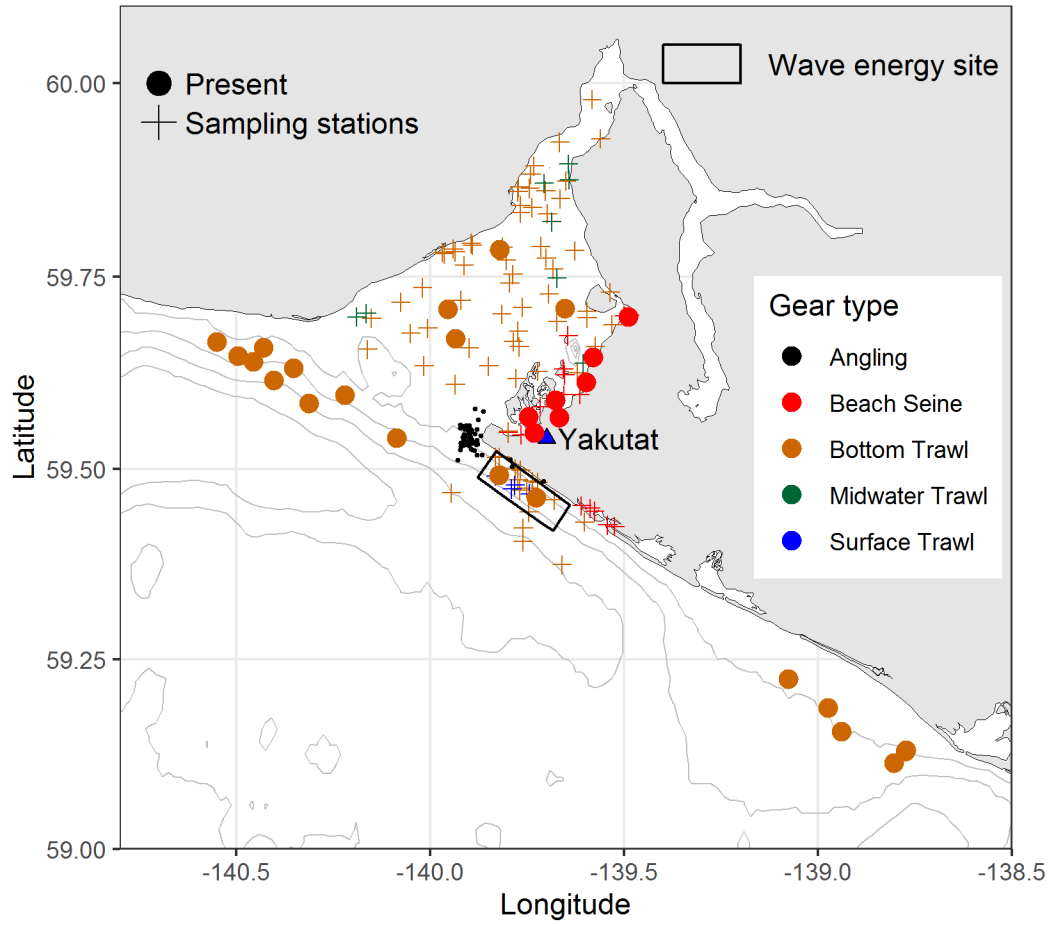
Kelp Greenling
Hexagrammos decagrammus



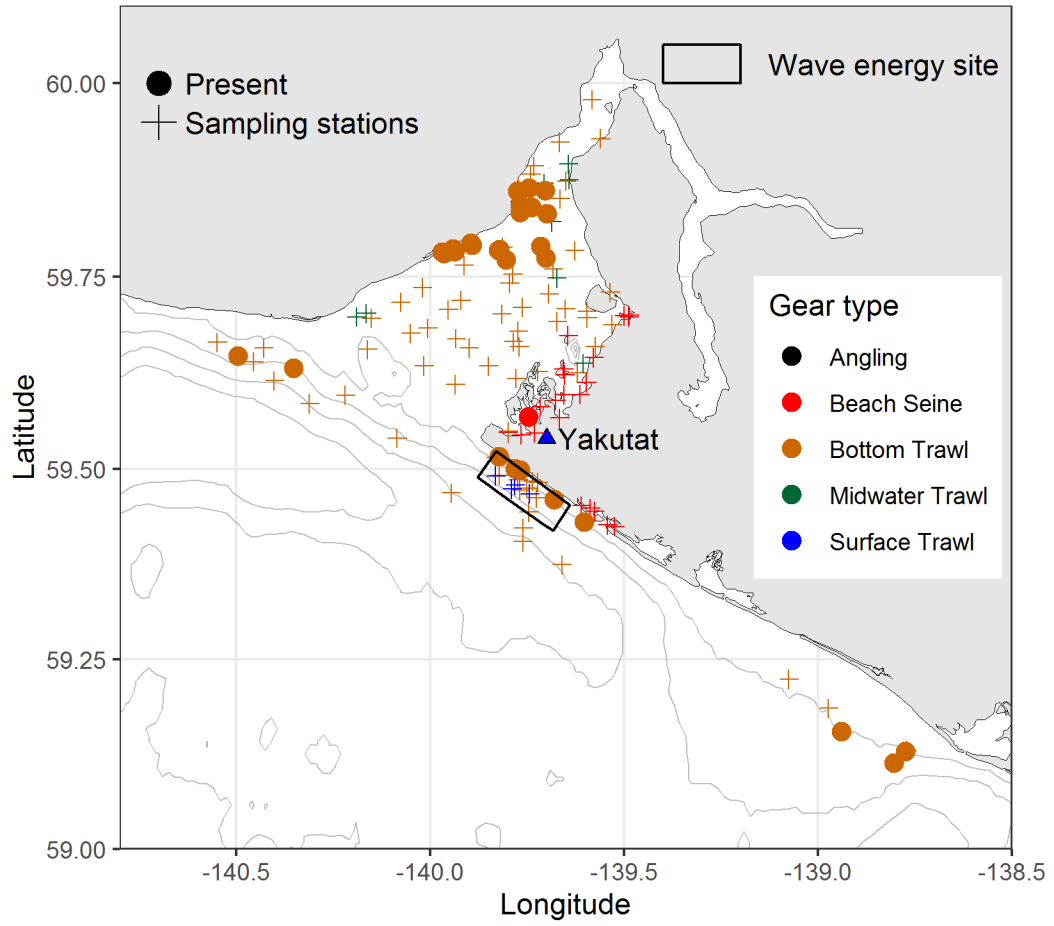
Leister Sculpin
Enophrys lucasi



Lingcod
Ophiodon elongatus

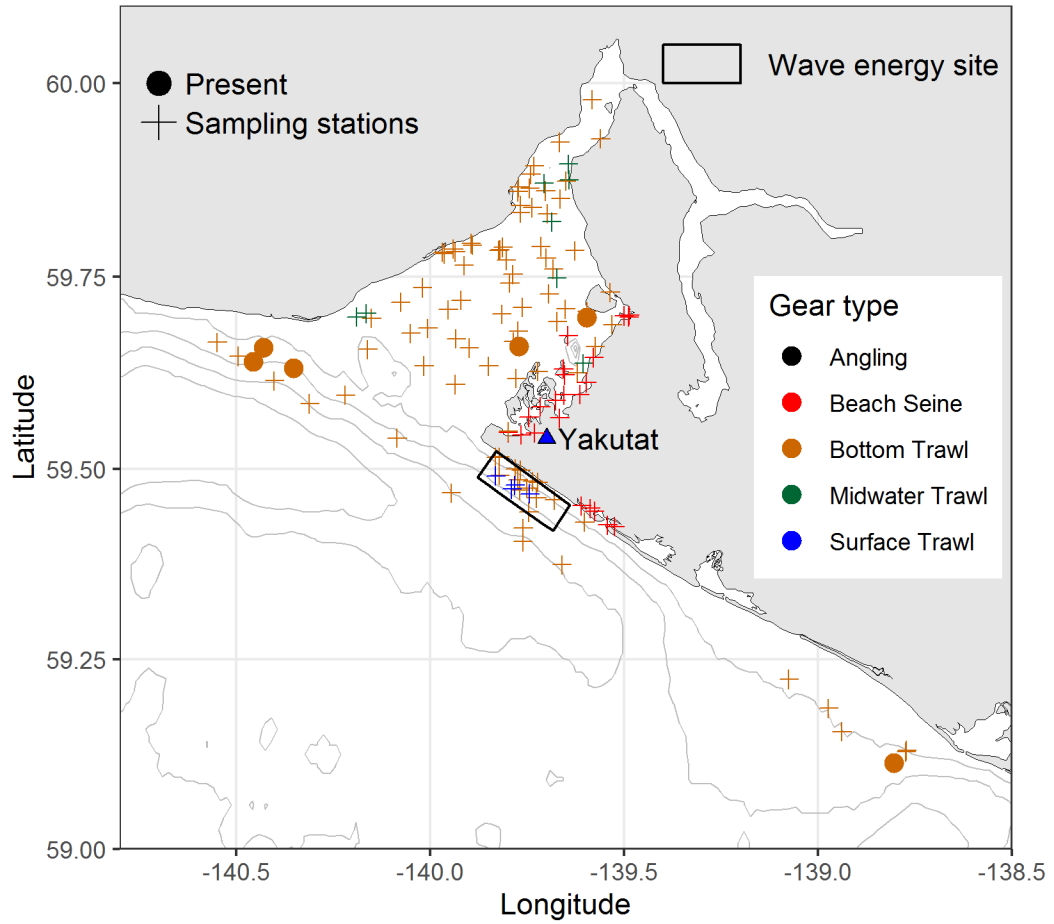


Longfin Smelt
Spirinchus thaleichthys



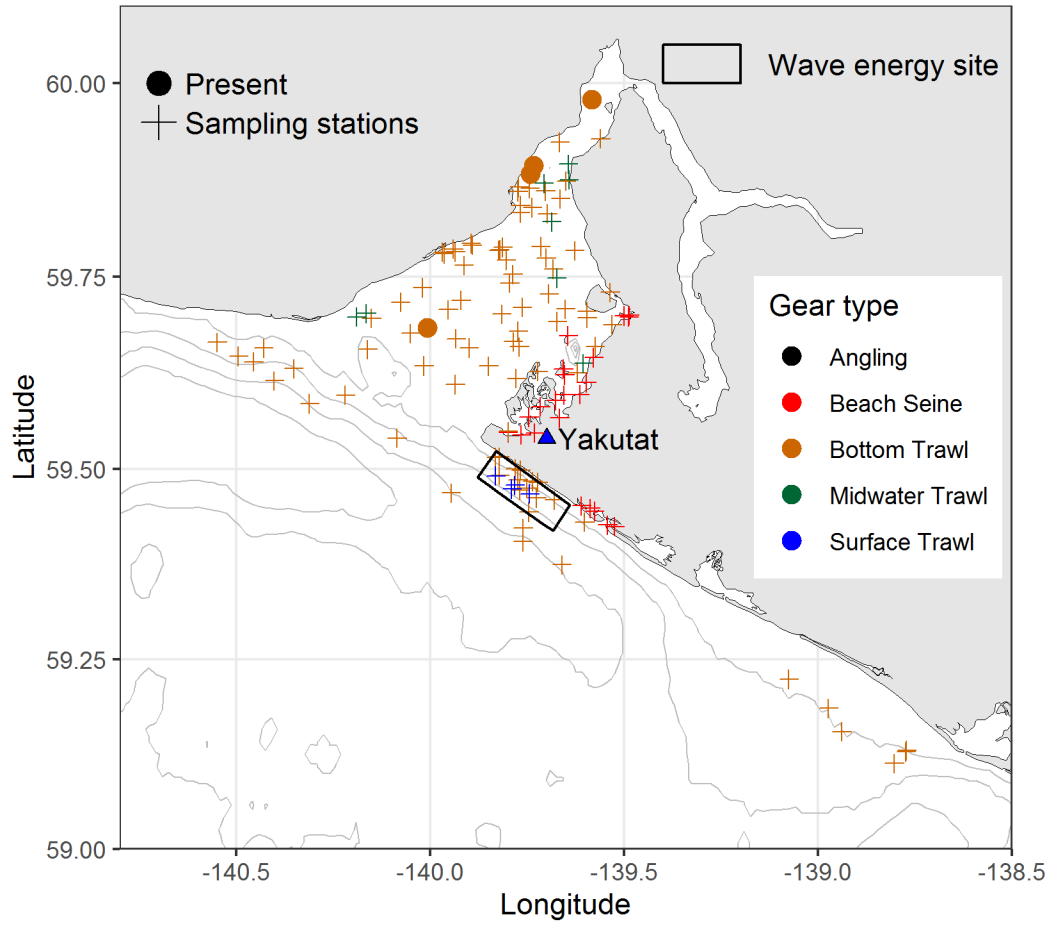
Longnose Skate

Raja rhina

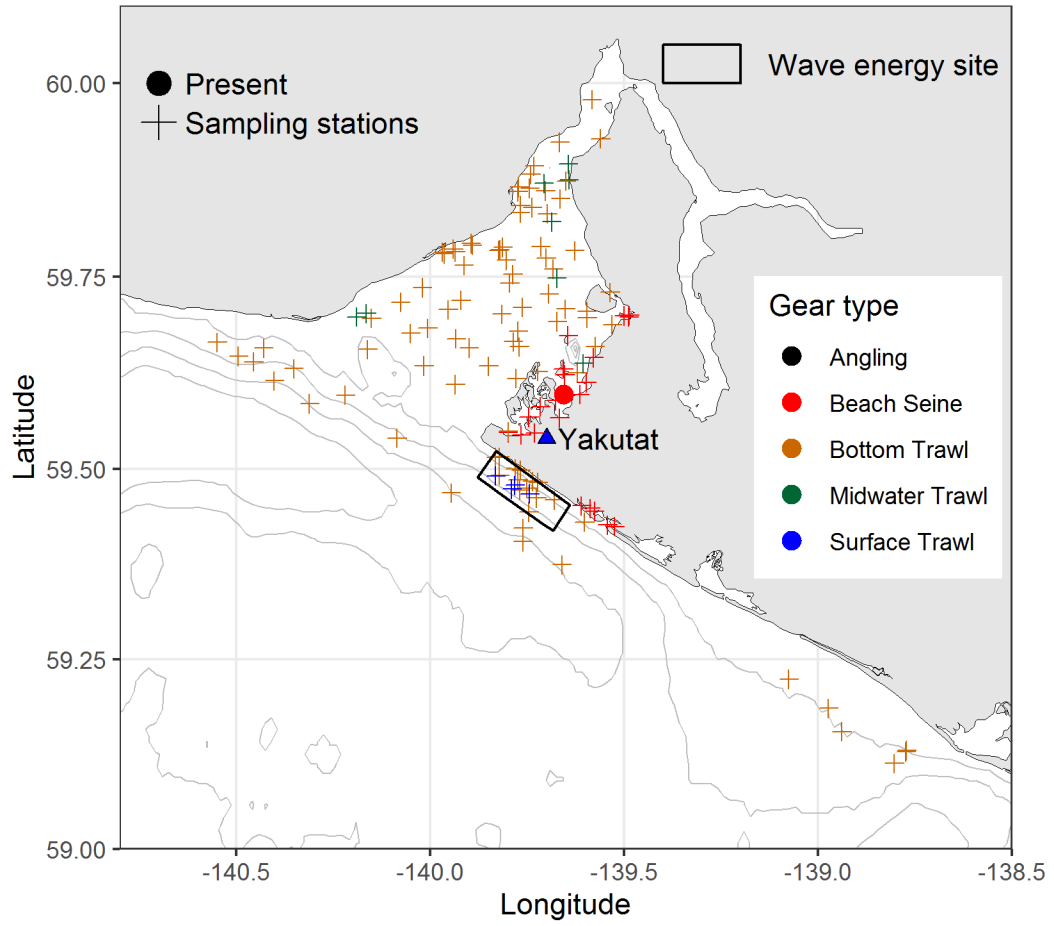


Longsnout Prickleback

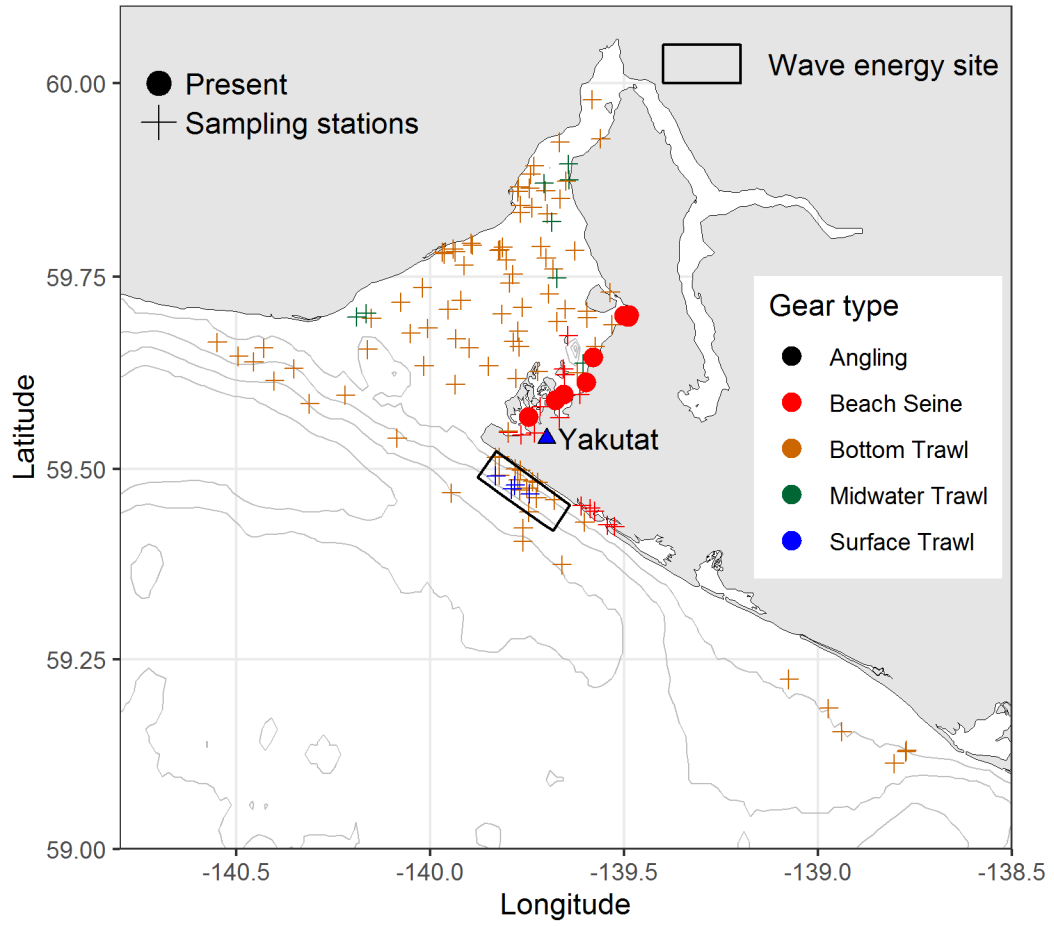
Lumpenella longirostris



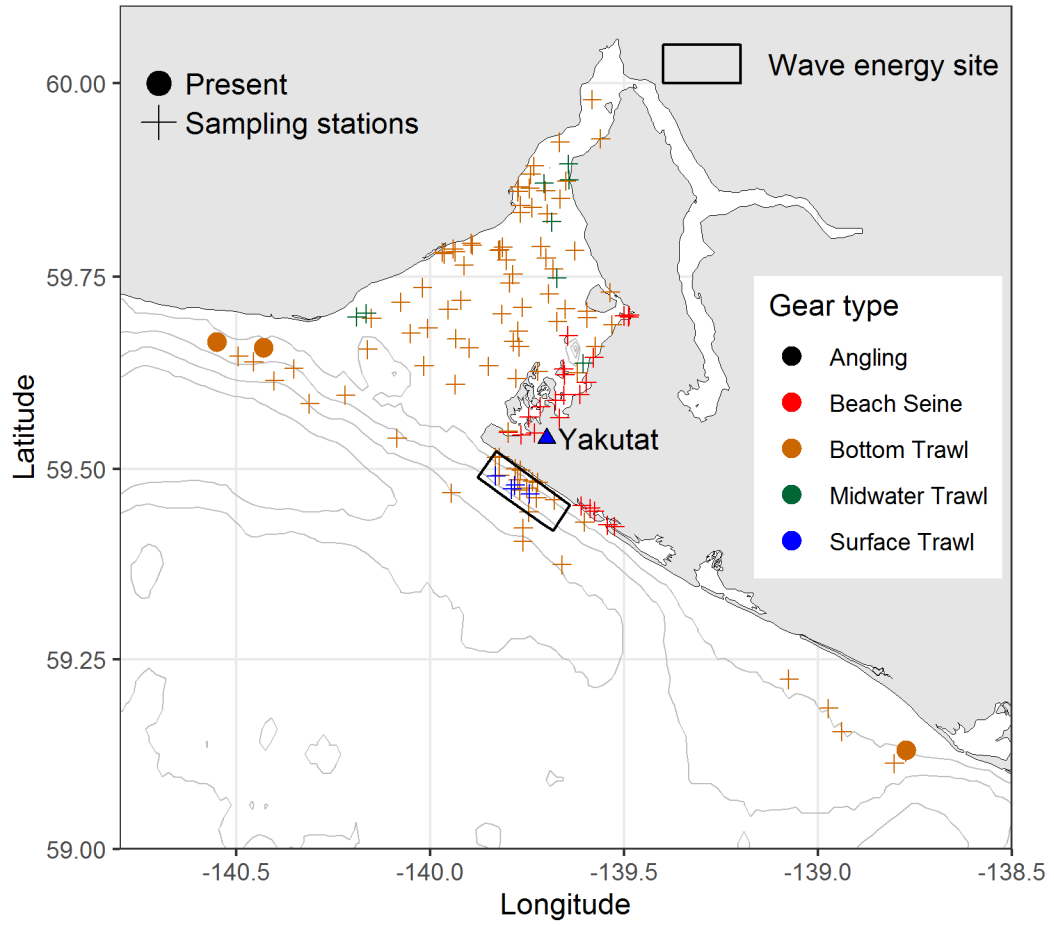
Manacled Sculpin
Synchirus gilli



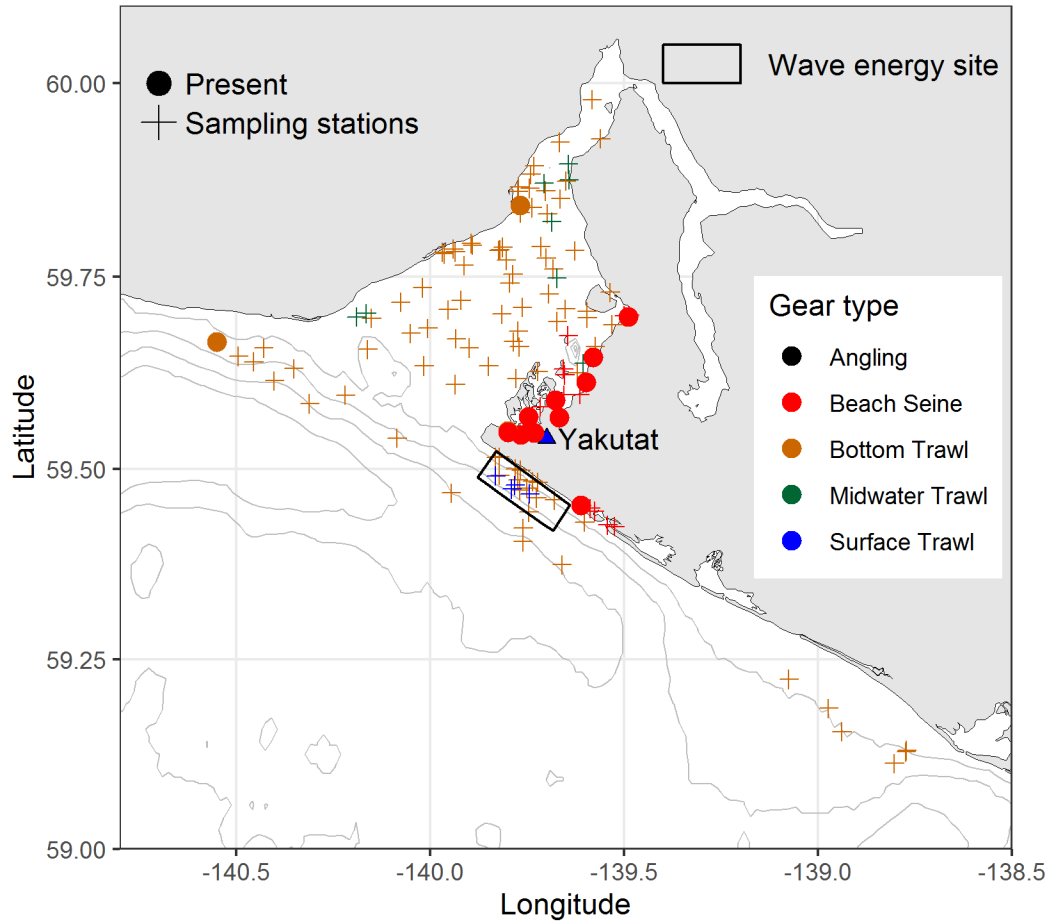
Masked Greenling
Hexagrammos octogrammus



Night Smelt
Spirinchus starksi

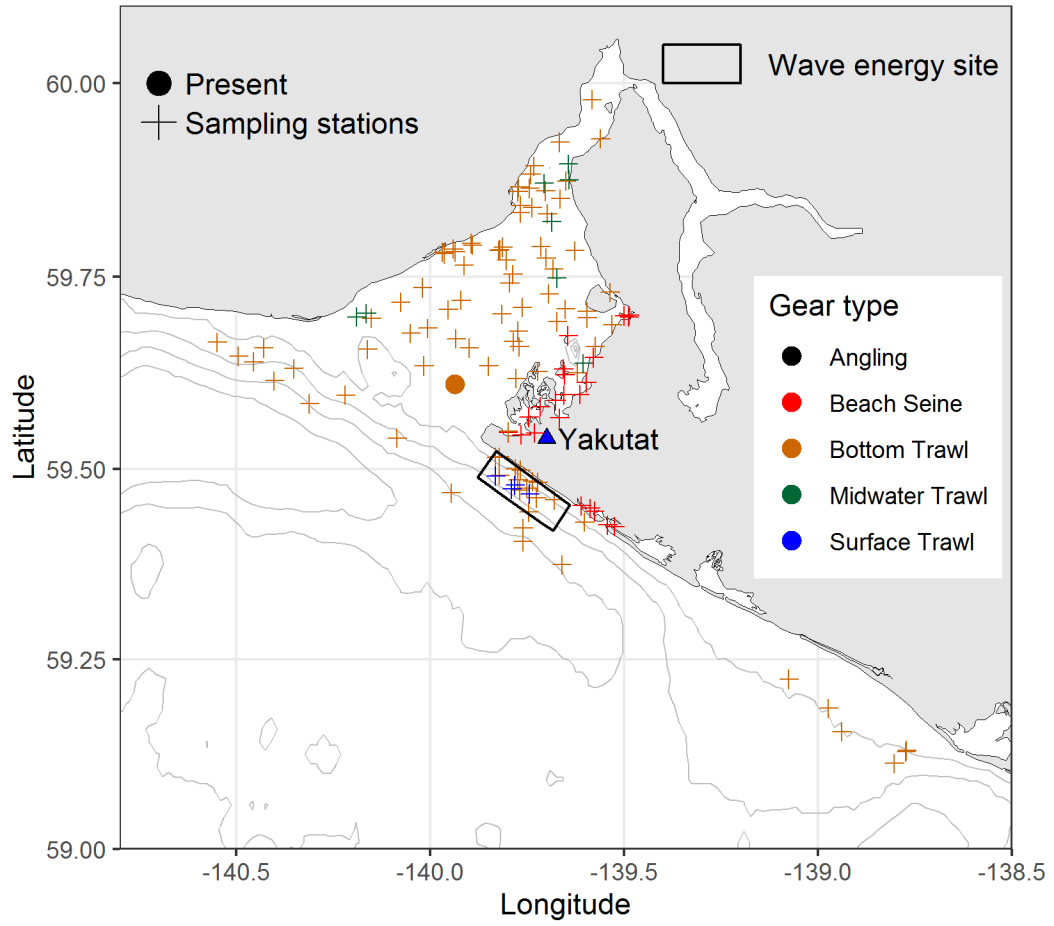


Northern Rock Sole
Lepidopsetta polyxystra



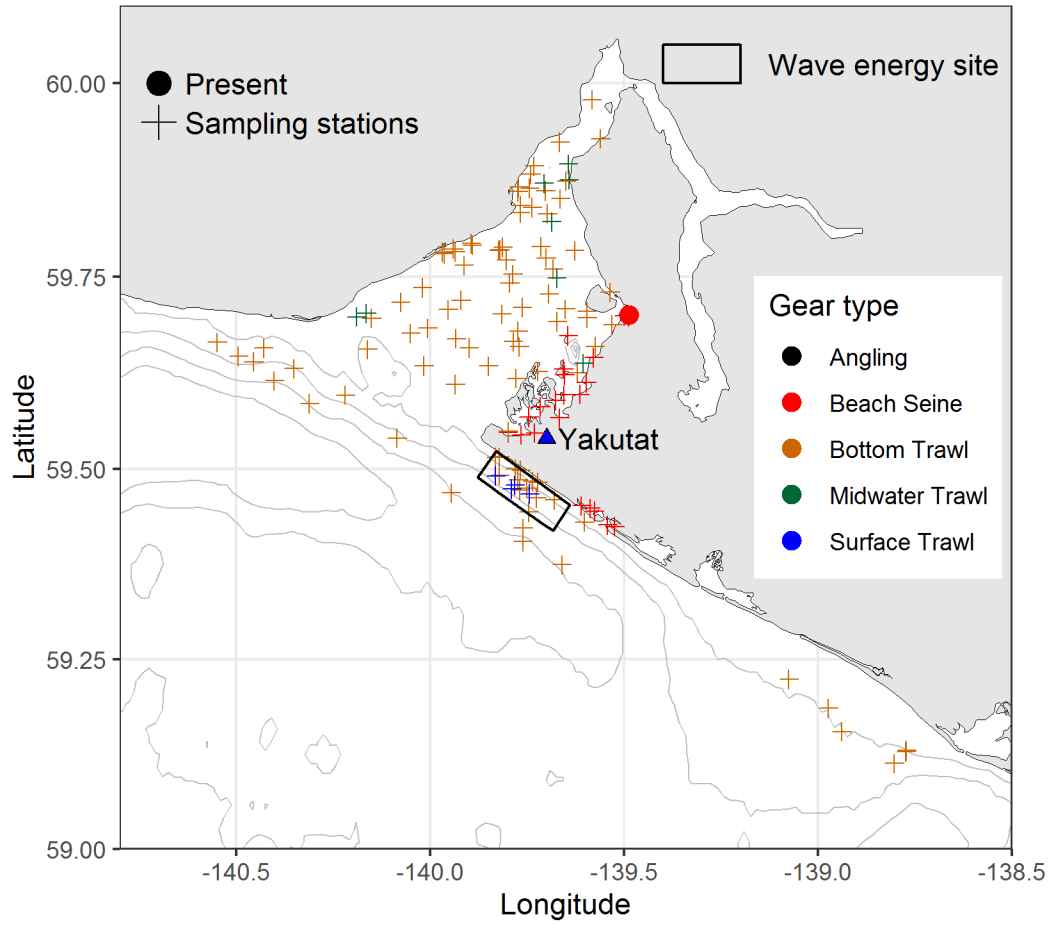
Northern Ronquil

Ronquilus jordani

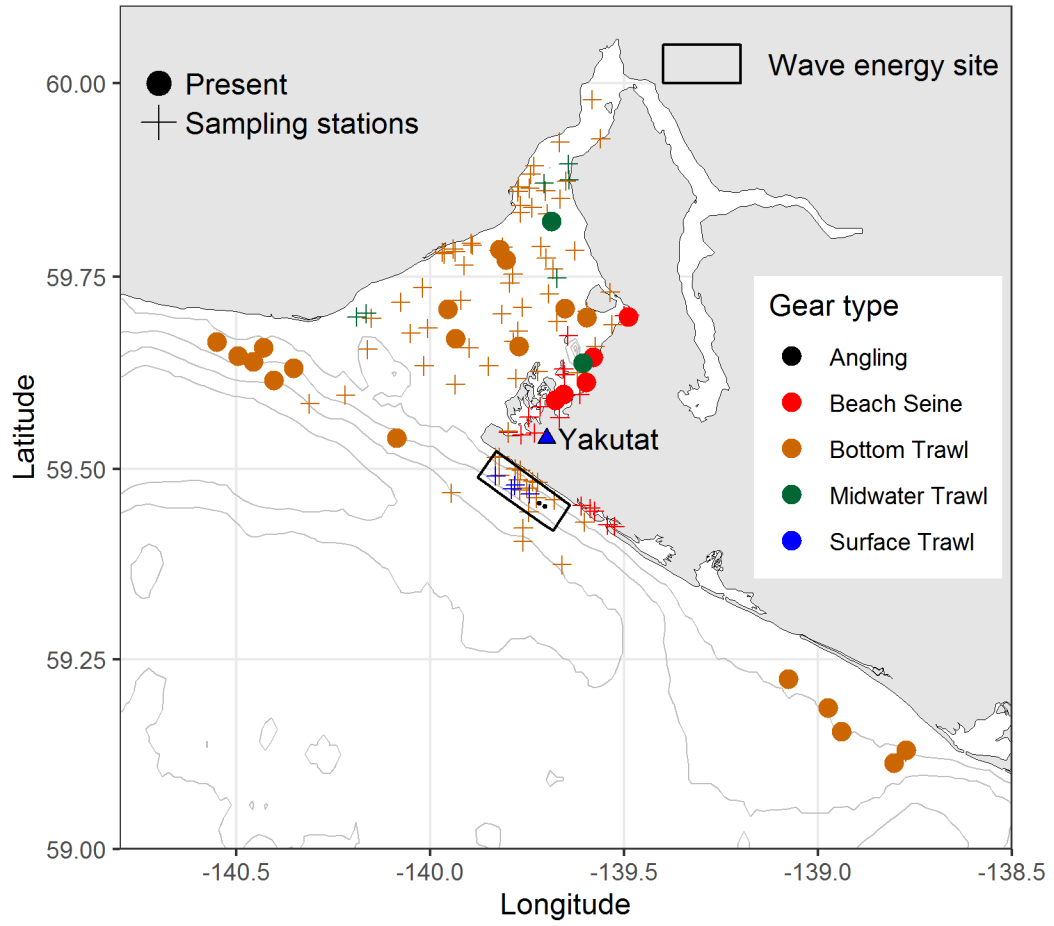


Northern Sculpin

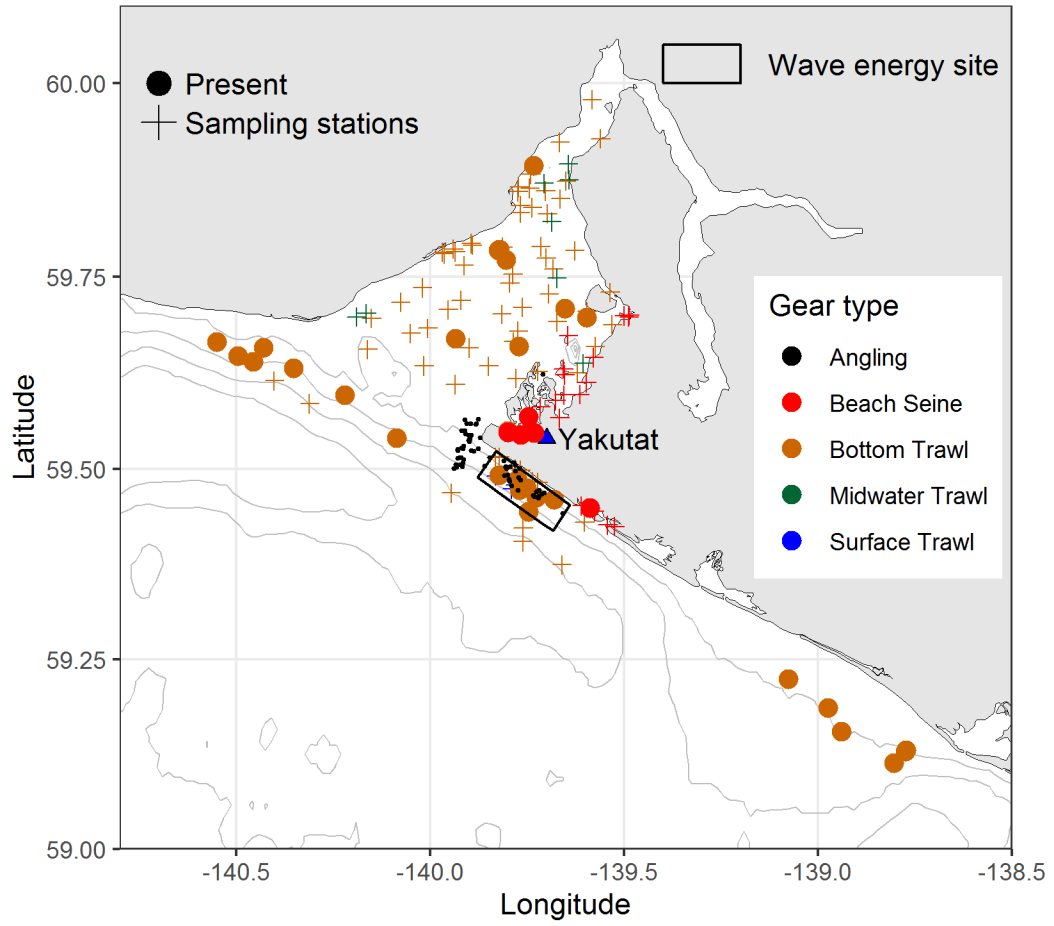
Icelinus borealis



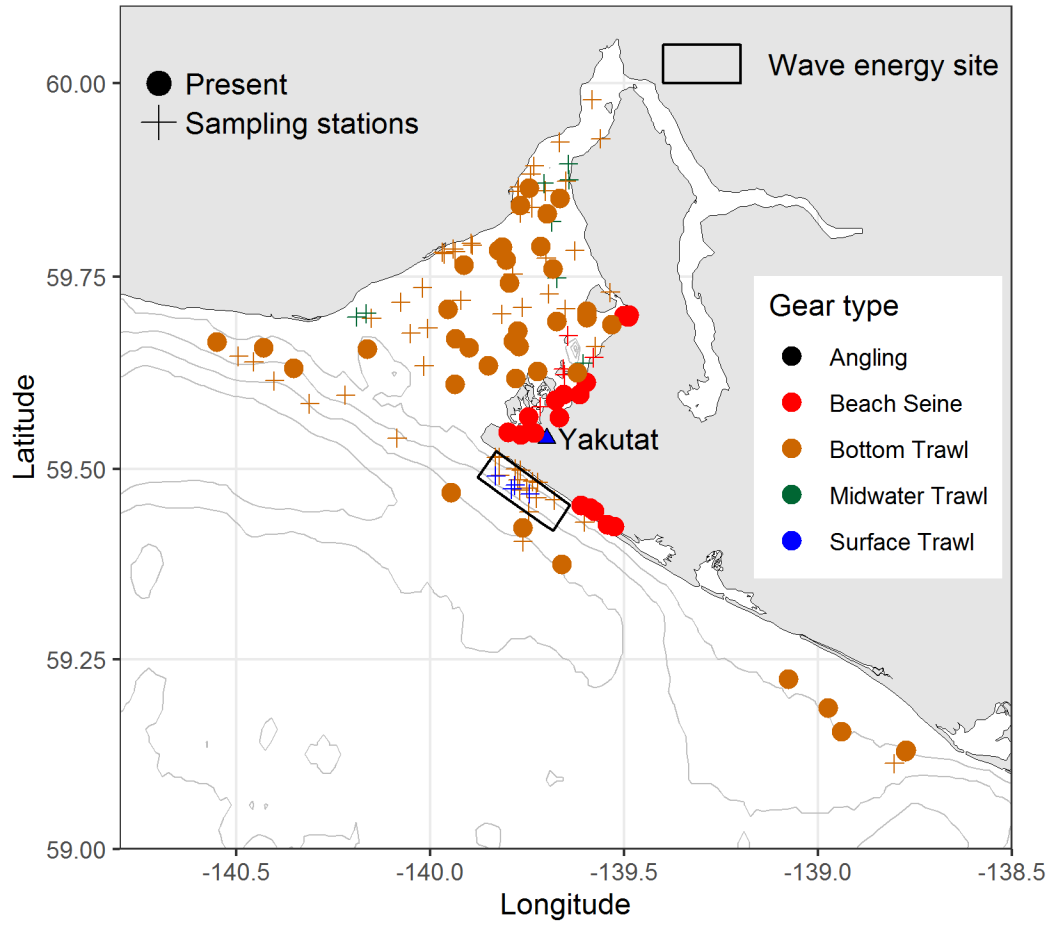
Pacific Cod
Gadus macrocephalus



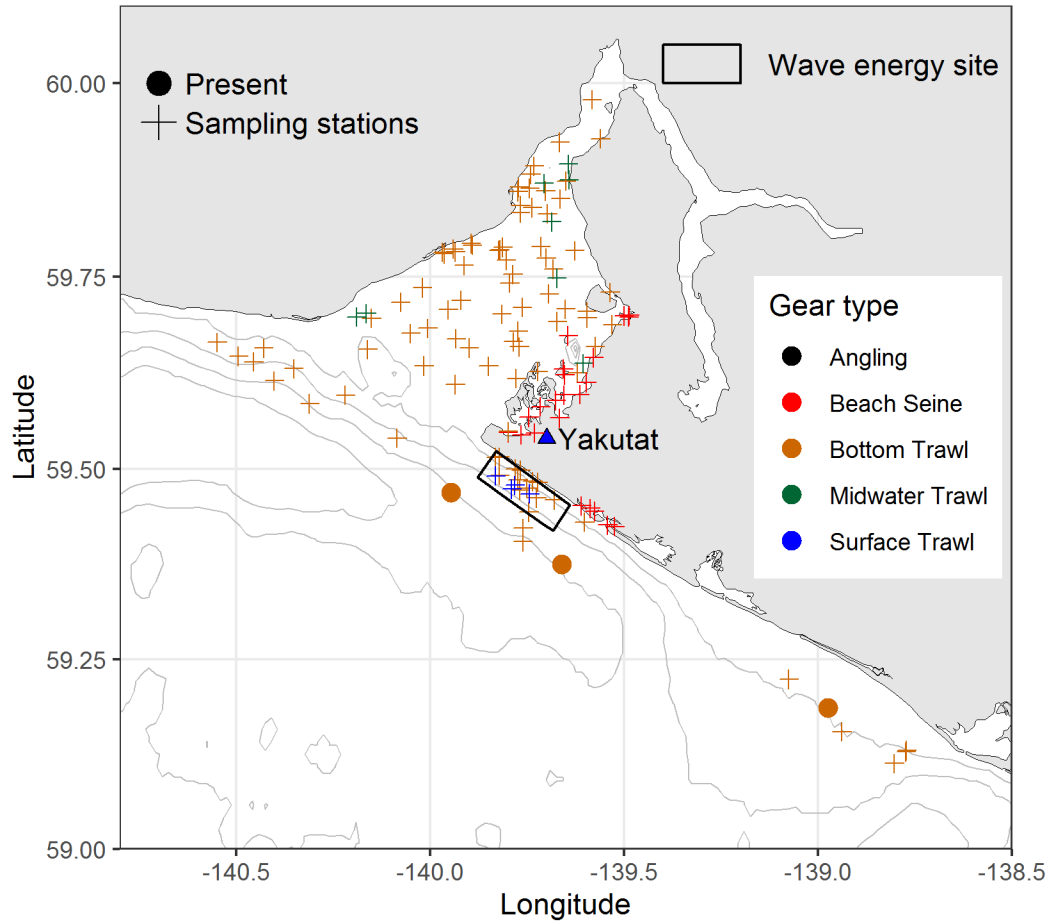
Pacific Halibut
Hippoglossus stenolepis



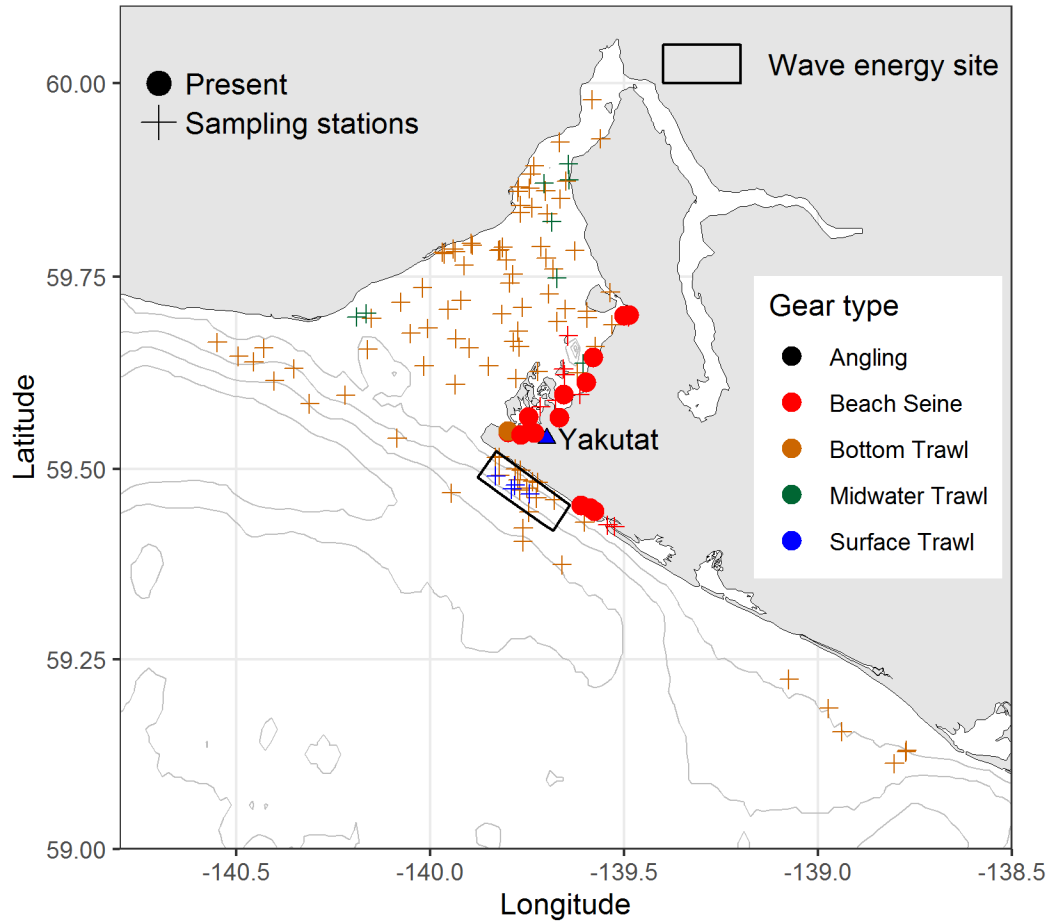
Pacific Herring
Clupea pallasii



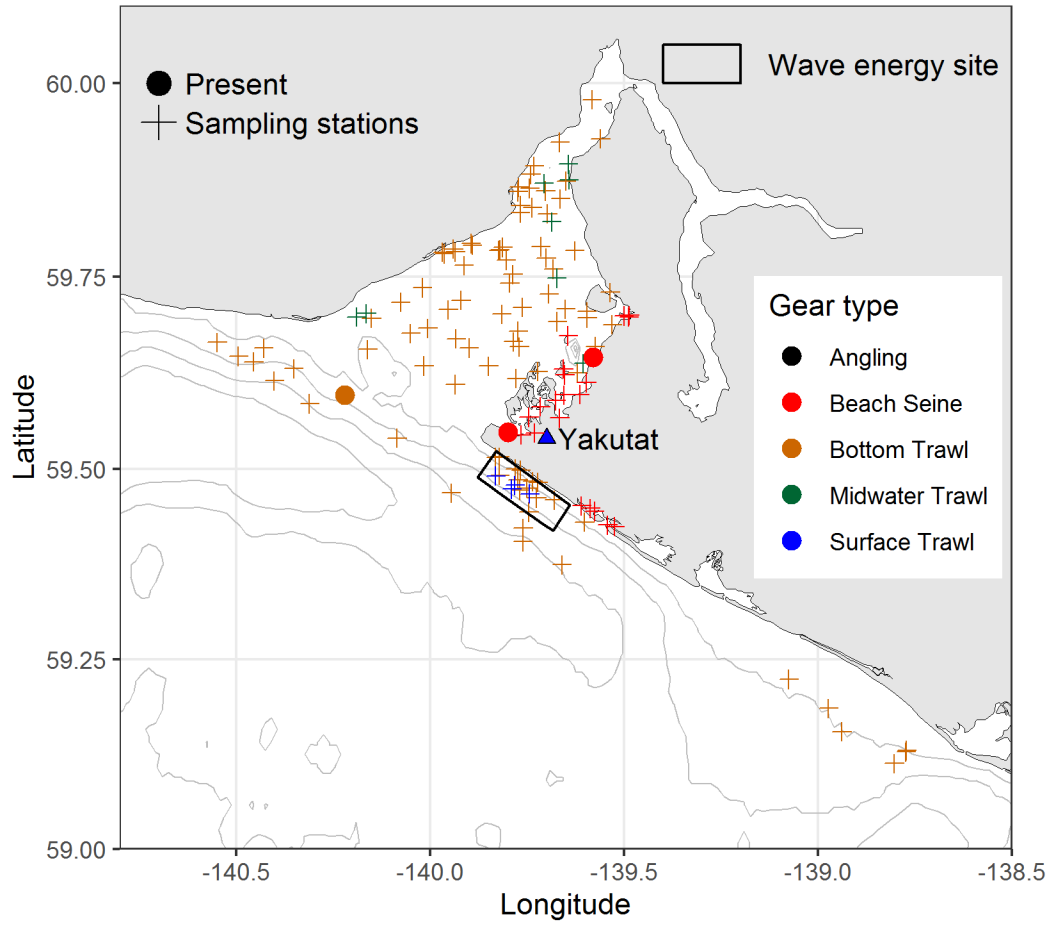
Pacific Ocean Perch
Sebastes alutus



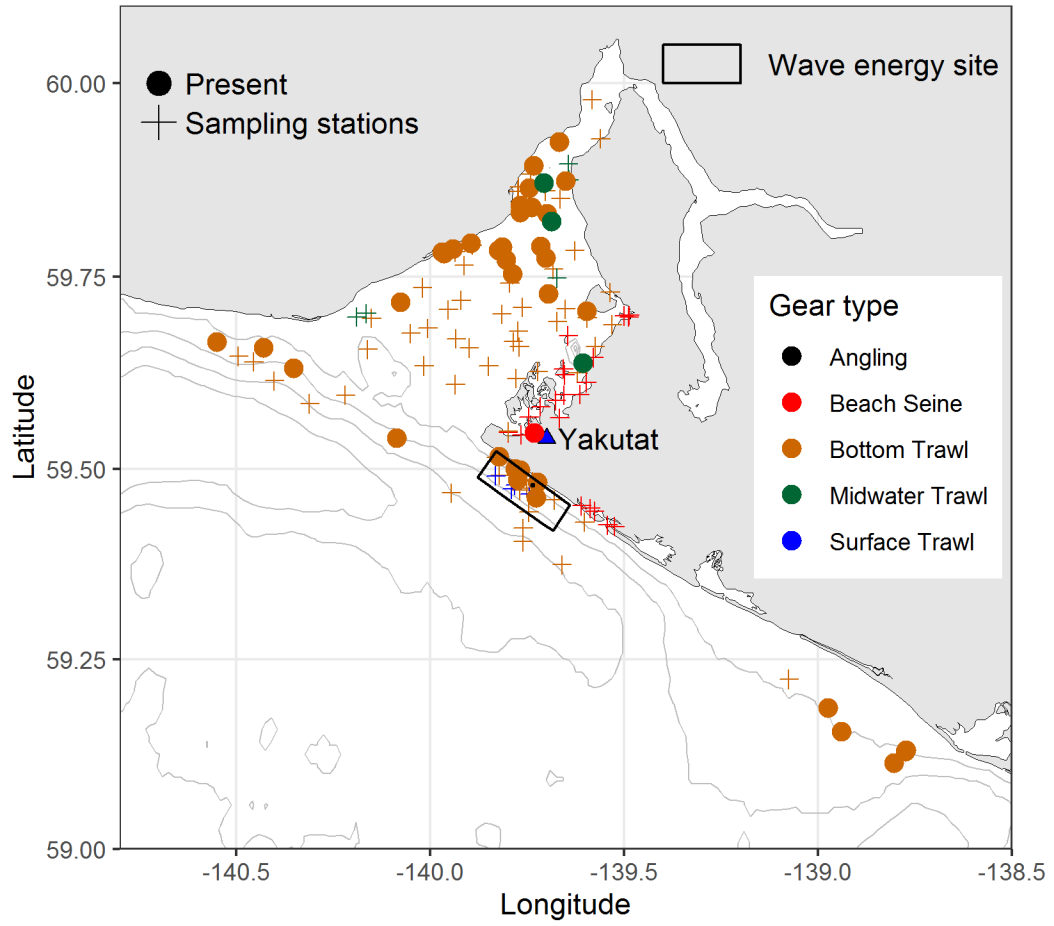
Pacific Sand Lance
Ammodytes personatus



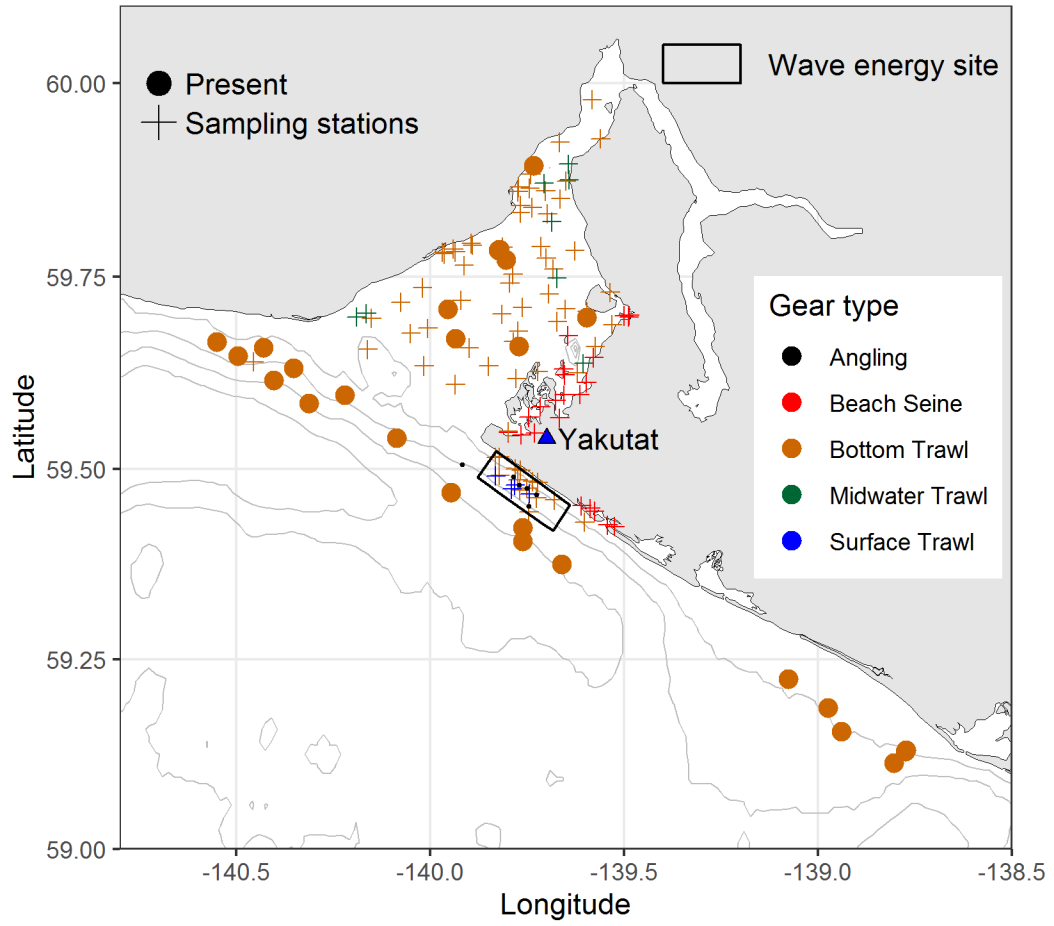
Pacific Sanddab
Citharichthys sordidus



Pacific Sandfish
Trichodon trichodon

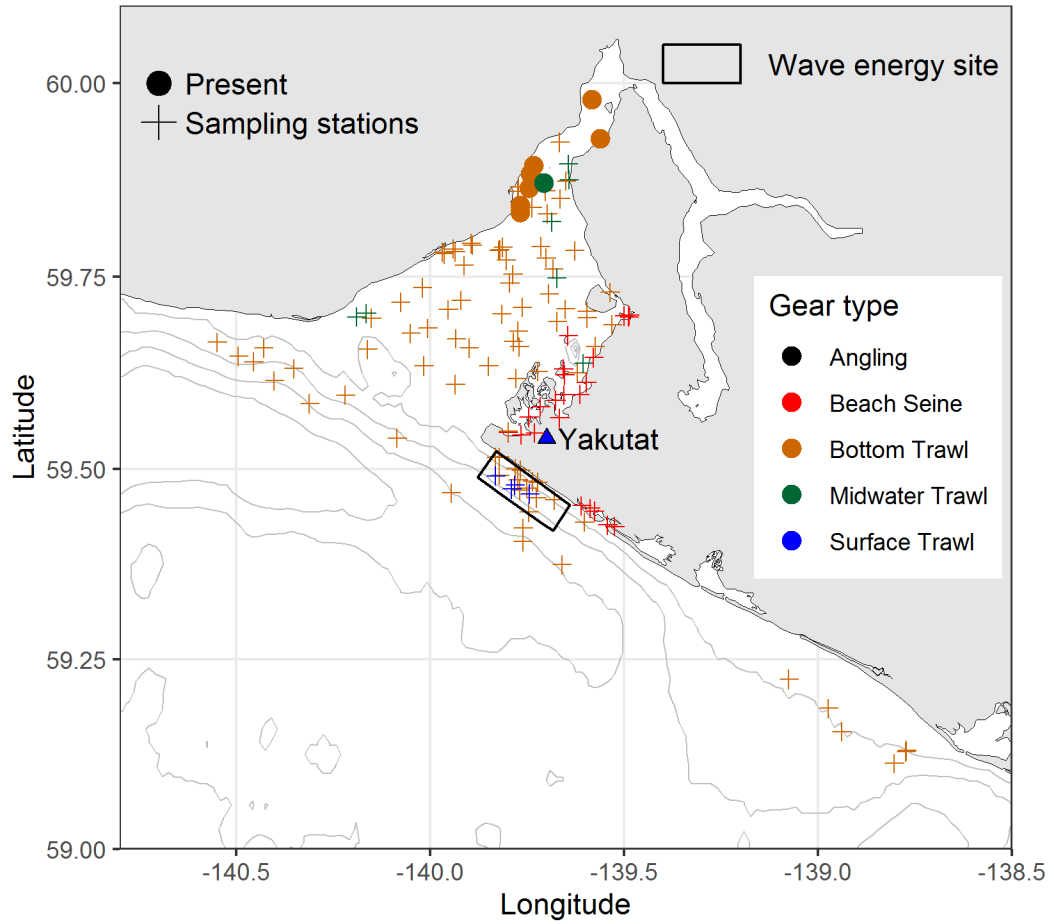


Pacific Spiny Dogfish
Squalus suckleyi



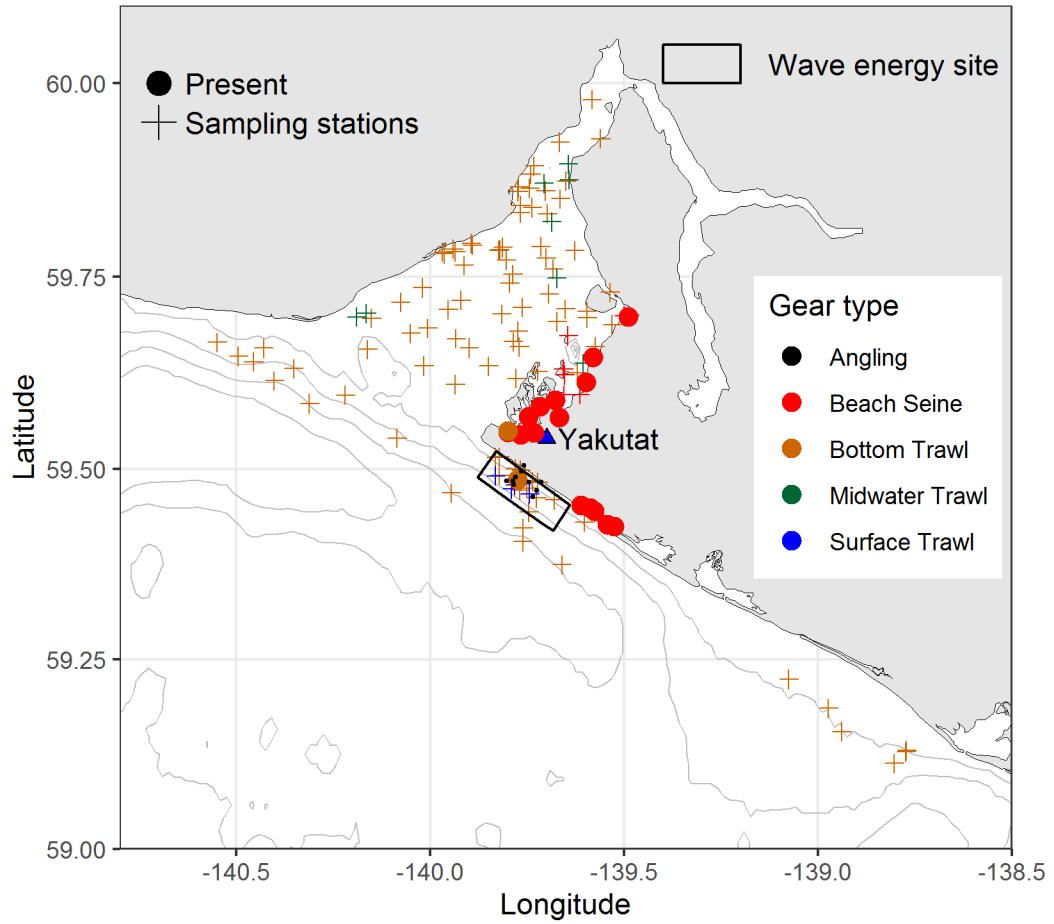
Pacific Spiny Lumpsucker

Eumicrotremus orbis

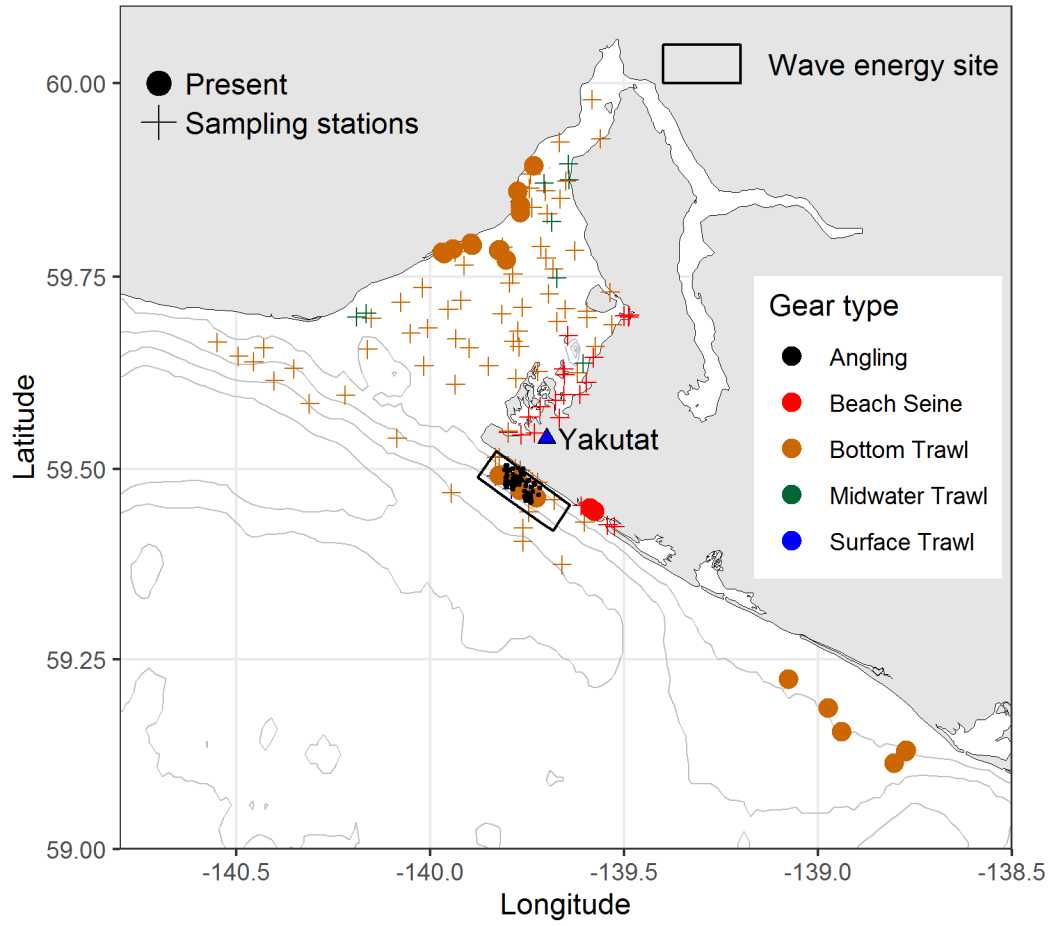


Pacific Staghorn Sculpin

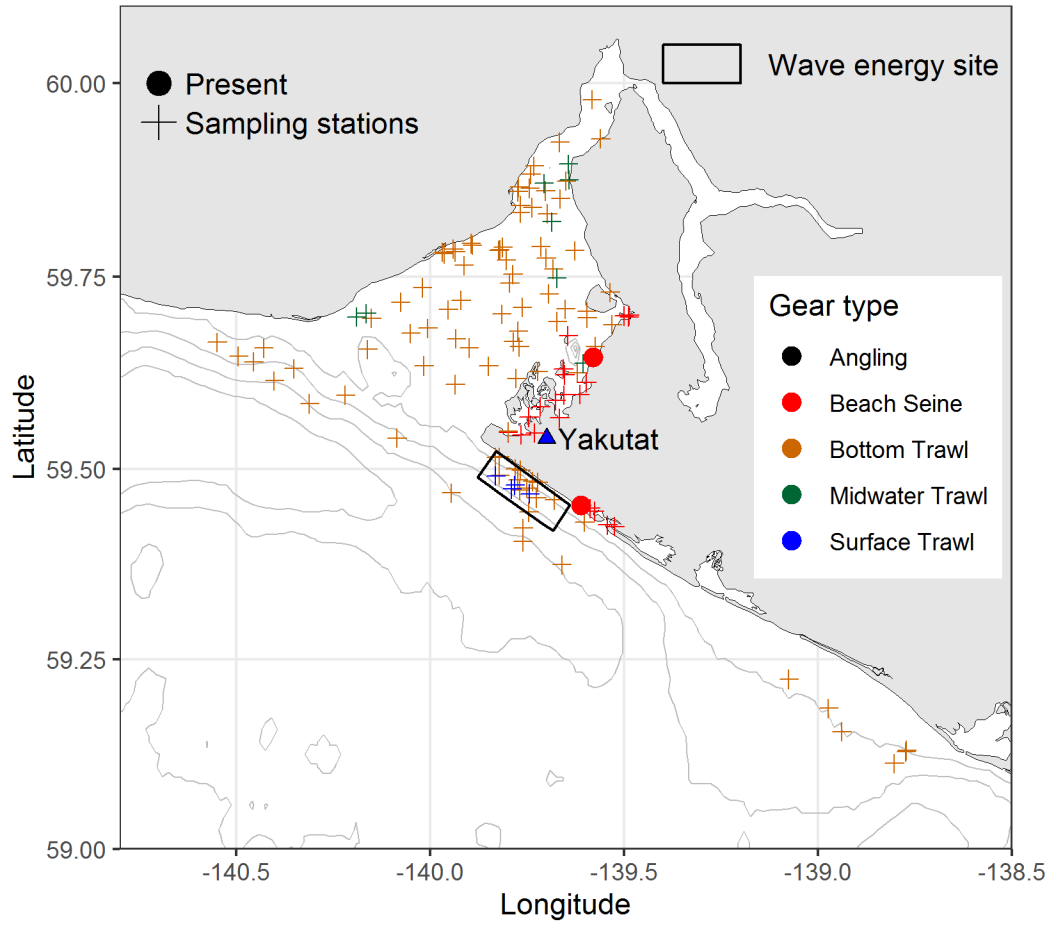
Leptocottus armatus



Pacific Tomcod
Microgadus proximus

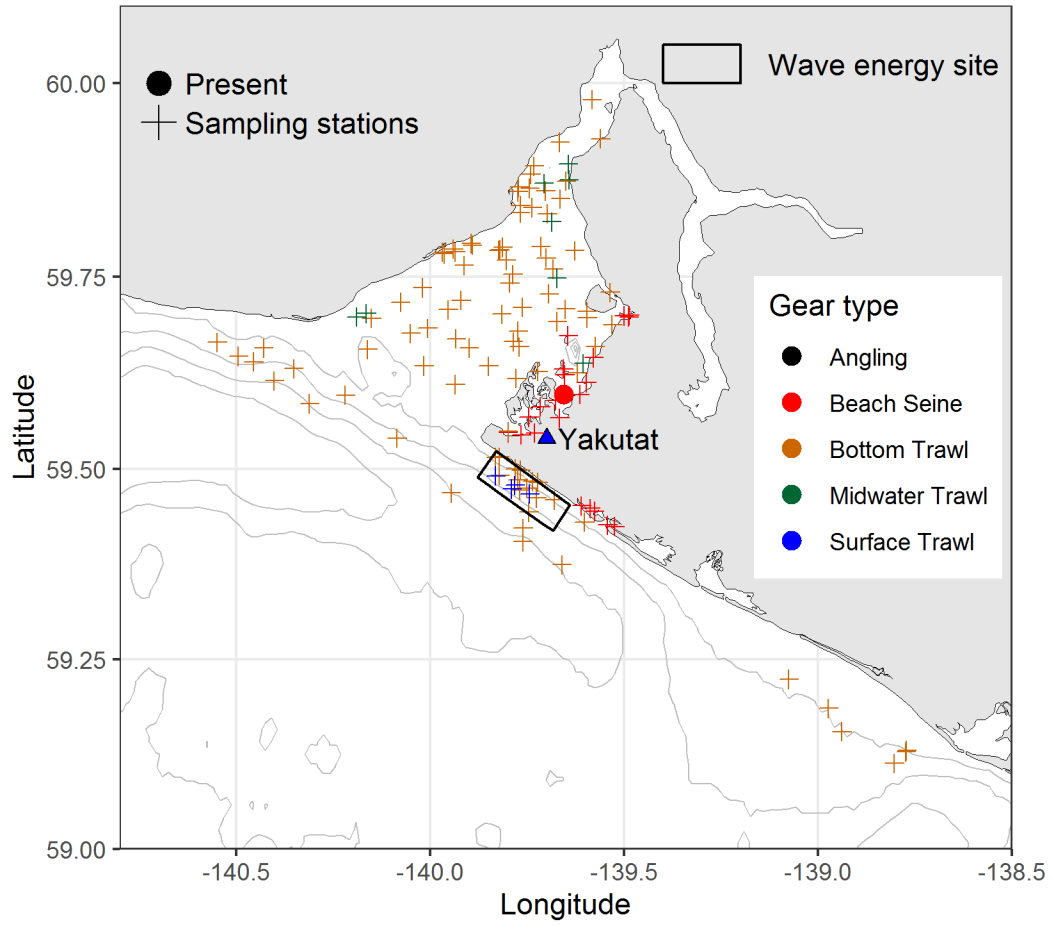


Padded Sculpin
Artedius fenestralis

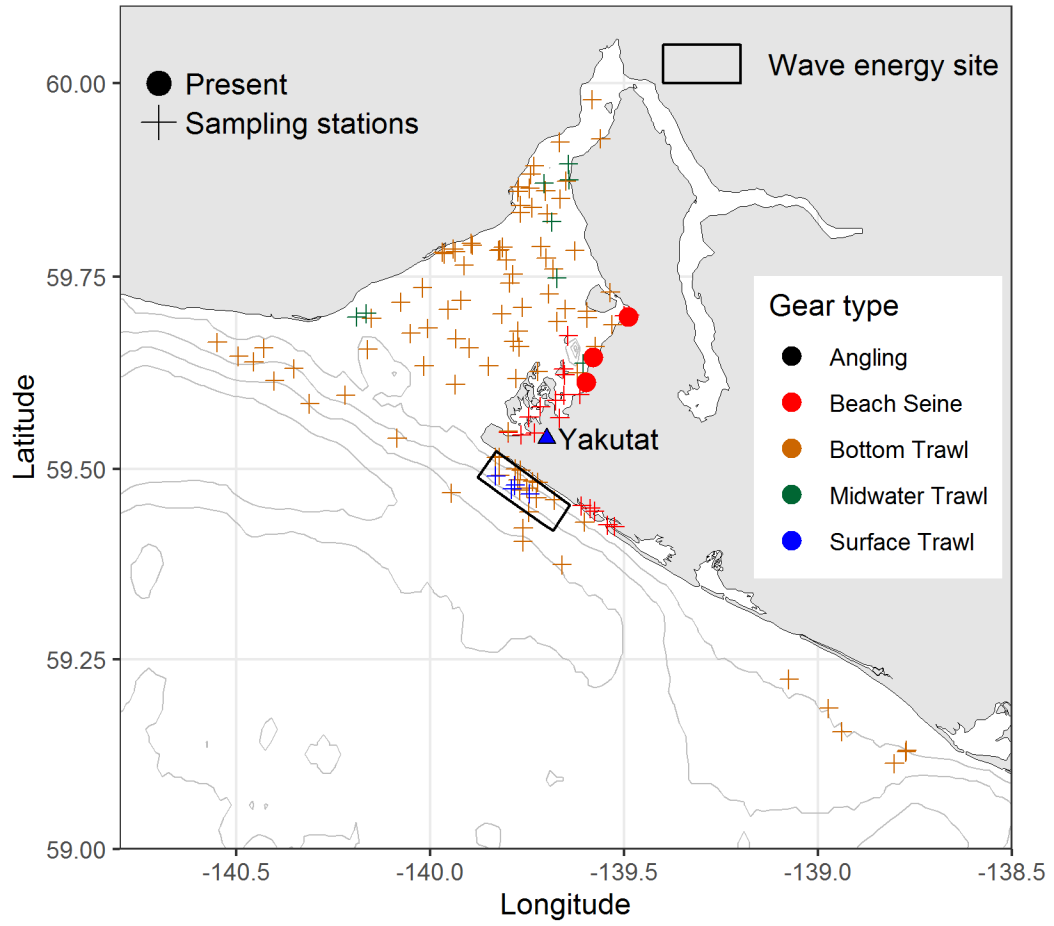


Painted Greenling

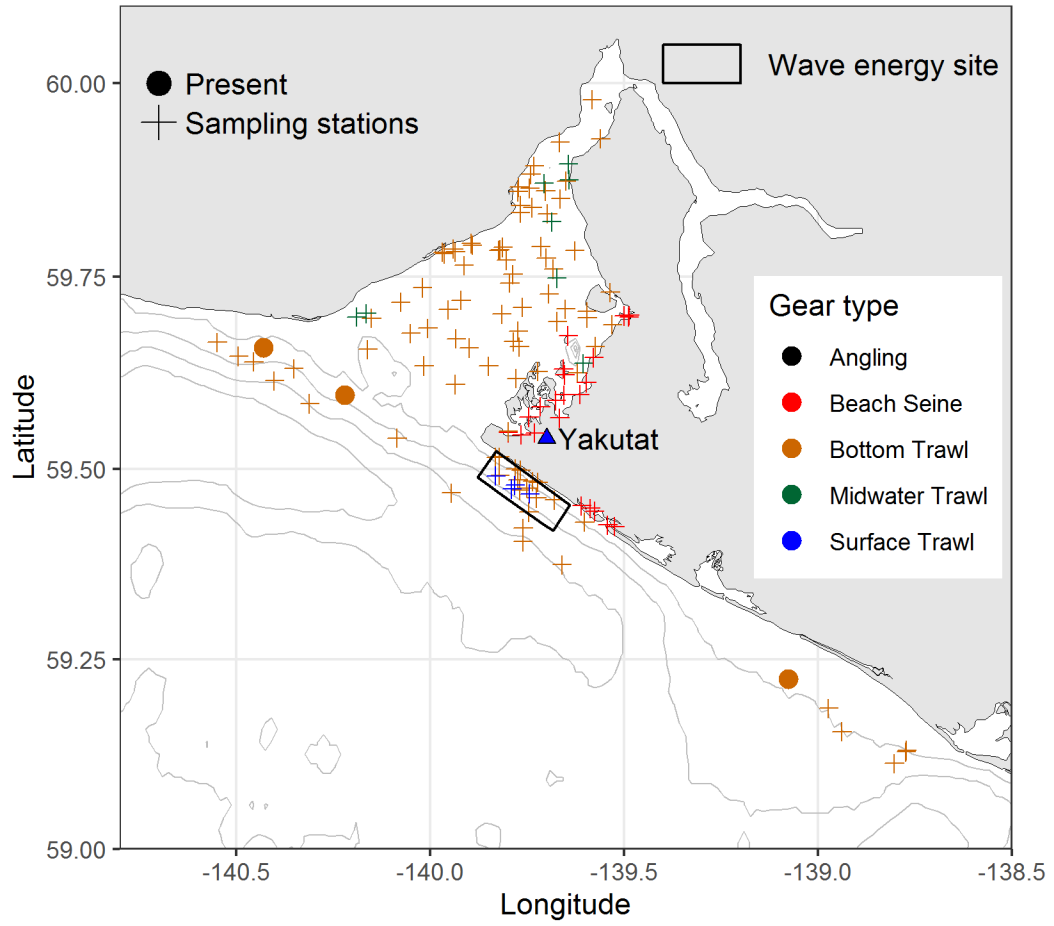
Oxylebius pictus



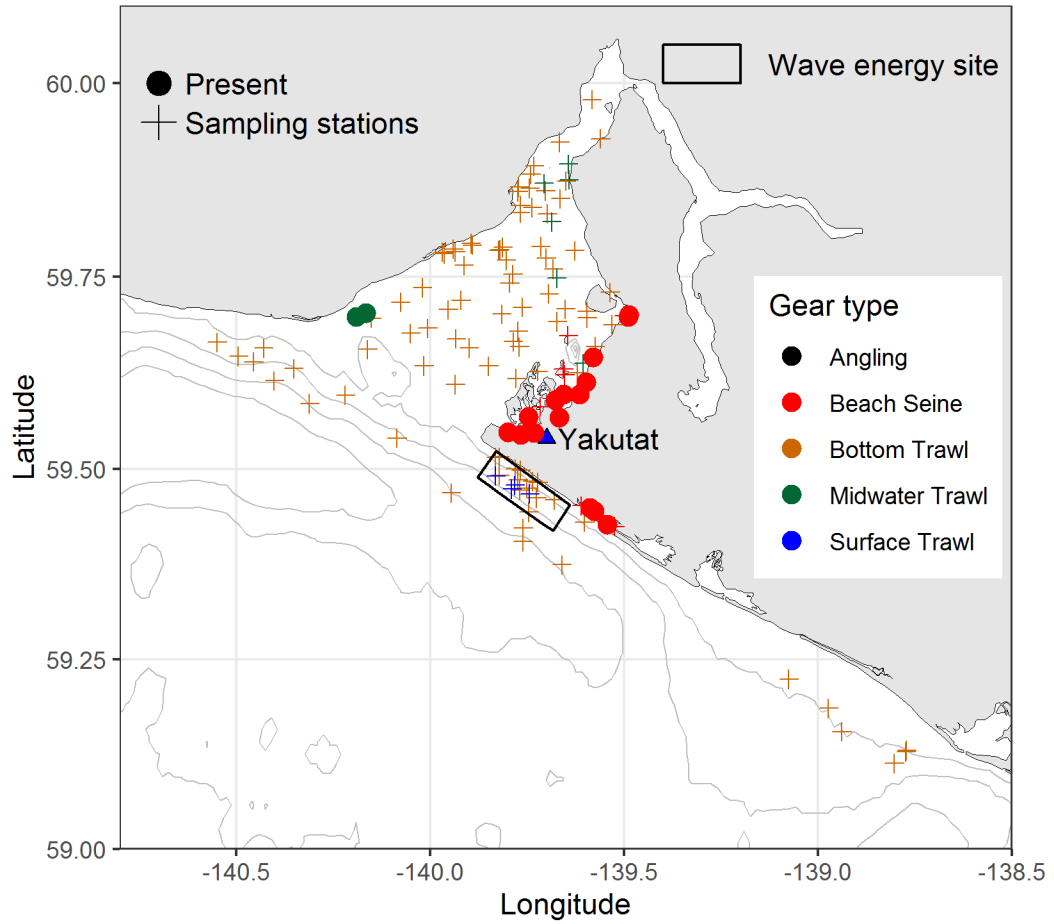
Penpoint Gunnel
Apodichthys flavidus



Petrale Sole
Eopsetta jordani

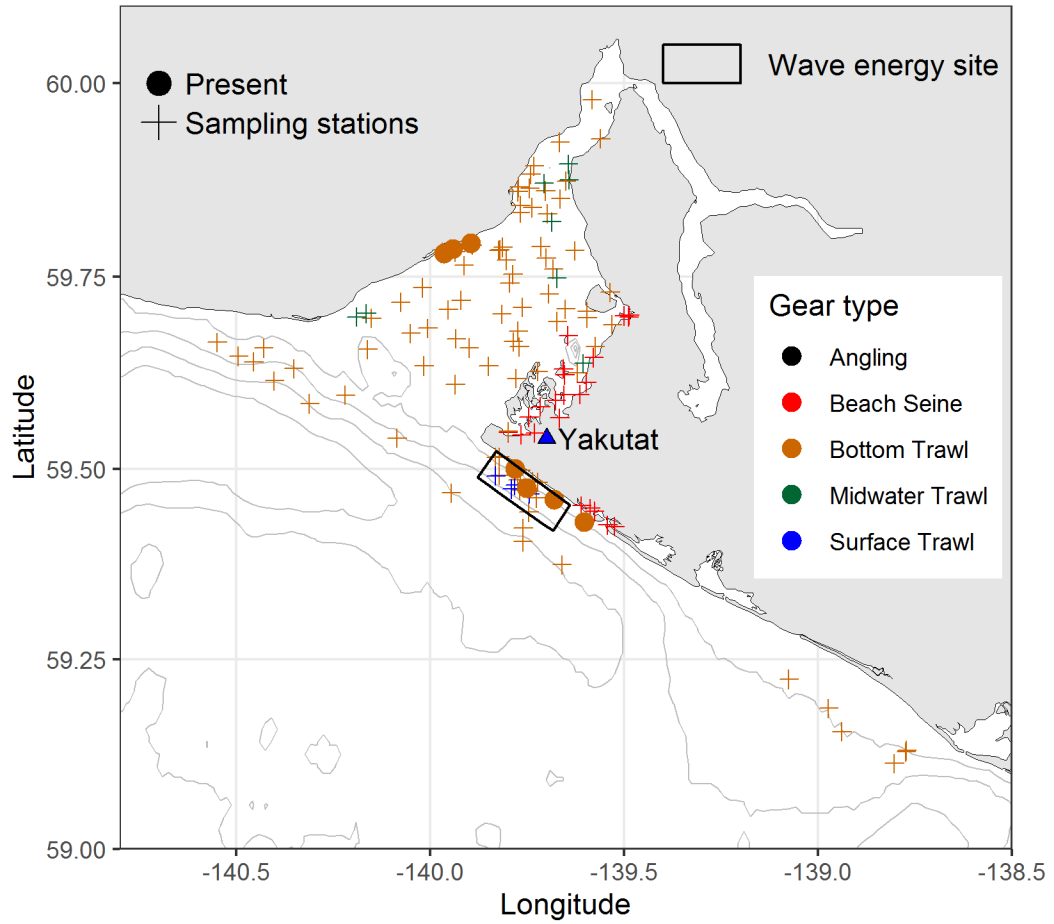


Pink Salmon
Oncorhynchus gorbuscha



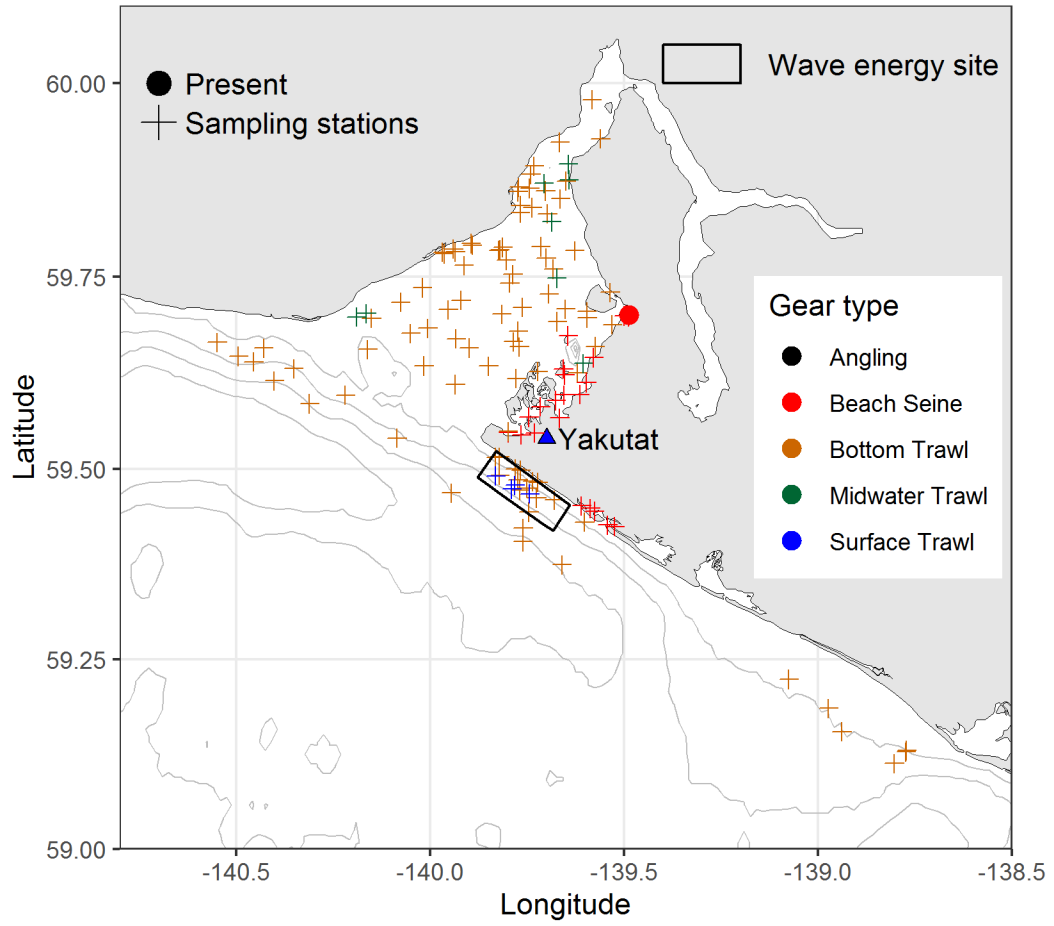
Pricklebreast Poacher

Stellerina xyosterna

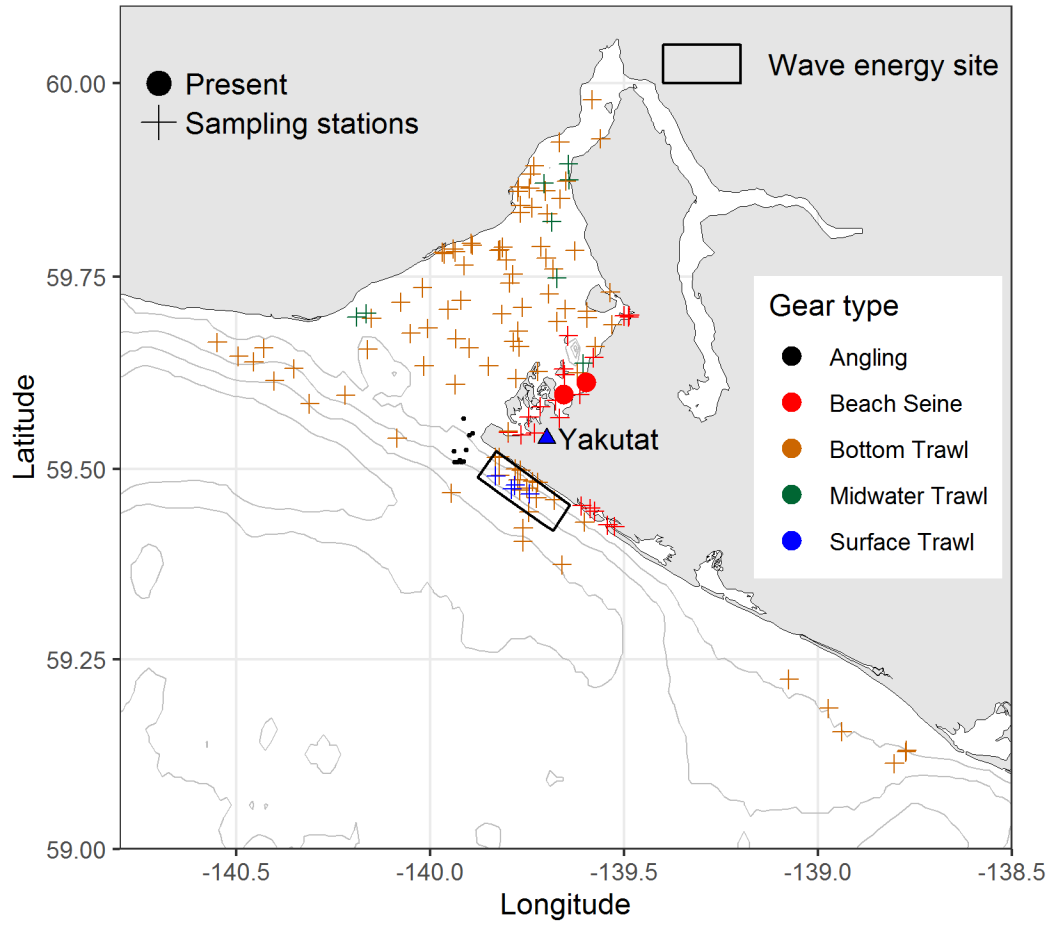


Puget Sound Rockfish

Sebastes emphaeus

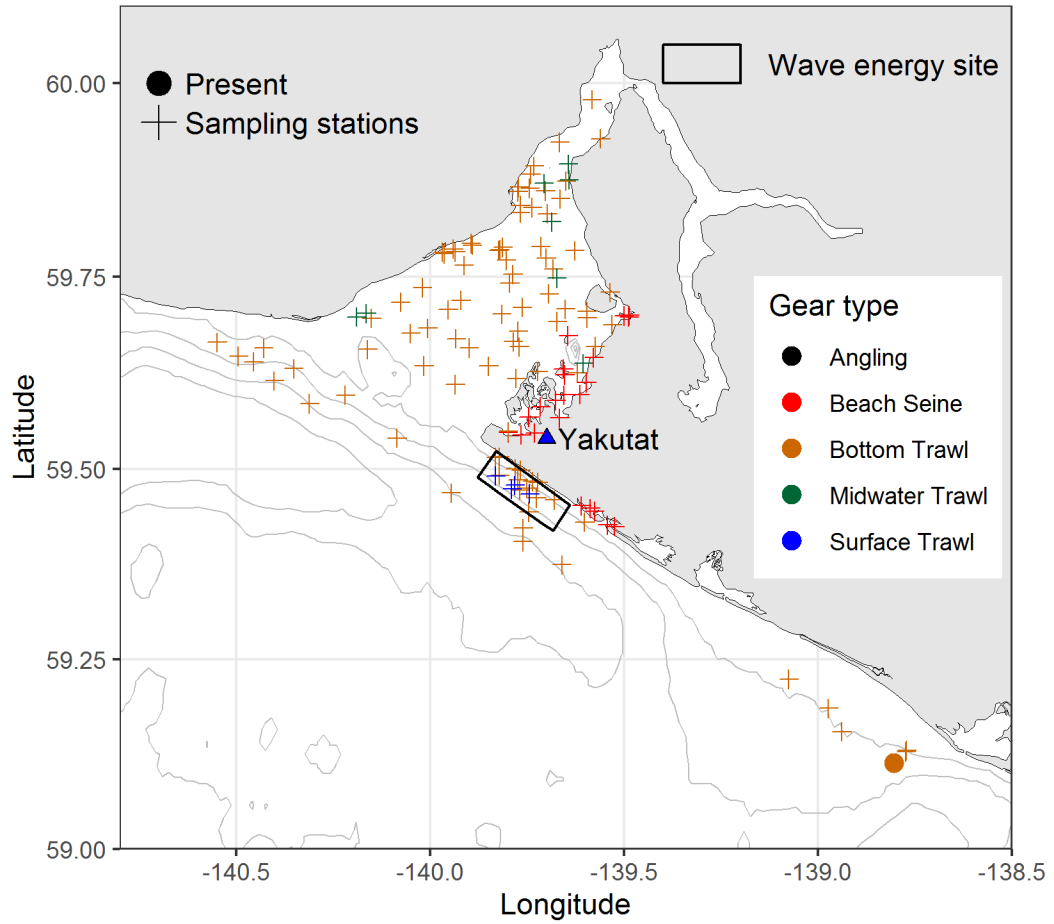


Quillback Rockfish
Sebastes maliger

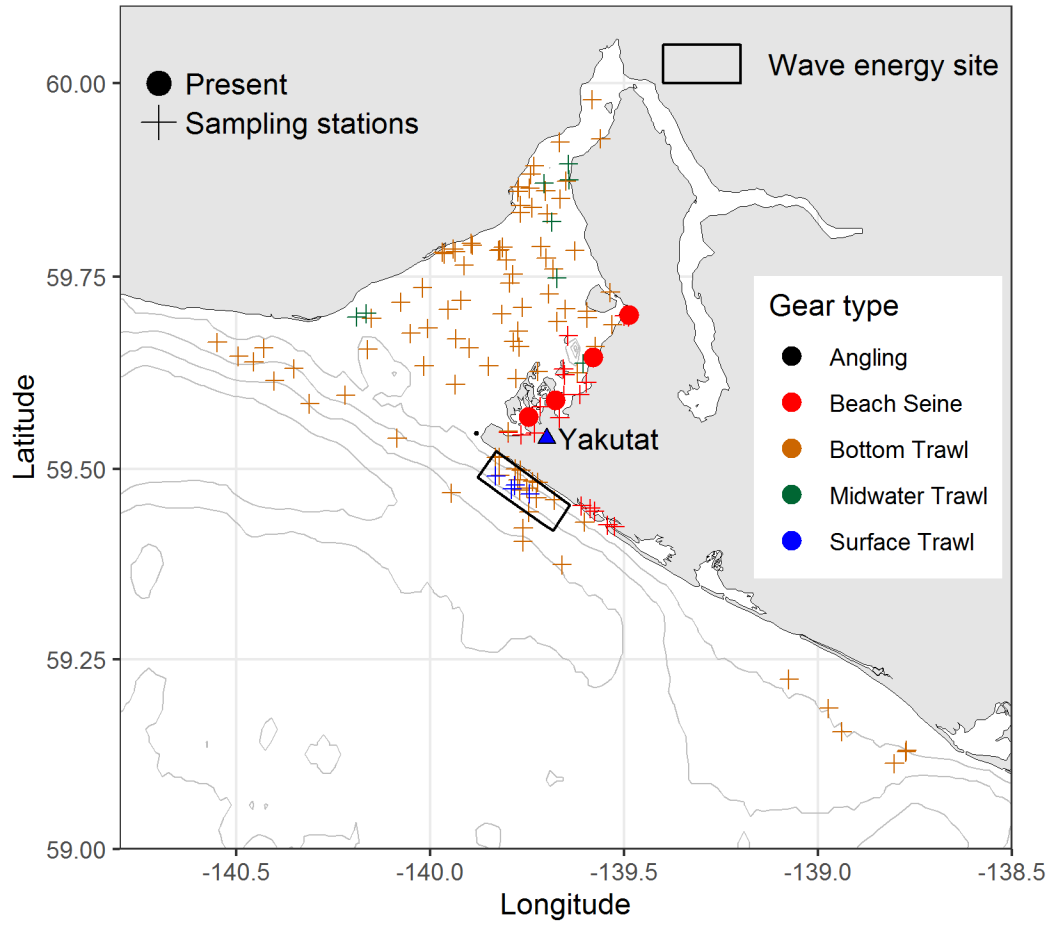


Rainbow Smelt

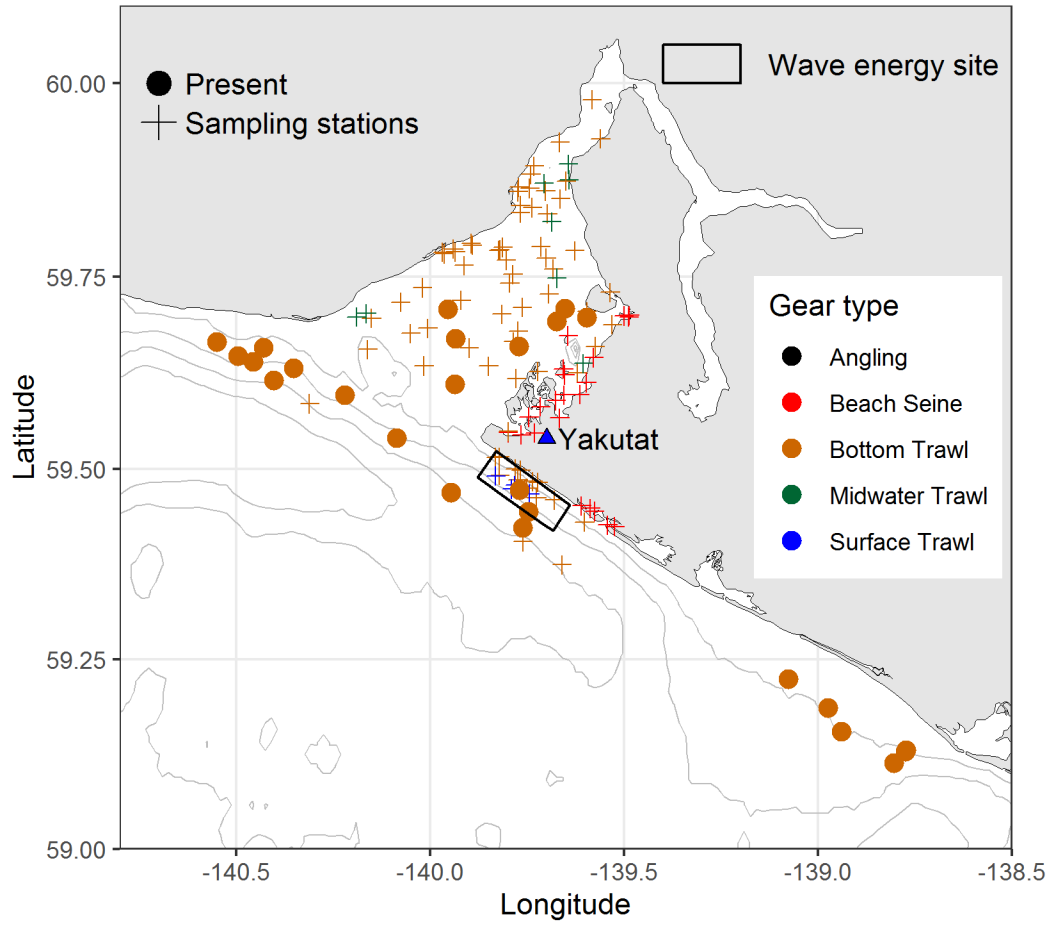
Osmerus mordax



Red Irish Lord
Hemilepidotus hemilepidotus

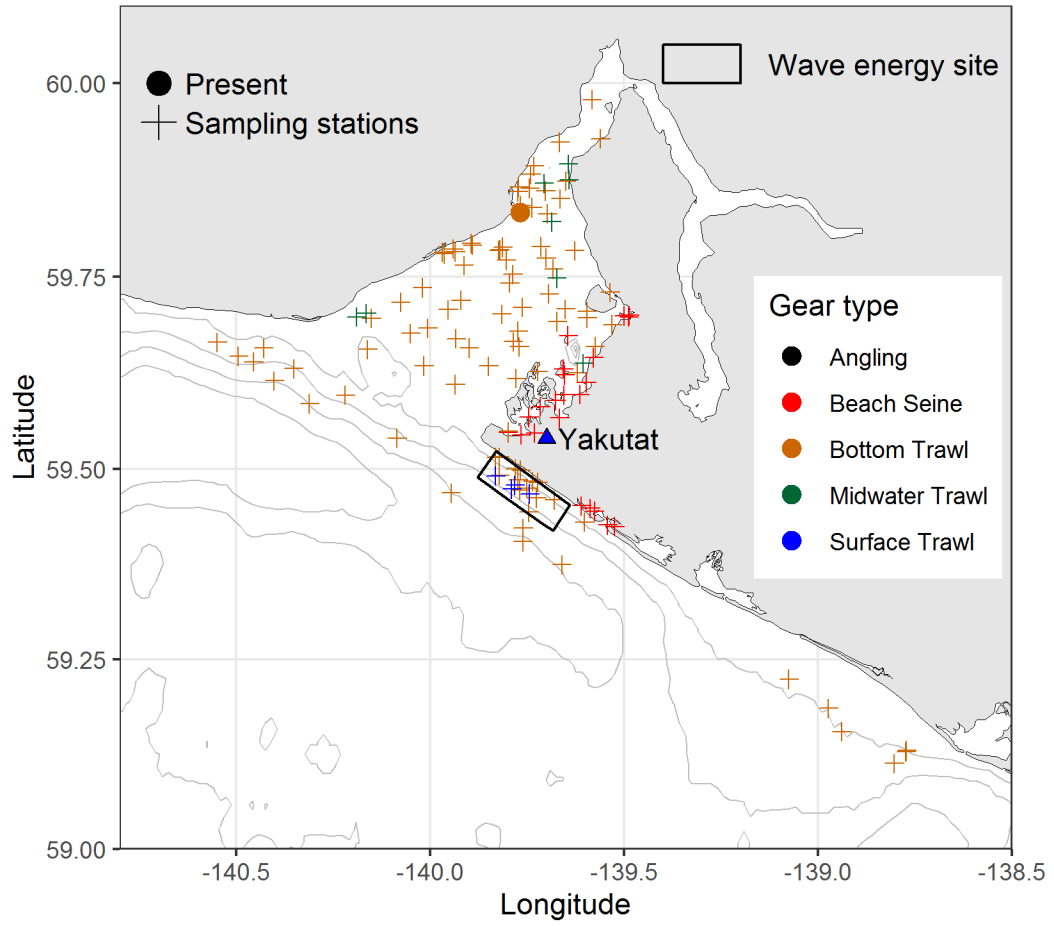


Rex Sole
Glyptocephalus zachirus

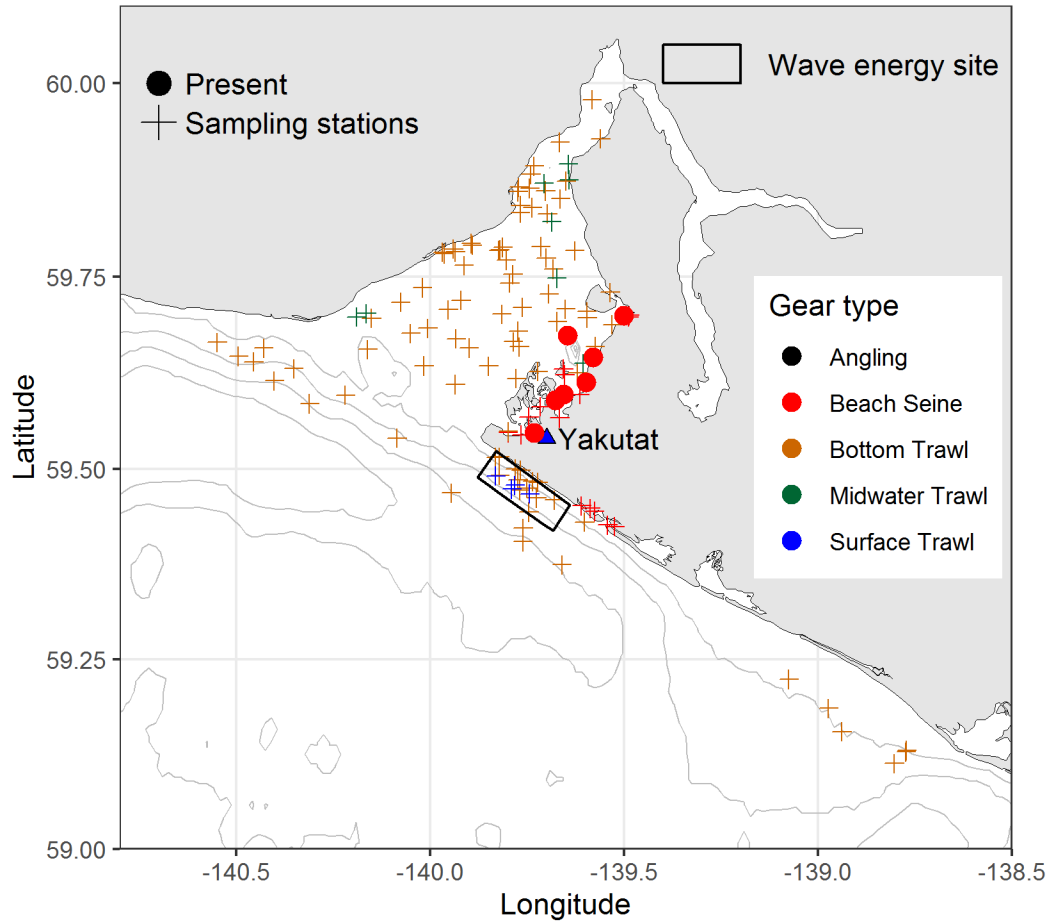


Ringtail Snailfish

Liparis rutteri

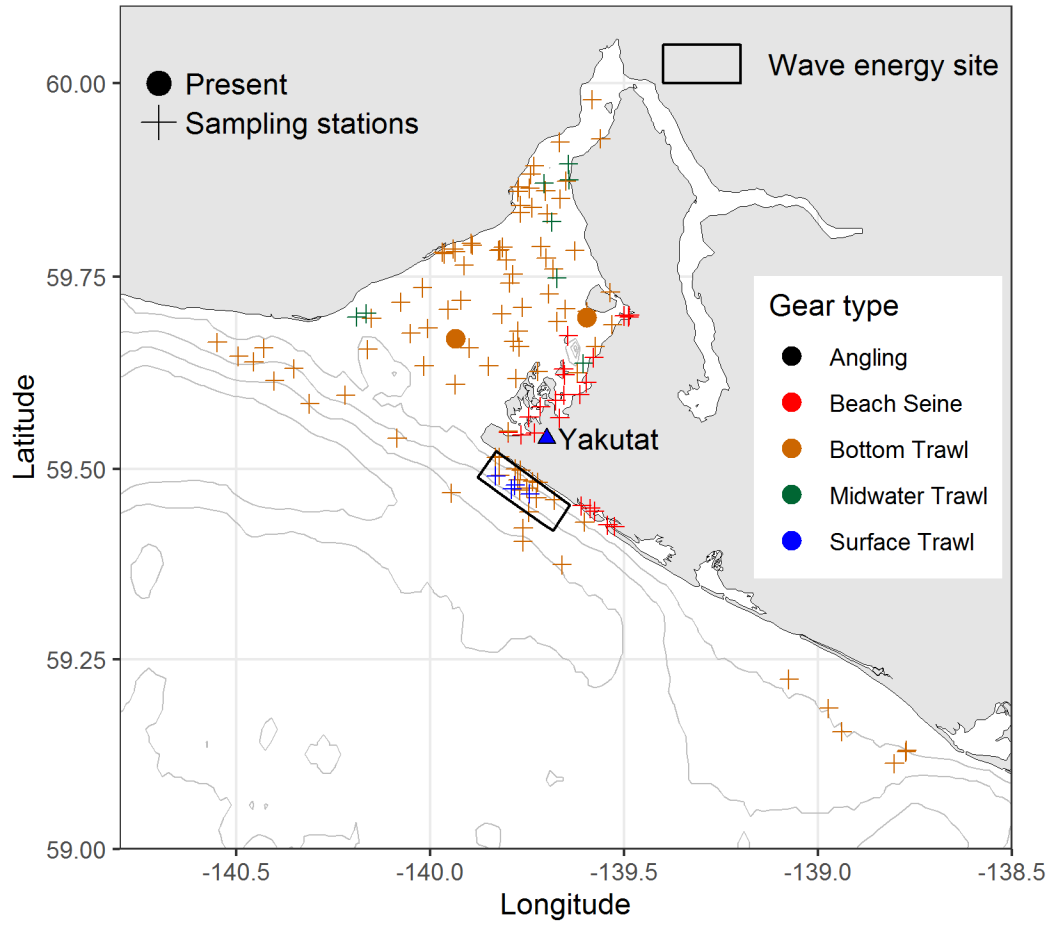


Rock Greenling
Hexagrammos lagocephalus

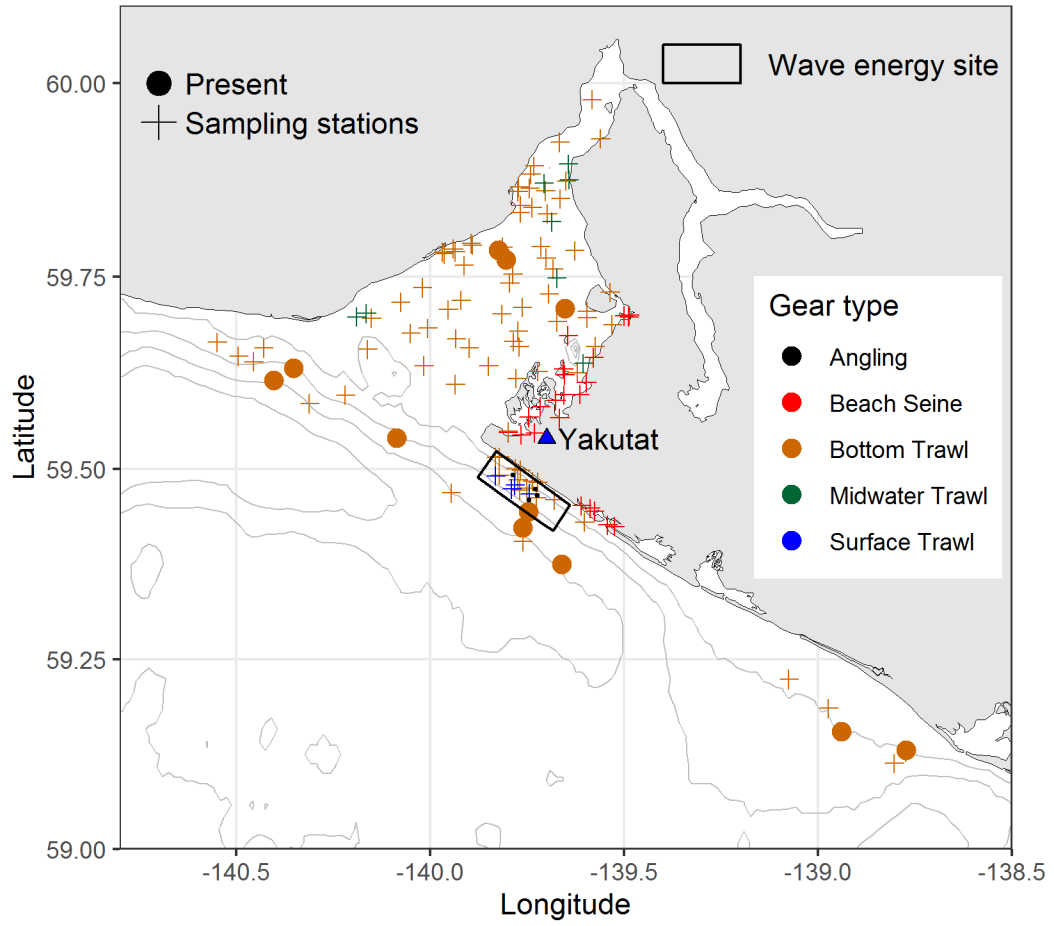


Rougheye Rockfish

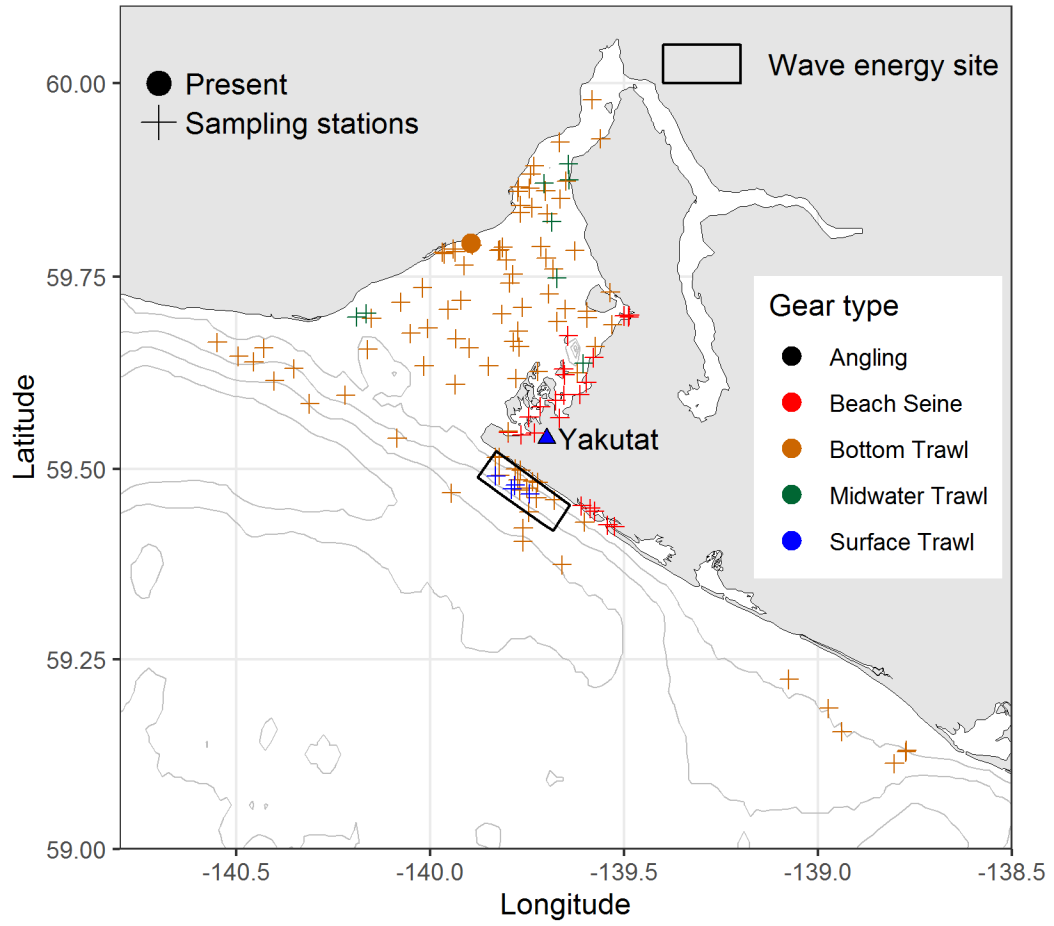
Sebastes aleutianus



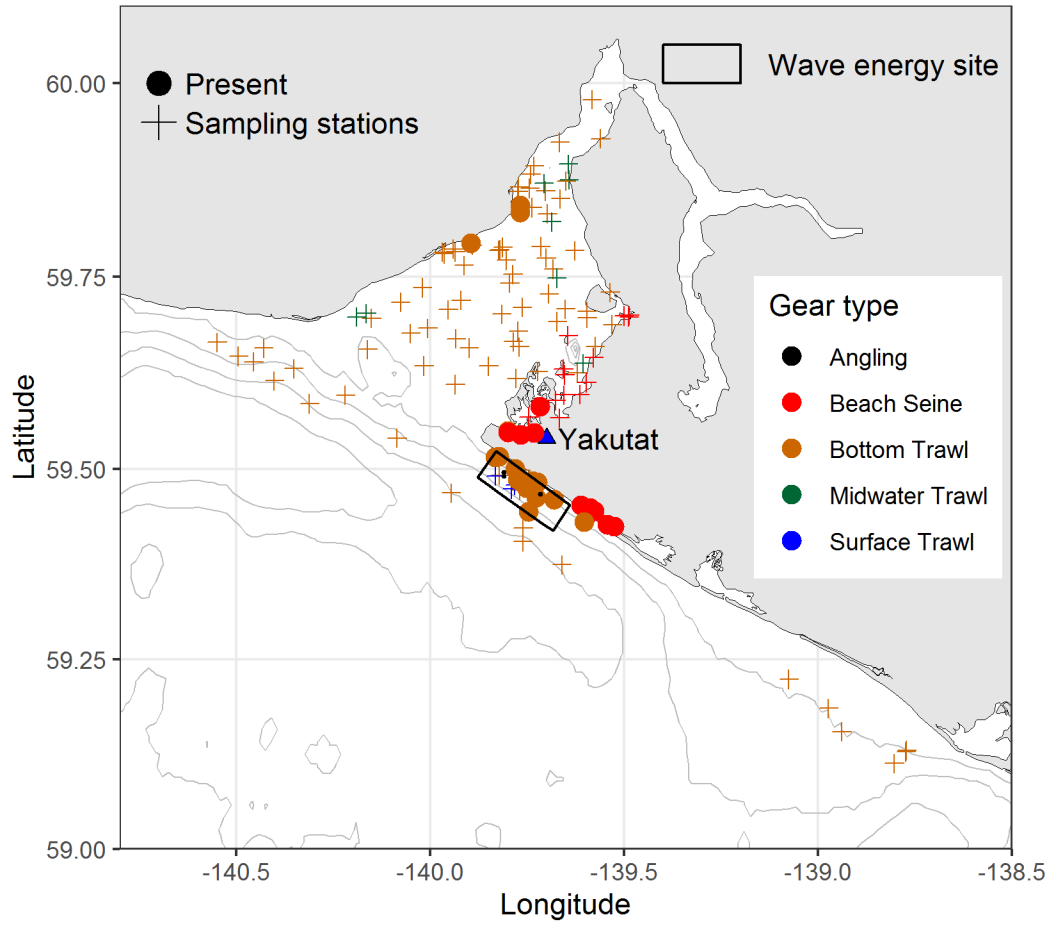
Sablefish
Anoplopoma fimbria



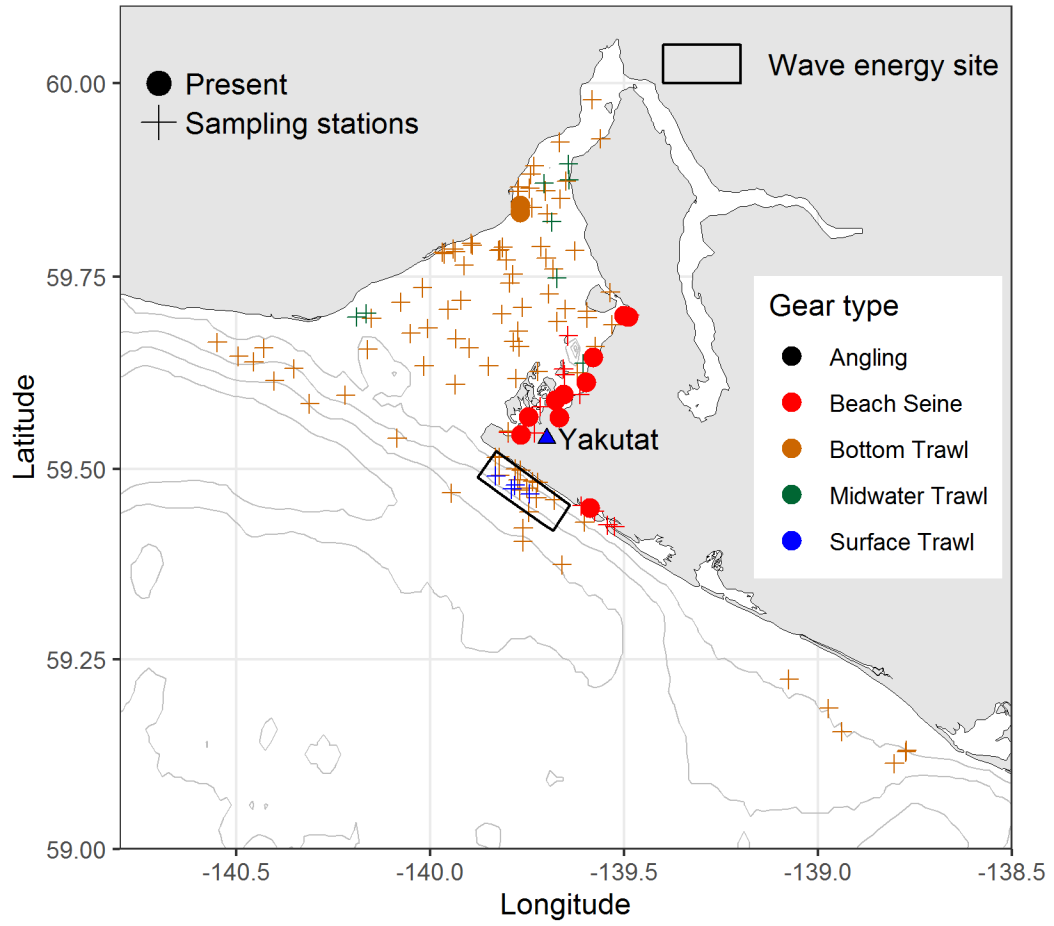
Saffron Cod
Eleginus gracilis



Sand Sole
Psettichthys melanostictus

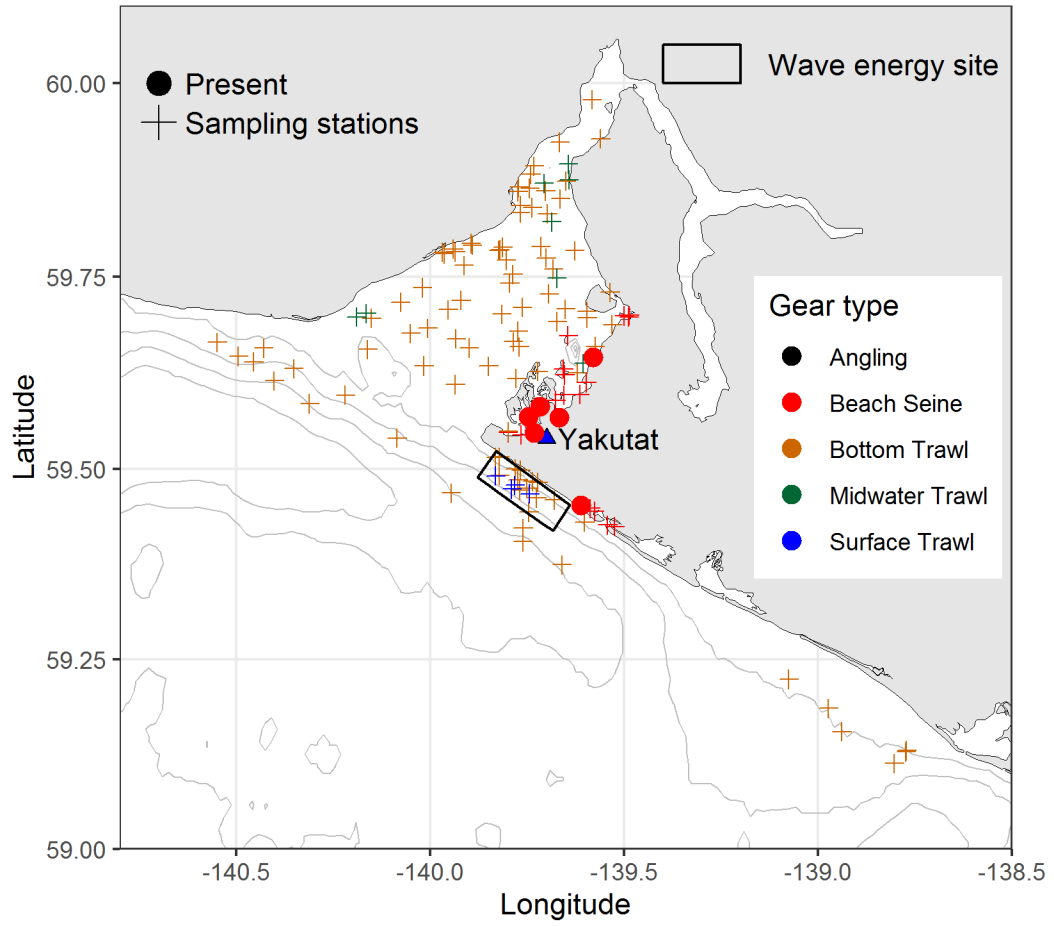


Scalyhead Sculpin
Artedius harringtoni

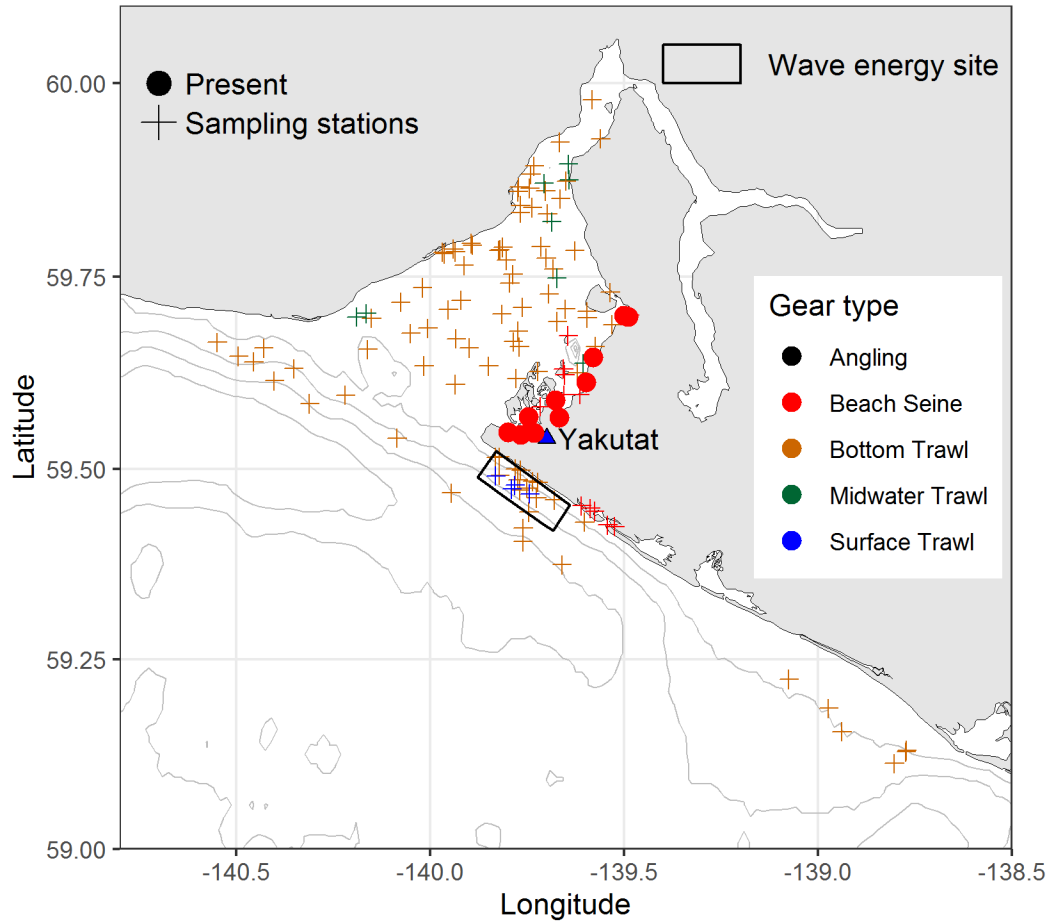


Sharpnose Sculpin

Clinocottus acuticeps

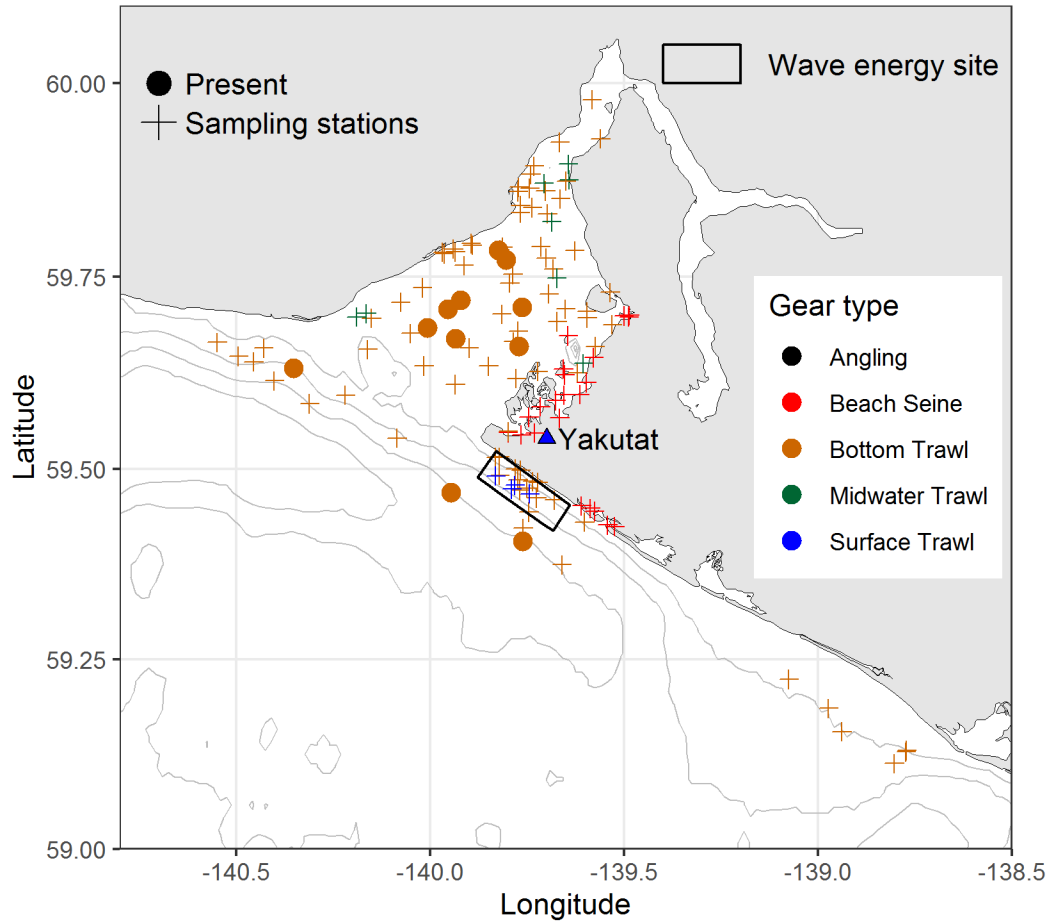


Shiner Perch
Cymatogaster aggregata

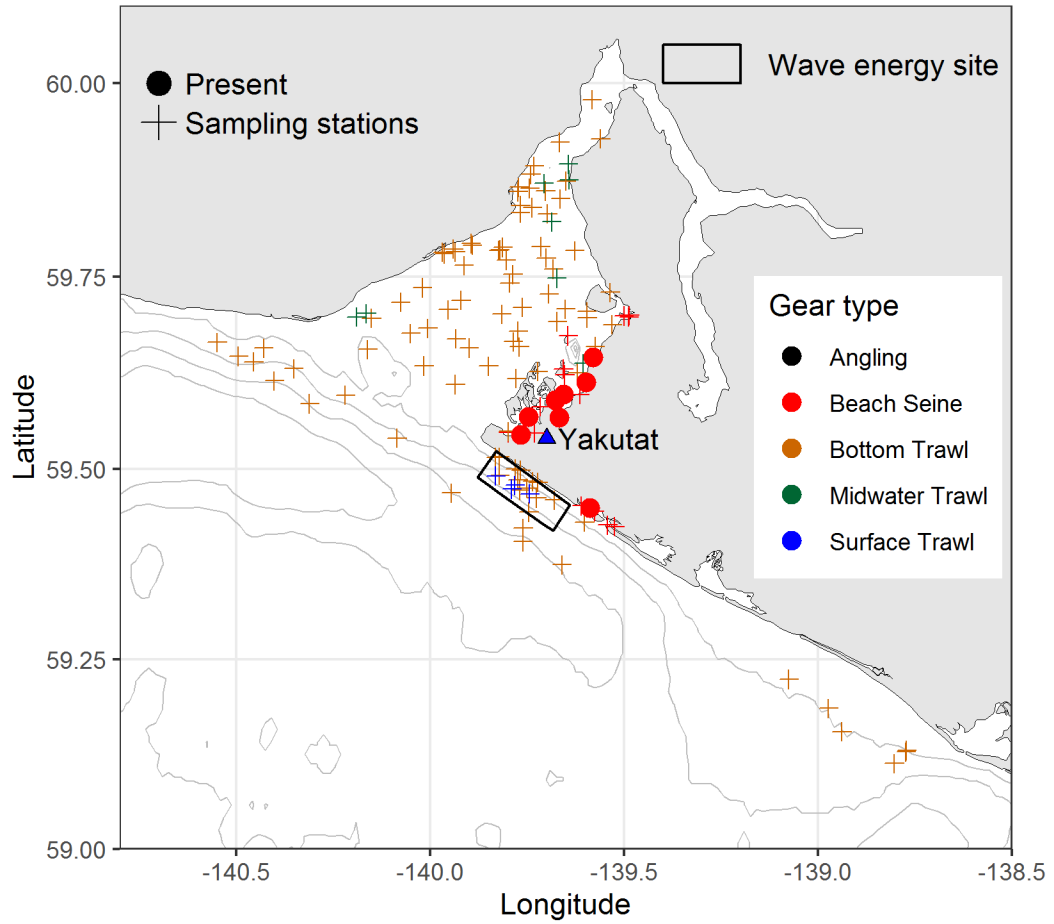


Shortfin Eelpout

Lycodes brevipes

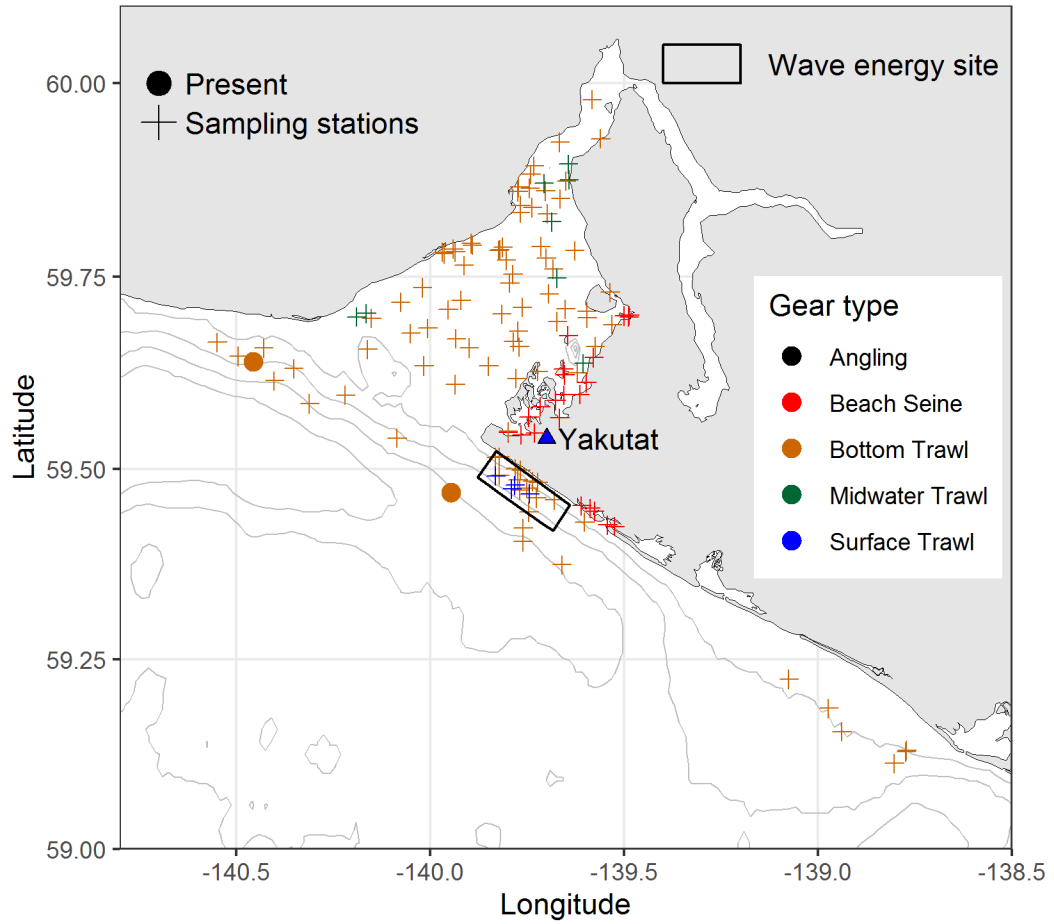


Shorthorn Sculpin
Myoxocephalus scorpius



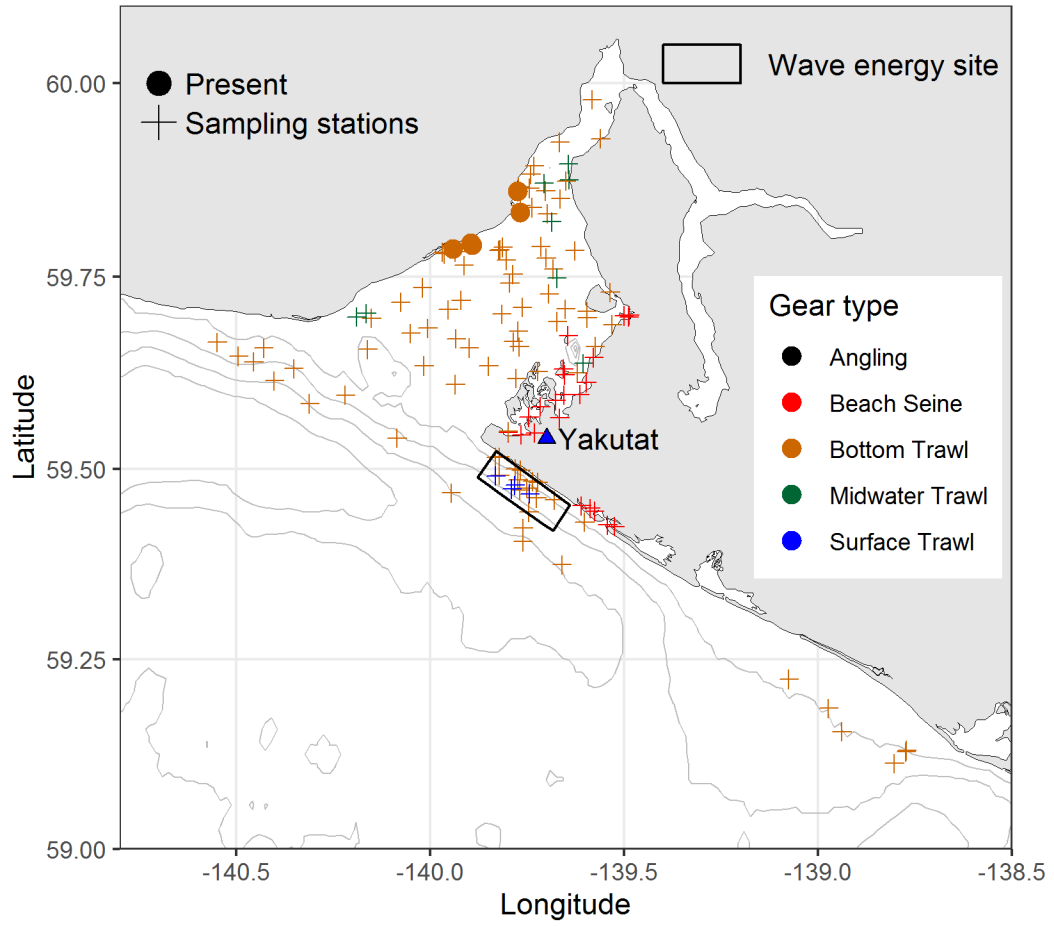
Shortspine Thornyhead

Sebastolobus alascanus



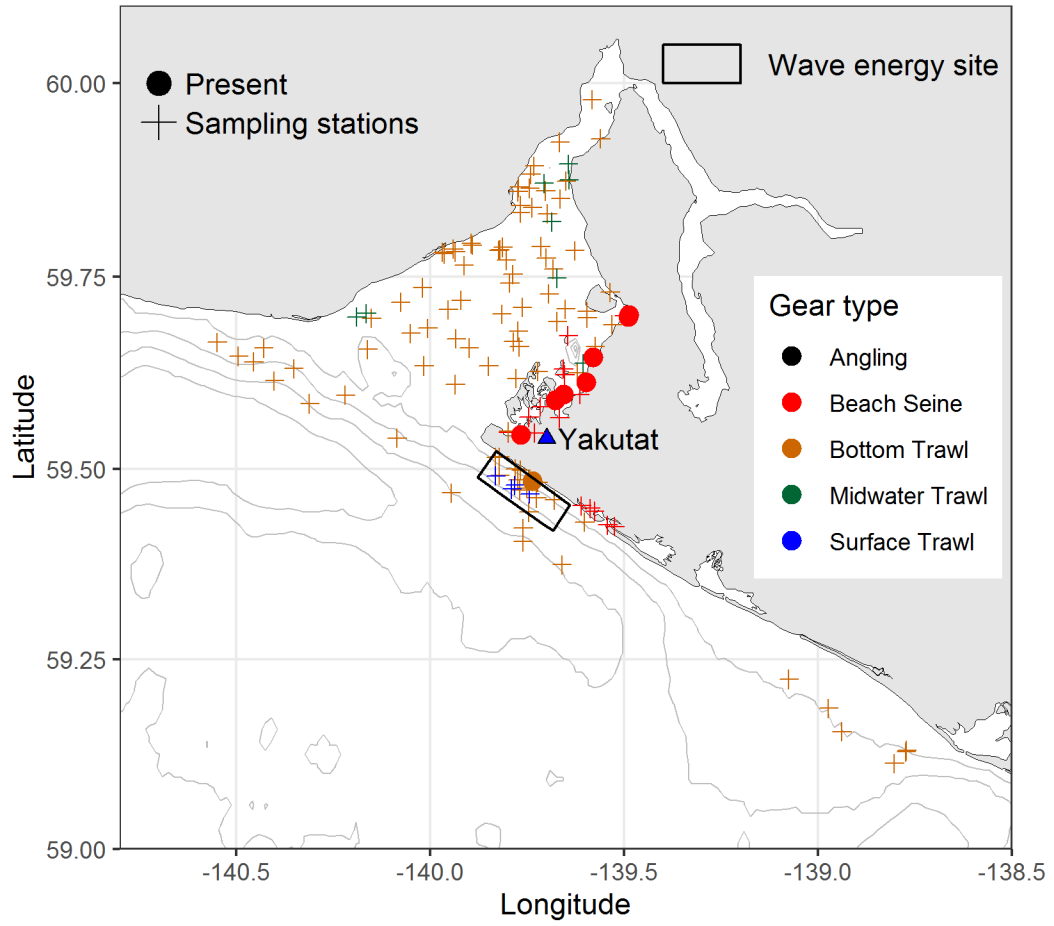
Showy Snailfish

Liparis pulchellus



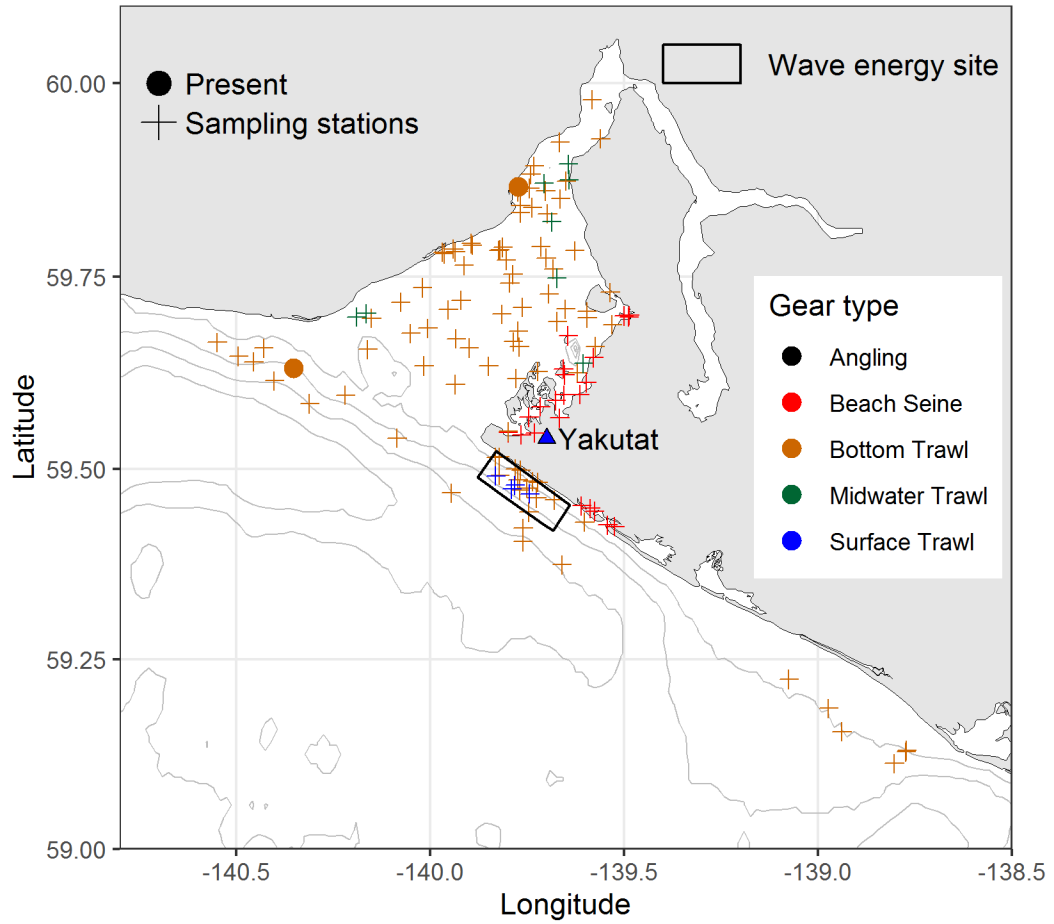
Silverspotted Sculpin

Blepsias cirrhosus



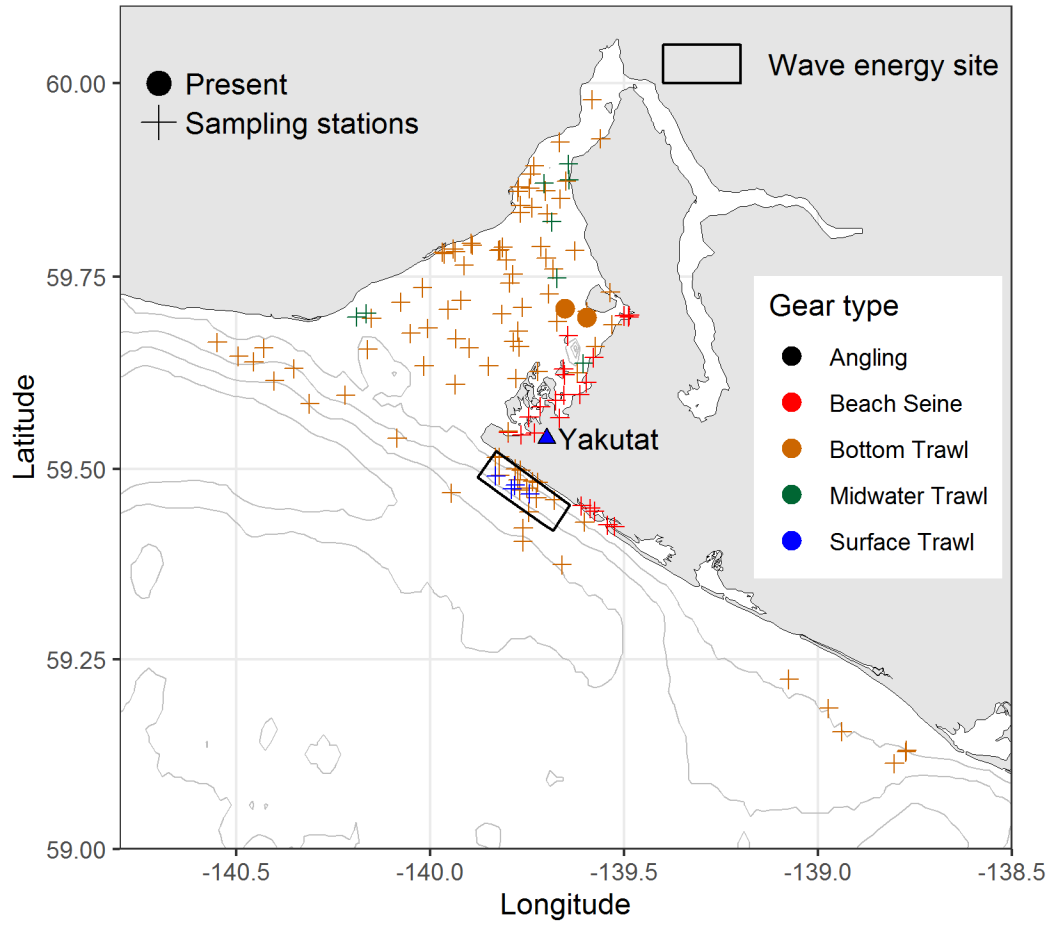
Slender Sole

Lyopsetta exilis



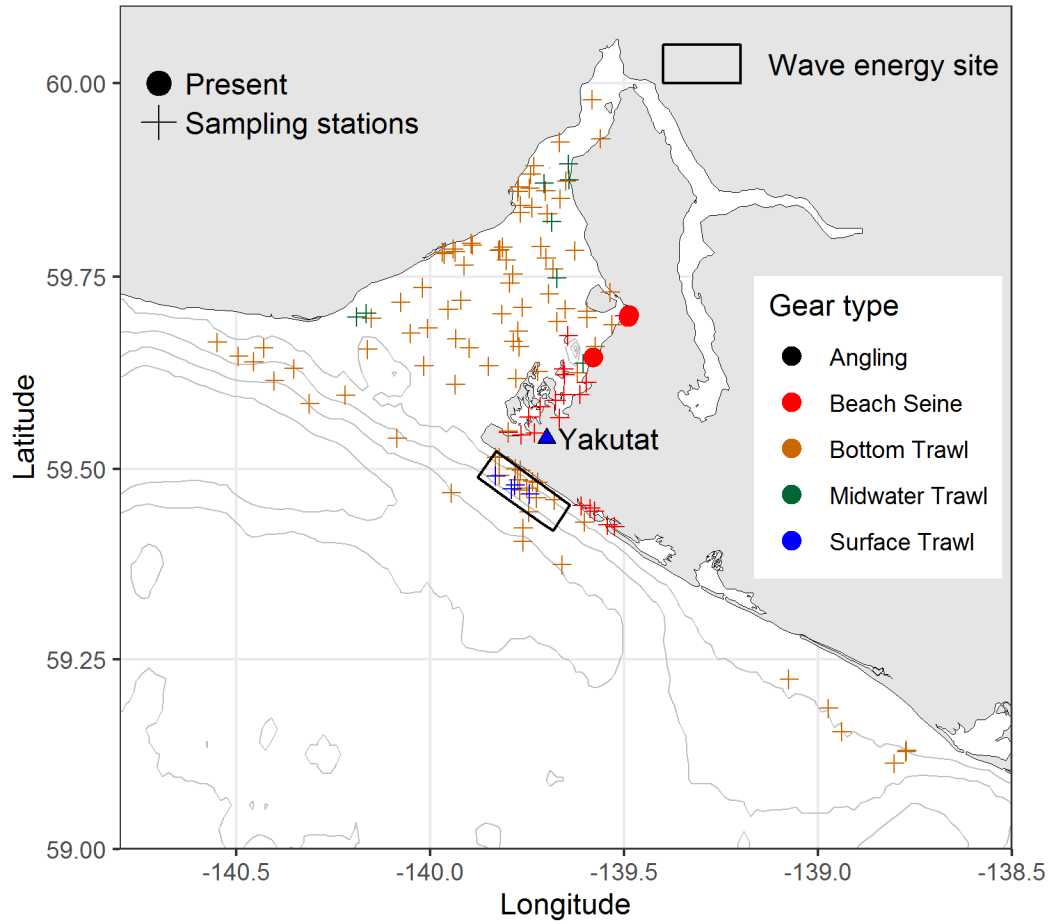
Smooth Lump sucker

Aptocyclus ventricosus



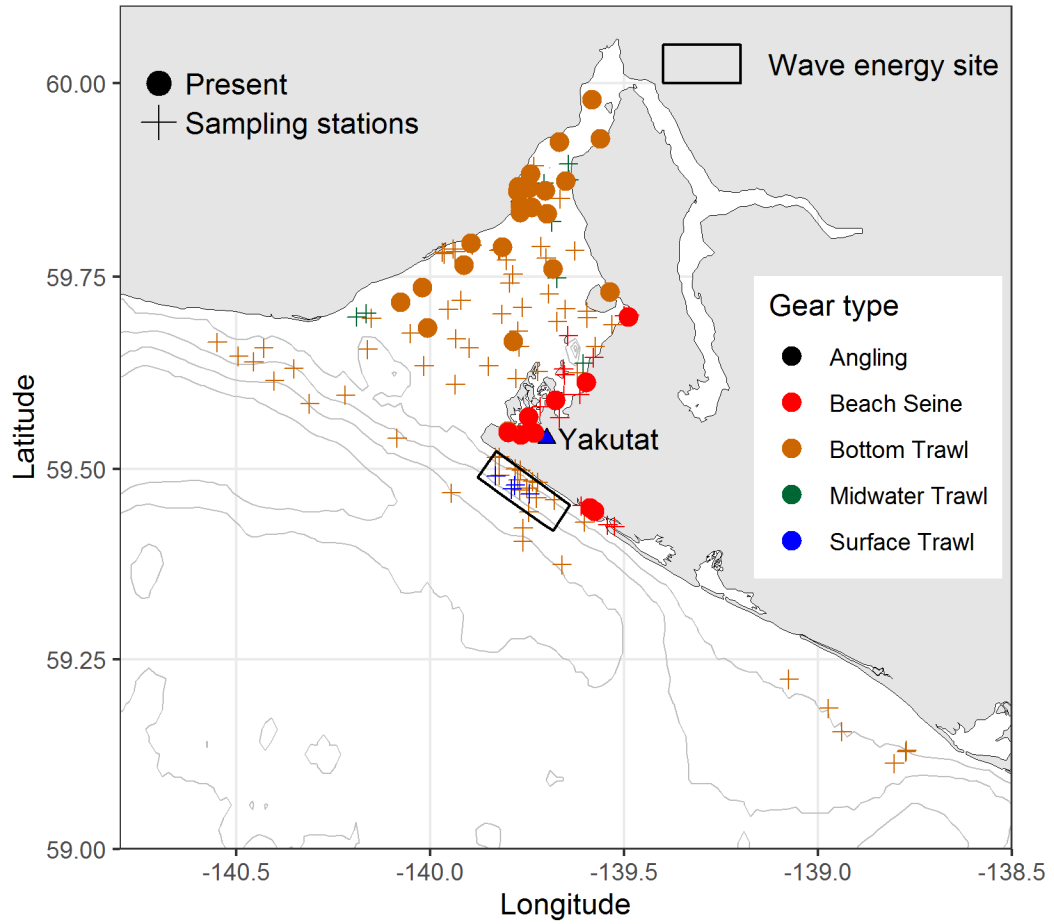
Smoothhead Sculpin

Artedius lateralis

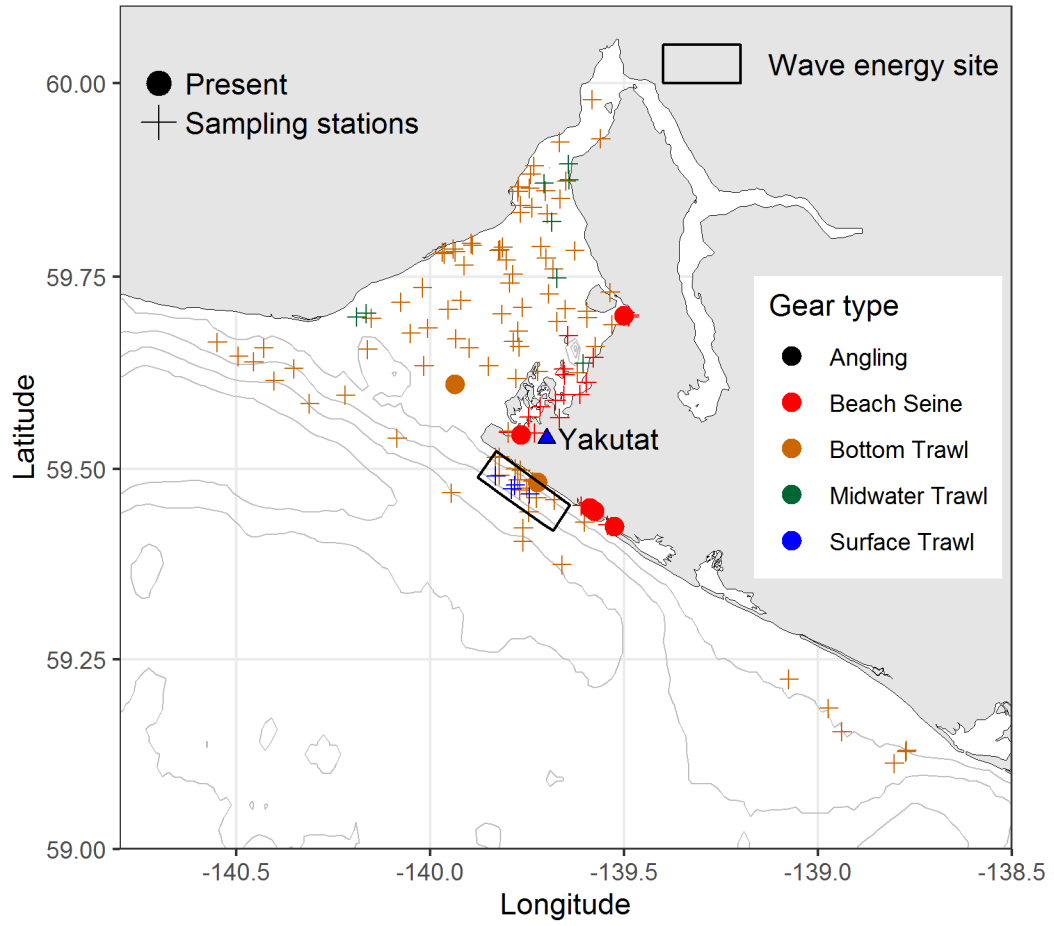


Snake Prickleback

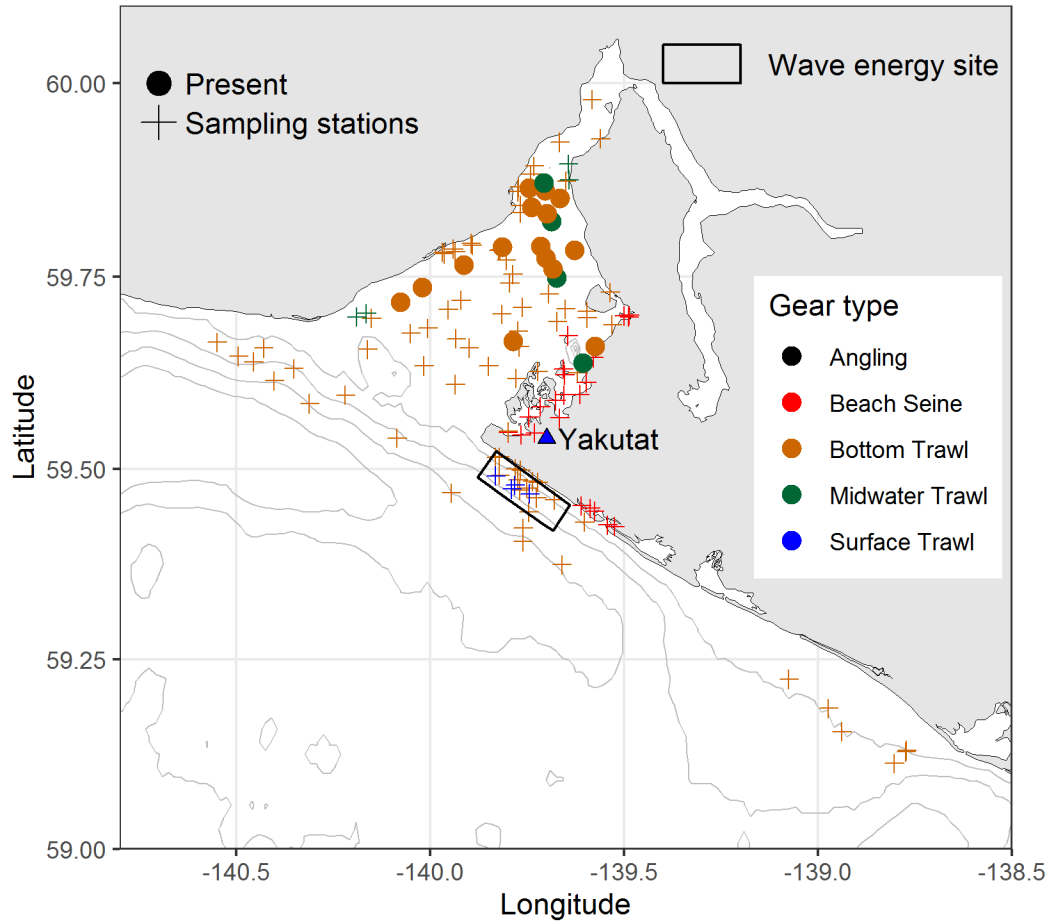
Lumpenus sagitta



Sockeye Salmon
Oncorhynchus nerka

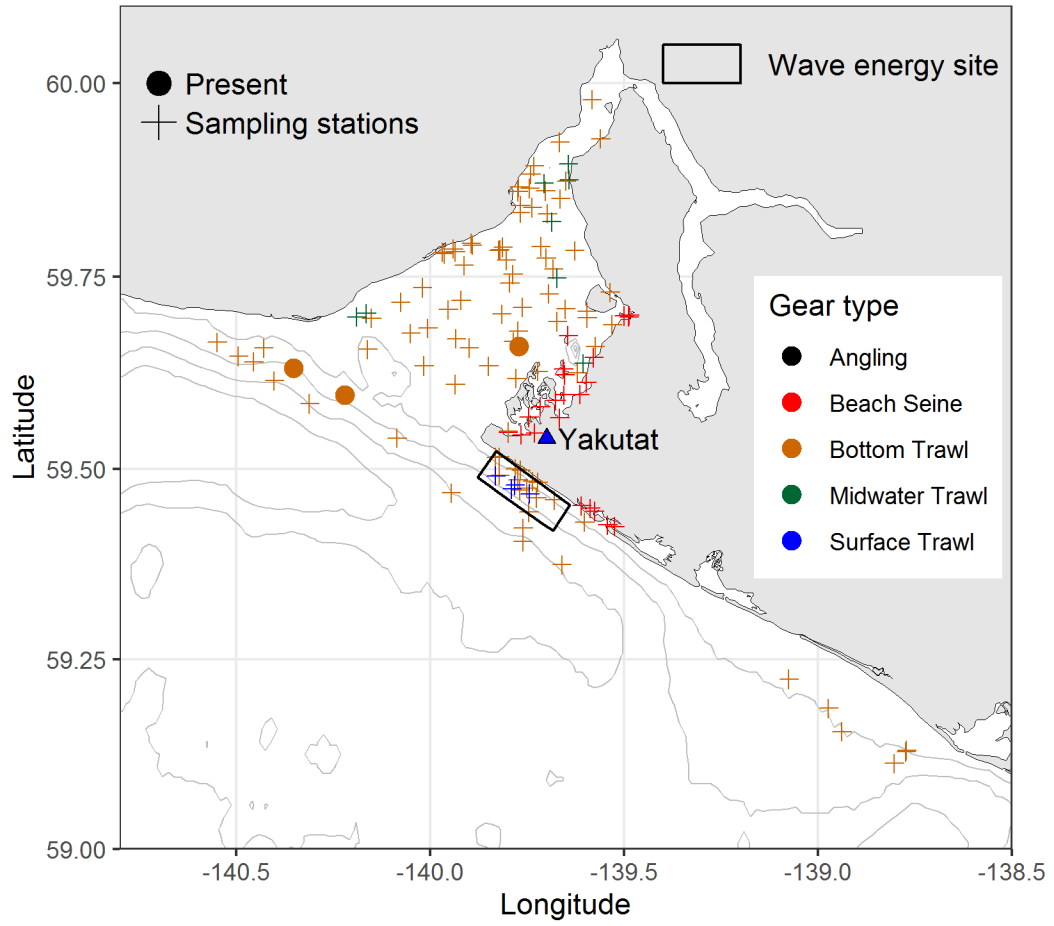


Soft Sculpin
Psychrolutes sigalutes

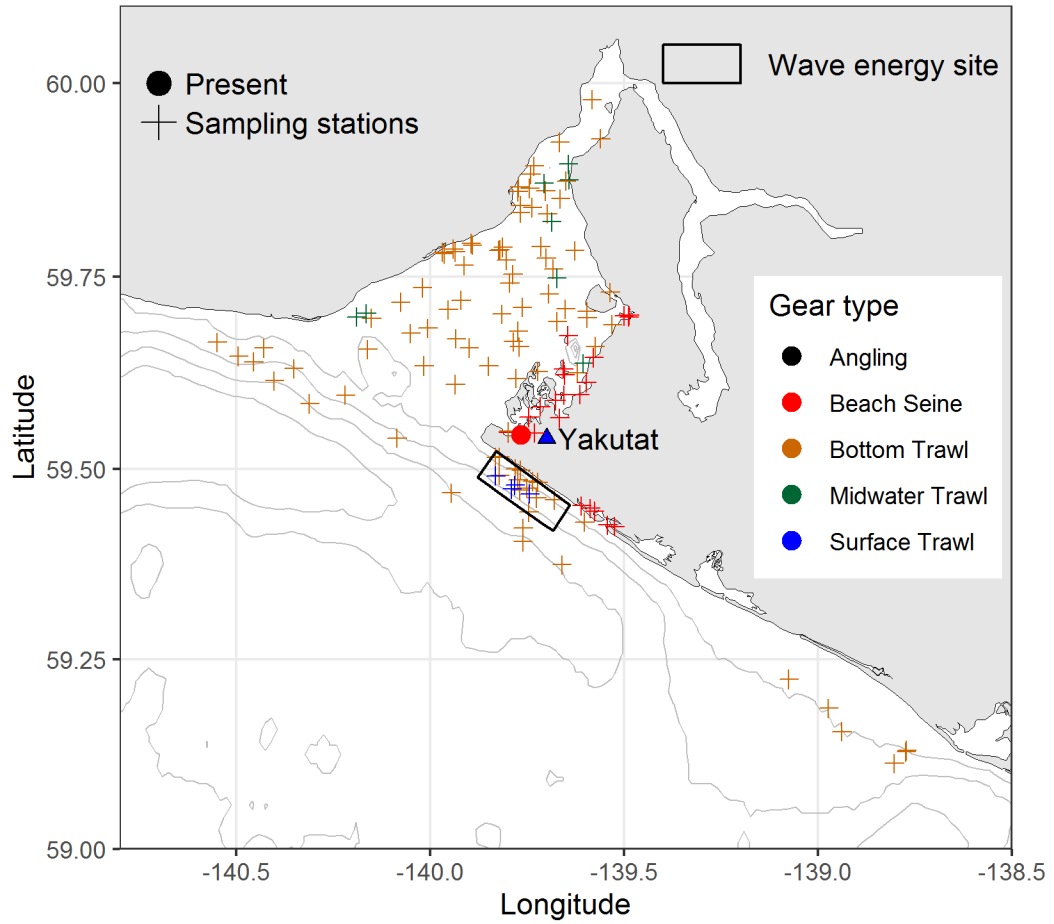


Southern Rock Sole

Lepidopsetta bilineata

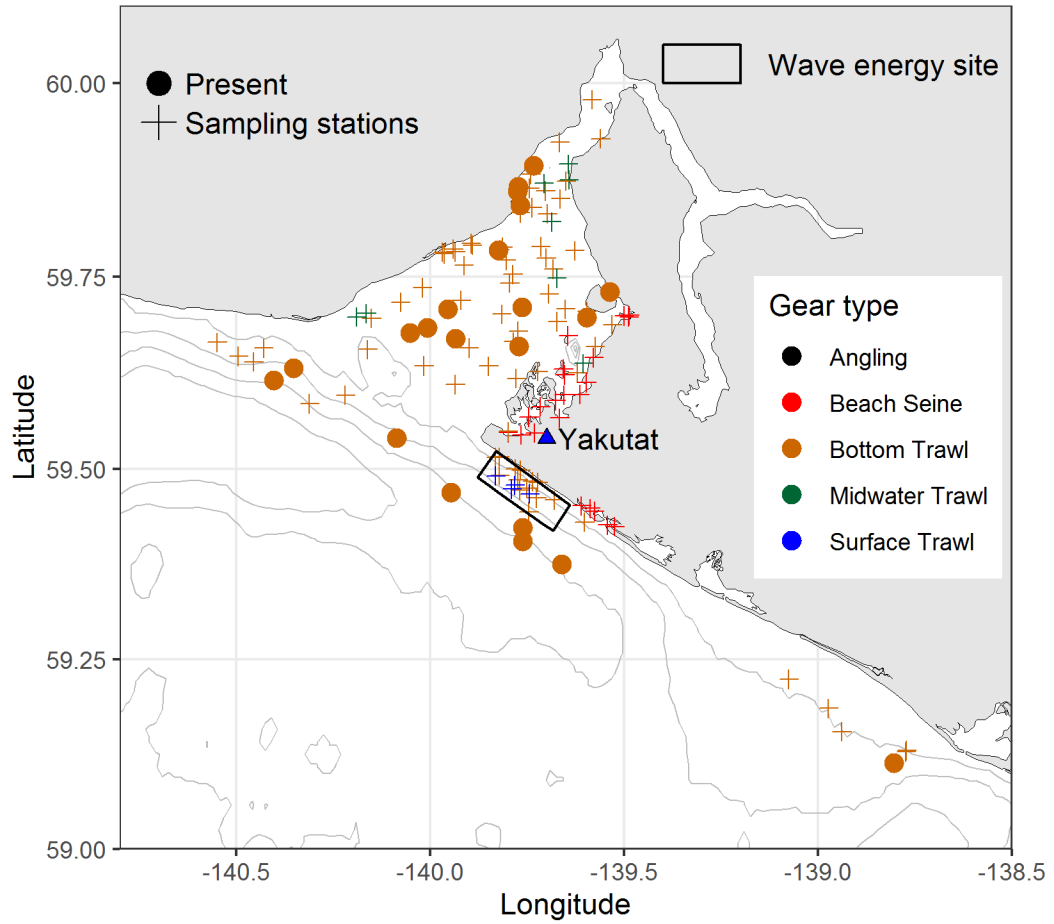


Speckled Sanddab
Citharichthys stigmaeus



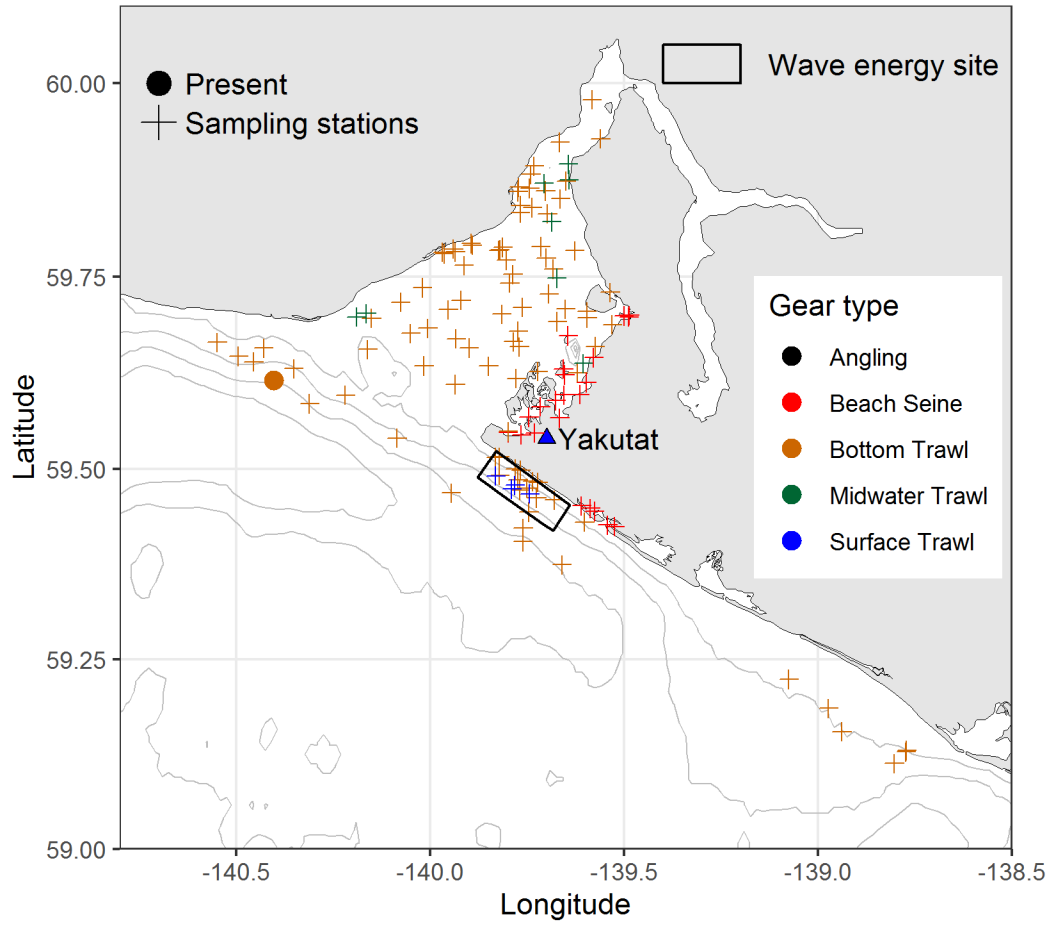
Spinyhead Sculpin

Dasycottus setiger

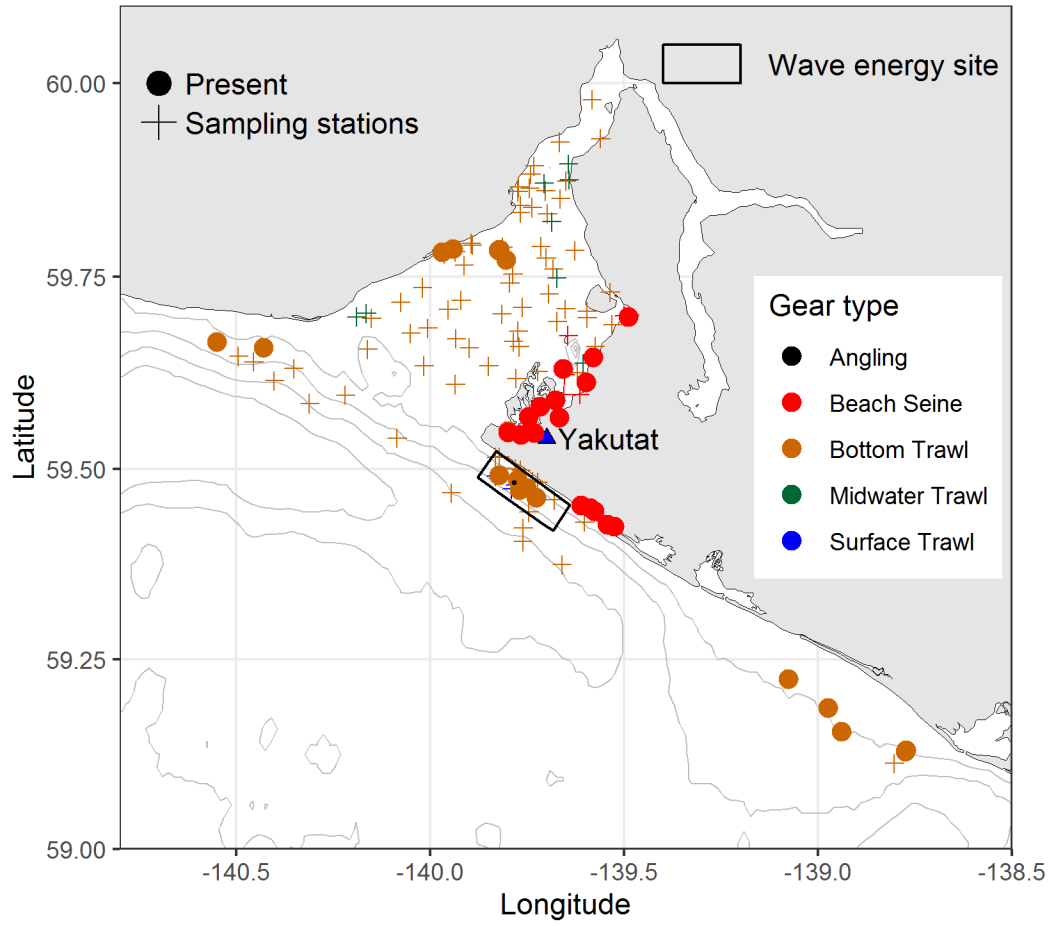


Spotted Ratfish

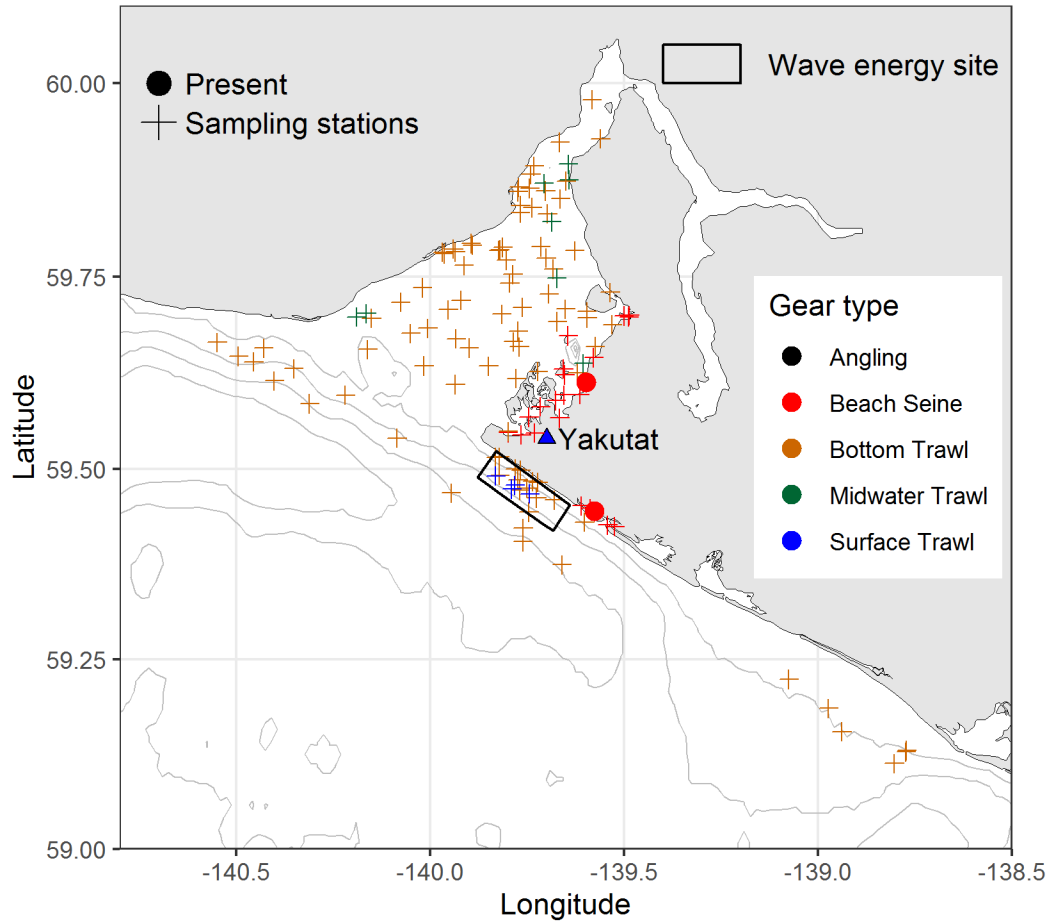
Hydrolagus colliei



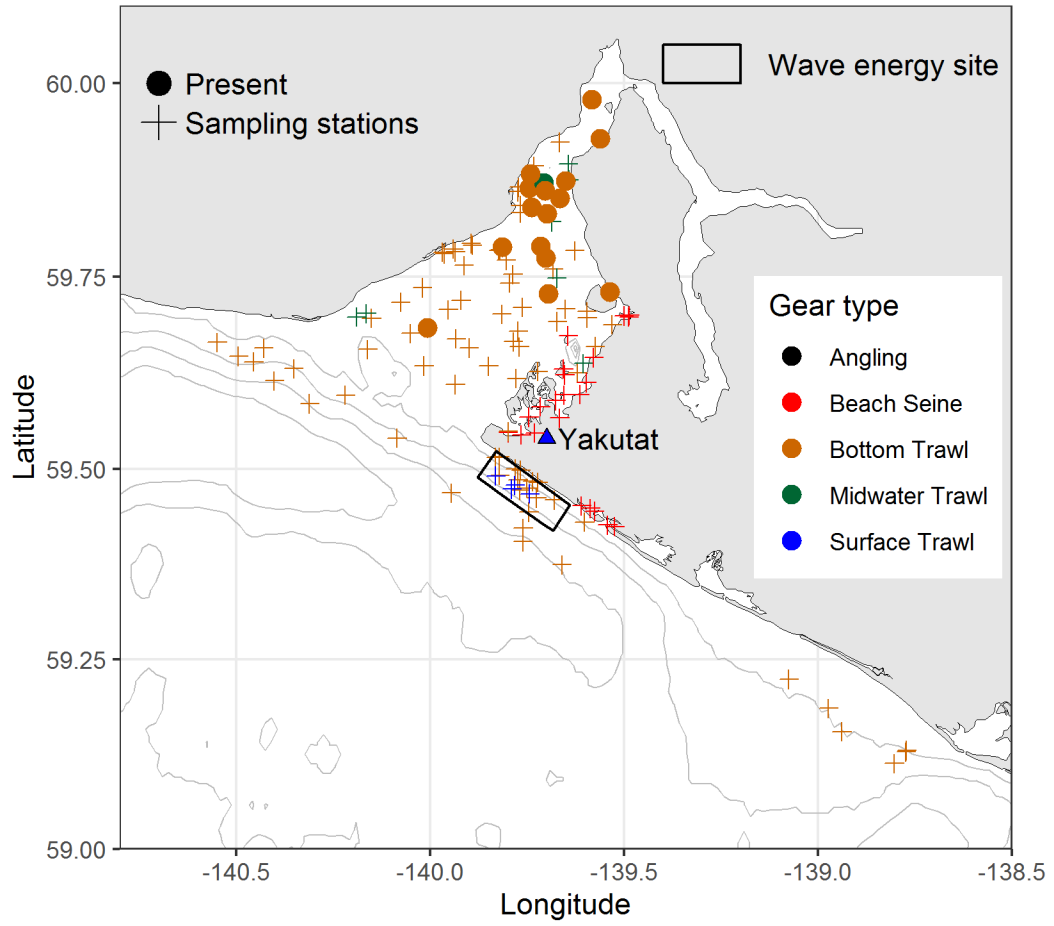
Starry Flounder
Platichthys stellatus



Steelhead Trout
Oncorhynchus mykiss

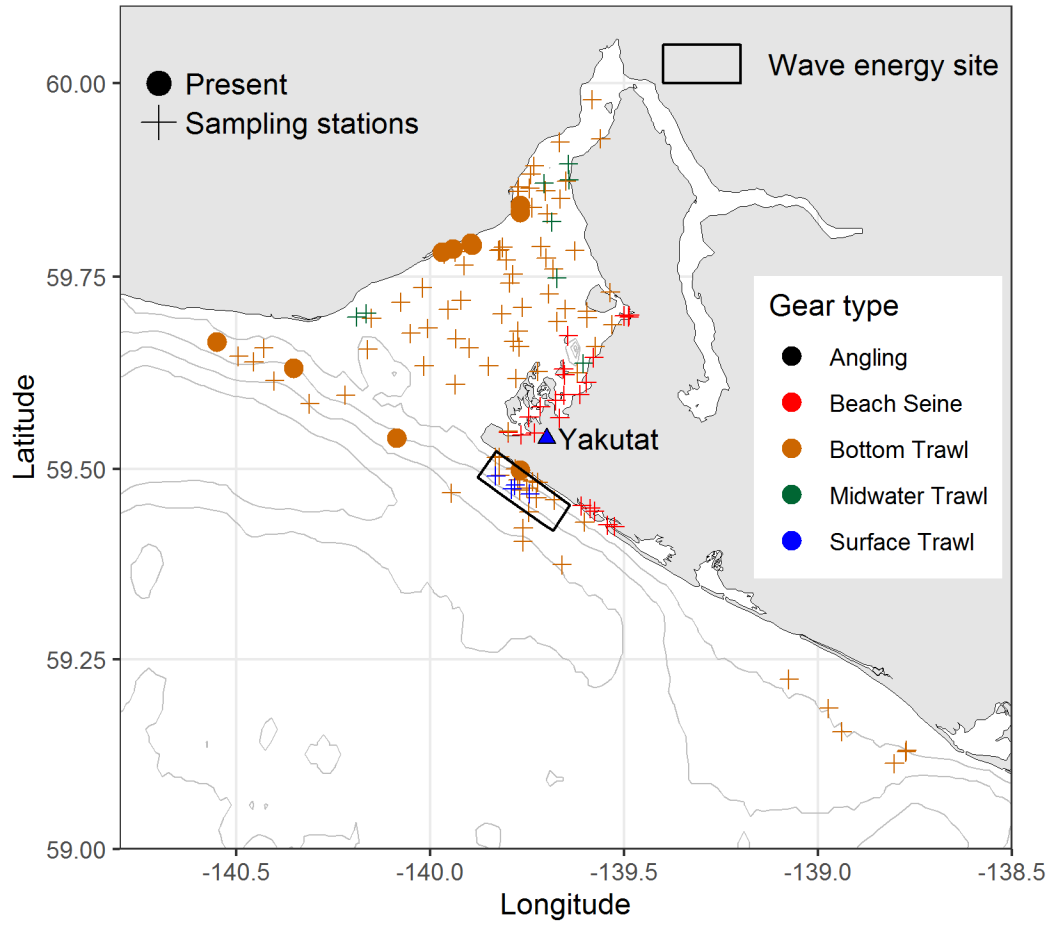


Stout Eelblenny
Anisarchus medius

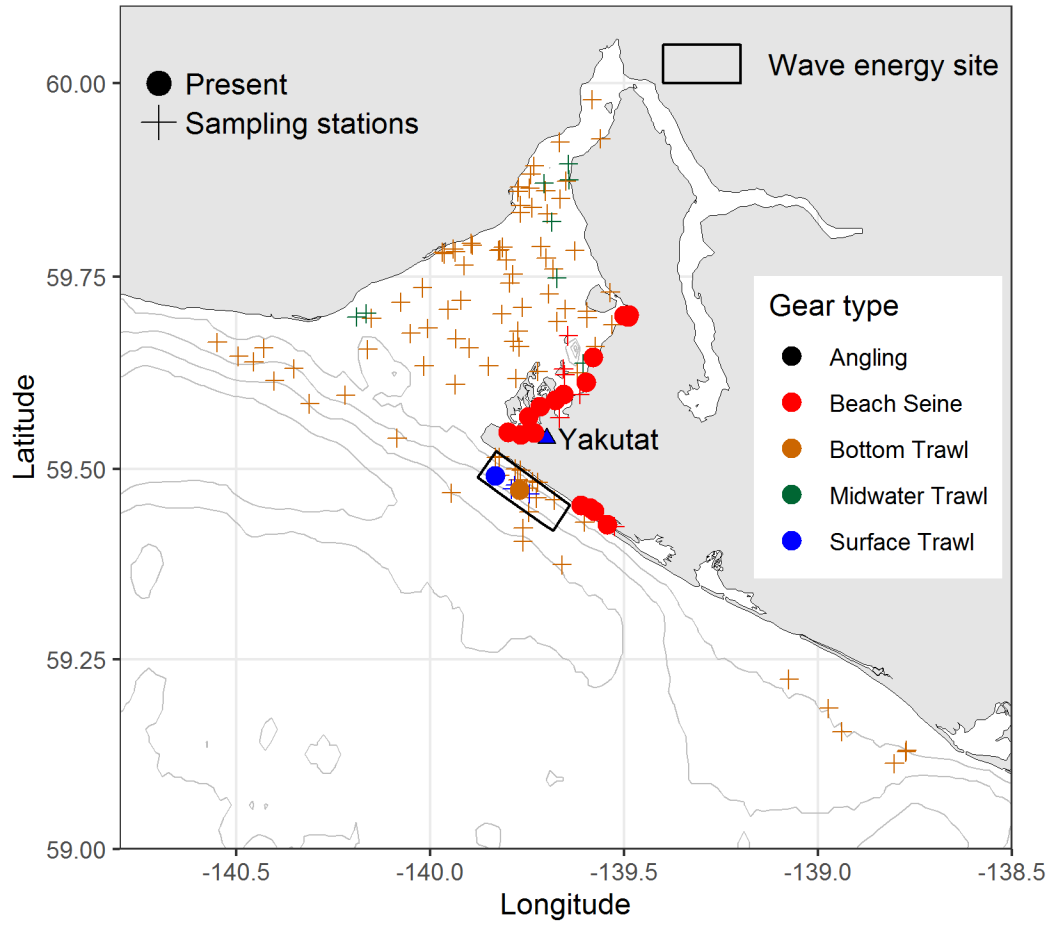


Sturgeon Poacher

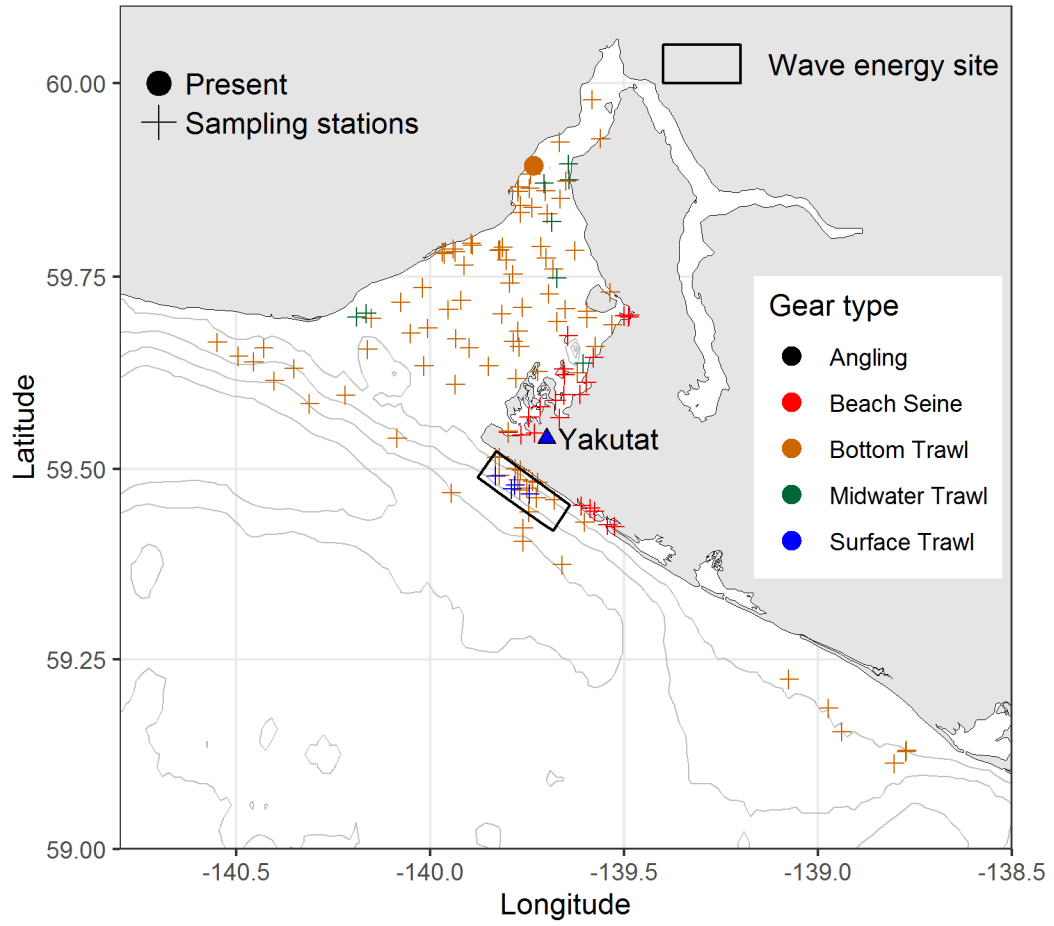
Podotheucus accipenserinus



Surf Smelt
Hypomesus pretiosus

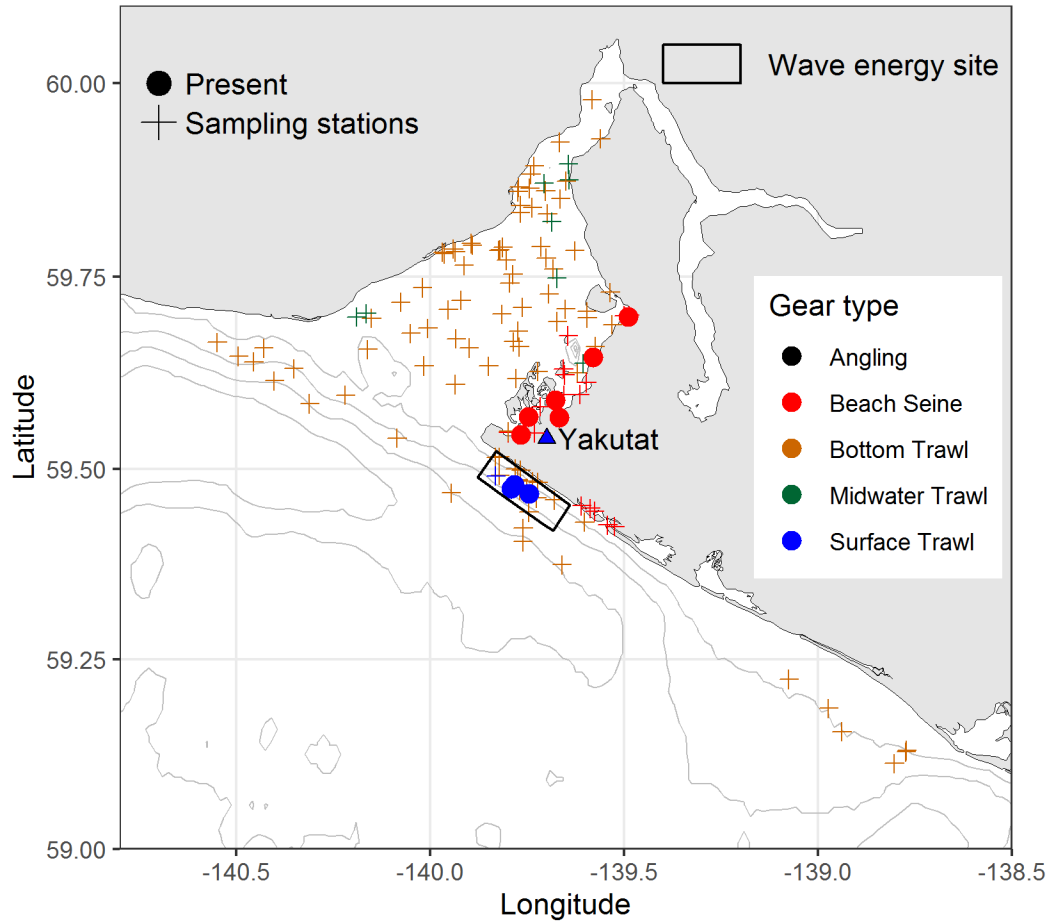


Tadpole Sculpin
Psychrolutes paradoxus

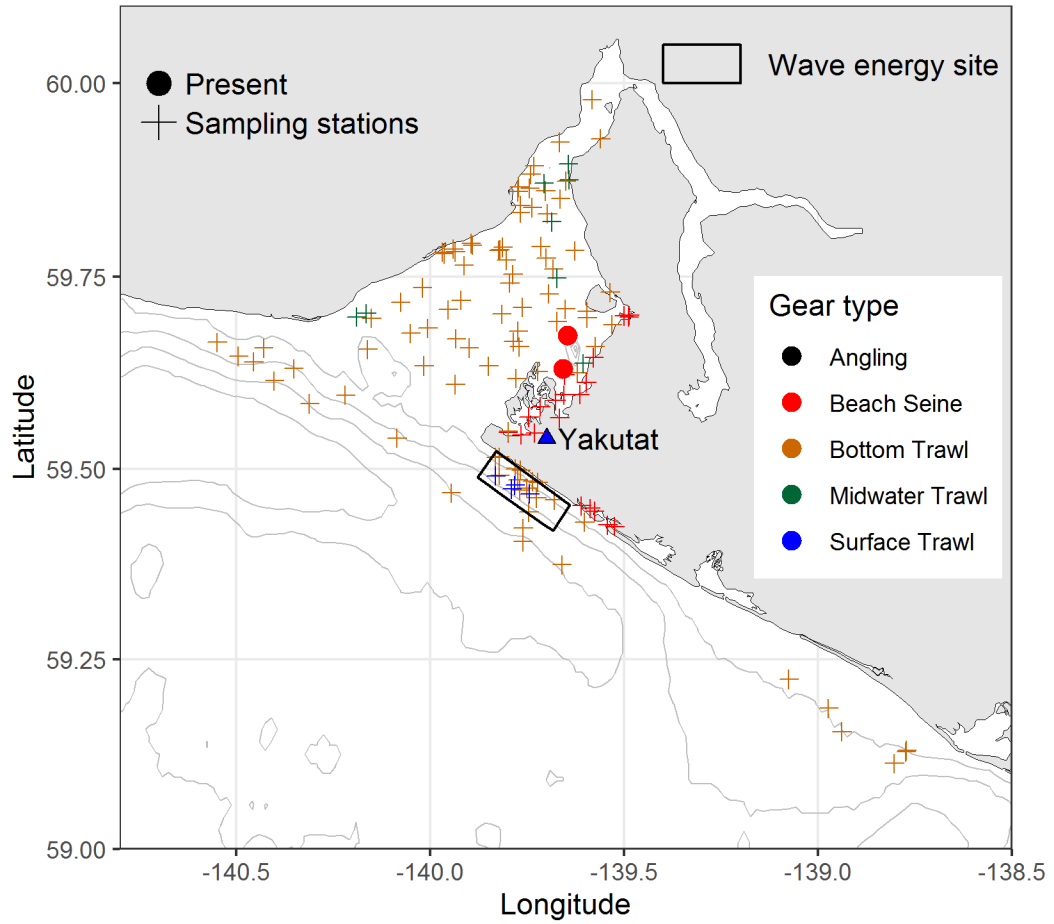


Threespine Stickleback

Gasterosteus aculeatus

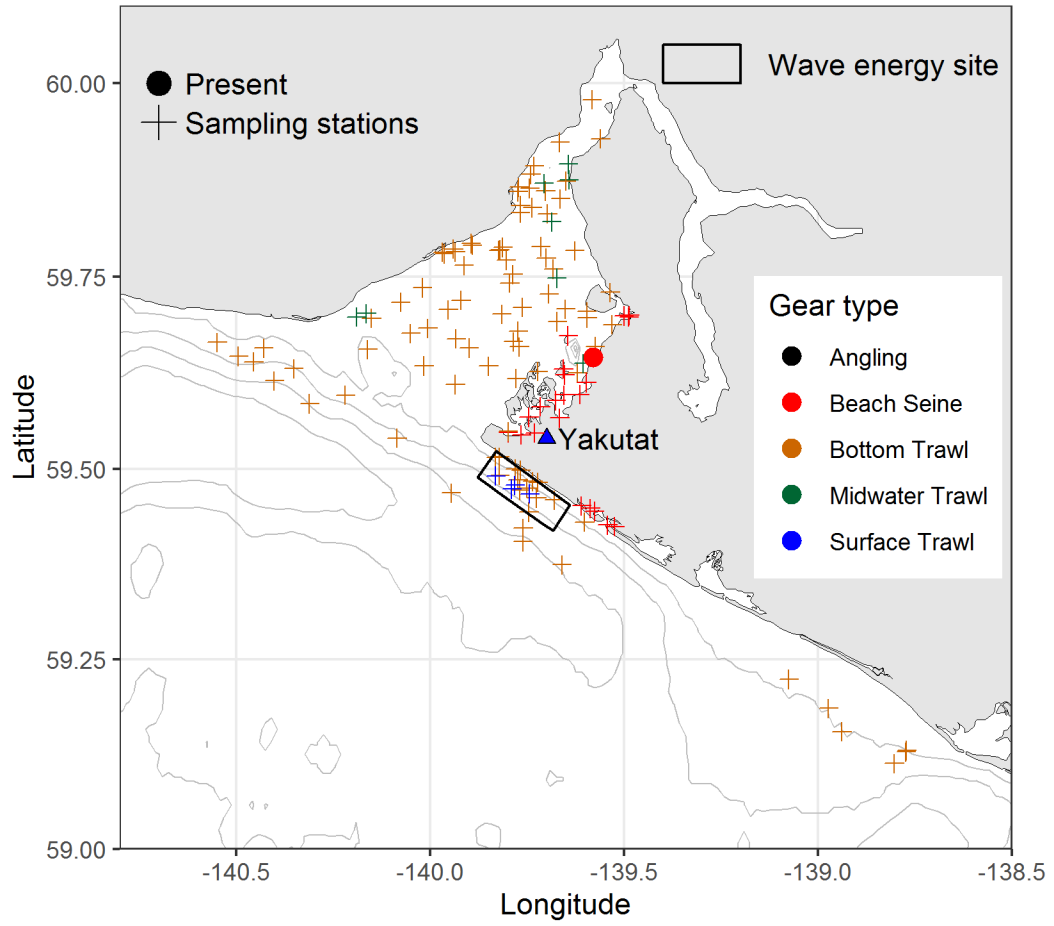


Tidepool Sculpin
Oligocottus maculosus



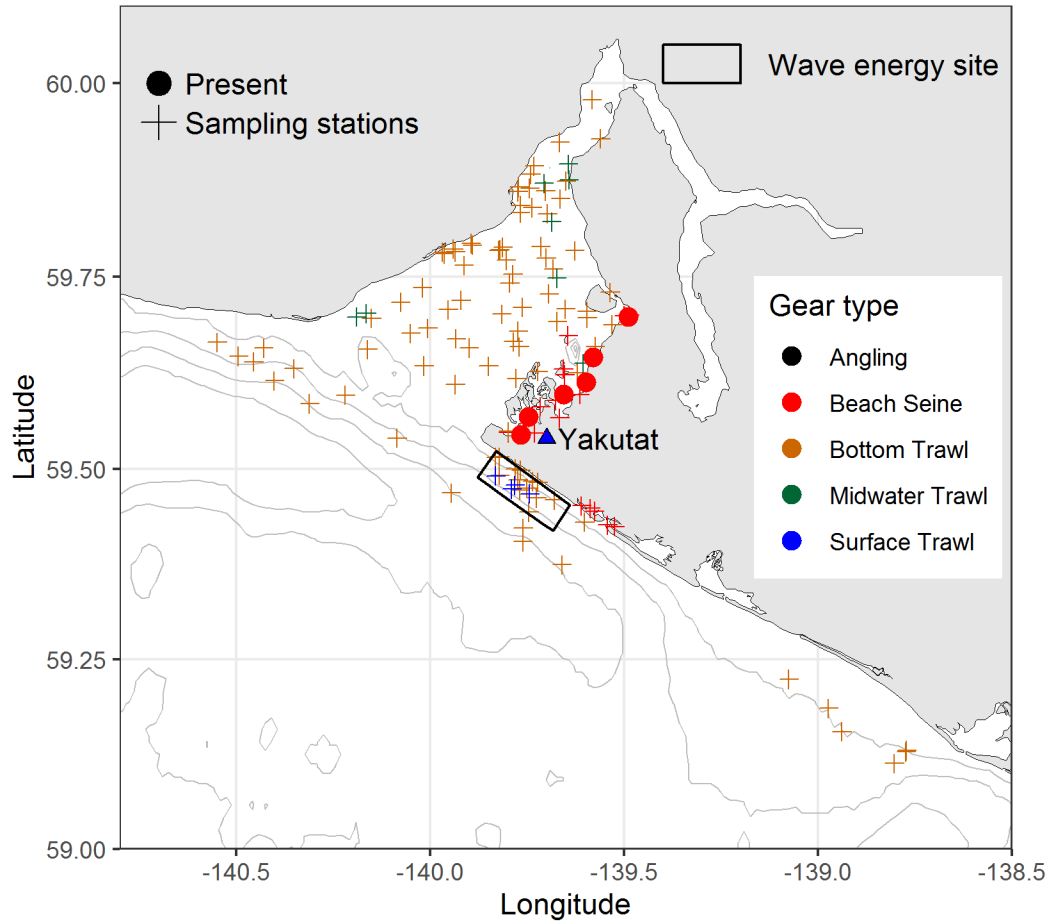
Tidepool Snailfish

Liparis florae

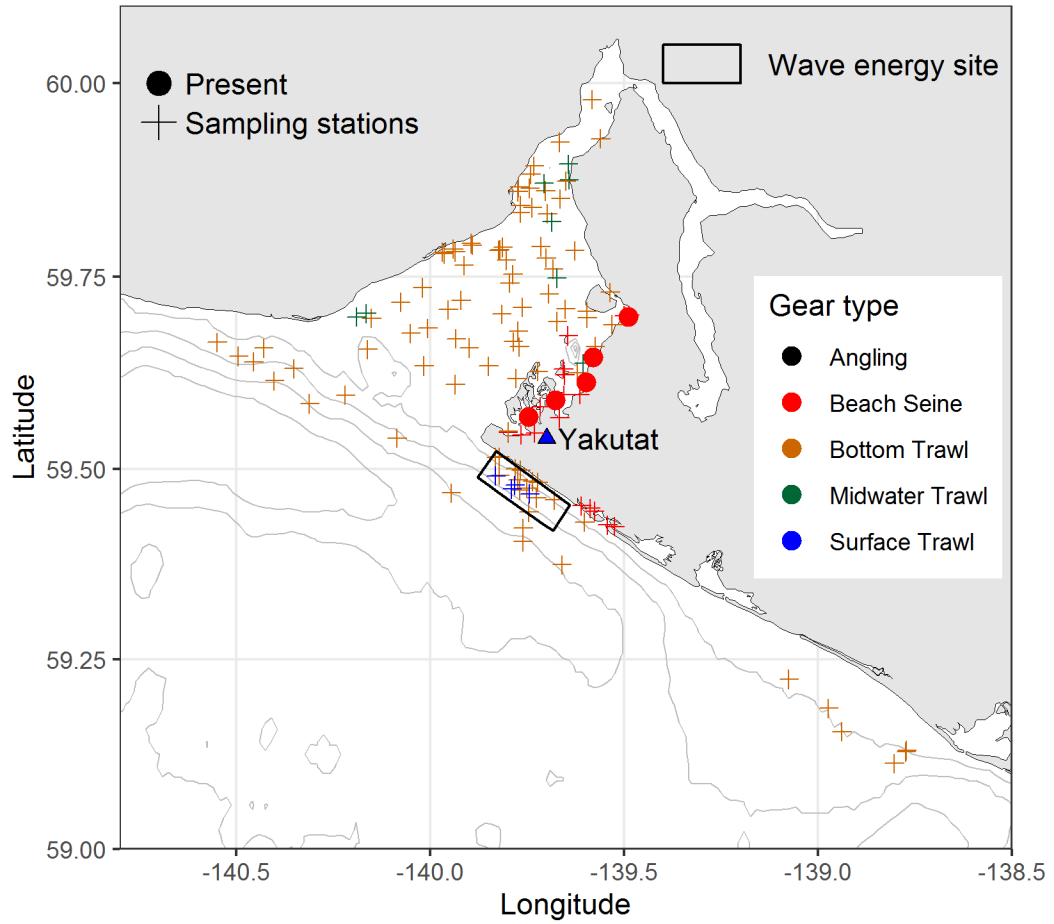


Tubenose Poacher

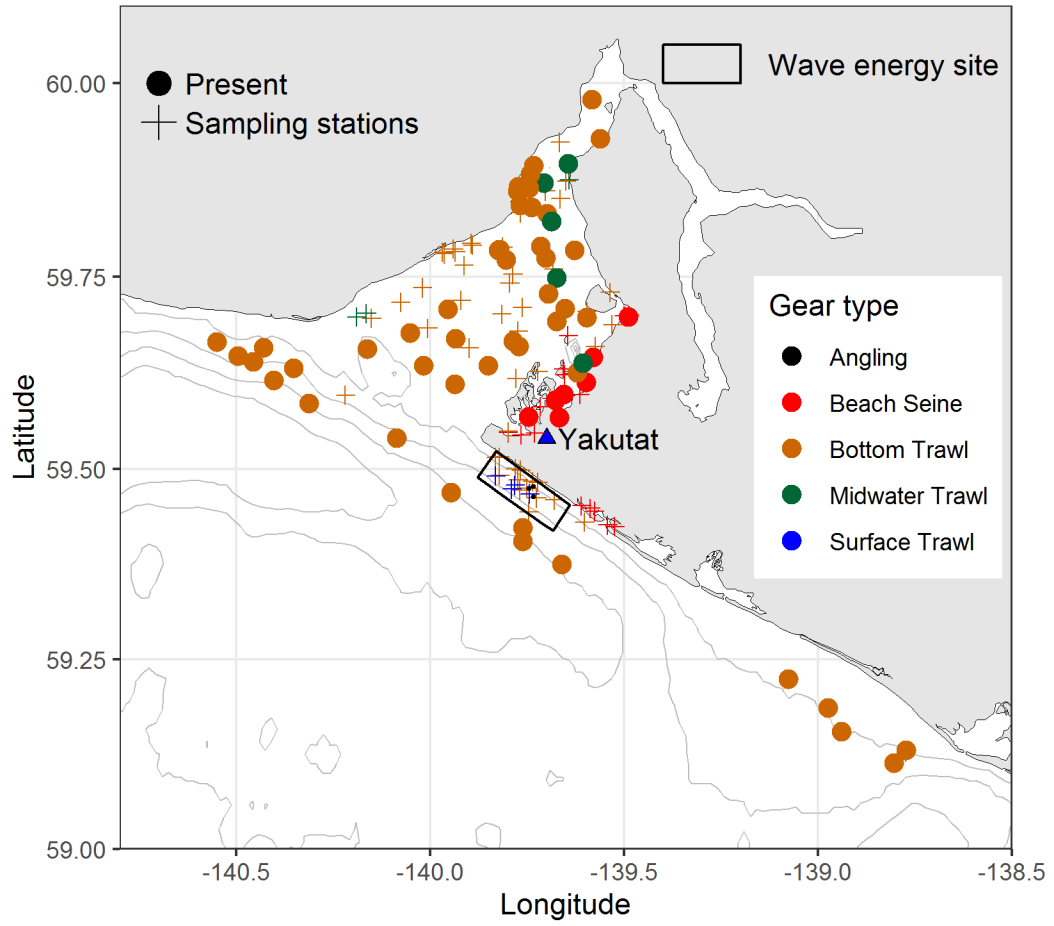
Pallasina barbata



Tubesnout
Aulorhynchus flavidus

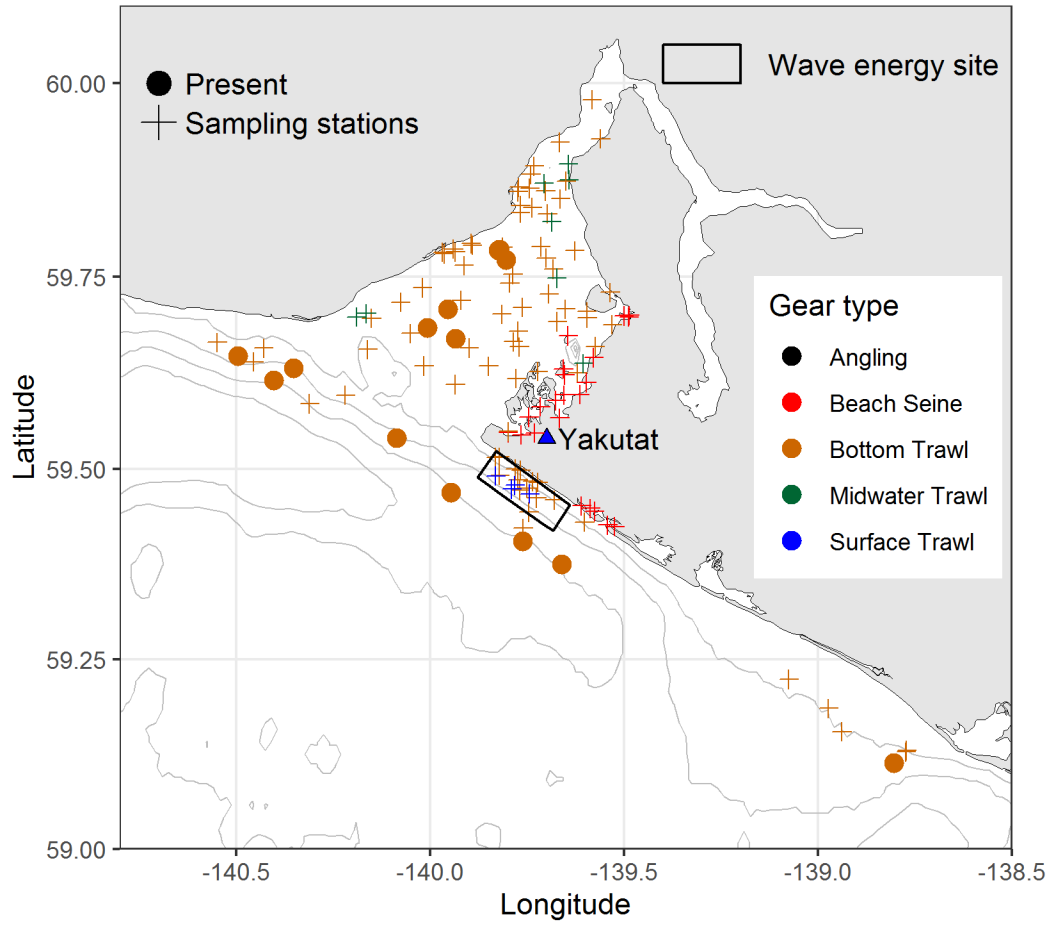


Walleye Pollock
Gadus chalcogrammus



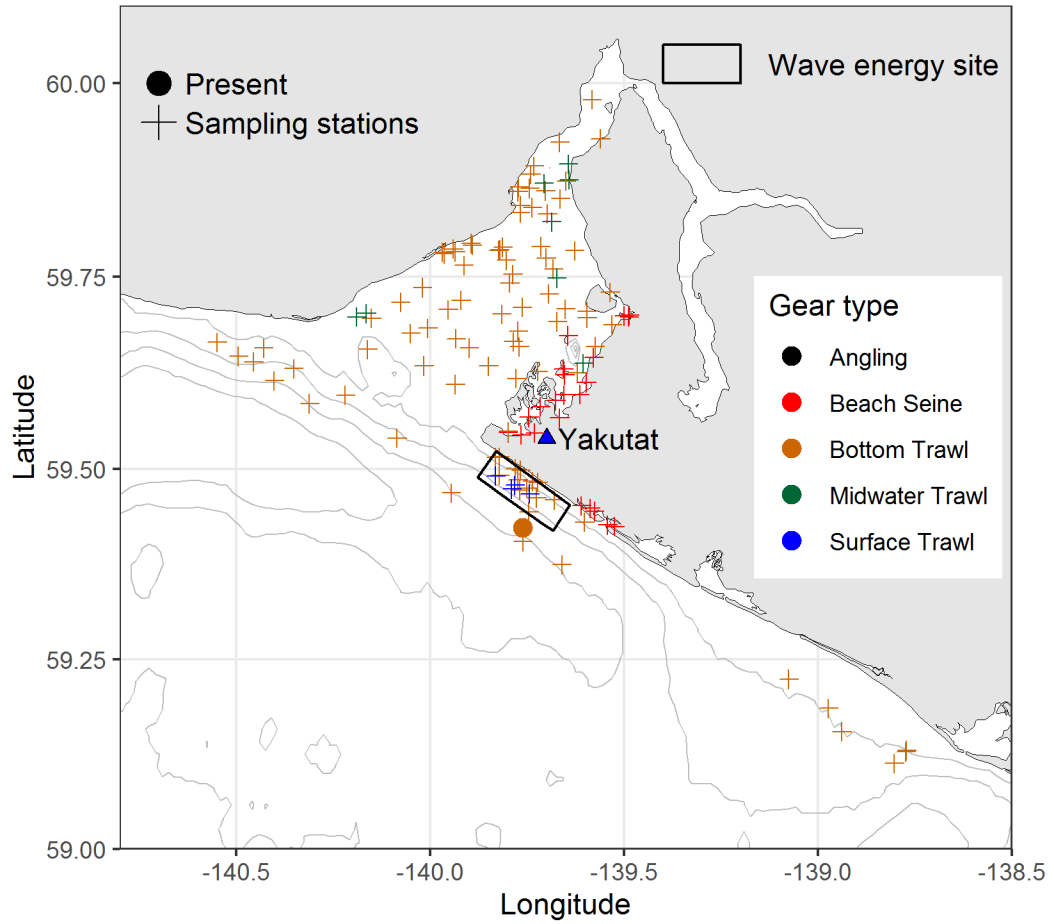
Wattled Eelpout

Lycodes palearis



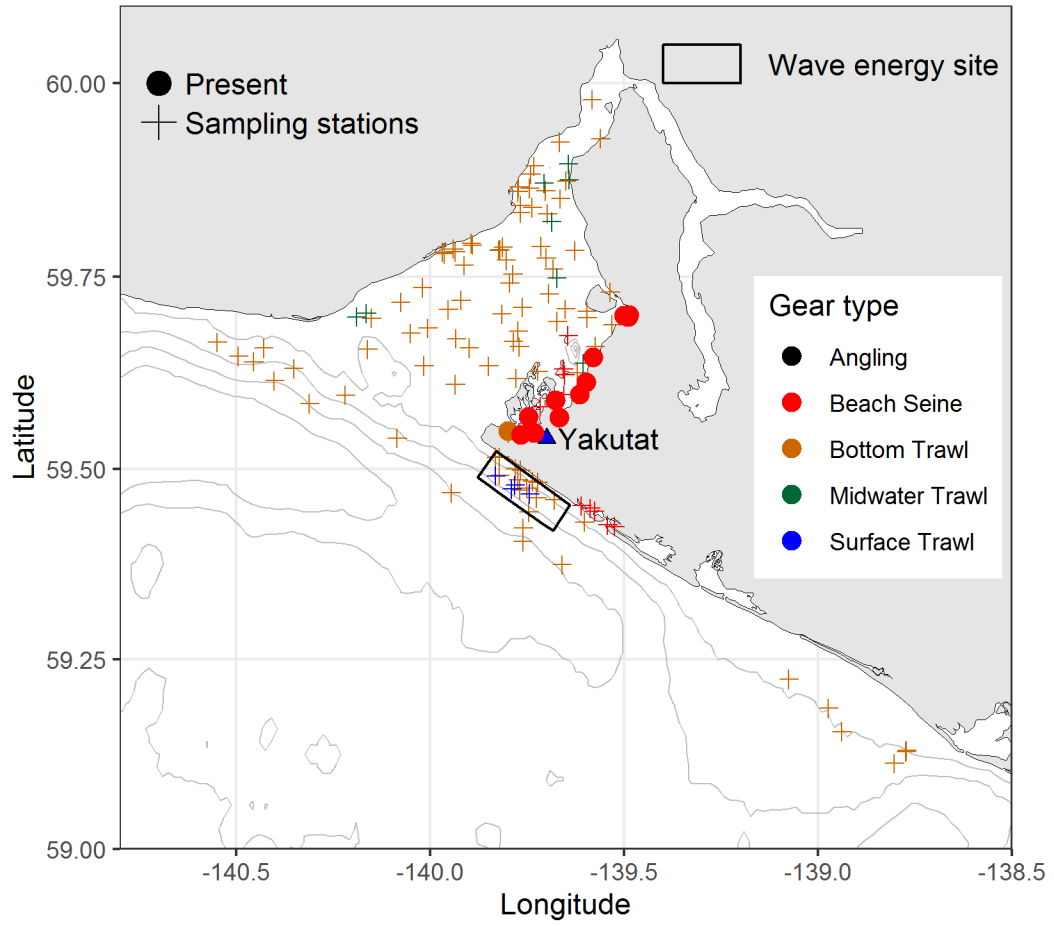
Whitebarred Prickleback

Poroclinus rothrocki

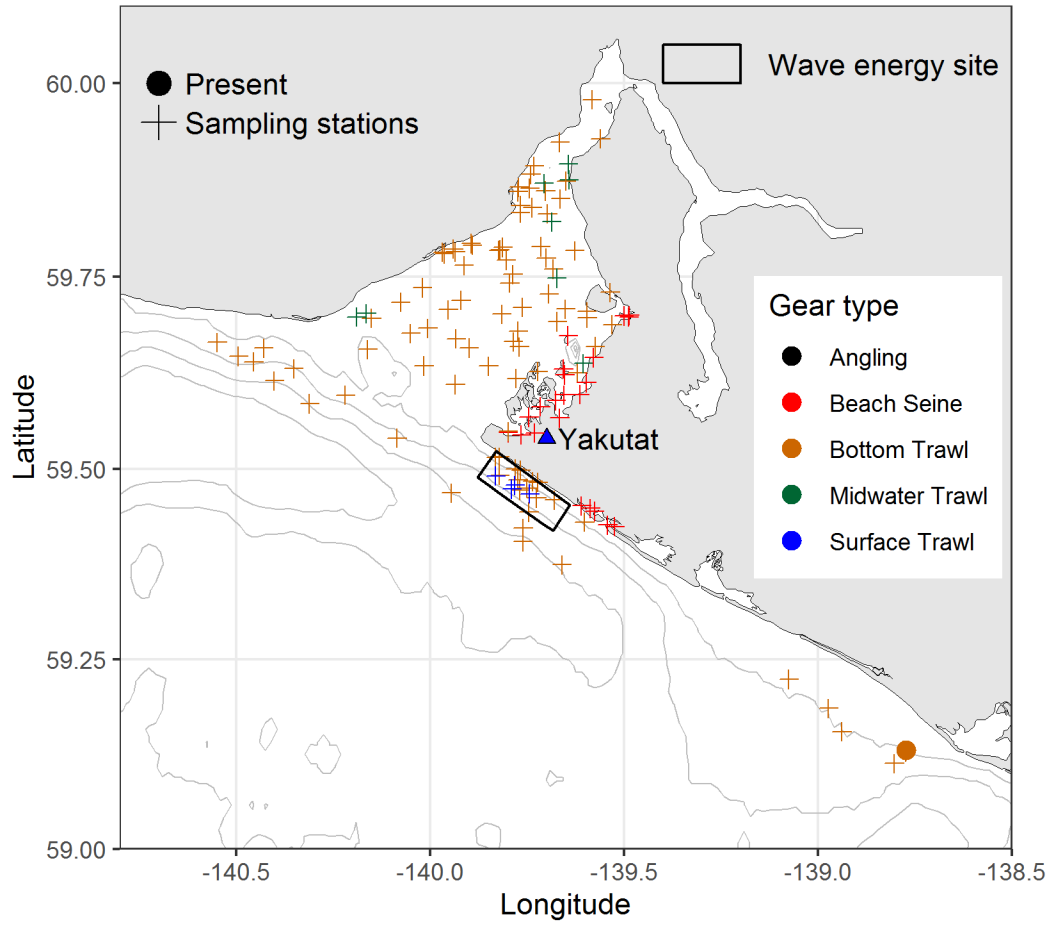


Whitespotted Greenling

Hexagrammos stelleri

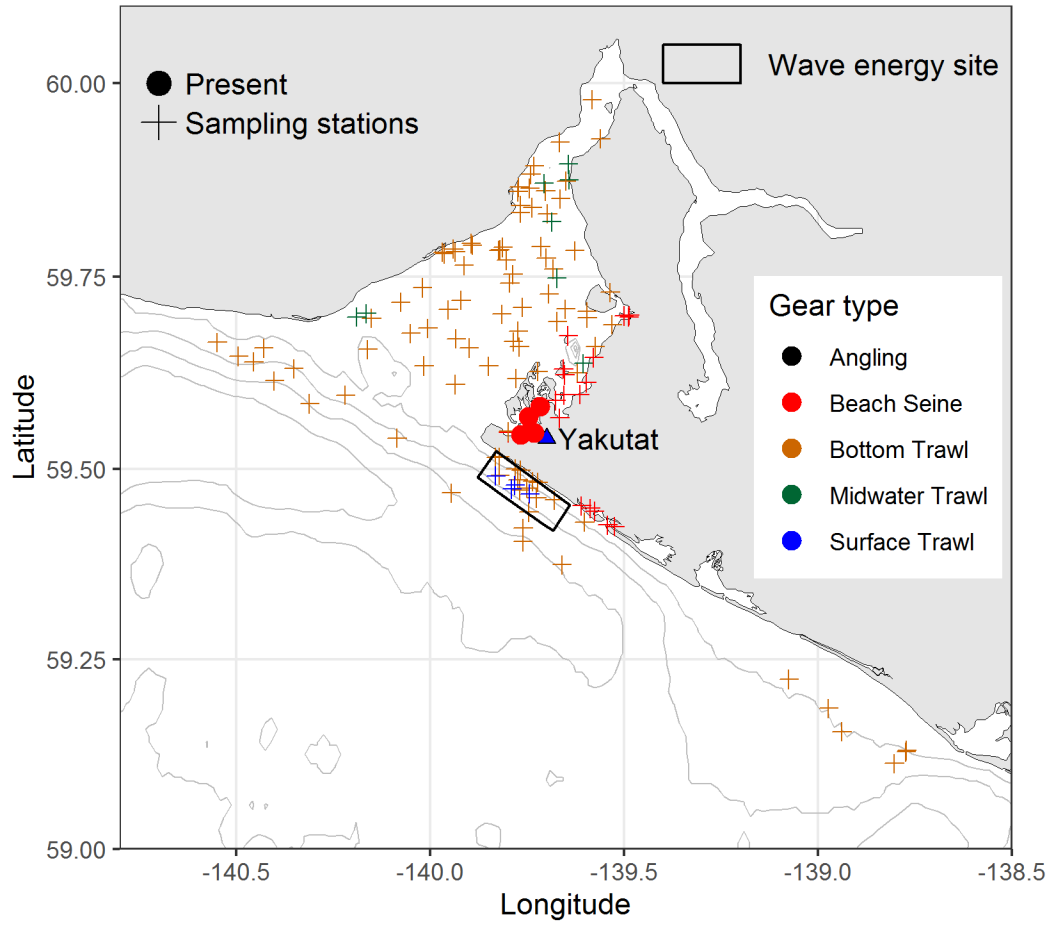


Wolf-Eel
Anarrhichthys ocellatus



Yellowfin Sole

Limanda aspera



● Appendix B

Sieve and Pipette Method for Analyzing Sediment Texture

Scope and Application

This method is recommended for academic research that is investigating properties related specifically to texture. The method employed by CAL splits the sand sized fraction into five classes, and splits silt into two size classes. Generally, the reproducibility is considered to be $\pm 2\%$.

Summary

Prior to starting the particle size separation steps the sample is dried and particles greater than 2 mm are removed, the sample is precisely weighed, then organic matter and any other potential cementing-agents are removed. Sodium hexametaphosphate is added to the suspension and placed on a shaker overnight to overcome flocculation during settling. Sand size fractions are separated through a wet sieve, oven dried, and sieved through a series of sieves. The silt and clay suspension is brought to a volume of 1L and specific aliquots of the fluid are removed by pipette at a specific depth at specific time points to capture the silt and clay sized particles in accordance with Stokes' Law. The fluid is dried, weighed, and the weight used in calculations to determine the final texture.

Equipment and Materials

- 2 mm sieve
- 0.05 mm sieve
- Sieve stack (US or FAO size grouping)
- Accujet pipette dispenser
- 20 mL glass pipettes
- Analytical balance (0.0001g accuracy)
- 30 mL beakers
- 1000 mL graduated cylinders
- Pipette slide apparatus
- Stop watch
- Large funnel
- Squirt bottle
- 500 mL texture bottles
- 500 mL bottle lids
- Data sheet
- 105C oven
- Thermometer
- Flat bottomed stirring rod

Reagents

- 30% Hydrogen peroxide (H_2O_2)
- Sodium Hexametaphosphate $Na_6P_6O_{18}$ (solution of 10% $Na_6P_6O_{18}$)

Procedure

A: Sample Preparation

1. Weigh approximately 50g of air dried soil that has been sieved through a 2 mm sieve and place into a labeled 500 mL texture bottle

B: Sample dispersion and removal of cementing agents

2. Assess sample for need to remove carbonates (pH greater than 7.3) or iron cementing agents (visual inspection for iron oxides).
3. Add 100 mL of deionized water using a bottletop dispenser.
4. Add 8 mL of 30% H₂O₂ using repeater pipette.
5. Gently swirl the bottle to mix the soil, water, and H₂O₂ together. Use a squirt bottle of deionized water to rinse the sides of the texture bottle to make sure all soil particles are in contact with the water and H₂O₂ slurry.
6. Let stand ~4 hours while periodically swirling the texture bottle and rinsing the sides of the bottle with deionized water. Do not let the soil dry out.
7. After ~4 hours, add 50 mL of Na₆P₆O₁₈ solution using a bottletop dispenser.
8. Secure cap on bottle, and place on reciprocating shaker set to “Low”.
9. After ~2 hours, take the bottles off the shaker and open each bottle to allow H₂O₂ fumes to release.
10. Put the lids back on the bottles and place the bottles back on the shaker. Set the shaker to “Low” and shake overnight.
11. Pull bottles off the shaker the following morning and proceed with ‘Separation of fractions’.

C: Separation of fractions

12. Remove samples from reciprocating shaker.
13. Label a 100 to 150 mL glass beaker with sample ID, place beaker in 105C oven for 5 minutes, then dessicate for 5 minutes, and record weight of empty beaker with a 0.0001g balance.
 - a. This beaker will be used to collect sand sized particles after silt and clay are rinsed through the sieve.
14. Set up sand sieving apparatus:
 - a. Place ring stand in the sink with funnel holder.
 - b. Place large funnel in funnel holder.
 - c. Place a 50µm sieve above the funnel.
 - d. Place a 1000 mL graduated cylinder below the funnel.
15. While the sample is still in the texture bottle, gently shake the bottle to ensure that none of the sample is stuck to the bottom of the bottle.
16. Pour dispersed sample over the sieve screen ensuring all smaller particles enter cylinder.
17. Use a rinse bottle with deionized water to rinse all particles out of the texture bottle and onto the sieve screen.
18. **Pay special attention to the volume of liquid in the graduated cylinder as you are transferring the sample from the texture bottle to the sieve screen. Do not fill the cylinder over the 1000 mL mark.**
19. Use a rinse bottle with deionized water to rinse all remaining particles on top of the sieve screen until there is only sand-sized particles left on top of the sieve screen.
20. Remove the sieve from the sand sieving apparatus and use a rinse bottle with deionized water to carefully transfer the remaining sand into pre-labeled and pre-weighed beaker. Place beaker onto a heat-safe tray and place the tray into 105C oven.
21. Dry beaker with sand fraction overnight in a 105C oven. After 24 hours, place the beakers in a dessicator for 20 minutes, then weigh beakers to 0.0001g.
22. Keep the sample in the beaker and prepare to separate the sand into different particle size classes using a sieve stack.
23. Stack the sieve sizes of choice with the largest on top, with decreasing sieve openings
 - a. We will use 1000, 500, 250, 106, 53µm sieve openings for our stack

24. After ensuring that you have recorded the weight of the dried beaker, transfer the dried sample onto the top sieve (1000 um). You will need to scrape the sides and bottom of the beaker to ensure that all of the sample has been transferred from the beaker into the sieve stack.
25. Using your hands or a Vortex shaker, shake the sieve stack for 30 – 60 seconds. Apply pressure to the top and bottom of the sieve stack to ensure that no sample is being lost between sieves.
26. After shaking, place each individual sieve onto a 0.0001g balance and record the weight. Repeat this process for all sieves of the sieve stack.
27. If any material makes it through ALL of the sand sieves, it should be transferred to the graduated cylinder for the pipette determination.
28. After ensuring that you have recorded a weight for each sieve in the sieve stack, use the sieve brush to thoroughly clean each sieve before reassembling the sieve stack. Proceed with the remaining samples.

D: Pipette fine fractions from depth

29. Gather enough 30 mL beakers needed for taking 3 aliquots of each texture sample
30. Label each 30 mL beaker with sample ID and pipette time point (i.e. 0 min, 5 min, 5.5 hr). Be sure to label a trio of beakers for Blank determination. (i.e. Blank 0 min, Blank 5 min, Blank 5.5 hr).
31. Place all 30 mL beakers in 105C oven for at least 10 minutes. After a minimum of 10 minutes, place beakers in dessicator, and then record the weight for each empty beaker to 0.0001g.
32. In the Texture room, line up all cylinders directly behind the yellow line on the bench. Using DI water, fill graduated cylinders to exactly 1000 mL.
33. Place the 0 min and 5 min oven dried, weighed, and labeled 30 mL beakers in front of each cylinder. Set the 5.5 hr 30 mL beakers aside.
34. Install a 20 mL glass pipette in the pipette slide apparatus.
35. Check the temperature of the room to determine appropriate sampling depth.
36. Set the pipette apparatus depth according to Table 1 at the end of this protocol. It is helpful to use a piece of lab tape to mark the 0 min and 5 min pipette depths on the pipette slide apparatus.
37. Rigorously stir/pump the silt and clay fraction with the flat bottomed stirring rod until thoroughly mixed. Do not break the surface of the water, focus on getting sediment up from the bottom of the cylinder and making sure the suspension is well distributed.
38. Immediately after mixing the suspension, lower the pipette to the desired sampling depth inside the graduated cylinder using the slide apparatus.
39. Remove 20 mL using the top button on the Accujet automatic pipetter. Pull the slide apparatus up and deposit the suspension into the 30 mL beaker labeled “0 min” using the down button on the Accujet. Ensure all of the suspension is dispensed by hitting the down button again after all of the suspension has been dispensed.
40. Proceed to stirring the next cylinder.
41. Carefully follow the timing schedule in Table 2 **at the end of this protocol**.
42. Precisely five minutes after you stop stirring each cylinder, pipette a second sample from the cylinder and deposit into the 30 mL beaker labeled “5 min”.
43. Place the 0 min and 5 min 30 mL beakers with suspension onto a heat safe tray and place tray into a 105C oven.
44. Precisely 5.5 hours after the first sample is removed from the cylinder, pipette a third sample from the cylinder and deposit into the 30 mL beaker labeled “5.5 hr”.
45. Place the beakers with suspension onto a heat safe tray and place in 105C oven.
46. The next day, remove all 30 mL beakers from the 105C oven and place in a dessicator for at least 30 minutes.
47. Weigh all 30 mL beakers and record the sample mass onto the datasheet.

48. Enter all data into the spreadsheet.

E: Blank Determination

1. Make a blank solution using 50 mL of 10% NaHMP and dilute to 1000 mL with DI water.
2. Follow pipetting steps 37 - 44 for this blank sample at each measurement point.
3. Determine the weight of salts added to the soil suspension for calculation purposes by drying and weighing each 30 mL beaker of the pipetted blank sample.

Calculations

1. A spreadsheet has been developed and provided to help make calculations
2. Enter all weights into the spreadsheet
3. Determine relative portion of fractions as follows; very coarse sand <2-1 mm, coarse sand <1-0.5 mm, medium sand <0.5-0.25 mm, fine sand <0.25-0.1 mm, and very fine sand <0.1-0.05 mm, coarse silt <0.05-0.02 mm, fine silt <0.02-0.002 mm, and clay <0.002 mm.

Table 1. Appropriate depth at which to take the sample with pipette by temperature

Temperature	Depth (cm)	Depth (cm)
°C	5 min.	5½ hrs.
19	10.5	6.9
20	10.8	7.1
21	11.0	7.2
22	11.3	7.4
23	11.6	7.6
24	11.9	7.8
25	12.1	8.0
26	12.4	8.2
27	12.7	8.4
28	13	8.6
29	13.3	8.8
30	13.6	9
31	13.9	9.1
32	14.2	9.3
33	14.4	9.5
34	14.8	9.7
35	15.1	9.9
36	15.4	10.1

Table 2. Timing schedule for pipette procedure

Minutes	Sample #	Action
0	1	Start Stir
0.5	1	Stop stir, start timer, & pull sample 1.1 (0 min)
2.5	2	Start stir
3	2	Stop stir and pull sample 2.1 (0 min)
5	1	Pull sample 1.2 (5 min)
5.5	3	Star Stir
6	3	Stop stir & pull sample 3.1 (0 min)
8	2	Pull sample 2.2 (5 min)
8.5	4	Start stir
9	4	Stop stir and pull sample 4.1 (0 min)
11	3	Pull sample 3.2 (5 min)
16	4	Pull sample 4.2 (5 min)
333 (5.5 hr)	1	Pull sample 1.3 (5.5 hr)
336	2	Pull sample 2.3 (5.5 hr)
339	3	Pull sample 3.3 (5.5 hr)
342	4	Pull sample 4.3 (5.5 hr)



Department of the Interior (DOI)

The Department of the Interior protects and manages the Nation's natural resources and cultural heritage; provides scientific and other information about those resources; and honors the Nation's trust responsibilities or special commitments to American Indians, Alaska Natives, and affiliated island communities.



Bureau of Ocean Energy Management (BOEM)

The mission of the Bureau of Ocean Energy Management is to manage development of U.S. Outer Continental Shelf energy and mineral resources in an environmentally and economically responsible way.

BOEM Environmental Studies Program

The mission of the Environmental Studies Program is to provide the information needed to predict, assess, and manage impacts from offshore energy and marine mineral exploration, development, and production activities on human, marine, and coastal environments. The proposal, selection, research, review, collaboration, production, and dissemination of each of BOEM's Environmental Studies follows the DOI Code of Scientific and Scholarly Conduct, in support of a culture of scientific and professional integrity, as set out in the DOI Departmental Manual (305 DM 3).